

December 2019

Targeting the Γ -Aminobutyric Acid a Receptor (gabaar) to Alleviate Inflammation for Asthma and Neuropathic Pain

Amanda Nicole Nieman
University of Wisconsin-Milwaukee

Follow this and additional works at: <https://dc.uwm.edu/etd>



Part of the [Biochemistry Commons](#)

Recommended Citation

Nieman, Amanda Nicole, "Targeting the Γ -Aminobutyric Acid a Receptor (gabaar) to Alleviate Inflammation for Asthma and Neuropathic Pain" (2019). *Theses and Dissertations*. 2325.
<https://dc.uwm.edu/etd/2325>

This Dissertation is brought to you for free and open access by UWM Digital Commons. It has been accepted for inclusion in Theses and Dissertations by an authorized administrator of UWM Digital Commons. For more information, please contact open-access@uwm.edu.

TARGETING THE γ -AMINOBTYRIC ACID A RECEPTOR (GABA_AR)
TO ALLEVIATE INFLAMMATION FOR ASTHMA AND NEUROPATHIC PAIN

by

Amanda N. Nieman

A Dissertation Submitted in
Partial Fulfillment of the
Requirements for the Degree of

Doctor of Philosophy
in Chemistry

at

The University of Wisconsin – Milwaukee

December 2019

ABSTRACT

TARGETING THE γ -AMINO BUTYRIC ACID A RECEPTOR (GABA_AR)
TO ALLEVIATE INFLAMMATION FOR ASTHMA AND NEUROPATHIC PAIN

by

Amanda N. Nieman

The University of Wisconsin – Milwaukee, 2019
Under the Supervision of Professor Alexander (Leggy) Arnold

The γ -Aminobutyric Acid A Receptor (GABA_AR) is a ligand-gated, pentameric chloride channel composed of subunits that include α 1-6, β 1-3, γ 1-3, δ , ϵ , π , θ , ρ 1-3.¹⁻² The most common arrangement includes two α subunits, two β subunits, and a γ subunit.³ This receptor includes two binding sites for the endogenous ligand γ -aminobutyric acid (GABA) between the α and β subunits and a binding site between the α and γ subunit for benzodiazepines, a large family of positive allosteric modulators.⁴⁻⁵

Benzodiazepines are one of the most prescribed classes of pharmaceuticals to treat anxiety, insomnia, and epilepsy as well as for muscle relaxation.⁶⁻⁷ However, adverse effects are also associated with benzodiazepine use, including tolerance, dependence, sedation, amnesia, and severe withdrawal symptoms.^{6,8} Physiological effects of these compounds corresponds to their selectivity towards GABA_ARs containing specific alpha subunits.⁸ This is also the case for non-neuronal cells as these cells express narrower subsets of GABA_AR subunits.⁹⁻¹¹ A high-throughput assay was developed using automated patch clamp and cell lines stably expressing functional GABA_ARs to determine subtype selectivity.

To determine any adverse CNS effects of novel imidazodiazepines, the rotarod assay was employed. Traditionally, this assay has been used to detect neurological deficits caused by muscle

relaxants, convulsants, and CNS depressants since the 1950's.¹² It is one of the most commonly used sensorimotor assays because of its sensitivity and reliability. After its implementation, hundreds of compounds have been screened in the recent years by members of the Arnold group.

Subtype-selective imidazodiazepines without CNS effects were used to target non-neuronal cell types in an effort to alleviate inflammation in asthma and neuropathic pain (NP). Many cell types play a role in the airway inflammatory response, including T-lymphocytes, alveolar macrophages, and eosinophils.¹³ CD4⁺ T-lymphocytes¹⁴ and macrophages¹⁵ have both been shown to express GABA_AR, however eosinophils have not previously been investigated.¹⁶⁻¹⁷ Herein, it is demonstrated that eosinophils express GABA_AR subunits.

The ability of imidazodiazepines to reduce inflammation was investigated by measuring the production of nitric oxide (NO) in activated macrophages. NO can cause vasodilation¹⁸, increase in mucus secretion¹⁸, recruit eosinophils¹⁸, cause cell injury and airway remodeling¹⁹, and mediate steroid resistance.¹⁹ Exhaled NO is used to determine the severity of lung inflammation of asthmatics.¹⁹ Among many compounds investigated, a novel imidazodiazepine was identified with the ability to reduce NO production.

Lymphocytes mediate the inflammatory response in asthma by infiltrating the airway and secreting inflammatory mediators, such as cytokines and chemokines.²⁰ Functional GABA_AR were confirmed on lymphocytes and targeted with novel imidazodiazepines to reduce IL-2, a cytokine associated with asthma exacerbations.²¹ The reduction of IL-2 was accompanied by a reduction of intracellular calcium, a signaling molecule that underlies many inflammatory processes.²²

Alveolar macrophages have been successfully targeted with novel imidazodiazepines.²³⁻²⁴ Interestingly, these cells have been reported to be developmentally related to other resident macrophages, including microglia, the resident macrophages in the central nervous system.²⁵ Microglia have been shown to express GABA_AR subunits¹¹, however a full characterization was not completed.

It is demonstrated that human and mouse microglia express functional GABA_AR that can be modulated with novel imidazodiazepines.

Neuropathic pain has been suggested to be caused by hyper-excitability of neurons, however new evidence showed that the underlying cause is inflammation as a result of microglial activation.²⁶⁻²⁷ Upon nerve injury, microglia are stimulated to cause an influx of intracellular calcium²⁸⁻²⁹, which leads to upregulation of numerous inflammatory mediators, including cytokines, chemokines, and cytotoxic compounds; substances known to contribute to allodynia, hyperalgesia, and nociception.³⁰⁻³² Novel imidazodiazepines have been identified among many compounds that reduce NO production, a key inflammatory modulator that causes extensive cell damage.³³ Further experiments showed that this reduction was caused by a decrease in intracellular calcium, which in turn downregulated transcription and translation of iNOS, the enzyme responsible for generating nitric oxide during the inflammatory response.³⁴ Initial experiments showed that these compounds have a stronger interaction with the κ opioid receptor than with GABA_AR.

© 2019 Amanda N. Nieman
All Rights Reserved

To
my parents,
my husband,
and my daughter.

TABLE OF CONTENTS

ABSTRACT	ii
LIST OF FIGURES	xi
LIST OF TABLES	xxviii
LIST OF ABBREVIATIONS	xxix
ACKNOWLEDGEMENTS	xxxii
CHAPTER 1	1
1.1 γ-Aminobutyric Acid (GABA)	2
1.1.1 Discovery of GABA	2
1.1.2 Formation of GABA	2
1.2 The γ-Aminobutyric Acid A Receptor ($GABA_A$R)	3
1.2.1 Discovery of the $GABA_A$ R	3
1.2.2 Structure of the $GABA_A$ R.....	4
1.3 Modulating the $GABA_A$R	7
1.3.1 The GABA Binding Site	7
1.3.2 The Chloride Channel.....	9
1.3.3 The Benzodiazepine Binding Site	10

1.4 Distribution of GABA _A R	12
CHAPTER 2	15
2.1 Background	16
2.2 Automated Patch Clamp	17
2.2.1 Instrumentation	17
2.2.2 Assay Format.....	19
2.3 Stable Cell Line Patch Clamp	20
2.3.1 Experimental	20
2.3.2 Results: GABA Concentration Responses.....	24
2.3.3 Results: Control Compounds.....	26
2.3.4 Results: Troubleshooting	32
2.3.5 Discussion.....	49
2.4 <i>Novel Imidazodiazepine Testing</i>	54
2.4.1 Experimental	54
2.4.2 Results	54
2.4.3 Discussion.....	59
2.5 Alternative Methods.....	61
CHAPTER 3	62
3.1 Background	63
3.2 Instrumentation	64

3.3 Initial Protocol	65
3.3.1 Experimental.....	65
3.3.2 Results.....	65
3.3.3 Discussion.....	66
3.4 Improved Protocol	68
3.4.1 Experimental.....	68
3.4.2 Results.....	68
3.4.3 Discussion.....	73
3.5 Conclusion	73
CHAPTER 4	75
4.1 Background	76
4.2 Targeting GABA_AR on Lymphocytes	79
4.2.1 Experimental.....	79
4.2.2 Results.....	85
4.2.3 Discussion.....	93
4.3 Targeting GABA_AR on Other Immune Cell Types	95
4.3.1 Experimental.....	95
4.3.2 Results: Eosinophils.....	96
4.3.3 Results: Macrophages.....	97
4.3.4 Discussion.....	98

4.4 Conclusion.....	99
CHAPTER 5	101
5.1 Background	102
5.2 Targeting GABA _A R on Astrocytes	105
5.2.1 Experimental	105
5.2.2 Results	108
5.2.3 Discussion.....	111
5.3 Targeting GABA _A R on Microglia	112
5.3.1 Experimental	112
5.3.2 Results	120
5.3.3 Discussion.....	149
5.4 Conclusion.....	152
REFERENCES.....	153
APPENDICES.....	163
Appendix A – Asthma Compound Structures	164
Appendix B – Pain Compound Structures	166
CURRICULUM VITAE	171

LIST OF FIGURES

Figure 1. GABA Shunt GABA-T: GABA α -oxoglutarate transaminase, GAD: glutamic acid decarboxylase, SSADH: succinic semialdehyde dehydrogenase ⁴	3
Figure 2. Cryo-electron microscopy structure of GABA_AR composed of α 1, β 2, and γ 2 subunits with GABA and Flumazenil bound as determined by Zhu et al. ⁴⁹ In red and yellow are antibodies used for isolation of the protein. Accessed from the Protein Data Bank (PDB: 6D6U)	4
Figure 3. Structure of the GABA_AR A typical GABA _A R contains two α subunits, two β subunits, and one γ subunit, forming two extracellular binding sites between α and β subunits for the endogenous ligand GABA and one extracellular binding site between α and γ subunits for benzodiazepines.	5
Figure 4. Structure of Flumazenil	6
Figure 5. Structure of Muscimol and its derivative Gaboxadol	7
Figure 6. Structure of Bicuculline	8
Figure 7. Structure of Gabazine	9
Figure 8. Structure of Picrotoxin Picrotoxin is an equal mixture of picrotoxinin and picrotin.	10
Figure 9. Subtype Specific Benzodiazepine Pharmacology Experiments with knock-in mice have allowed researchers to correlate GABA _A R subunits with pharmacological effects. ⁸	11
Figure 10. Structure of Ro15-4513	12
Figure 11. IonFlux Microplate Pattern consists of eight compound addition wells (C1-8), an inlet for cell suspension (in), an outlet for waste collection (out), and two traps (T1-2). Traps contain combs with twenty patch pipettes that seal to individual cells. Reprinted with permission from GEN. ⁸⁶	18
Figure 12. Compound Application Scheme A screenshot from the IonFlux control software showing the timing of compound applications. A brief washout period is permitted between 3 second applications.	

Six applications from compound well 1 is followed by a longer washout period before two applications each from compound wells 2-8. Washout times are increased as concentration increases to ensure total removal of the compound. 20

Figure 13. $\alpha 1\beta 3\gamma 2$ Stable Cell Line GABA Concentration Response Cells were patched and exposed to increasing concentrations of GABA. Results were normalized such that 0% represented the response to ECS buffer only and 100% was the maximum response to GABA. 24

Figure 14. $\alpha 2\beta 3\gamma 2$ Stable Cell Line GABA Concentration Response Results were normalized such that 0% represented the response to ECS buffer only and 100% was the maximum response to GABA. 25

Figure 15. $\alpha 3\beta 3\gamma 2$ Stable Cell Line GABA Concentration Response Results were normalized such that 0% represented the response to ECS buffer only and 100% was the maximum response to GABA. 25

Figure 16. $\alpha 4\beta 3\gamma 2$ Stable Cell Line GABA Concentration Response Results were normalized such that 0% represented the response to ECS buffer only and 100% was the maximum response to GABA. 26

Figure 17. $\alpha 5\beta 3\gamma 2$ Stable Cell Line GABA Concentration Response Results were normalized such that 0% represented the response to ECS buffer only and 100% was the maximum response to GABA. 26

Figure 18. $\alpha 1\beta 3\gamma 2$ Control Compound Responses Compounds were co-applied with 400nM GABA, the approximate EC_{20} value determined by the GABA concentration response. Left: Responses were normalized such that 100% represented the response to GABA alone. Right: Sweeps graphs depict the current responses to 3 second applications of the respective concentrations. 28

Figure 19. $\alpha 2\beta 3\gamma 2$ Control Compound Responses Compounds were co-applied with 1 μ M GABA. Left: Responses were normalized such that 100% represented the response to GABA alone. Right: Sweeps graphs depict the current responses to 3 second applications of the respective concentrations. 29

Figure 20. $\alpha 3\beta 3\gamma 2$ Control Compound Responses Compounds were co-applied with 430 nM GABA, the approximate EC_{20} value determined by the GABA concentration response. Left: Responses were

normalized such that 100% represented the response to GABA alone. Right: Sweeps graphs depict the current responses to 3 second applications of the respective concentrations..... 30

Figure 21. $\alpha 4\beta 3\gamma 2$ Control Compound Responses Compounds were co-applied with 600nM GABA, the approximate EC_{20} value determined by the GABA concentration response. Left: Responses were normalized such that 100% represented the response to GABA alone. Right: Sweeps graphs depict the current responses to 3 second applications of the respective concentrations..... 31

Figure 22. $\alpha 5\beta 3\gamma 2$ Control Compound Responses Compounds were co-applied with 600nM GABA, the approximate EC_{20} value determined by the GABA concentration response. Left: Responses were normalized such that 100% represented the response to GABA alone. Right: Sweeps graphs depict the current responses to 3 second applications of the respective concentrations..... 32

Figure 23. Clone Comparison in GABA Concentration Response Three new clones along with the established CL1 clone were tested in GABA Concentration Response. Results were normalized such that 0% represented the response to ECS buffer only and 100% was the maximum response to GABA. 33

Figure 24. Clone Comparison in Diazepam Concentration Response Three new clones along with the established CL1 clone were tested in Diazepam Concentration Response. Diazepam was co-applied with 600 nM GABA, the approximate EC_{20} as determined by the GABA Concentration Response. Responses were normalized such that 100% represented the response to GABA alone. 33

Figure 25. $\alpha 4\beta 3\gamma 2$ Control Compounds in CL13 and CL17 Compounds were co-applied with 600nM GABA, the approximate EC_{20} as determined by the GABA Concentration Response. Responses were normalized such that 100% represented the response to GABA alone. 34

Figure 26. Cell Culture Changes Compounds were co-applied with 1.5 μ M GABA and responses were normalized such that 100% represented the response to GABA alone. (A) Cells were cultured in DMEM High media with 100 μ g/mL of hygromycin. (B) Cells were cultured in DMEM High media with 300 μ g/mL

of hygromycin and supplemented with non-essential amino acids. Cells were also cultured using matrigel.

..... 35

Figure 27. Brand Change for Cell Culture Flasks Cells were cultured in identical media in Nunc EasY flasks and CellStar Flasks. Results were normalized such that 0% represented the response to ECS buffer only and 100% was the maximum response to GABA. Sweeps corresponding to the concentration curve (left) are shown on the right..... 36

Figure 28. Cell Preparation Modifications Cells were prepared for patch clamp experiments through three blank media washes followed by three ECS washes (6X Wash) or the ECS washes alone (3X wash). Results were normalized such that 0% represented the response to ECS buffer only and 100% was the maximum response to GABA. Sweeps corresponding to the concentration curve (left) are shown on the right. 37

Figure 29. Holding Voltage Changes Compounds were co-applied with 400 nM GABA, the approximate EC_{20} identified by the GABA concentration curve shown in **Figure 18**. Responses were normalized such that the response to GABA alone was 100% (A) Holding voltage during data acquisition was set to -80 mV, the standard previously used for all GABA_AR stable cell lines. (B) Holding voltage was changed to -70 mV during data acquisition. 38

Figure 30. Effects of Physiological Temperature Compounds were co-applied with 400 nM GABA, the approximate EC_{20} determined by the GABA concentration response. Responses were normalized such that the response to GABA alone was 100%. (A) Concentration responses of four novel imidazodiazepines at room temperature. (B) Sweeps for GL-II-75 corresponding to the concentration response curve in A. (C) Concentration responses of four novel imidazodiazepines at 37°C, physiological temperature. (B) Sweeps for GL-II-75 corresponding to the concentration response curve in C. 39

Figure 31. Testing $\alpha 5\beta 3\gamma 2$ Standards Using Buffers with Varying Chloride Concentrations The $\alpha 5\beta 3\gamma 2$ stable cell line was tested with standard buffers (A-B) and new buffers that altered the internal and external chloride concentrations (C-D). Responses were normalized such that the response to GABA alone

was 100% (A,C) and representative sweeps are displayed for SH053-2'F-R-053, a compound selective for receptors containing $\alpha 5$ subunits (B,D). 41

Figure 32. Standard Buffers vs. IonFlux Buffers The $\alpha 3\beta 3\gamma 2$ stable cell line was tested with standard buffers (A-B) and IonFlux buffers (C-D), the composition of which can be found in **Table 5**. Responses were normalized such that the response to GABA alone was 100% (A,C) and representative sweeps are displayed for SH053-2'F-R-053, a compound selective for receptors containing $\alpha 5$ subunits (B,D)..... 43

Figure 33. Differences in Buffer Recipes from Yuan⁸⁴ The $\alpha 1\beta 3\gamma 2$ cell line was tested in GABA concentration response with the buffers described in **Table 6**. The results were normalized such that 0% represented the response to ECS alone and 100% was the maximum response to GABA. Sweeps corresponding to the concentration curve (left) are shown on the right. 44

Figure 34. Addition of Inlet DMSO Patch clamp readings were taken with and without 0.1% DMSO added to inlet wells. The results were normalized such that 0% represented the response to ECS alone and 100% was the maximum response to GABA. Sweeps corresponding to the concentration curve (left) are shown on the right. 46

Figure 35. Increased Concentration of Initial GABA Application Initial concentration of GABA was increased from 0.43 μ M (A-B) to 1 μ M (C-D). Responses were normalized such that the response to GABA alone was 100% (A,C) and representative sweeps are displayed for XHE-III-74 (B,D). 47

Figure 36. Compound Protocol Changes to Shorten Assay Time The $\alpha 1\beta 3\gamma 2$ cell line was tested in GABA concentration response with the 2X protocol, which applied two rounds of each compound solution and the 6X2X protocol, which applied six applications of the first compound solution and two applications of the remaining solutions. The results were normalized such that 0% represented the response to ECS alone and 100% was the maximum response to GABA. Sweeps corresponding to the concentration curve (left) are shown on the right..... 48

Figure 37. Structure of RJ-02-50 that combines the ethyl ester functionality of XHE-III-74 Ethyl Ester with the increased hydrophilicity of XHE-III-74 Acid to generate a new lead compound. RJ-02-50 was synthesized by Rajwana Jahan of the James Cook Lab.²³ 54

Figure 38. Subtype Selectivity of RJ-02-50 Compound was co-applied with 400 nM with the $\alpha1\beta3\gamma2$ cell line and 600nM with the $\alpha4\beta3\gamma2$ cell line. Left: Responses were normalized such that 100% represented the response to GABA alone. Right: Sweeps graphs depict the current responses to 3 second applications of the respective concentrations. 55

Figure 39. Structure of MRS-01-66 which was synthesized through published routes by Michael Rajesh Stephen of the James Cook Lab.⁷² 55

Figure 40. Subtype Selectivity of MRS-01-66 Compound was co-applied with 400 nM with the $\alpha1\beta3\gamma2$ cell line and 800 nM with the $\alpha4\beta3\gamma2$ cell line. Left: Responses were normalized such that 100% represented the response to GABA alone. Right: Sweeps graphs depict the current responses to 3 second applications of the respective concentrations. 56

Figure 41. Structure of MIDD0301 which was synthesized by Guanguan Li of the James Cook lab according to a published procedure.²⁴ 56

Figure 42. MIDD0301 Response in the $\alpha4\beta3\gamma2$ Stable Cell Line Compound was co-applied with 600nM. Left: Responses were normalized such that 100% represented the response to GABA alone. Right: Sweeps graphs depict the current responses to 3 second applications of the respective concentrations..... 57

Figure 43. Compounds Designed to be $\alpha2$ Selective to Treat Depression and Anxiety Compounds were synthesized according to published routes by Guanguan Li.⁶⁸ (A) GL-II-74 (B) GL-II-74 (C) GL-II-75 (D) GL-II-76 58

Figure 44. Electrophysiological Response of Depression/Anxiety Compounds in $\alpha1\beta3\gamma2$ Stable Cell Line Compounds were co-applied with 600 nM GABA in three second applications..... 59

Figure 45. Structure of MQ-DS This ratiometric dye produces dual fluorescence emissions with a single excitation at 405 nm. The methoxyquinolinium group (blue) emits at 440 nm and decreases in signal as chloride concentration increases. The dansyl group (red) emits at 560 nm and is insensitive to chloride ions, providing a baseline on which to normalize the response of the methoxyquinolinium group (F_{560}/F_{440}).
..... 61

Figure 46. Mice running on the RotaRod Apparatus The RotaRod apparatus has individual compartments for each mouse to maintain the animal’s focus. The area beneath the rod is enclosed to contain the animals if they fall. The rod is high enough to encourage the animals to stay on the rod, but not so high as to cause injury if they do fall. 64

Figure 47. Initial RotaRod Studies with Male BALB/c Mice (A) Trained mice (n = 8) were placed on the RotaRod set at a constant speed of 15 RPM. Results are presented as the percent success rate. (B) Structure of Diazepam (Valium®), which was used as a positive control. (C) Structure of XHE-III-74 Acid (D) Structure of XHE-III-74 Ethyl Ester (EE). 66

Figure 48. RotaRod Controls with Female Swiss Webster Mice Trained mice (n = 10) were placed on the RotaRod set at a constant speed of 15 RPM at various time points post-injection. Vehicle only was used as a negative control, and 5 mg/kg diazepam was used as a positive control. All compounds were administered i.p. 69

Figure 49. Asthma Compounds with Amide Functionality Compounds were synthesized according to a published procedure by Jahan et al.⁷² The table indicates the X and Y groups of the scaffold. 69

Figure 50. Rotatod Study of Imidazobenzodiazepines with Non-Amide Functionalities Trained mice (n = 10) were placed on the RotaRod set at a constant speed of 15 RPM at various time points. Vehicle only was used as a negative control, and 5 mg/kg diazepam was used as a positive control. All compounds were administered i.p. at 40 mg/kg. 70

Figure 51. Imidazobenzodiazepines with Non-Amide Functionalities Compounds were synthesized according to published routes by Jahan et al.⁷² (A) Structure of scaffold with indicated X and Y substituents in table to right. (B) Structure of KRM-II-68..... 71

Figure 52. RotaRod of Additional Asthma Compounds Trained mice (n = 10) were placed on the RotaRod set at a constant speed of 15 RPM. Vehicle only was used as a negative control, and 5 mg/kg diazepam was used as a positive control. All compounds were administered i.p.. Compounds that were not soluble at an initial concentration of 500 μ M in DMSO were excluded from testing because the resulting suspension was not injectable..... 72

Figure 53. Structures of Novel Imidazodiazepines Identified as Lead Compounds for Potential Asthma Treatments Two different scaffolds were utilized based on previously tested compounds that were determined to be α 4 (top) or α 5 (bottom) subtype selective GABA_AR modulators.^{109,110} 85

Figure 54. T-Lymphocytes contain GABA_AR mRNA mRNA was isolated from Jurkat T-lymphocytes and analyzed via RT-qPCR. Quantification was completed using QuantiFast SYBR green RT-qPCR kit. Cycle numbers from each subunit were normalized to GAPDH..... 86

Figure 55. GABA_AR on Lymphocytes are Functional Primary CD4⁺ T-Lymphocytes were isolated from spleens of male BALB/c mice via magnetic negative selection and utilized in the automated patch clamp assay. GABA was applied in concentrations ranging from 10nM to 1mM. Data were normalized such that 0 represents the response to 10nM GABA and 100 represents the response to 1mM GABA. 87

Figure 56. GABA_AR on Lymphocytes can be Modulated by Imidazodiazepines CD4⁺ T-Lymphocytes were isolated from male BALB/c mice via magnetic negative selection. The purified cells were utilized in the patch clamp assay, which tested concentrations of four novel imidazodiazepines ranging from 100nM to 30 μ M in combination with 600 nM GABA. Responses were normalized such that 100% represented the response to GABA alone. 88

Figure 57. Receptors are Still Activated by Modulators after Repeated In Vivo Dosing CD4⁺ T-Lymphocytes were isolated from male BALB/c mice via magnetic negative selection. The purified cells were utilized in the patch clamp assay, which tested concentrations of four novel imidazodiazepines ranging from 100nM to 30µM in combination with 600 nM GABA. Responses were normalized such that 100% represented the response to GABA alone. 89

Figure 58. Intracellular Calcium Levels are Reduced by Targeting GABA_AR Intracellular calcium levels were investigated with the Fluo-4 NW Calcium Assay. Jurkat T-lymphocytes were plated, treated 30 minutes prior to reading, and activated immediately before reading with 50ng/mL PMA and 1µg/mL PHA. Fluorescence (ex: 494 nm, em: 516 nm) was recorded over 5 minutes at 10 second intervals. Results were normalized such that 100% represents the maximum response in the activated cells. 90

Figure 59. Intracellular Calcium Response in the Presence of Imidazodiazepines Intracellular calcium levels were investigated with the Fluo-4 NW Calcium Assay. Jurkat T-lymphocytes were plated, treated 30 minutes prior to reading, and activated immediately before reading with 50ng/mL PMA and 1µg/mL PHA. Fluorescence (ex: 494 nm, em: 516 nm) was recorded over 5 minutes at 10 second intervals. Results were normalized such that 100% represents the maximum response in the activated cells. 91

Figure 60. IL-2 Production in the Presence of GABA Jurkat T-lymphocytes were activated with 50 ng/mL PMA and 1 µg/mL PHA, and treated with increasing concentrations of γ-aminobutyric acid (GABA) and incubated for 24 hours. Supernatant was analyzed with the BD Biosciences Human IL-2 ELISA kit. 91

Figure 61. Novel Imidazodiazepines Reduce Cytokine Production Jurkat T-lymphocytes were activated with 50ng/mL PMA and 1µg/mL PHA, and treated with XHE-III-74 Ethyl Ester (EE) and XHE-III-74 Acid (Acid) with and without 1mM GABA for 24 hours. Supernatant was analyzed with the BD Biosciences Human IL-2 ELISA kit. 92

Figure 62. Imidazodiazepines Do Not Reduce Inflammatory Cell Proliferation Splenocytes were isolated from asthmatic mice and cultured with 100 µg/mL of the allergen ovalbumin (A) or without the allergic

stimulus to control for toxicity (B). Cells were incubated in the presence of compounds (1μM) for 48 hours. ATP levels were quantified by the Cell Titer Glo kit as a measure of proliferation..... 93

Figure 63. GABA_AR Subunits in Primary Human Eosinophils Eosinophils were isolated from human blood using magnetic negative selection. mRNA was isolated and analyzed using RT-qPCR to identify GABA_AR subunits..... 97

Figure 64. Nitric Oxide Production in Response to Imidazodiazepines RAW264.7 Mouse Macrophages were activated with interferon γ (IFNγ) and lipopolysaccharide (LPS) and treated with 20μM of each compound for 24 hours. Supernatant was analyzed with the Griess Assay..... 97

Figure 65. Reduction of Nitric Oxide with MRS-III-90 RAW264.7 Mouse Macrophages were activated with interferon γ (IFNγ) and lipopolysaccharide (LPS) and treated with varying concentrations of MRS-III-90 in combination with 1 μM GABA for 24 hours. Half of the supernatant was removed and analyzed with the Griess Assay. ATP levels were quantified by the Cell Titer Glo kit as a measure of proliferation using the cells and remaining supernatant. 98

Figure 66. Structure of MP-III-080 MP-III-080 was synthesized by Mike Poe of the Prof. Cook Lab according to established routes.¹⁴³ 106

Figure 67. Rat Astrocytes Contain GABA_AR mRNA mRNA was isolated from DI TNC1 Rat Astrocytes and whole rat brain. 10 ng of mRNA was used to assess GABA_AR subunits in whole rat brain due to the expected high expression. 50 ng of mRNA was used for rat astrocytes due to unknown expression. Quantification was completed using QuantiFast SYBR green RT-qPCR kit. Cycle numbers for each subunit were normalized to GAPDH using the ΔC_t method. 109

Figure 68. GABA_AR on Rat Astrocytes are Functional Astrocytes were analyzed in the patch clamp assay with increasing concentrations of GABA ranging from 1 nM to 1 mM. Data were normalized such that 0 represented the response to ECS buffer only applications and 100 represents the response to 1 mM GABA. 110

Figure 69. Imidazodiazepines can Potentiate GABA-induced Currents in Rat Astrocytes MP-III-080 was co-applied with 10 nM GABA in concentrations ranging from 0.1 nM to 30 μ M. Responses were normalized such that 100 represented the response to 0.1 nM MP-III-080. 111

Figure 70. Structure of Lead Compounds for Neuropathic Pain Compounds were synthesized by Mike Poe and Guanguan Li of the Prof. Cook Lab according to established routes.^{143, 149} 114

Figure 71. GABA_AR on Human Microglia are Functional HMC3 Microglia were analyzed in the patch clamp assay with increasing concentrations of GABA ranging from 1 nM to 1 mM in IonFlux Buffers. Data were normalized such that 0 represented the response to 1 nM GABA applications and 100 represents the response to 1 mM GABA. 120

Figure 72. Imidazodiazepines can Potentiate GABA-induced Currents in HMC3 Human Microglia KRM-II-81 was co-applied with 100 nM GABA in concentrations ranging from 0.1 nM to 30 μ M in IonFlux Buffers. Responses were normalized such that 100 represented the response to 1 nM MP-III-080 applications. 121

Figure 73. Immortalized Human Microglia Contain GABA_AR mRNA mRNA was isolated from human microglia immortalized at Case Western University¹⁴⁵ and whole human brain. 10 ng of mRNA was used to assess GABA_AR subunits in whole brain due to the expected high expression. 50 ng of mRNA was used for microglia due to unknown expression. Quantification was completed using QuantiFast SYBR green RT-qPCR kit. Cycle numbers for each subunit were normalized to GAPDH using the Δ Ct method. 122

Figure 74. GABA_AR on Human Microglia are Functional Microglia were analyzed in the patch clamp assay with increasing concentrations of GABA ranging from 1 nM to 1 mM. Data were normalized such that 0 represented the response to ECS buffer only applications and 100 represents the response to 1 mM GABA. 122

Figure 75. Immortalized Mouse Microglia Contain GABA_AR mRNA mRNA was isolated from microglia immortalized at Case Western University¹⁴⁵ and whole mouse brain. 10 ng of mRNA was used to assess

GABA_AR subunits in whole mouse brain due to the expected high expression. 50 ng of mRNA was used for microglia due to unknown expression. Quantification was completed using QuantiFast SYBR green RT-qPCR kit. Cycle numbers for each subunit were normalized to GAPDH using the Δ Ct method..... 123

Figure 76. GABA_AR on Mouse Microglia are Functional Microglia were analyzed in the patch clamp assay with increasing concentrations of GABA ranging from 1 nM to 1 mM. Data were normalized such that 0 represented the response to ECS buffer only applications and 100 represents the response to 1 mM GABA. 124

Figure 77. Imidazodiazepines can Potentiate GABA-induced Currents in Microglia MP-III-080 was co-applied with 50 nM GABA in concentrations ranging from 0.1 nM to 30 μ M. Responses were normalized such that 100 represented the response to 1 nM MP-III-080 applications..... 125

Figure 78. Rotarod Performance of Mice Treated with MP-III-080 Mice were orally dosed with MP-III-080 at 40, 80, 100, 120, and 150 mg/kg and placed on the Rotarod apparatus at various time post-treatment to determine if MP-III-080 caused any detrimental sensorimotor effects. Data Courtesy of Alex Kehoe and Ian Luecke. 126

Figure 79. Intracellular Calcium Levels are Reduced by Targeting GABA_AR with MP-III-080 Intracellular calcium levels were investigated with the Fluo-4 NW Calcium Assay. Mouse Microglia were plated, treated 30 minutes prior to reading, and purigenic calcium channels were activated immediately before reading with 100 μ M ATP. Fluorescence (ex: 494 nm, em: 516 nm) was recorded over 3 minutes at 10 second intervals..... 128

Figure 80. MP-III-080 has no Effect on Nitric Oxide Production Mouse Microglia were activated with interferon γ (IFN γ) and lipopolysaccharide (LPS) and treated with 1 – 100 μ M of MP-III-080 for 24 hours. Supernatant was analyzed with the Griess Assay..... 129

Figure 81. First Round of Compound Screening Mouse Microglia were activated with LPS and IFN γ and treated with 1 μ M GABA co-applied with 50 μ M of compounds of interest for 24 hours. Half of the

supernatant was removed and analyzed with the Griess Assay. ATP levels were quantified by the Cell Titer Glo kit as a measure of toxicity using the cells and remaining supernatant. Data courtesy of Brandon Mikulsky. 130

Figure 82. Structures of Compounds that Reduced Nitric Oxide Compounds were synthesized by Mike Poe and Guanguan Li of the Prof. Cook Group according to established routes.^{143, 149} 130

Figure 83. Concentration Response of Compounds that Showed NO Reduction in Screening Assay Mouse Microglia were activated with LPS and IFN γ and treated with 1 μ M GABA co-applied with 1 nM - 50 μ M of compounds of interest for 24 hours. Half of the supernatant was removed and analyzed with the Griess Assay. ATP levels were quantified by the Cell Titer Glo kit as a measure of toxicity using the cells and remaining supernatant. Data courtesy of Brandon Mikulsky..... 131

Figure 84. Concentration Response of Compounds that Showed NO Reduction in Screening Assay in Mouse Macrophages RWA264.7 Mouse Macrophages were activated with LPS and IFN γ and treated with 1 μ M GABA co-applied with 100 nM - 50 μ M of compounds of interest for 24 hours. Half of the supernatant was removed and analyzed with the Griess Assay. ATP levels were quantified by the Cell Titer Glo kit as a measure of toxicity using the cells and remaining supernatant. 132

Figure 85. Cytotoxicity of MP-IV-010 Mouse Microglia were treated with 1 nM – 200 μ M of MP-IV-010 for 24 hours. Cytotoxicity was measured based on the cells’ metabolic reduction capabilities with the Cell Titer Blue Assay..... 132

Figure 86. Rotarod Performance of Mice Treated with MP-IV-010 Mice were orally dosed with MP-IV-010 at 40, 80, and 120 mg/kg and placed on the Rotarod apparatus at various time post-treatment to determine if MP-IV-010 caused any detrimental sensorimotor effects. Data Courtesy of Alex Kehoe and Ian Luecke. 133

Figure 87. PDSP Secondary Screening Data Dose dependent binding was determined for the κ Opioid receptor, the Sigma2 receptor, and the rat brain benzodiazepine site utilizing, Salvinorin A, Haloperidol, and Clonazepam respectively as positive controls. 135

Figure 88. Antagonizing the GABA_AR to Reverse NO Reduction Mouse Microglia were incubated for 24 hours with LPS and IFN γ , 1 μ M GABA, 50 μ M MP-IV-010, and maximum concentrations of antagonists determined by solubility in DMSO. Flumazenil was used to antagonize the benzodiazepine binding site on the GABA_AR, Picrotoxin was used to block the chloride channel of the GABA_AR, and Bicuculline inhibits the binding of GABA. Half of the supernatant was removed and analyzed with the Griess Assay. ATP levels were quantified by the Cell Titer Glo kit as a measure of toxicity using the cells and remaining supernatant. Data courtesy of Brandon Mikulsky..... 136

Figure 89. Antagonizing Other Receptors to Reverse NO Reduction Mouse Microglia were incubated for 24 hours with LPS and IFN γ , 1 μ M GABA, 50 μ M MP-IV-010, and maximum concentrations of antagonists determined by solubility in DMSO. PK-11195 antagonizes the peripheral benzodiazepine receptor (PBR) and Norbinaltorphimine antagonizes the κ Opioid Receptor (KOR). Half of the supernatant was removed and analyzed with the Griess Assay. ATP levels were quantified by the Cell Titer Glo kit as a measure of toxicity using the cells and remaining supernatant. Data courtesy of Brandon Mikulsky..... 137

Figure 90. Reducing Nitric Oxide Production through the Peripheral Benzodiazepine Receptor (PBR) Mouse Microglia were incubated for 24 hours with LPS and IFN γ . Cells were either treated with the PBR agonist 100 μ M 4'Chlorodiazepam or 1 μ M GABA with and without 50 μ M MP-IV-010, and. Half of the supernatant was removed and analyzed with the Griess Assay. ATP levels were quantified by the Cell Titer Glo kit as a measure of toxicity using the cells and remaining supernatant. Data courtesy of Brandon Mikulsky. 138

Figure 91. Intracellular Calcium Levels are Reduced by Targeting GABA_AR with MP-IV-010 Intracellular calcium levels were investigated with the Fluo-4 NW Calcium Assay. Mouse Microglia were plated, treated

30 minutes prior to reading, and purigenic calcium channels were activated immediately before reading with 100 μ M ATP. Fluorescence (ex: 494 nm, em: 516 nm) was recorded over 3 minutes at 10 second intervals..... 139

Figure 92. 24 Hour MP-IV-010 Treatment Does Not Reduce iNOS Transcription Mouse Microglia were activated for 24 hours with IFN γ and LPS and treated with 50 μ M MP-IV-010. mRNA was isolated and quantified using QuantiFast SYBR green RT-qPCR kit. Cycle numbers for each sample were normalized to GAPDH using the Δ Ct method..... 140

Figure 93. iNOS Activity after 24 Hour Treatment with MP-IV-010 Mouse Microglia were treated for 24 hours with IFN γ , LPS, and 50 μ M MP-IV-010. Protein was harvested and 100 μ g was incubated with cofactors and substrates from the Abcam iNOS Activity Assay kit to determine nitric oxide production by isolated iNOS..... 140

Figure 94. Nitric Oxide Production from MP-IV-010 Treated Protein Protein was isolated from Mouse Microglia activated with IFN γ and LPS. 100 μ g of protein was incubated with 50 μ M MP-IV-010 and cofactors and substrates from the Abcam iNOS Activity Assay kit for 2 hours before measurement..... 141

Figure 95. Second Round of Compound Screening Mouse Microglia were activated with LPS and IFN γ and treated with 1 μ M GABA co-applied with 10 μ M of compounds of interest for 24 hours. Half of the supernatant was removed and analyzed with the Griess Assay. ATP levels were quantified by the Cell Titer Glo kit as a measure of toxicity using the cells and remaining supernatant. 142

Figure 96. Structures of Compounds that Reduced Nitric Oxide Compounds were synthesized by Mike Poe and Guanguan Li of the Prof. Cook Lab according to established routes.^{143, 149} 143

Figure 97. Concentration Response of Compounds from Second Screening Assay in Mouse Microglia Mouse Microglia were activated with LPS and IFN γ and treated with 1 μ M GABA co-applied with 100 nM - 30 μ M of compounds of interest for 24 hours. Half of the supernatant was removed and analyzed with

the Griess Assay. ATP levels were quantified by the Cell Titer Glo kit as a measure of toxicity using the cells and remaining supernatant. 143

Figure 98. Second Round of Compound Screening in Mouse Macrophages RAW264.7 Mouse

Macrophages were activated with LPS and IFN γ and treated with 1 μ M GABA co-applied with 10 μ M of compounds of interest for 24 hours. Half of the supernatant was removed and analyzed with the Griess Assay. ATP levels were quantified by the Cell Titer Glo kit as a measure of toxicity using the cells and remaining supernatant. 144

Figure 99. Concentration Response of Compounds from Second Screening Assay in Mouse Macrophages

RWA264.7 Mouse Macrophages were activated with LPS and IFN γ and treated with 1 μ M GABA co-applied with 1 nM - 10 μ M of compounds of interest for 24 hours. Half of the supernatant was removed and analyzed with the Griess Assay. ATP levels were quantified by the Cell Titer Glo kit as a measure of toxicity using the cells and remaining supernatant..... 145

Figure 100. Rotarod Performance of Mice Treated with GL-IV-03 Mice were orally dosed with 40 mg/kg

GL-IV-03 and placed on the Rotarod apparatus at various time post-treatment to determine if GL-IV-03 caused any detrimental sensorimotor effects. Data Courtesy of Alex Kehoe and Ian Luecke..... 146

Figure 101. Rotarod Performance of Mice Treated with GL-IV-03 Mice were dosed I.P. with 10 or 40

mg/kg GL-IV-03 and placed on the Rotarod apparatus at various time post-treatment to determine if GL-IV-03 caused any detrimental sensorimotor effects. Data Courtesy of Nicolas Zahn. 146

Figure 102. GL-IV-03 Regulates iNOS Transcription Mouse Microglia were activated with IFN γ and LPS (A)

and treated with 10 μ M GL-IV-03 (G) for 3, 6, 12, 18, and 24 hours. mRNA was isolated and quantified using QuantiFast SYBR green RT-qPCR kit. Cycle numbers for each sample were normalized to GAPDH using the Δ Ct method. 147

Figure 103. GL-IV-03 Regulates iNOS Transcription at Early Time Points Mouse Microglia were activated

with IFN γ and LPS (A) and treated with 10 μ M GL-IV-03 (G) for 15 minutes, 1, 3, and 6 hours. mRNA was

isolated and quantified using QuantiFast SYBR green RT-qPCR kit. Cycle numbers for each sample were normalized to GAPDH using the ΔC_t method. 148

Figure 104. iNOS Protein Levels after 24 Hour Treatment with GL-IV-03 Mouse microglia were activated with IFN γ and LPS and treated with 10 μ M GL-IV-03 for 24 hours. Protein was extracted and analyzed with the Mouse iNOS ELISA kit from ABCAM. 148

LIST OF TABLES

Table 1. Distribution of GABA_AR Alpha Subunits in Human Tissues⁷⁷⁻⁷⁹	14
Table 2. Automated Patch Clamp Buffer Components	21
Table 3. Instrumental Settings for Patch Clamp Experiments	23
Table 4: Altering Chloride Concentration in ECS and ICS Buffers	40
Table 5. IonFlux Buffers	42
Table 6. Differences between Standard Recipe and Yuan’s Recipe for ECS Buffer⁸⁴	44
Table 7. Human GABA_AR Subunit qPCR Primers	80
Table 8. Automated Patch Clamp Buffer Components	82
Table 9. Instrumental Settings for Patch Clamp Experiments	83
Table 10. Rat GABA_AR Subunit RT-qPCR Primers	106
Table 11. Automated Patch Clamp Buffer Components	107
Table 12. Instrumental Settings for Patch Clamp Experiments	108
Table 13. Human GABA_AR Subunit qPCR Primers	113
Table 14. Mouse GABA_AR Subunit RT-qPCR Primers	114
Table 15. Automated Patch Clamp Buffer Components	115
Table 16. PDSP Primary Screening Data for MP-III-080	127
Table 17. PDSP Primary Screening Data for MP-IV-010	134

LIST OF ABBREVIATIONS

AHR: Airway Hyperresponsiveness

ASM: Airway Smooth Muscle

ATP: Adenosine Triphosphate

BALF: Bronchoalveolar Lavage Fluid

BCA: Bicinchoninic Acid

bp: base pair

BZP: Benzodiazepine

CFW: Swiss Webster (strain of mouse)

CNS: Central Nervous System

CRAC: Calcium Release Activated Channel

DMSO: Dimethyl Sulfoxide

DNA: Deoxyribonucleic Acid

EC: Effective Concentration

ECS: Extracellular Solution

EE: Ethyl Ester

ELISA: Enzyme-Linked Immunosorbent Assay

eNOS: Epithelial Nitric Oxide Synthase

FBS: Fetal Bovine Serum

GABA: γ -Aminobutyric Acid

GABA_AR: γ -Aminobutyric Acid Type A Receptor

GABA-T: γ -Aminobutyric Acid Transaminase

GAD: Glutamic Acid Decarboxylase

GAT: γ -Aminobutyric Acid Transporter

HIV: Human Immunodeficiency Virus

IACUC: Institutional Animal Care and Use Committee

IC: Inhibitory Concentration

ICS: Intracellular Solution

ICS: Inhaled Corticosteroids

IFN γ : Interferon- γ

IL: Interleukin

iNOS: Inducible Nitric Oxide Synthase

IP: Intraperitoneal

KOR: κ Opioid Receptor

LABA: Long-Acting Beta-Agonists

LPS: Lipopolysaccharide

MAPK: Mitogen-Activated Protein Kinase

MBP: Major Basic Protein

mRNA: Messenger Ribonucleic Acid

NIMH: National Institute of Mental Health

nNOS: Neuronal Nitric Oxide Synthase

NO: Nitric Oxide

NP: Neuropathic Pain

ns/n.s.: Not Significant

Ova: Ovalbumin

PBR: Peripheral Benzodiazepine Receptor

PBS: Phosphate Buffered Saline

PDSP: Psychoactive Drug Screening Program

PHA: Phytohaemagglutinin

PMA: Phorbol 12-Myristate 13-Acetate

PSI: Pounds per Square Inch

RBC: Red Blood Cell

RNA: Ribonucleic Acid

RPM: Rounds per Minute

RT-qPCR: Reverse Transcription Quantitative Polymerase Chain Reaction

SSADH: Succinic Semialdehyde Dehydrogenase

TNF β : Tumor Necrosis Factor β

UWM: University of Wisconsin – Milwaukee

ACKNOWLEDGEMENTS

First and foremost, I want to thank my advisor Dr. Leggy Arnold for welcoming me into his group, applying for grant after grant to fund my research, and advising me the last five years. I am a better scientist because of his encouragement to always go one step further and think outside the box. A doctoral advisor can make or break your graduate career, and I am grateful to have had such a supportive mentor.

I also want to thank my committee members, Dr. Douglas Stafford, Dr. Nicholas Silvaggi, Dr. David Frick, Dr. James Cook, and Dr. Mitchell Grayson. My research has greatly benefitted from their collective knowledge and opinions. Additional gratitude is extended to Dr. Stafford for his regular contributions to my research goals and additional support for major presentations and Dr. Frick for use of his thermocycler and imaging system.

Thank you to all my friends for understanding when I had nothing to talk about except cells or mice and feigning interest. An extra dose of gratitude goes out to my graduate school friends, who went above and beyond the conventional friendship duties to keep spirits and motivation high when stress was overwhelming, be great resources while teaching, and provide invaluable suggestions when discussing research.

I would not be where I am today without all of my incredible family. They say it takes a village to raise a child, and over the last year my family has really pulled together. I am very appreciative to my parents, my parents-in-law, my Grandma Janet, and my future sister-in-law Ally for many hours of babysitting to ensure that I had the time I needed to dedicate to my studies. I would also like to thank my brother, grandmas, and other extended family for their invaluable support and encouragement.

For the last twenty five years, my parents have been the greatest proponents of my education. They have woken up at 2 a.m. to do a paper route before work to help fund my undergraduate degree, tried to keep up with my ever evolving research project, and are always willing to lend an ear and encouragement when I need it most. I am truly blessed to have such amazing parents.

My greatest thanks goes to my husband, Mark and daughter, Charlotte. Mark is the most patient, level-headed, and encouraging person I know. He has been my rock to lean on through the inevitable failures and stress, but most importantly he celebrated my successes as if they were his own. He is an amazing father to our little girl; a fact I was thankful for while I spent evenings away finishing experiments and writing. Becoming a mother during graduate school was an added challenge, but one that opened many new doors for me. When I became discouraged, a few minutes watching Charlotte play would remind me to continue wondering about the world and the value of curiosity.

Last but not least, I need to thank two very special pets. Gus was the only mouse I ever knew that could endear himself so completely. After he was retired from RotaRod due to poor performance, he spent two blissful years entertaining and endlessly running on his saucer. Finally, thank you to my faithful pup Daphne. She spent many hours by my side as I analyzed data, reviewed literature, and wrote my dissertation.

CHAPTER 1

Introduction to the γ -Aminobutyric Acid A Receptor

1.1 γ -Aminobutyric Acid (GABA)

1.1.1 Discovery of GABA

γ -Aminobutyric Acid (GABA) was initially found in plants in the 1800's, where it was deemed part of the Krebs's Cycle.³⁵ It was then discovered to accumulate in the brain in large amounts, up to 1000 times greater than any neurotransmitter, in the 1950's.³⁶⁻³⁷ Eugene Roberts and Sam Frankel recognized it as the major amine in the brain through simple paper chromatograms and ninhydrin stains.³⁶⁻³⁷

It was not identified as an inhibitory neurotransmitter until a few years later when a compound, then called Substance I, inhibited crayfish neurons and was recognized as GABA.^{36, 38-39} GABA was initially questioned as a neurotransmitter because of the absence of rapid inactivation.⁴⁰⁻⁴¹ However, subsequent studies revealed that inactivation was achieved through rapid intracellular uptake⁴² and that GABA hyperpolarized neocortical neurons⁴³. From then on, GABA was classified as an inhibitory neurotransmitter.

1.1.2 Formation of GABA

GABA is formed through a pathway referred to the GABA shunt (**Figure 1**). The first step involves the formation of α -ketoglutarate from succinic semialdehyde through the Krebs cycle. The Krebs cycle related formation of GABA prompted the initial hypotheses that GABA plays a role in metabolism.³⁵ Subsequently, α -ketoglutarate is converted by GABA-transaminase (GABA-T) to glutamate in the mitochondria.⁴ Glutamate decarboxylase (GAD), which is found in the presynaptic terminals, converts glutamate into GABA.⁴ Two forms of GAD have been detected: GAD₆₅ and GAD₆₇.⁴ GAD₆₇ is constitutively producing GABA, whereas GAD₆₅ is activated in demand for additional GABA for neurotransmission.⁴⁴

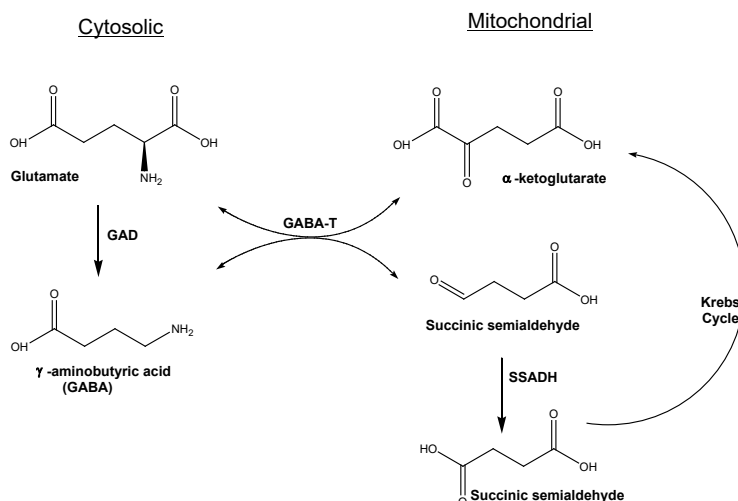


Figure 1. GABA Shunt GABA-T: GABA α -oxoglutarate transaminase, GAD: glutamic acid decarboxylase, SSADH: succinic semialdehyde dehydrogenase⁴

GABA is released into the synaptic cleft when presynaptic neurons are depolarized.⁴ After crossing the synaptic cleft and binding to receptors on the postsynaptic cell surface of receiving cells, GABA is up-taken by GABA transporter (GAT) to prevent spill-over to neighboring synapses.⁴⁵ This happens in light of the unfavorable concentration gradient, as the internal concentration of GABA is approximated to be 200 times higher than the external concentration.⁴ GABA is then either reused by neurons or converted to succinic semialdehyde by GABA-T to enter the Krebs Cycle.⁴ When glia uptake GABA, it is converted through the Krebs Cycle to glutamine, which can be used to generate GABA.⁴

1.2 The γ -Aminobutyric Acid A Receptor (GABA_AR)

1.2.1 Discovery of the GABA_AR

The receptors for GABA took three decades to identify. The first structure was suggested in 1990.⁴⁶ During that time, other neurotransmitter receptors such as the nicotinic acetylcholine, glycine, and 5HT₃ receptors, were discovered and found to exhibit significant sequence homology with the GABA_AR, especially in the ligand binding regions.⁴⁷ Together, this group of receptors would be known as the Cys loop ligand-gated ion channel superfamily.⁴⁸ Through functional and mutagenesis studies,

approximations were made as to where GABA and other modulators may bind, however these were not confirmed until the crystal structure of a GABA_AR was determined.⁴⁹⁻⁵⁰ In 2018, a heteropentameric GABA_AR structure was elucidated through high-resolution cryo-electron microscopy confirming the binding site of GABA and flumazenil, an allosteric modulator.⁴⁹

1.2.2 Structure of the GABA_AR

The GABA_AR is a heteropentameric, membrane bound receptor¹ formed from nineteen possible subunits (α 1–6, β 1–3, γ 1–3, δ , ϵ , π , θ , ρ 1-3).² From the cryo-electron microscopy structure (**Figure 2**), it was determined that each subunit had a similar structure consisting of an extracellular domain containing the signature cys loop and 10 β -strands in a β -sandwich, followed by four α -helices, which form the membrane bound ion channel.⁴⁹

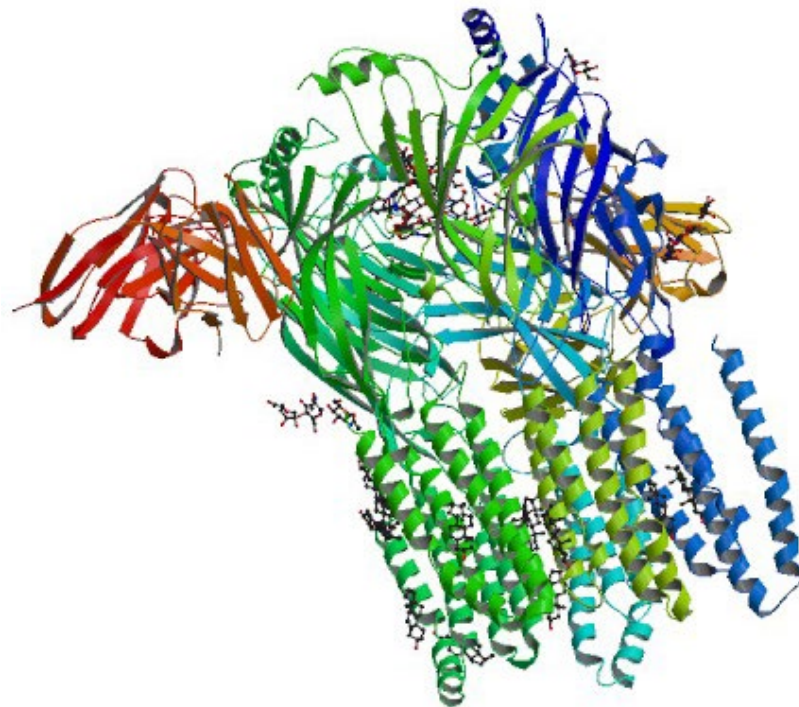


Figure 2. Cryo-electron microscopy structure of GABA_AR composed of α 1, β 2, and γ 2 subunits with GABA and Flumazenil bound as determined by Zhu et al.⁴⁹ In red and yellow are antibodies used for isolation of the protein. Accessed from the Protein Data Bank (PDB: 6D6U)

Classical GABA_ARs consist of two α , two β , and one tertiary subunit (γ or δ) (**Figure 3**).³ Expression of these subunits is very heterogeneous across cell and tissue types, and will be discussed further in **1.4 Distribution of GABAAR**.⁵¹ The receptor represented by cryo-electron microscopy structure is an $\alpha 1\beta 2\gamma 2$ receptor, the most common receptor in the brain.⁴⁹ The protein was isolated using monoclonal antibodies, which bound to the extracellular domain of the $\alpha 1$ subunits seen in red and yellow (**Figure 2**).⁴⁹

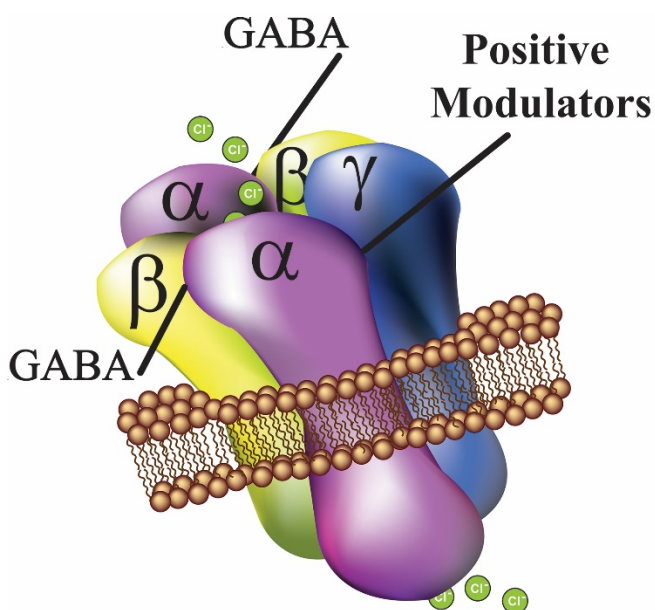


Figure 3. Structure of the GABA_AR A typical GABA_AR contains two α subunits, two β subunits, and one γ subunit, forming two extracellular binding sites between α and β subunits for the endogenous ligand GABA and one extracellular binding site between α and γ subunits for benzodiazepines.

GABA_ARs have many ligand binding sites that are targeted by a plethora of molecules, including GABA, pharmaceuticals, and drugs of abuse. These molecules will be further discussed in **1.3 Modulating the GABAAR**. Three main binding sites discussed herein are the GABA site, the chloride channel, and the benzodiazepine site, though binding sites for additional allosteric modulators such as neurosteroids, barbiturates, and ethanol are also part of the receptor.⁴⁻⁵

The intersections between α and β subunits form two binding sites for the endogenous ligand γ -aminobutyric acid (GABA).⁴⁻⁵ The structure confirmed GABA binding between the $\alpha 1$ and $\beta 2$ subunits of the isolated receptor.⁴⁹ Three tyrosine and one phenylalanine form an 'aromatic glove' that interact with the nitrogen of GABA (structure of GABA found in **Figure 1**).⁴⁹ An additional interaction between the carboxylate group on GABA and a threonine group further stabilizes the binding.⁴⁹

Flumazenil (**Figure 4**) was found between the $\alpha 1$ and $\gamma 2$ subunits on the extracellular side of the receptor as expected.⁴⁹ The molecule sits in the binding pocket with the fluorobenzene interacting with the $\alpha 1$ subunit and the ethyl ester with the $\gamma 2$ subunit.⁴⁹ A large number of aromatic residues form the benzodiazepine binding site, including a phenylalanine, two tyrosine, two serine, and one threonine from the alpha subunit and a phenylalanine, a tyrosine, and a threonine from the gamma subunit.⁴⁹ A histidine on the $\alpha 1$ subunit forms a hydrogen bond with the fluorine on Flumazenil, and this residue is conserved through $\alpha 1-3$ and $\alpha 5$ subunits.⁴⁹ $\alpha 4$ and $\alpha 6$ subunits contain an arginine residue at this position, which renders the receptor diazepam insensitive.⁴⁹

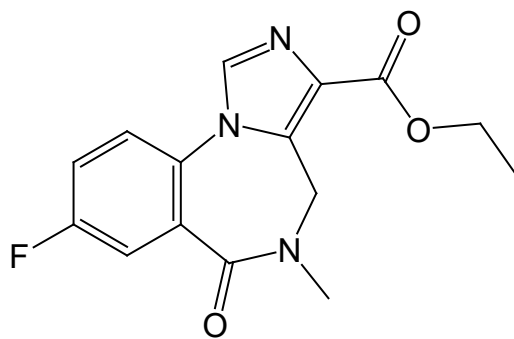


Figure 4. Structure of Flumazenil

1.3 Modulating the GABA_AR

1.3.1 The GABA Binding Site

Agonists

The GABA_A receptor can be activated by agonists other than endogenous ligands. Muscimol (**Figure 5**) is an isoxazole isolated from the psychoactive mushroom *Amanita muscaria* first discovered in the 1960's.⁵²⁻⁵³ It acts similarly to GABA because it has a highly similar structure, though conformationally restrained.⁵³ Muscimol's activity is fairly subtype-independent, however it acts as a "super agonist" at $\alpha 4$ -containing receptors.⁵³

Additional agonists were developed from the muscimol structure, including 4,5,6,7-tetrahydroisoxazolo(5,4-c)pyridine-3-ol (THIP) otherwise known as Gaboxadol (**Figure 5**).⁵³ Gaboxadol was investigated as a potential sleep aid, because of its unique dependence on the δ subunit being part of the GABA_AR⁵⁴, however its development was discontinued after it was determined to have limited efficacy and adverse psychiatric effects.⁵⁵

Gaboxadol is a super agonist at $\alpha 4$ -containing receptors, inducing nearly twice the response elicited by GABA or muscimol.⁵³ It is less potent however, with EC₅₀ values over 30 times higher than either GABA or muscimol.⁵³ Interestingly, GABA and muscimol binding was enhanced when diazepam was bound to the benzodiazepine site, however Gaboxadol binding was unaltered, supporting the idea that Gaboxadol is part of a different class of agonist despite the structural similarity.⁵⁶

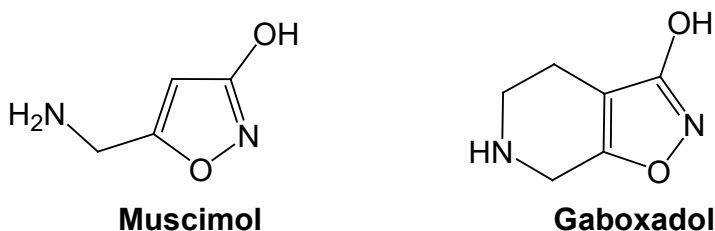


Figure 5. Structure of Muscimol and its derivative Gaboxadol

Antagonists

Bicuculline (**Figure 6**) is an alkaloid that was first characterized in 1970 as the first GABA_AR selective antagonist.⁵⁷ When the convulsant activities of bicuculline were evaluated, it was discovered that it had limited solubility and stability.^{52, 57} Bicuculline salts were generated, such as bicuculline methiodide or methochloride, however with limited success.⁵⁷ They are less selective and interact with other proteins resulting in confounding results.⁵⁷ GABA_AR subunit composition has little effect on bicuculline action, however $\alpha 6$ -containing receptors are slightly less sensitive.⁵⁸

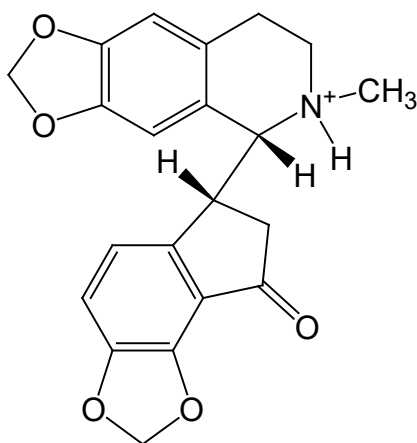


Figure 6. Structure of Bicuculline

Gabazine (**Figure 7**) is an additional GABA binding site antagonist, as proved by the reversal of its effects by muscimol⁵⁹ and mutational studies of the GABA binding site⁶⁰. It was introduced in 1986 after studies of arylaminopyridazine derivatives of GABA.⁵⁷ Though gabazine and bicuculline have similar mechanisms of action, they interact with different residues of the GABA binding site.⁵⁷ In comparison, gabazine is more potent with an IC₅₀ of 0.2 μ M compared to 0.9 μ M for bicuculline.⁶⁰

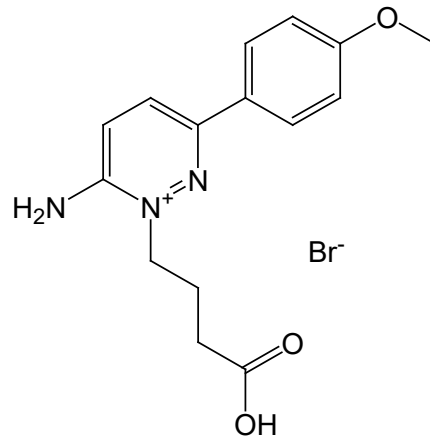


Figure 7. Structure of Gabazine

1.3.2 The Chloride Channel

Antagonists

Picrotoxin is a non-competitive antagonist of GABA_AR with universal efficacy isolated from moonseed plants.⁶¹⁻⁶² It is an equal mixture of picrotoxinin and picrotin (**Figure 8**), however picrotoxinin has been shown to be 30 times more potent than picrotin.⁶³ It is hypothesized that it binds within the chloride pore of GABA_ARs, interacting with one of the alpha helices bound in the cell membrane.⁶¹ Mutational studies suggest that picrotoxin binds in the region of V257 of the α 1 subunit.⁶⁴ While the fact that picrotoxin binds within the chloride channel is well known, the interactions are hypothesized based on structurally similar nicotinic acetylcholine receptors, which are homopentameric in contrast to GABA_AR, which are heteropentameric.⁶¹

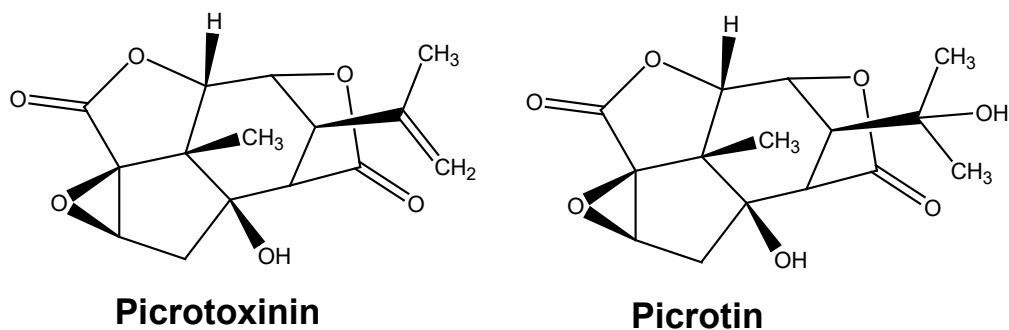


Figure 8. Structure of Picrotoxin Picrotoxin is an equal mixture of picrotoxinin and picrotin.

1.3.3 The Benzodiazepine Binding Site

Positive Allosteric Modulators

Benzodiazepines were discovered through clever molecular manipulation of benzheptodiazines, which were originally investigated in a search for new dyestuff.⁶⁵ However, after these compounds failed in their original purpose, they were investigated as potential tranquilizers because they were fairly unexplored, readily accessible, easily varied and transformed, offered interesting chemical problems, and “looked like” they could be biologically active.⁶⁵ After many years of trial, error, and failure, one compound (and its salt) stood out as being overlooked during a final cleaning and both were subsequently sent for biological testing. These tests confirmed improved muscle relaxant and anticonvulsant activities than chlorpromazine, the current standard of the day.⁶⁵

This compound was eventually approved by the FDA and was the first benzodiazepine on the market: Librium.⁶⁵ Three years later, diazepam was introduced to the market under the trade name Valium®.⁶⁵ Research into benzodiazepines soared, allowing researchers to better understand the structure-activity relationships. Numerous compounds began flooding the market, including clonazepam in 1975 and lorazepam in 1977.⁶⁵ Alprazolam and clonazepam were the 23rd and 38th most prescribed drugs in 2018.⁶⁶

More recently, knock-in mice have been developed that mutate specific residues in each α subunit.⁸ This allowed for pharmacological and behavioral studies that linked each α subtype to certain

physiological effects. These results are summarized in **Figure 9**. Many clinically relevant effects such as anxiolysis and muscle relaxation can be achieved though targeting the $\alpha 2$ or $\alpha 3$ subunit-containing GABA_AR, while avoiding the $\alpha 1$ subunit-containing GABA_AR can greatly reduce adverse effects such as unwanted amnesia or addiction.⁸

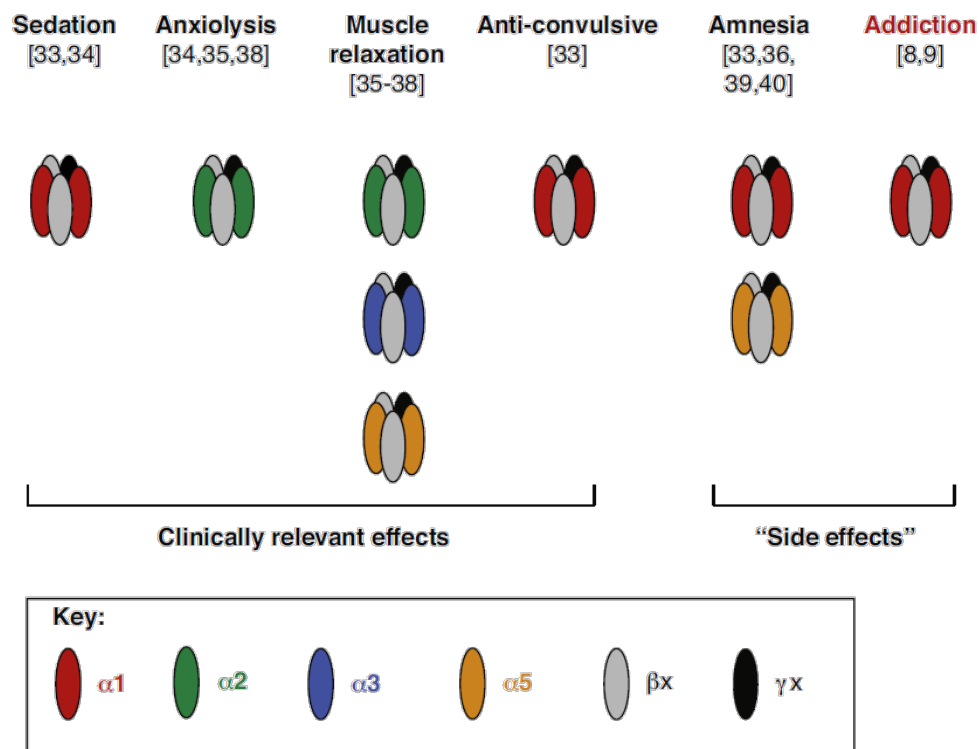


Figure 9. Subtype Specific Benzodiazepine Pharmacology Experiments with knock-in mice have allowed researchers to correlate GABA_AR subunits with pharmacological effects.⁸

To achieve subtype-selectivity of novel benzodiazepines, Professor James Cook developed a pharmacophore model to guide synthesis towards compounds that selectively bind at certain α subunit-containing GABA_AR.⁶⁷ This model has helped generate subtype selective imidazodiazepines targeting numerous diseases ranging from central nervous system diseases such as depression⁶⁸, schizophrenia⁶⁹, and neuropathic pain⁷⁰ to pulmonary diseases such as asthma^{23-24, 71-72}. Biological results pertaining to novel imidazodiazepines used for asthma and neuropathic pain will be discussed in Chapter 4 and 5, respectively.

Negative Allosteric Modulators

Flumazenil (**Figure 4**) is an imidazodiazepine that antagonizes α 1-3 and α 5-containing GABA_AR. Clinically, flumazenil is used to reverse the effects of benzodiazepines, such as diazepam-induced sedation, by competing for the benzodiazepine binding site.⁷³ Interestingly, flumazenil acts as a weak partial agonist for α 4/6-containing receptors.⁷⁴⁻⁷⁵

An analog of flumazenil, Ro15-4513 was first reported as a behavioral alcohol antagonist, as it reverses ethanol-enhanced GABA_AR currents through α 4/6 and δ -containing GABA_AR.⁶² Flumazenil is not capable of blocking the effects of ethanol though, and it is thought that the long nitrogen tail of Ro15-4513 blocks the ethanol binding site on the δ subunit, whereas the analogous fluorine on Flumazenil cannot.⁷⁶

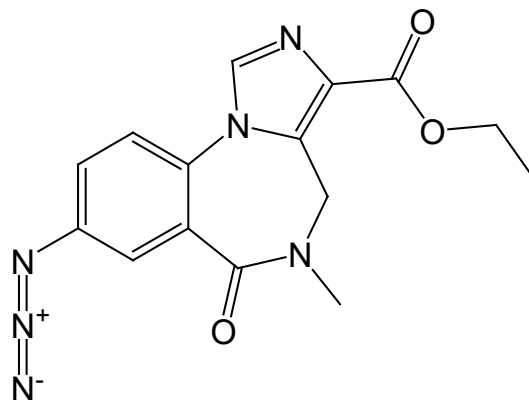


Figure 10. Structure of Ro15-4513

1.4 Distribution of GABA_AR

GABA_AR are highly expressed in the brain, where they mediate inhibitory neurotransmission. However, GABA_AR are being discovered in peripheral tissues as well, including lung, endocrine tissues, muscle tissues, lymphoid tissues, and bone marrow. **Table 1** contains excerpts from the Human Protein Atlas (www.proteinatlas.org), which collects information relating to the human proteome, including breakdowns of protein expression by tissue, cell, pathology, among other cellular effects.⁷⁷⁻⁷⁹

This project combines data from three individual projects: Human Protein Atlas, Genotype-Tissue Expression, and the FANTOM5 project, normalizes the expression determined in each project, and combines it for a composite look at expression displayed as a unitless normalized expression of RNA transcribed.

Table 1 shows the distribution of alpha subunits in various tissue types. In the brain, expression of alpha subunits varies widely by region. For example, the cerebral cortex has very high expression of α 1-3 and α 5 subunits, nearly three times higher than α 4 and fifty times as high as α 6 expression. However, α 6 expression is highly concentrated in the cerebellum, where it has a normalized concentration ten times higher than any other alpha subunit.

In contrast to the brain where normalized expression of alpha subunits can be as high as 96.4 normalized units, peripheral tissues have much lower GABA_AR expression, typically at normalized levels of approximately 1. The normalization procedure is complex and described at <https://www.proteinatlas.org/about/assays+annotation>. Individual cell types within these tissues have more distinct GABA_AR expression profiles and will be further discussed in Chapters 4 and 5.

Table 1. Distribution of GABA_AR Alpha Subunits in Human Tissues⁷⁷⁻⁷⁹

	Tissue Type	GABA _A R Subunit					
		α1	α2	α3	α4	α5	α6
Brain	Olfactory Region	22	31	10.5		15.2	0
	Cerebral Cortex	58.6	52.6	30.1	16.1	52.6	1.6
	Hippocampal Formation	10.5	38.9	10.9	1.9	20.9	0
	Amygdala	8.5	38.5	7.7	2.7	12	0
	Basal Ganglia	21.9	34.4	15.2	8.9	48.2	0
	Hypothalamus	8.8	7.7	15.9	1.4	6	0
	Thalamus	0	7.1	1.1		2	0
	Midbrain	6.7	3.7	4.7	1	2.3	0
	Pons and Medulla	7.4	10.5	6.2		1	2.6
	Cerebellum	35.2	10.4	1.3	0.3	0.1	96.4
	Corpus Callosum	1.8	4.9	3.3		0.8	0
	Spinal Cord	1.3	6.9	2.1	0	0.3	0.7
	Lung	Lung	1	1	0.7	0	0.8
Endocrine Tissues	Thyroid Gland	1	1.1	0.7	0	0.9	0
	Parathyroid Gland	1	0.9	0.6	0	0.7	0
	Adrenal Gland	2.6	1.3	0.7	0.1	0.8	0
	Pituitary Gland	0.1	0.6	0.9	0.2	0.1	0
Muscle Tissues	Heart Muscle	1	1	0.7	4	0.9	0
	Smooth Muscle	1	1.3	0.8	0	1.4	0
	Skeletal Muscle	1	1	0.8	0	0.7	0
Lymphoid Tissues	Thymus	0	0	0		1.3	0
	Appendix	1	1.4	0.6	0.1	0.8	0
	Spleen	1.1	2.3	0.7	0	0.8	0
	Lymph Node	1	1.4	0.7	0	0.8	0
	Tonsil	1.3	1.4	0.9	0	1.1	0
	Bone Marrow	1	1.2	0.7	0	0.8	0

Because tissues outside the brain have been shown to express GABA_AR, it makes them novel and attractive targets for new pharmaceuticals. The well-established pharmaceutical class of benzodiazepines can now be tailored to new targets and new diseases while maintaining the safety and efficacy of tried and true drugs. The work herein seeks to support the use of imidazodiazepines to target non-neuronal cell types in diseases such as asthma and neuropathic pain.

CHAPTER 2

Determining GABA_AR Subtype Selectivity of Novel Imidazodiazepines

2.1 Background

The γ -aminobutyric acid A receptor (GABA_AR) is a heteropentameric chloride ion channel that is found in the cell membrane and enables anions such as chloride to cross.¹ Endogenous γ aminobutyric acid (GABA) binds between the alpha and beta subunits of the receptor and opens the channel for ion transport.⁵ In addition, allosteric GABA_AR agonists such as benzodiazepines can bind between the alpha and gamma subunits and potentiate the GABA response.⁵

Six different GABA_AR alpha subunits exist, and their expression varies widely³. On neurons, the α 1 and γ 2 subunits are relatively ubiquitous, and have been shown to group with any of the three beta subunits to constitute a majority of neuronal GABA_ARs.⁵¹ In addition, delta and alternative gamma GABA_AR subunits can be part of a functional receptor in distinct brain locations.⁸⁰

Physiological effects of GABA_ARs follow a general pattern based on the alpha subunit that is present. Using knockout mouse models and subtype-selective GABA_AR modulators, it has been shown that α 1 containing GABA_AR mediate amnesia and addiction.⁸ These receptors are also responsible for clinically relevant effects, such as anti-convulsion and sedation.⁸ Anxiolysis and muscle relaxation are typically controlled through α 2, α 3, and α 5 containing GABA_AR receptors.^{80,8} Therefore, subtype-selective GABA_AR modulators can induce a specific pharmacological response.

Subtype-selectivity can also be exploited for targeting non-neuronal GABA_ARs, which have been recently characterized on peripheral cell types such as immune and smooth muscle cells. These cells exhibit a more distinct expression of GABA_AR subunits. For example, murine CD4⁺ T-Lymphocytes exhibited α 2, α 3, β 3, γ 3, and δ subunits⁹, whereas human airway smooth muscle displayed α 4, α 5, β 3, and γ 2 subunits.¹⁰ Variation of subunit expression also exists over the same cell type across species.⁸¹ Therefore, it is important to confirm the subtype-selectivity of a GABA_AR modulator to avoid adverse CNS effects and ensure the compound's ability to affect the cells of interest.

Assessing GABA_AR subtype selectivity is typically done by patch clamp with cells that are transiently transfected with GABA_AR subunits.^{82,71,23,24} Patch clamp was first described in 1976 by Neher and Sakmann as an adaptation of earlier voltage clamp methods⁸³, who were awarded the 1991 Nobel Prize in Physiology or Medicine. Briefly, they described that cytoplasmic readings could be obtained through a glass pipette with a 3-5 μM diameter end that was placed against a cell. Negative pressure was applied through the pipette to attain giga-ohm ($\text{G}\Omega$) seal and any current fluctuations through the channel within the section of membrane attached to the pipette could be measured.

Further alterations were made to this method, including different recording modes. Whole-cell recording utilizes the same technique, however, a brief but strong pulse of suction through the pipette after the $\text{G}\Omega$ seal ruptures the membrane and allows cytosolic replacement with a buffer. This improves the uniformity of the readings for membrane-bound channels that do not require any cytosolic factors⁸⁴.

Traditional patch clamp requires an intricate experimental set up to produce reliable results, including a stage, micromanipulators, a microscope, and electronics. The elaborate setup ensures that vibrations will not jostle the delicate seals⁸⁵. Other factors can also affect the quality of the data, such as the composition of intracellular and extracellular buffers. The ion concentrations should mimic the *in vivo* conditions to ensure proper ion channel function. Furthermore, pH and osmolarity are key constraints for patch clamp buffers. If a cell shrinks because of the buffer, the membrane will wrinkle and prevent a high-quality seal. If the cell expands too much the membrane will lyse⁸⁵.

2.2 Automated Patch Clamp

2.2.1 Instrumentation

Traditional patch clamp recordings are very time consuming and only reliable in the hands of skilled operators. Recent innovations have removed many of these barriers to gain access to high quality electrophysiological recordings through automation. Many types of automated patch clamp systems are

currently on the market, including Fluxion Bioscience's IonFlux. This system utilizes 96 or 384-well plates with built in microfluidic channels. Users only need to fill the plate with buffers, cell solution, and compounds of interest; the entire assay is automated.

The multi-well plates are divided into 12-well patterns (eight patterns in the 96-well plate). Each pattern contains an inlet for the cell solution, and outlet for waste collection, eight compound addition wells, and two traps that each contain twenty patch pipettes for data generation (**Figure 11**). A pneumatic interface seals to the top of the plates within the instrument to regulate pressure and vacuum and controlling the electrodes for data collection.

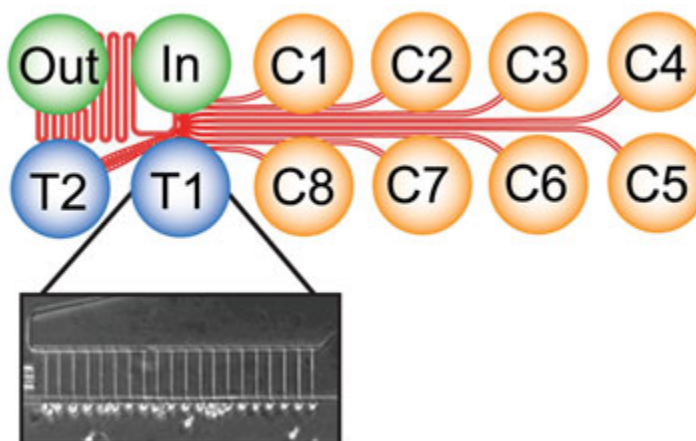


Figure 11. IonFlux Microplate Pattern consists of eight compound addition wells (C1-8), an inlet for cell suspension (in), an outlet for waste collection (out), and two traps (T1-2). Traps contain combs with twenty patch pipettes that seal to individual cells. Reprinted with permission from GEN.⁸⁶

Regular maintenance of the electrodes is necessary between experiments for successful patch clamp readings. Because the IonFlux utilizes Ag/AgCl electrodes, it is essential that the chloride ions on the electrodes be replenished frequently to avoid contact between the silver and proteins. This is simply done with frequent bleach soaks, followed by a PBS rinse before any experiments.

Once an IonFlux plate is prepared and inserted into the instrument, there are necessary steps to prepare the plate before the experiment. First, any remaining storage solution in the microfluidics needs to be replaced through positive pressure on all wells. Next, the cells need to be moved into the traps. Positive pressure is used again to move cells from the inlet into the traps, and negative pressure on the

traps attaches the cells to the patch pipettes. During this trapping period, the flow is repeatedly stopped for a brief moment to allow the negative pressure in the traps to patch the cells onto the pipettes. Finally, a brief but strong pulse of suction through the patch pipettes breaks the attached portion of membrane for the whole-cell patch clamp assay. At this point, data acquisition is possible.

2.2.2 Assay Format

Assay optimization had been performed by Nina Yuan, a previous graduate student in the Arnold Group.⁸⁴ Briefly, the original assay format from Fluxion suggested one well for GABA alone, one well for solvent alone, three wells for increasing concentrations of modulator alone, and three for increasing concentrations of modulator + GABA. Initially, GABA alone is applied. Next, modulator alone is applied followed by modulator + GABA. This would show that the modulator alone does not produce a response but when co-applied with GABA, the response would increase with increasing concentrations.

Due to limited space on the plate, however, this only allowed for three concentrations to be tested per plate, which is rather low throughput. Nina adjusted the protocol to allow for seven concentrations to be used per plate, sacrificing the modulator only wells. There are six initial applications of ECS (extracellular solution) for GABA concentration response experiments or EC₂₀ concentrations of GABA in ECS for modulator concentration response experiments to ensure a quality baseline reading. This was followed by two applications from each compound well C2-C8 contained increasing concentrations of GABA or increasing concentrations of modulator with EC₂₀ concentration of GABA for a concentration response curve (**Figure 12**).

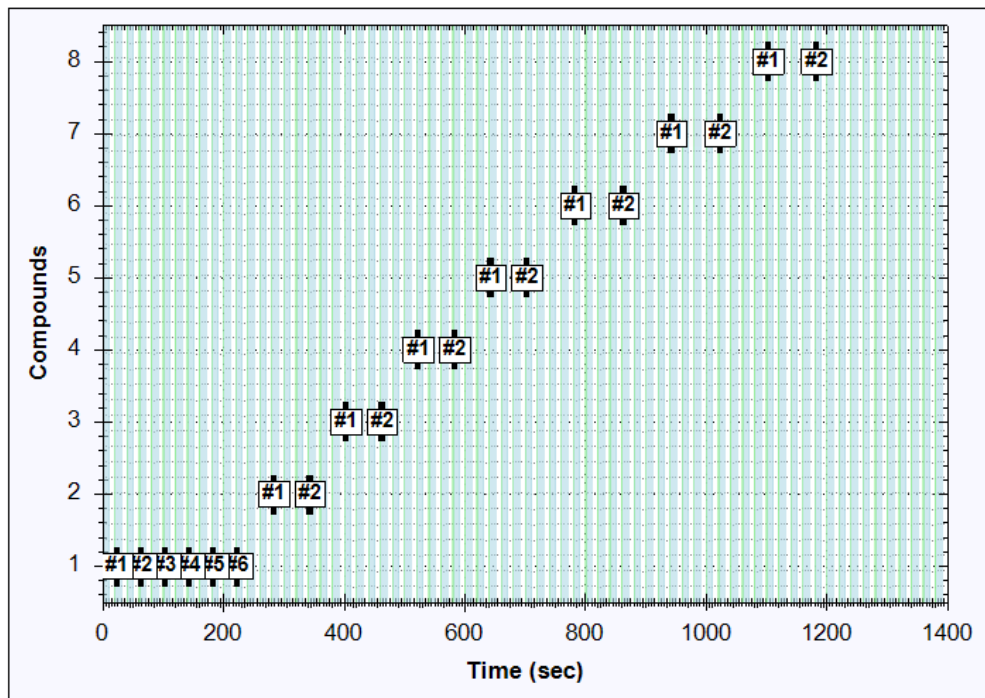


Figure 12. Compound Application Scheme A screenshot from the IonFlux control software showing the timing of compound applications. A brief washout period is permitted between 3 second applications. Six applications from compound well 1 is followed by a longer washout period before two applications each from compound wells 2-8. Washout times are increased as concentration increases to ensure total removal of the compound.

2.3 Stable Cell Line Patch Clamp

2.3.1 Experimental

Cell Culture

HEK293T stable cell lines expressing α 1-6, β 3, and γ 2 were generated by Nina Yuan.⁸⁴ The cells were maintained in DMEM/High Glucose (Hyclone, SH30243.01) supplemented with 10% heat-inactivated fetal bovine serum (Corning, 35011CV), 100 U/mL penicillin and 100 μ g/mL streptomycin (Hyclone, SV30010), and 300 μ g/mL hygromycin (Invitrogen, 10687-010). Cultures were incubated at 37°C and 5% CO₂ in T75 flasks (Thermo Scientific, 156499). Cells were passaged every 3-4 days or when cultures reached 90% confluency. Cells were passaged using 0.05% Trypsin (Hyclone, SH30236.01).

Buffers

All buffers were made with the following chemicals: NaCl (Fisher, BP358-1), KCl (Fisher, BP366-1), MgCl₂ (Sigma, M8266), CaCl₂ (Acros Org, 123350025), CsCl (Sigma, 203025), Glucose (Sigma, G0350500), HEPES (Fisher, BP410-500), and EGTA (Sigma, E4378). Buffers were filter sterilized before being stored in autoclaved glass bottles.

Table 2. Automated Patch Clamp Buffer Components

	ECS (M)	ICS (M)
NaCl	0.14	
KCl	0.005	
MgCl ₂	0.001	0.001
CaCl ₂	0.002	0.001
Glucose	0.005	
HEPES	0.01	0.01
KF		
EGTA		0.011
CsCl		0.14
pH	7.4	7.2

Automated Patch Clamp Electrophysiology

Electrodes were prepared through chlorination before experimentation each day. 300 μ L of bleach was dispensed into the solid bottom plate in columns 1, 2, 7, and 8. The preset ‘chloride’ protocol was run. After completion, the solid bottom plate was rinsed with deionized water and the same wells were filled with 300 μ L of calcium and magnesium free PBS (Hyclone, SH30256.01). The ‘hydrate’ protocol was run.

The IonFlux plate was gently rinsed three times with deionized water to remove any storage solution from the wells. 250 μ L of MilliQ water was dispensed into every well except the outlet, which received 50 μ L to allow space in the well to collect waste. The ‘water rinse’ protocol was run to ensure the storage solution was removed from the microfluidics. The water was emptied from the plate and dried well by lightly tapping the plate on a paper towel.

Experimental solutions were then distributed into the plate. 250 μ L of ICS was dispensed into each trap, 250 μ L of ECS into the inlet, and 50 μ L of ECS into the outlet to ensure the microfluidics remained wet. Compounds were first serially diluted in DMSO, then diluted into ECS to achieve the desired concentration with 0.1% DMSO. 250 μ L of each solution was dispensed into corresponding concentration wells. The 'prime' protocol was run.

Cells were harvested for patch clamp analysis using Detachin (Genlantis, T100100), which is gentler than traditional trypsin and therefore leaves membranes intact for higher quality seals with the patch pipet. Serum free media was used for three consecutive washes, followed by three additional washes with ECS. Cells were suspended in ECS at a final density of 5×10^6 cells/mL and 250 μ L was dispensed into each of the eight inlets.

There are four main parts to the experimental protocol: prime, trap, break, and data acquisition. During the prime phase, cell solution is moved from the inlet into the microfluidics. The trap phase moves the cells from the main channel to the patch pipettes. As the flow is quick to move the cells to the traps, brief pauses are necessary to allow the cells to attach to the pipettes. Twelve cycles of fast flow followed by a pause allows for multiple attempts to ensure all pipette tips are occupied. The break phase is responsible for breaking the membrane to allow for whole cell recording. A strong pulse of suction on the traps achieves this. Finally, the data acquisition phase can begin. Voltages and pressures for each phase of the experiment are detailed in **Table 3**.

Table 3. Instrumental Settings for Patch Clamp Experiments

		Pressure	Voltage
Prime	Main Channel	1 PSI, 45 s 0.4 PSI, 10 s	-80 mV, 50 ms -90 mV, 50 ms -80 mV, 50 ms
	Traps	6 PSI, 40 s 1.5 PSI, 15 s 2 PSI, 5 s	
	Compound Wells	6 PSI, 40 s 1.5 PSI, 15 s	
Trap	Main Channel	0.2 PSI, 2 s 0 PSI, 4.2 s 0.35 PSI, 0.8 s (repeat 12 times) 0.2 PSI, 8 s	-80 mV, 20 ms -100 mV, 30 ms
	Traps	5 PSI, 70 s	
	Compound Wells		
Break	Main Channel	0.05 PSI, 25 s	-80 mV, 50 ms -90 mV, 50 ms -80 mV, 50 ms
	Traps	5 PSI, 5 s 10 PSI, 15 s 5 PSI, 5 s	
	Compound Wells		
Data Acquisition	Main Channel	0.15 PSI for duration of experiment	-80 mV, 200 ms -80 mV, 200 ms -90 mV, 200 ms -80 mV, 9850 ms
	Traps	5 PSI for duration of experiment	
	Compound Wells		

Data Analysis

Data were exported to excel by concentration well. Because the IonFlux records over 5000 data points per compound application per trap, the data were cut down to 30 data points through averaging to allow for further processing. From there, it was reorganized from compound application into the eight patterns from the plate to generate concentration dependent sweeps and concentration response curves.

2.3.2 Results: GABA Concentration Responses

GABA concentration response curves were generated for five stable cell lines. The $\alpha 1\beta 3\gamma 2$ cell line was exposed to GABA concentrations ranging from 40nM to 30 μ M. The concentration response is depicted in **Figure 13** with an EC_{50} value of 2.319 μ M. This value was consistent with Nina's previously reported value of 3.41 μ M.⁸⁴ The maximum current was around -10,000 pA, which also consistent with previously determined values.

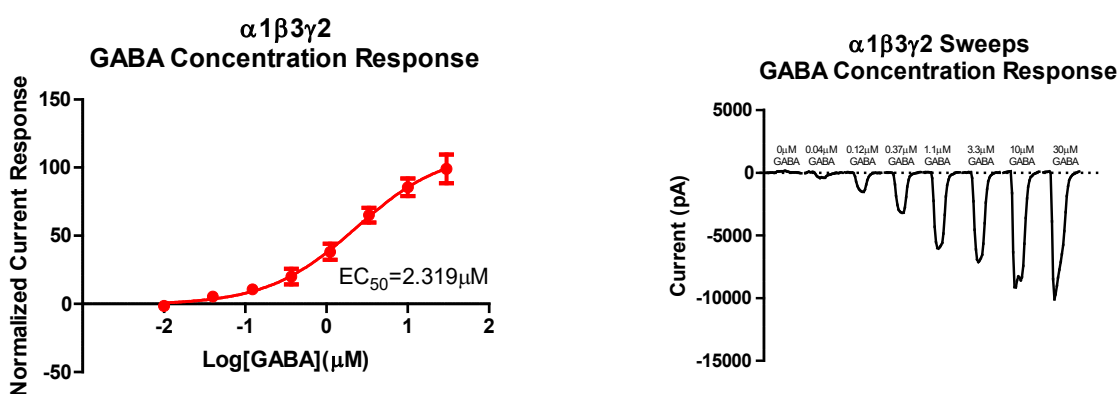


Figure 13. $\alpha 1\beta 3\gamma 2$ Stable Cell Line GABA Concentration Response Cells were patched and exposed to increasing concentrations of GABA. Results were normalized such that 0% represented the response to ECS buffer only and 100% was the maximum response to GABA.

The subsequent cell lines were exposed to GABA concentrations ranging from 1 nM to 1 mM to measure a larger concentration range. The concentration response for $\alpha 2\beta 3\gamma 2$ is depicted in **Figure 14** and an EC_{50} value of 2.224 μ M was calculated with a maximum current of response of approximately -1500 pA. Positive currents in the low concentrations were noted, however the results did not seem to be impacted as these values were consistent with previously reported experiments that determined the EC_{50} to be 1.07 μ M.⁸⁴ Troubleshooting for this issue is discussed in 2.3.4 *Troubleshooting*.

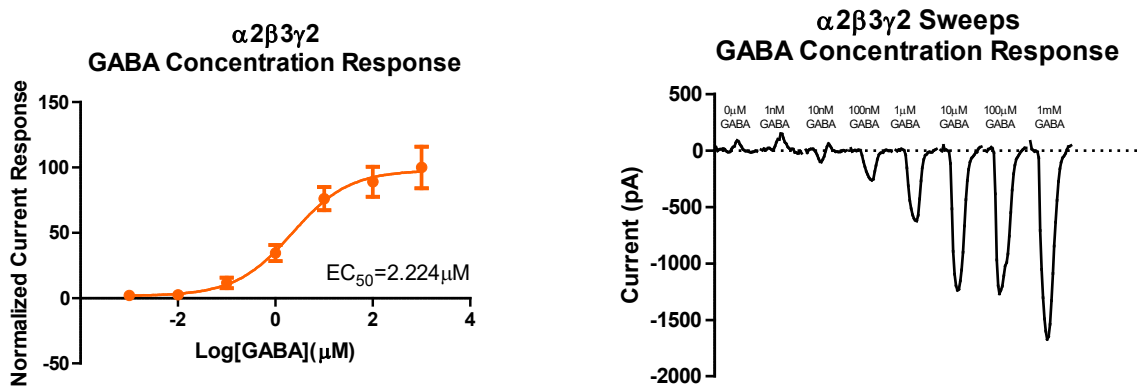


Figure 14. $\alpha 2\beta 3\gamma 2$ Stable Cell Line GABA Concentration Response Results were normalized such that 0% represented the response to ECS buffer only and 100% was the maximum response to GABA.

The $\alpha 3\beta 3\gamma 2$ cell line responded with an EC_{50} value of 2.205 μM and a maximum current of approximately -1000 pA (Figure 15), which was similar to the previously reported EC_{50} value of 1.05 μM .⁸⁴ Positive currents were again observed at lower concentrations and are addressed in 2.3.4 Troubleshooting.

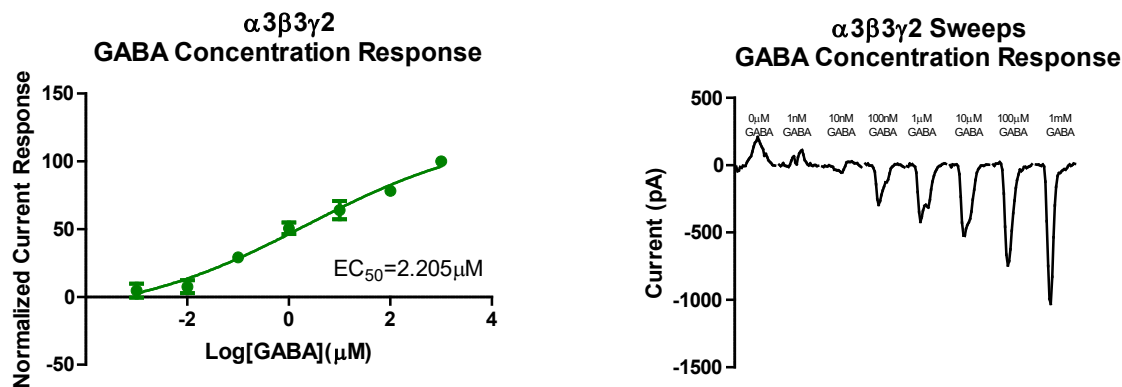


Figure 15. $\alpha 3\beta 3\gamma 2$ Stable Cell Line GABA Concentration Response Results were normalized such that 0% represented the response to ECS buffer only and 100% was the maximum response to GABA.

Figure 16 shows that the $\alpha 4\beta 3\gamma 2$ cell line responded with an EC_{50} value of 3.400 μM and a maximum current of approximately -2500 pA, which was again consistent to the previously reported value of 2.43 μM .⁸⁴ Positive currents were again a problem early in the experiment and are addressed in 2.3.4 Troubleshooting.

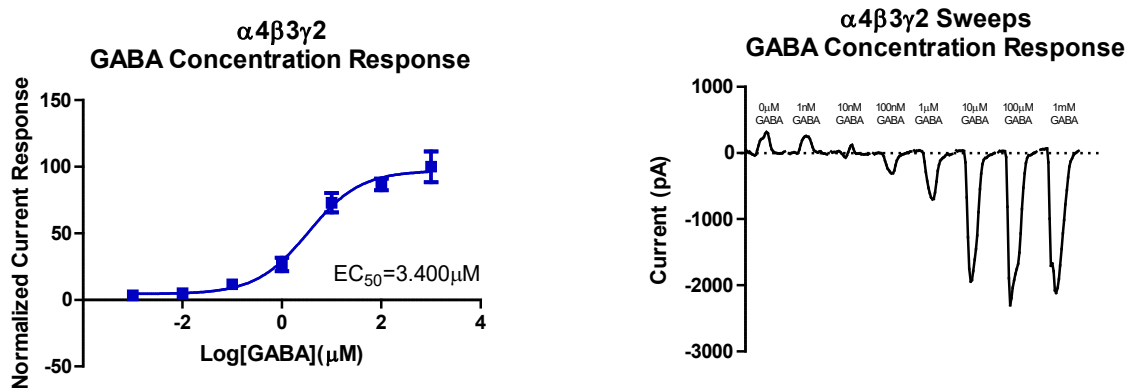


Figure 16. α4β3γ2 Stable Cell Line GABA Concentration Response Results were normalized such that 0% represented the response to ECS buffer only and 100% was the maximum response to GABA.

The α5β3γ2 cell line responded with an EC₅₀ value of 3.383 μM and a maximum current of approximately -2000 pA. The previously reported EC₅₀ value was 10.42 μM (**Figure 17**). Positive currents appeared in the ECS only and 1 nM concentration of GABA. Troubleshooting for these positive currents is addressed in 2.3.4 *Troubleshooting*.

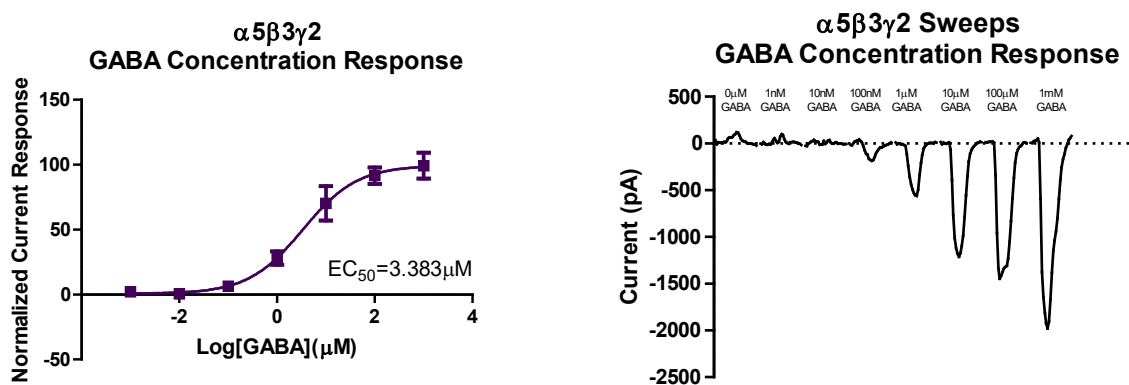


Figure 17. α5β3γ2 Stable Cell Line GABA Concentration Response Results were normalized such that 0% represented the response to ECS buffer only and 100% was the maximum response to GABA.

2.3.3 Results: Control Compounds

Because the stable cell lines were responding as expected to GABA, control compounds were tested for each cell line. Zolpidem is known to be a positive allosteric modulator of α1 subunit containing GABA_AR⁸⁷, and low activity has been reported with diazepam and Xhe-III-74^{87,75}. These compounds were

used in conjunction with Ro15-4513, which was used as a negative control as it has no reported activity at $\alpha 1$ subunit containing GABA_AR⁷⁵. These compounds were co-applied with an EC₂₀ concentration of GABA (400 nM). **Figure 18** shows that Zolpidem showed the greatest efficacy in the $\alpha 1\beta 3\gamma 2$ stable cell line as expected with a maximum potentiation of 250%, EC₅₀ value of 18.9 nM, and maximum current of -2000 pA. Diazepam and XHE-III-74 both showed moderate responses as expected. Diazepam had a maximum potentiation of 232%, a calculated EC₅₀ value of 77.3nM and a maximum current of -1500 pA. XHE-III-74 had a maximum potentiation of 186%, an EC₅₀ of 23.1 nM with a maximum current of -1750 pA. Ro15-4513 responded slightly more than expected, with a maximum potentiation of 163%, an EC₅₀ of 43.1 nM and a maximum current of -1500 pA.

Standard deviations are noticeably high, especially at higher concentrations, which is due to a great amount of variability between the dual applications within and between traps. This issue was intended to be analyzed during troubleshooting, however the project never progressed to a point where it was feasible to begin looking at this problem.

It is also noted that amplitude of the current sweeps does not always seem to match the normalized response in the concentration response graph. This is due to great inconsistency in the response to GABA alone. For instance, one trap reported a response of -90 pA when 400 nM GABA was applied, but another reported a response of -2000 pA. The GABA alone response is used as the baseline for normalization. Therefore, when wells were excluded for lack of response or electrophysiological abnormalities, the averaged responses that compose the sweep are disproportionately affected compared to the percent potentiation graph, especially in the later compound applications as the cells were prone to cease responding. Even though there were problems noted, the expected general trend was seen, so the $\alpha 1\beta 3\gamma 2$ stable cell line was deemed worthy for further studies.

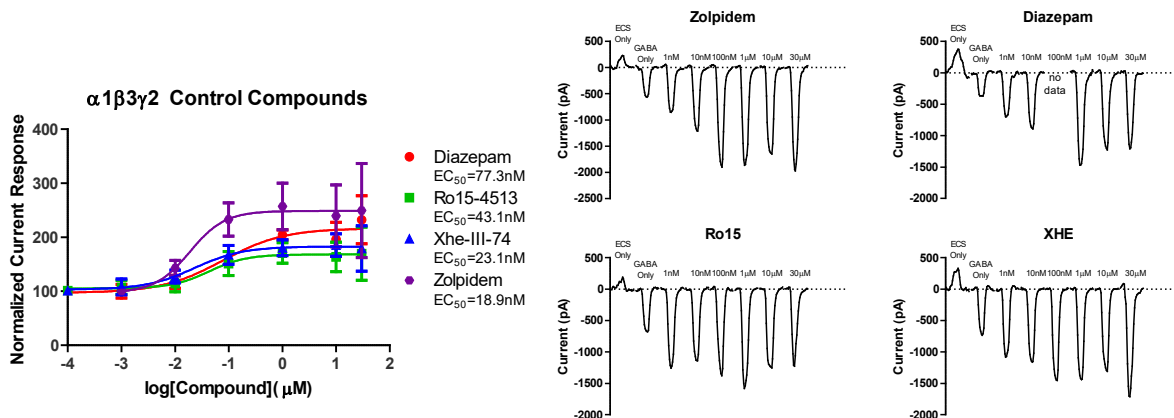


Figure 18. α1β3γ2 Control Compound Responses Compounds were co-applied with 400nM GABA, the approximate EC₂₀ value determined by the GABA concentration response. Left: Responses were normalized such that 100% represented the response to GABA alone. Right: Sweeps graphs depict the current responses to 3 second applications of the respective concentrations.

The α2β3γ2 cell line was tested with Diazepam, XHE-III-74, and Ro15-4513 co-applied with 1 μM GABA (**Figure 19**). The concentration of GABA used is higher than the EC₂₀ in a failed attempt to reverse the positive currents seen with applications of GABA only. Of these compounds, diazepam is expected to be the most efficacious, as it is well published to target α2 and α3 containing GABA_AR^{75,87}. XHE-III-74 has low activity at α2 containing receptors⁷⁵ and Ro15-4513 was again used as a negative control⁷⁵.

While the expected general trend was again seen, there were significant issues with positive currents in the GABA only application, which will be further discussed in 2.3.4 *Troubleshooting*. This led to issues normalizing the responses with respect to GABA alone. It is because of these issues that the percent potentiation is much higher than expected. Because of the inconsistent response of the α2β3γ2 line to GABA, the line was deemed unreliable and not used to test novel imidazodiazepines.

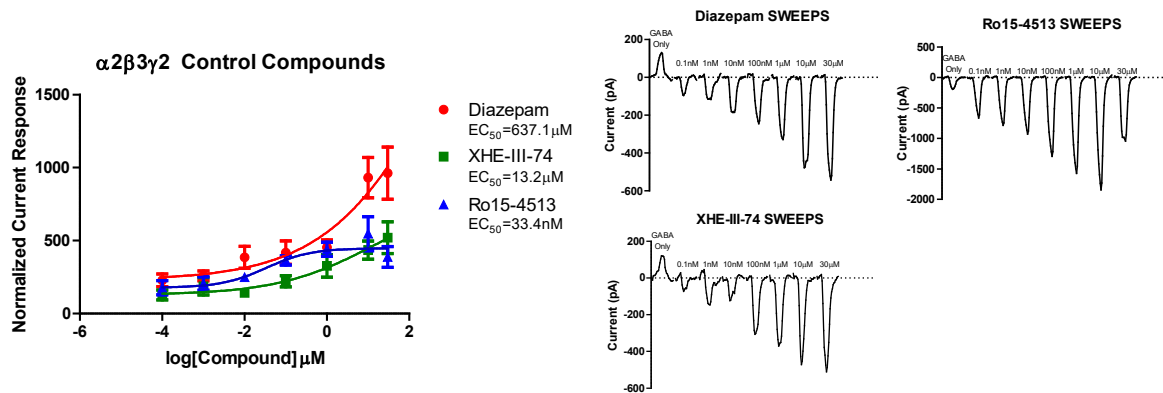


Figure 19. α2β3γ2 Control Compound Responses Compounds were co-applied with 1μM GABA. Left: Responses were normalized such that 100% represented the response to GABA alone. Right: Sweeps graphs depict the current responses to 3 second applications of the respective concentrations.

The α3β3γ2 cell line utilizes the same control compounds that have the same expected response trend, with diazepam being the highest, XHE-III-74 having a low response, and Ro15-4513 being utilized as a negative control.^{87,75} These compounds were co-applied with 430 nM GABA, the EC₂₀ determined by previous concentration responses. The results are depicted in **Figure 20**.

Highly inconsistent responses were seen with the initial application of ECS only, with maximum current responses ranging from -500 pA to 500 pA. The GABA only application is more consistent than the ECS application within the experiment, with responses ranging from -70 pA to 150 pA, however it was again inconsistent with the GABA concentration response. According to the concentration response, currents of approximately -500 pA would be expected. Because of these irregularities, the α3β3γ2 cell line was not utilized in determining subtype selectivity for novel imidazodiazepines.

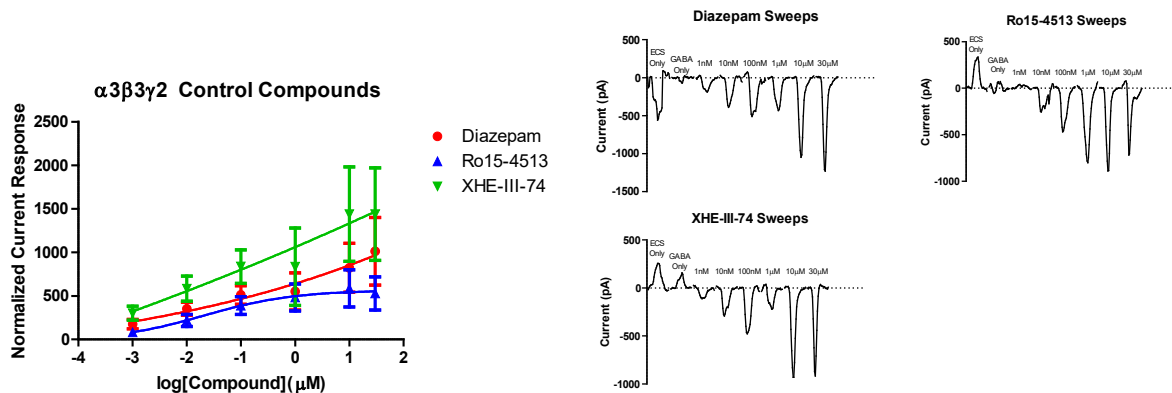


Figure 20. $\alpha 3\beta 3\gamma 2$ Control Compound Responses Compounds were co-applied with 430 nM GABA, the approximate EC_{20} value determined by the GABA concentration response. Left: Responses were normalized such that 100% represented the response to GABA alone. Right: Sweeps graphs depict the current responses to 3 second applications of the respective concentrations.

The $\alpha 4\beta 3\gamma 2$ cell line was tested using XHE-III-74, which was shown to be selective for $\alpha 4$ containing receptors⁷⁵ and Ro15-4513, which is selective for $\alpha 4$ containing GABA_AR but with lower efficacy.⁷⁶ $\alpha 4$ containing receptors are well known to be diazepam insensitive, so it was utilized as a negative control. Troubleshooting was carried out for this stable cell line (detailed in 2.3.4 *Troubleshooting*), however not all issues were overcome.

The best results for the $\alpha 4\beta 3\gamma 2$ control compounds after troubleshooting are shown in **Figure 21**. XHE-III-74 showed the highest response, with an EC_{50} of 69 nM, maximum current of approximately -1500 pA, and maximum potentiation of 2234%. Ro15-4513 showed the expected moderate response compared to XHE-III-74 with potentiation of 2039% and an EC_{50} of 57 nM and maximum current of 3000 pA. Diazepam showed the lowest response as expected at 938% potentiation with currents reaching -2500 pA and an EC_{50} of 75 nM.

The percent potentiation for these compounds overall is much higher than typically reported because the lack of response with the GABA only applications affected the normalization. Instead of normalizing to the GABA only application, normalization was based on the lowest concentration of modulator, with the assumption that no true modulation was occurring at such a low concentration.

Standard deviations are also noticeably high, which is due to a great amount of variability between the dual applications within and between traps. This issue was intended to be analyzed during troubleshooting, though the overall project never progressed to a point where it was feasible. When compared against each other, the trends between the compounds are as expected. The $\alpha 4\beta 3\gamma 2$ cell line was approved for further experiments with novel imidazodiazepines with additional troubleshooting planned to fine-tune the assay.

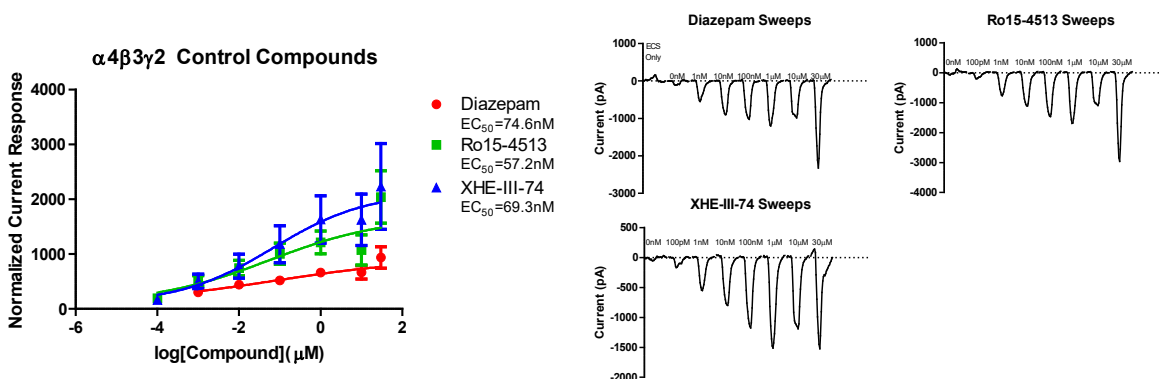


Figure 21. $\alpha 4\beta 3\gamma 2$ Control Compound Responses Compounds were co-applied with 600nM GABA, the approximate EC₂₀ value determined by the GABA concentration response. Left: Responses were normalized such that 100% represented the response to GABA alone. Right: Sweeps graphs depict the current responses to 3 second applications of the respective concentrations.

Many of the same problems that were observed for the $\alpha 2\beta 3\gamma 2$ and $\alpha 3\beta 3\gamma 2$ cell lines also affected the $\alpha 5\beta 3\gamma 2$ cell line (**Figure 22**). Positive currents were again seen in the GABA only applications and many of the lower concentrations of all compounds tested. Many troubleshooting measures were taken and are discussed in 2.3.4 *Troubleshooting*.

SH053-2'F-R-CH₃ is a known $\alpha 5\beta 3\gamma 2$ selective compound⁸⁷, however the maximum potentiation barely reached 300%, which is low considering diazepam was expected to have a moderately low response.^{87,75} Zolpidem and Ro15-4513 were expected to have baseline responses based on reported literature values.^{87,75,76} Given that the responses were inconsistent with both the GABA concentration curves previously discussed and literature responses, the $\alpha 5\beta 3\gamma 2$ was not utilized for future studies.

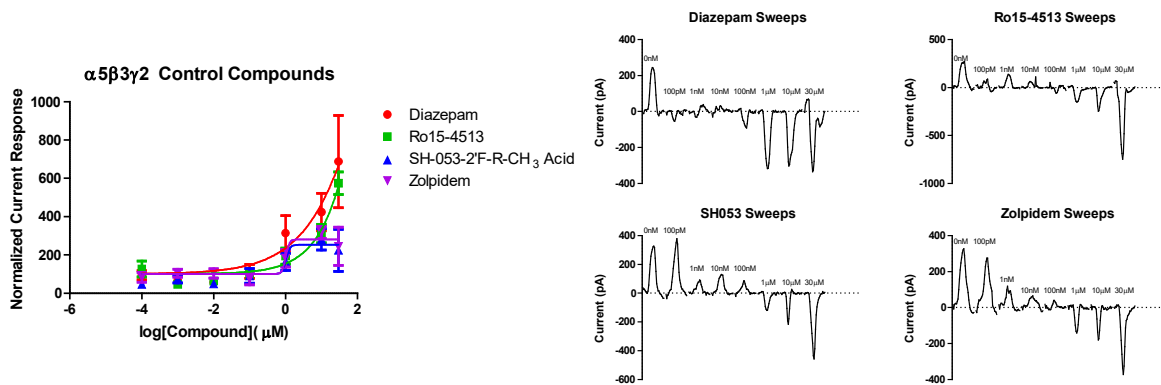


Figure 22. $\alpha 5\beta 3\gamma 2$ Control Compound Responses Compounds were co-applied with 600nM GABA, the approximate EC_{20} value determined by the GABA concentration response. Left: Responses were normalized such that 100% represented the response to GABA alone. Right: Sweeps graphs depict the current responses to 3 second applications of the respective concentrations.

2.3.4 Results: Troubleshooting

Stable Cell Line Changes

As work with the $\alpha 4\beta 3\gamma 2$ cell line began, it was clear that there were problems with the established line, clone 1 (CL1). High responses with diazepam were very unexpected and contrary to the literature. When the stable cell lines were generated, multiple clones were selected and tested as potential candidates.⁸⁴ In light of the issues, three other cell lines with high expression of each of the three subunits were selected and tested for insensitivity to diazepam along with CL1 for comparison.

As seen in **Figure 23**, all four clones responded similarly to increasing concentrations of GABA, however CL13 and CL17 had noticeably sigmoidal curves and similar EC_{50} values, whereas CL1 and CL5 did not.

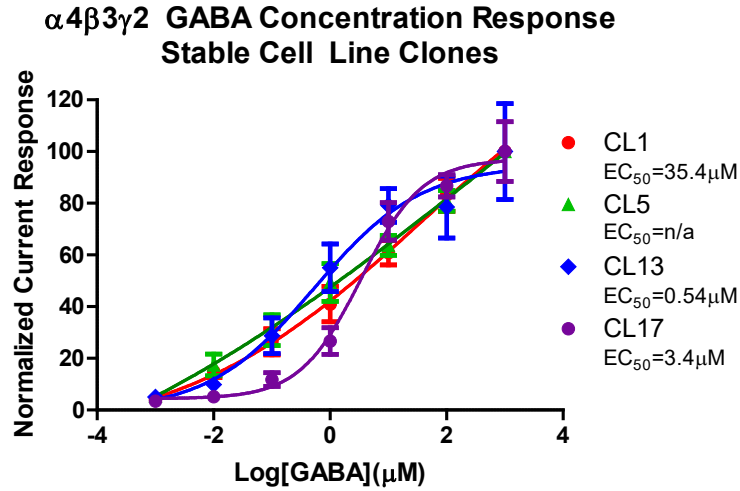


Figure 23. Clone Comparison in GABA Concentration Response Three new clones along with the established CL1 clone were tested in GABA Concentration Response. Results were normalized such that 0% represented the response to ECS buffer only and 100% was the maximum response to GABA.

All four lines were similarly tested with diazepam to identify any clones that were diazepam insensitive. CL1 and CL5 responded highly to diazepam applications, with potentiations of approximately 500% and 300% respectively (**Figure 24**). In contrast, CL13 and CL17 had much lower responses each with potentiations under 200%. These two clones were selected for further testing.

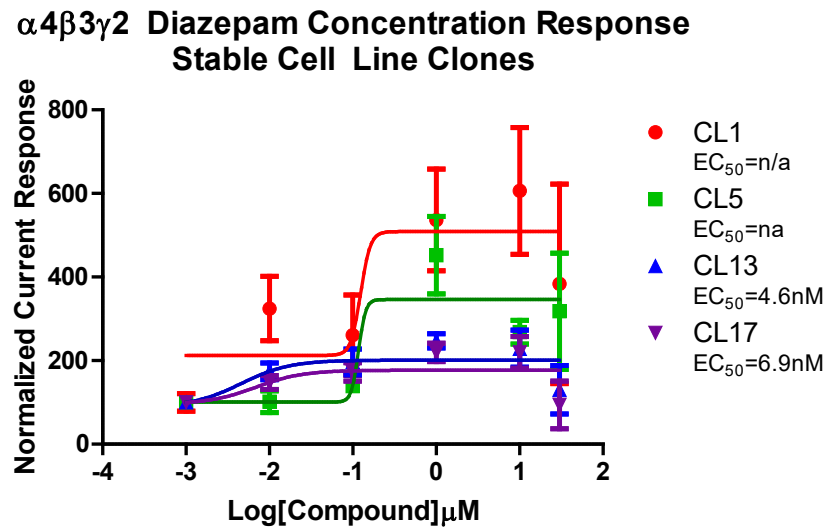


Figure 24. Clone Comparison in Diazepam Concentration Response Three new clones along with the established CL1 clone were tested in Diazepam Concentration Response. Diazepam was co-applied with 600 nM GABA, the approximate EC₂₀ as determined by the GABA Concentration Response. Responses were normalized such that 100% represented the response to GABA alone.

CL13 and CL17 were tested with XHE-III-74, Ro15-4513, and XHE-III-74, the three control compounds for the $\alpha 4\beta 3\gamma 2$ cell line (**Figure 25**). Both cell lines behaved similarly again, with maximum potentiations of approximately 300% for XHE-III-74, 200% for Ro15-4513. CL13 had a slightly higher response to diazepam at approximately 200% whereas CL17 responded to diazepam with potentiation around 175%. CL17 was chosen for future experiments.

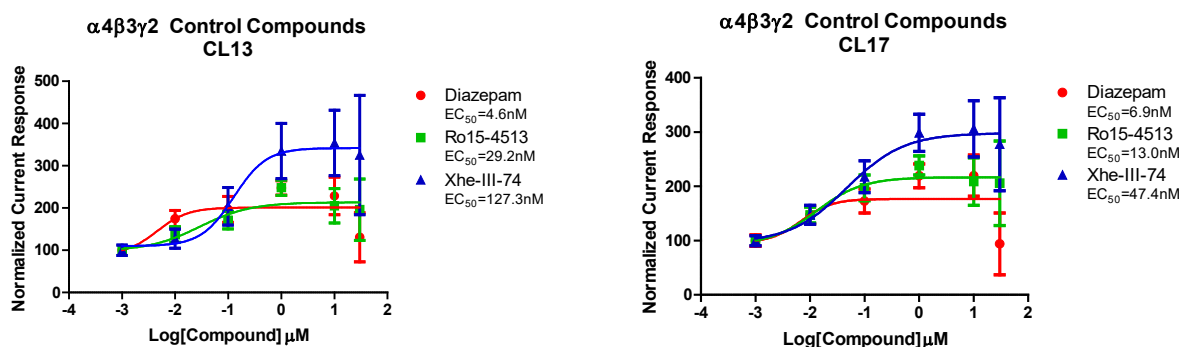


Figure 25. $\alpha 4\beta 3\gamma 2$ Control Compounds in CL13 and CL17 Compounds were co-applied with 600nM GABA, the approximate EC₂₀ as determined by the GABA Concentration Response. Responses were normalized such that 100% represented the response to GABA alone.

Cell Culture Modifications

Proper maintenance of the stable cell lines is essential for quality patch clamp experiments. The cell population needs to be homogenous in its high expression of GABA_AR and have strong, intact membranes to withstand the pressure changes and ensure a GΩ seal.

Poor responses to control compounds in the $\alpha 5\beta 3\gamma 2$ line prompted much troubleshooting, including culture changes. While positive currents were seen in initial applications of ECS only (data not shown), the more pressing issue was the lack of response to a known $\alpha 5\beta 3\gamma 2$ selective compound, SH053-2'F-R-CH₃ and the high response seen with Ro15-4513, a compound known to have no efficacy at $\alpha 5$ containing receptors.

To ensure optimal growth, non-essential amino acids were added to the media and matrigel was utilized to support attachment to the flask surface. Additionally, the selection antibiotic (hygromycin B)

concentration was increased from 100 $\mu\text{g}/\text{mL}$ to 300 $\mu\text{g}/\text{mL}$ to guarantee a homogenous population of cells with high expression of $\alpha 5\beta 3\gamma 2$ GABA_AR.

As **Figure 26** shows, these changes did not affect the cell line's response to SH053-2'F-R-CH₃, as the maximum potentiation remained at approximately 200%. The response to diazepam was reduced to be more in line with the expected low response, however the response to Ro15-4513 was not reduced to a level expected of a negative control, and the potentiation remained greater than 400%.

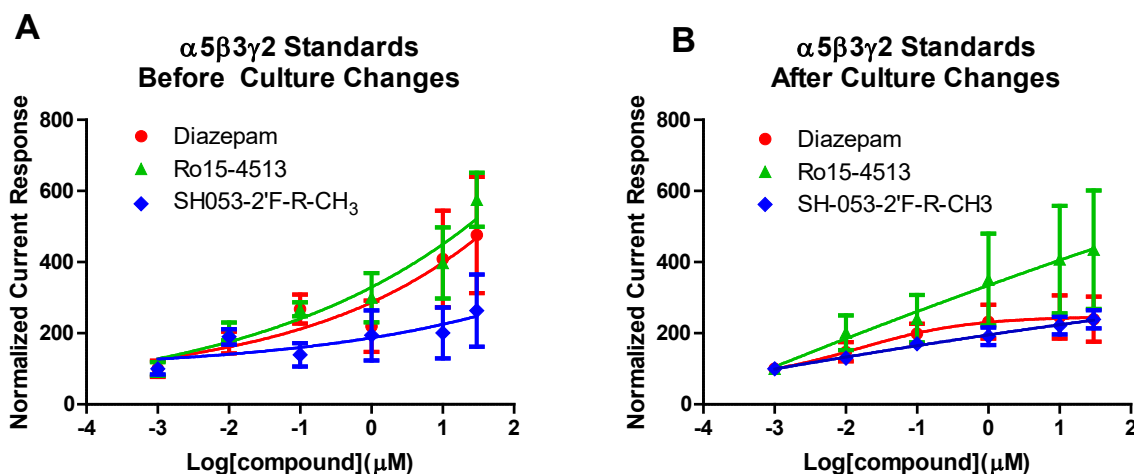


Figure 26. Cell Culture Changes Compounds were co-applied with 1.5 μM GABA and responses were normalized such that 100% represented the response to GABA alone. (A) Cells were cultured in DMEM High media with 100 $\mu\text{g}/\text{mL}$ of hygromycin. (B) Cells were cultured in DMEM High media with 300 $\mu\text{g}/\text{mL}$ of hygromycin and supplemented with non-essential amino acids. Cells were also cultured using matrigel.

Additional experiments investigated the effects of 500 $\mu\text{g}/\text{mL}$ hygromycin, though the results were still unchanged. Even though these culture changes did not affect the results for the $\alpha 5\beta 3\gamma 2$ cell line, the changes made were not detrimental to the cells and were therefore maintained to ensure high quality cells for all subsequent experiments.

Over time the quality of data seemed to be diminishing for unknown reasons. It was observed that the brand of flask used for cell culture was changed. **Figure 27** shows that regardless of the brand of flask used, the maximum current response and EC₅₀ were equal. The only difference seen between the two brands was the elimination of positive currents in the ECS only and 1nM applications when cells were

cultured in the Nunc EasY flasks. These flasks were utilized moving forward, however the positive currents did appear in other experiments regardless.

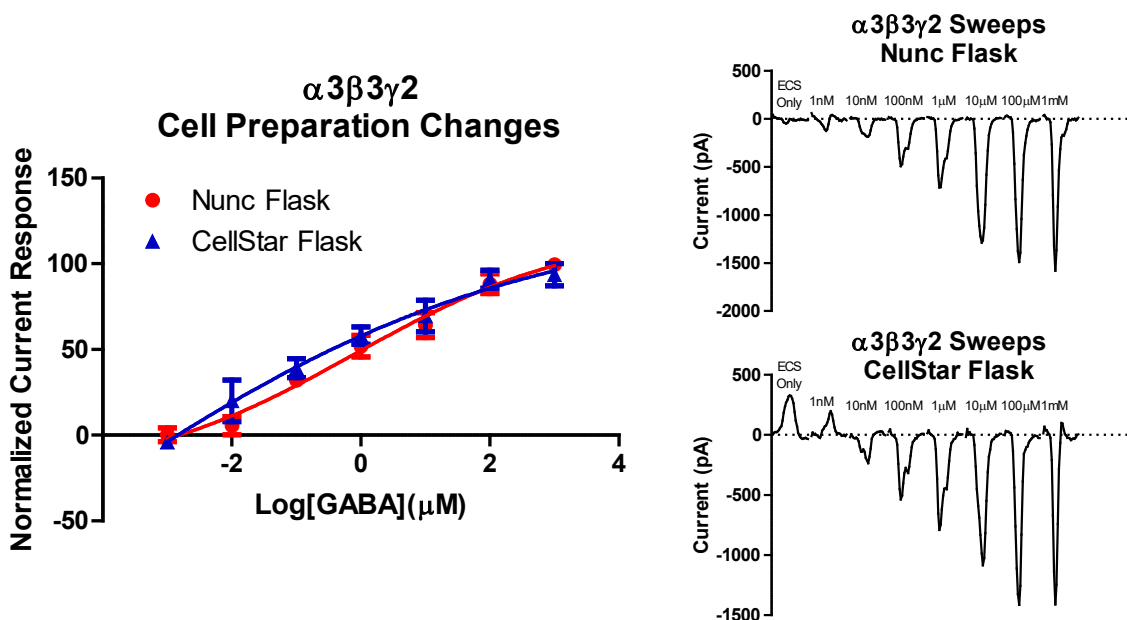


Figure 27. Brand Change for Cell Culture Flasks Cells were cultured in identical media in Nunc EasY flasks and CellStar Flasks. Results were normalized such that 0% represented the response to ECS buffer only and 100% was the maximum response to GABA. Sweeps corresponding to the concentration curve (left) are shown on the right.

Cell quality can also be affected during preparation for the experiment. Because patch clamp requires highly controlled buffers to measure current changes, cells need to be completely removed from media into ECS buffer. This requires multiple washes in blank media and ECS before cells are resuspended for the experiment. It was hypothesized that the current standard of three washes in blank media followed by three washes in ECS may be too hard on the cells.

The three blank media washes were removed in an effort to shorten the time the cells were in preparation before the experiment and to reduce the amount of centrifugation they underwent. The removal of blank media washes did not negatively impact the data, as the approximate EC_{50} and maximum potentiation remained unchanged (**Figure 28**). Moving forward, only three ECS washes were utilized to minimize the stress on the cells prior to experimentation.

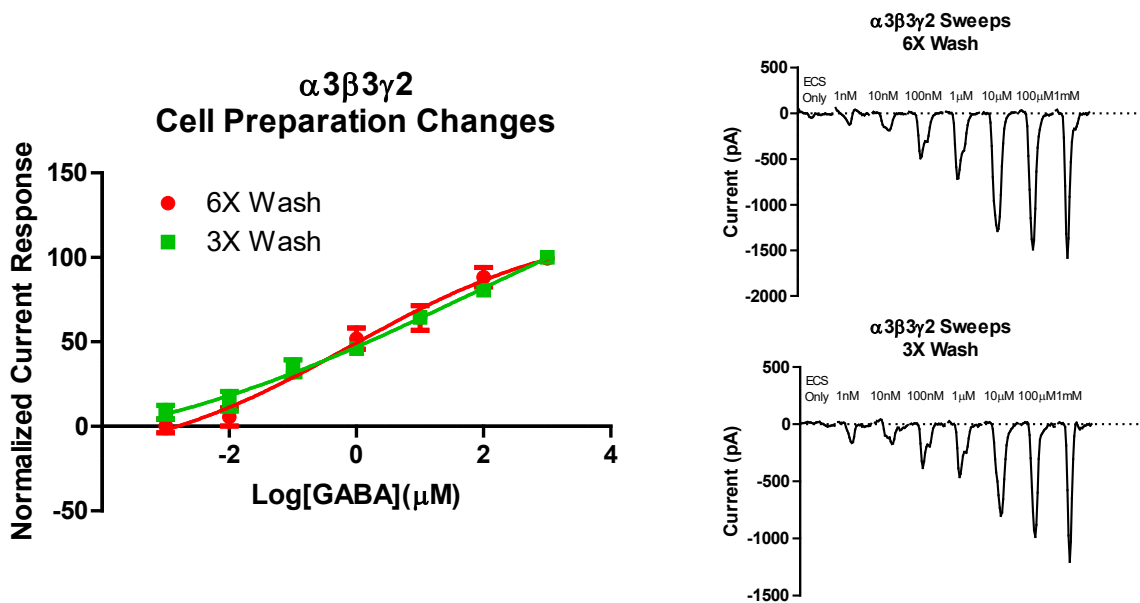


Figure 28. Cell Preparation Modifications Cells were prepared for patch clamp experiments through three blank media washes followed by three ECS washes (6X Wash) or the ECS washes alone (3X wash). Results were normalized such that 0% represented the response to ECS buffer only and 100% was the maximum response to GABA. Sweeps corresponding to the concentration curve (left) are shown on the right.

Instrument Setting Modifications

Sweeps seen in **Figure 18** show positive currents in the initial applications of ECS only with the $\alpha 1\beta 3\gamma 2$ cell line. In an effort to combat the positive currents seen in many initial applications across all cell lines, the holding voltage was changed from -80mV to -70mV . Because the holding voltage is higher and the interior of the cell less negative, it was hypothesized that fewer positive ions would pass through the membrane.

Figure 29A depicts response with control compounds using the conventional holding voltage of -80mV and **B** depicts the response after the holding voltage was increased. Positive currents were not eliminated (data not shown) and the differential response between compounds was lost. The holding voltage was set to -80mV for all subsequent experiments.

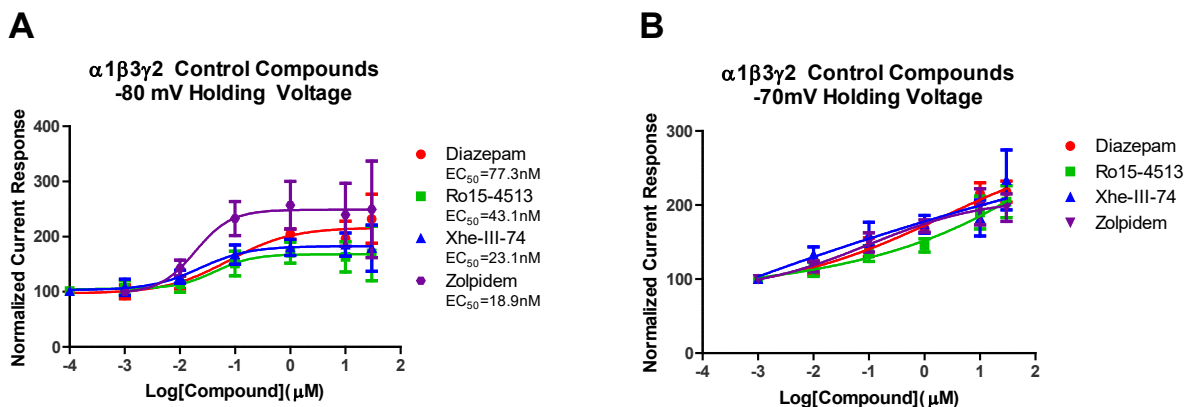


Figure 29. Holding Voltage Changes Compounds were co-applied with 400 nM GABA, the approximate EC_{20} identified by the GABA concentration curve shown in **Figure 18**. Responses were normalized such that the response to GABA alone was 100% (A) Holding voltage during data acquisition was set to -80 mV, the standard previously used for all GABA_AR stable cell lines. (B) Holding voltage was changed to -70 mV during data acquisition.

It was then hypothesized that the extensive time at room temperature may be affecting the cells' natural responses. At the time, subtype selectivity data were needed for the novel imidazodiazepines GL-II-73, GL-II-74, GL-II-75, and GL-II-76, which were synthesized by Guanguan Li working in the group of Prof. James Cook as antidepressants and anxiolytics.⁶⁸ However, buffer only applications were continuing to elicit positive currents (**Figure 30B**). In an effort to improve the results, the experimental temperature was changed from room temperature to 37°C (physiological temperature). However, the differential responses between the compounds were lost (**Figure 30C**) and the positive currents persisted (**Figure 30D**). All subsequent experiments were set at room temperature.

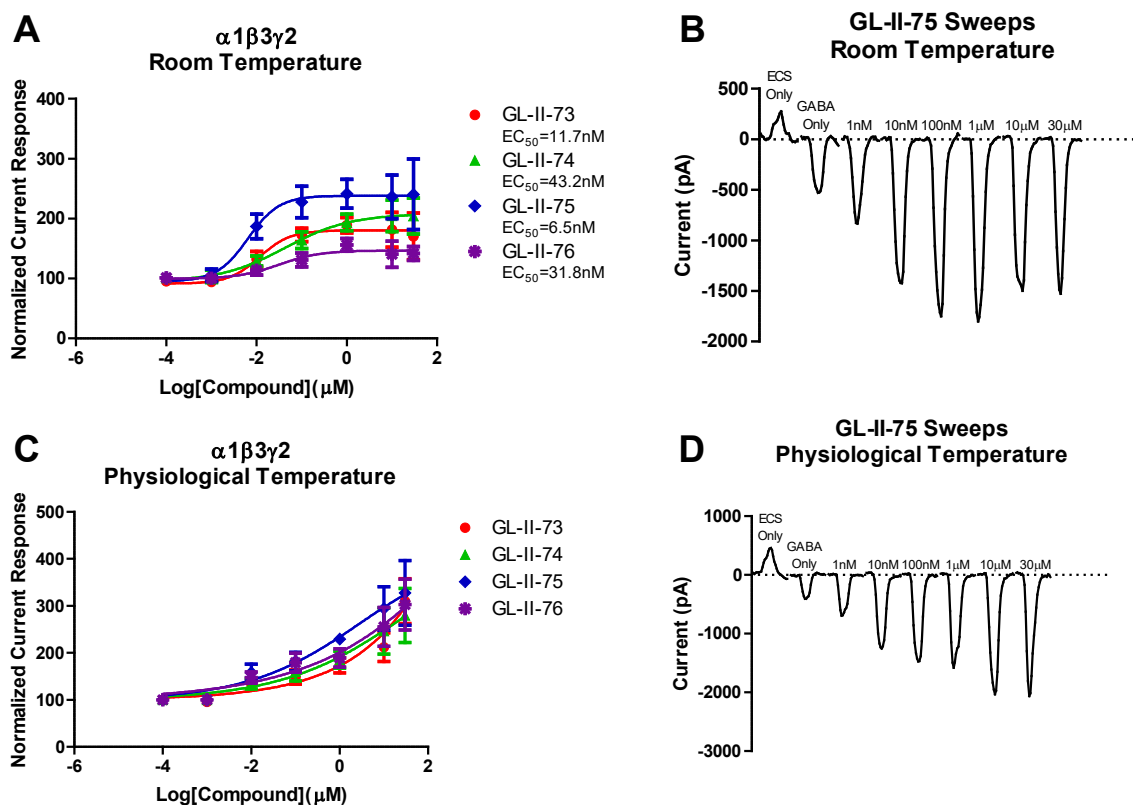


Figure 30. Effects of Physiological Temperature Compounds were co-applied with 400 nM GABA, the approximate EC_{20} determined by the GABA concentration response. Responses were normalized such that the response to GABA alone was 100%. (A) Concentration responses of four novel imidazodiazepines at room temperature. (B) Sweeps for GL-II-75 corresponding to the concentration response curve in A. (C) Concentration responses of four novel imidazodiazepines at 37°C, physiological temperature. (D) Sweeps for GL-II-75 corresponding to the concentration response curve in C.

Buffer Modifications

Buffers are one of the most important aspects of quality patch clamp data, as buffers are responsible for providing the ions for current changes and maintaining cellular shape and membrane integrity for a GΩ seal.

The standard buffers described in **Table 2** contain 150 mM of chloride ions in the ECS and 144 mM of chloride ions in the ICS. It was hypothesized that a higher chloride concentration inside the cell may be more physiologically relevant, so the buffers were altered as described in **Table 4**, to change the ECS concentration to 144 mM and the ICS concentration to 151 mM.

Table 4: Altering Chloride Concentration in ECS and ICS Buffers

	Standard ECS (M)	Standard ICS (M)	New ECS (M)	New ICS (M)
NaCl	0.14		0.133	
KCl	0.005		0.005	
MgCl ₂	0.001	0.001	0.001	0.001
CaCl ₂	0.002	0.001	0.002	0.001
Glucose	0.005		0.005	
HEPES	0.01	0.01	0.01	0.01
KF				
EGTA		0.011		0.011
CsCl		0.14		0.147
pH	7.4	7.2	7.4	7.2

These buffers were used in conjunction with the $\alpha 5\beta 3\gamma 2$ cell line in an effort to see responses more in line with published results, namely a high response with the $\alpha 5$ compound SH053-2'F-R-CH₃ and low responses from negative control compound Ro15-4513 and Zolpidem. The new buffers did decrease the response to zolpidem to much lower levels, however the response to Ro15-4513 remained high and the response to SH-053-2'F-R-CH₃ remained low (**Figure 31**).

Additionally, it was hypothesized that a reversal of the high and low chloride concentrations may affect the positive currents frequently seen with buffer only applications. However, this did not appear to be the case, as the positive currents actually increased. The current sweeps show that the response to the modulators was decreased, however, since the response was suppressed when 1 nM SH053-2'F-R-053 was added compared to the GABA alone.

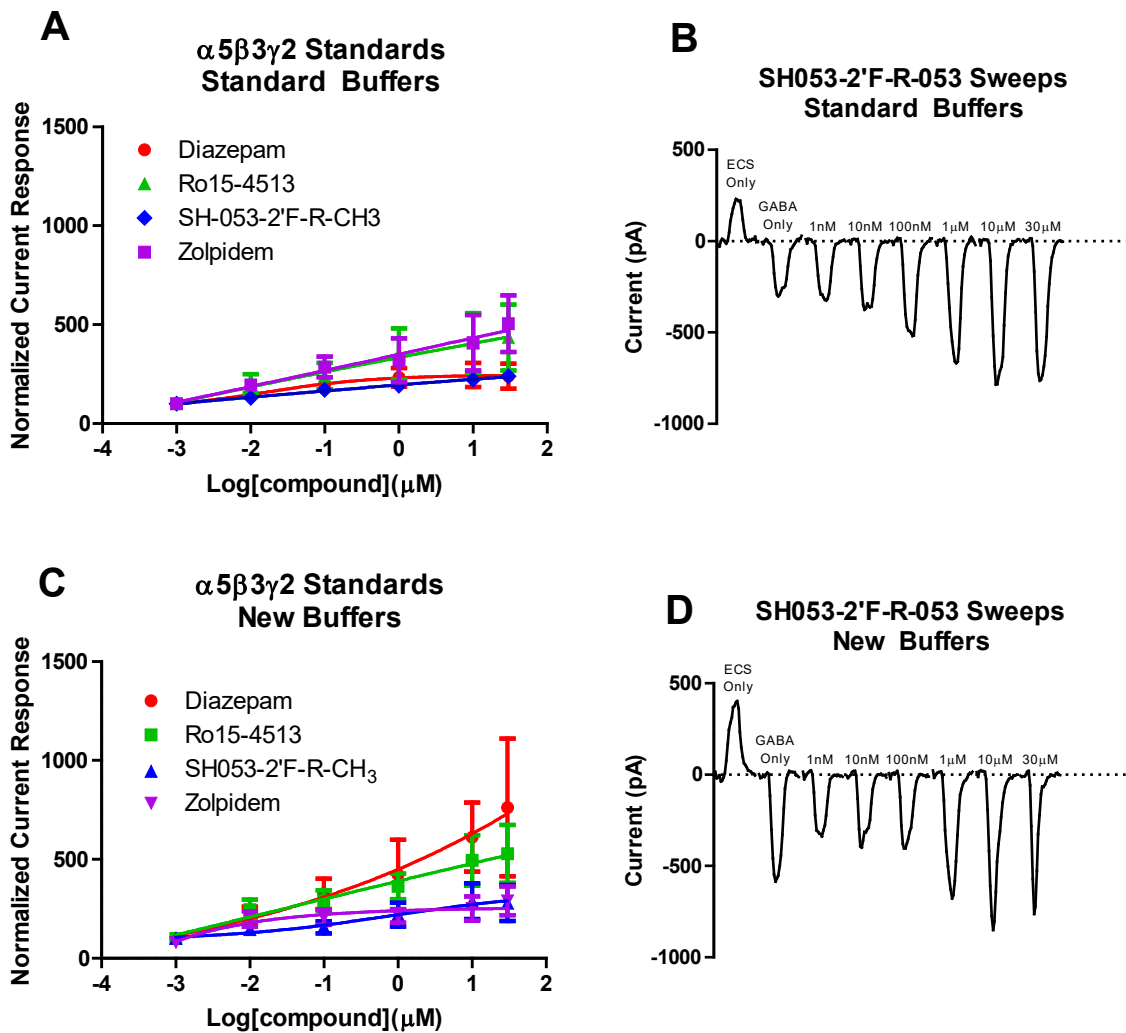


Figure 31. Testing $\alpha 5\beta 3\gamma 2$ Standards Using Buffers with Varying Chloride Concentrations The $\alpha 5\beta 3\gamma 2$ stable cell line was tested with standard buffers (A-B) and new buffers that altered the internal and external chloride concentrations (C-D). Responses were normalized such that the response to GABA alone was 100% (A,C) and representative sweeps are displayed for SH053-2'F-R-053, a compound selective for receptors containing $\alpha 5$ subunits (B,D).

Additional buffer changes were investigated as well. The standard buffers used for most experiments was optimized by Nina Yuan⁸⁴, however Fluxion suggests its own buffers for use with the IonFlux machine, which are detailed in **Table 5**. Nina had previously tested these buffers, however with lack of success.

The IonFlux ECS is highly similar to the standard ECS that had been used previously, however the ICS is drastically different. The ICS suggested by Fluxion contains NaCl and KCl as main sources of chloride

ions, whereas the current buffers utilized CsCl. The use of cesium had been optimized by Nina as it was reported that cesium prevents potassium leak current.⁸⁸

The results in the concentration curve appear consistent despite the drastically different buffer systems (**Figure 32A,C**), however the current sweeps show that the inclusion of cesium in the ICS is important as the sweeps appear much smoother and include fewer artifacts (**Figure 32B,D**). This is in line with what Nina had discovered as well.⁸⁴ The IonFlux buffers were not used for subsequent experiments.

Table 5. IonFlux Buffers

	Standard ECS (M)	Standard ICS (M)	IonFlux ECS (M)	IonFlux ICS (M)
NaCl	0.14		0.138	0.015
KCl	0.005		0.004	0.06
MgCl ₂	0.001	0.001	0.001	
CaCl ₂	0.002	0.001	0.0018	
Glucose	0.005		0.0056	0.005
HEPES	0.01	0.01	0.01	0.005
KF				0.07
EGTA		0.011		
CsCl		0.14		
pH	7.4	7.2	7.4	7.25

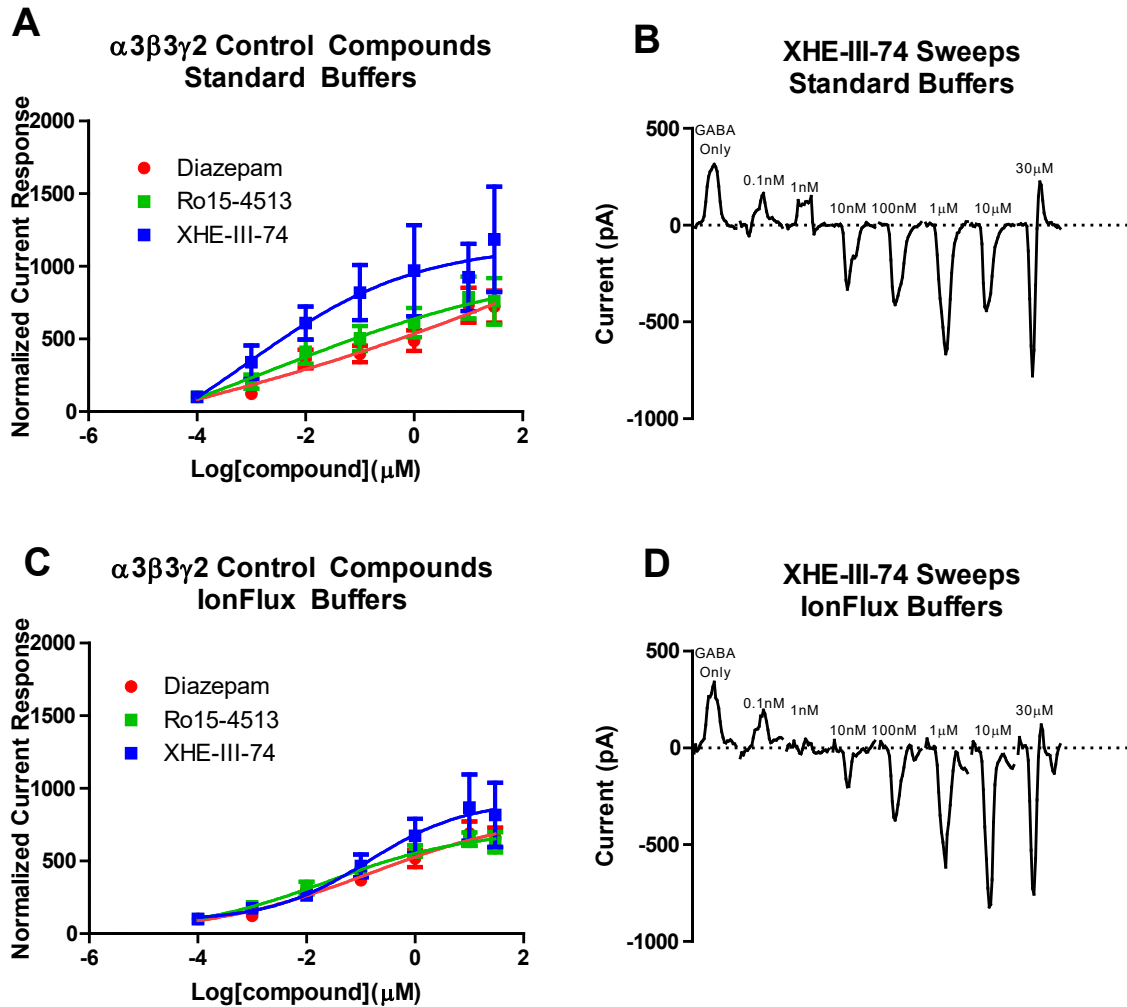


Figure 32. Standard Buffers vs. IonFlux Buffers The $\alpha 3\beta 3\gamma 2$ stable cell line was tested with standard buffers (A-B) and IonFlux buffers (C-D), the composition of which can be found in **Table 5**. Responses were normalized such that the response to GABA alone was 100% (A,C) and representative sweeps are displayed for SH053-2'F-R-053, a compound selective for receptors containing $\alpha 5$ subunits (B,D).

After further investigation into past experiments, it was discovered that the buffer recipe for ECS that was being used for all experiments as the standard buffer did not match the recipe published in Yuan.⁸⁴ The differences are shown in **Table 6**. The main variances are the omission of magnesium chloride from the published recipe and a lower overall concentration of chloride, although it is still higher than the chloride concentration in the ICS.

Table 6. Differences between Standard Recipe and Yuan's Recipe for ECS Buffer⁸⁴

	Standard ECS (M)	Yuan ECS (M)
NaCl	0.14	0.140
KCl	0.005	0.0054
MgCl ₂	0.001	
CaCl ₂	0.002	0.001
Glucose	0.005	0.01
HEPES	0.01	0.01
pH	7.4	7.4

The change in buffer composition did not change the concentration response curve, as shown in **Figure 33**, however the amplitude of the current response nearly doubled and the positive currents were drastically reduced. The magnesium-free buffer is the buffer of choice for any further experiments. However, by the time this buffer was discovered, the project was already coming to an end and was no longer necessary.

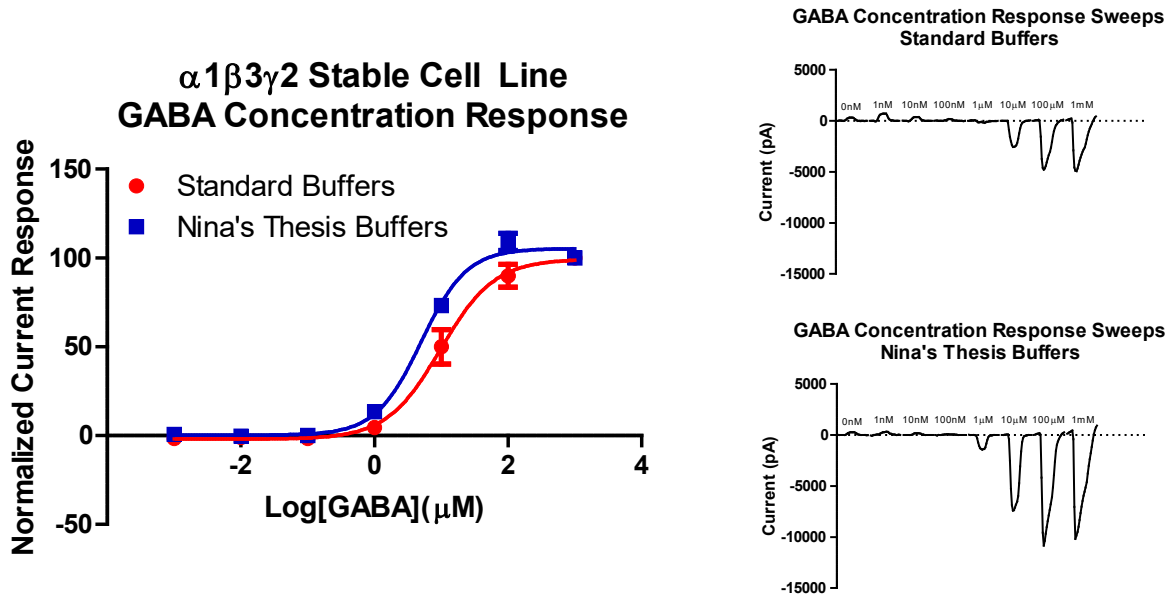


Figure 33. Differences in Buffer Recipes from Yuan⁸⁴ The $\alpha 1\beta 3\gamma 2$ cell line was tested in GABA concentration response with the buffers described in **Table 6**. The results were normalized such that 0% represented the response to ECS alone and 100% was the maximum response to GABA. Sweeps corresponding to the concentration curve (left) are shown on the right.

Assay Format Modifications (Experimental Solutions)

Changes to the experimental solutions were also attempted in response to the numerous issues. Because the automated patch clamp experiment utilizes microfluidics in the plates to deliver compounds of interest to the cells, it was hypothesized that micro air bubbles may be affecting the functionality of the microfluidics. Solutions were sonicated and degassed before experiments, but this seemed to have no effect on the end results (data not shown) and was thus discontinued.

Prior experiments have shown that these cells are sensitive to DMSO, so the DMSO concentration was equalized between compound wells to be 0.1%. However, there is no DMSO in the inlet. It was hypothesized that the introduction of DMSO to the cells from the first compound well may invoke a response that could be mitigated through the presence of DMSO to cells within the inlet.

There were no differences seen between the DMSO treated and non-treated cells, as shown in **Figure 34**. The concentration curves are highly comparable and the EC₅₀ values also reflect the similarity of response. The current responses are also similar, with the exception of the lack of response to 333 μ M GABA in solution without DMSO. This was an artifact of the experiment however, and does not support a necessary role for DMSO in the inlet. No DMSO was used in inlet wells in any other experiment.

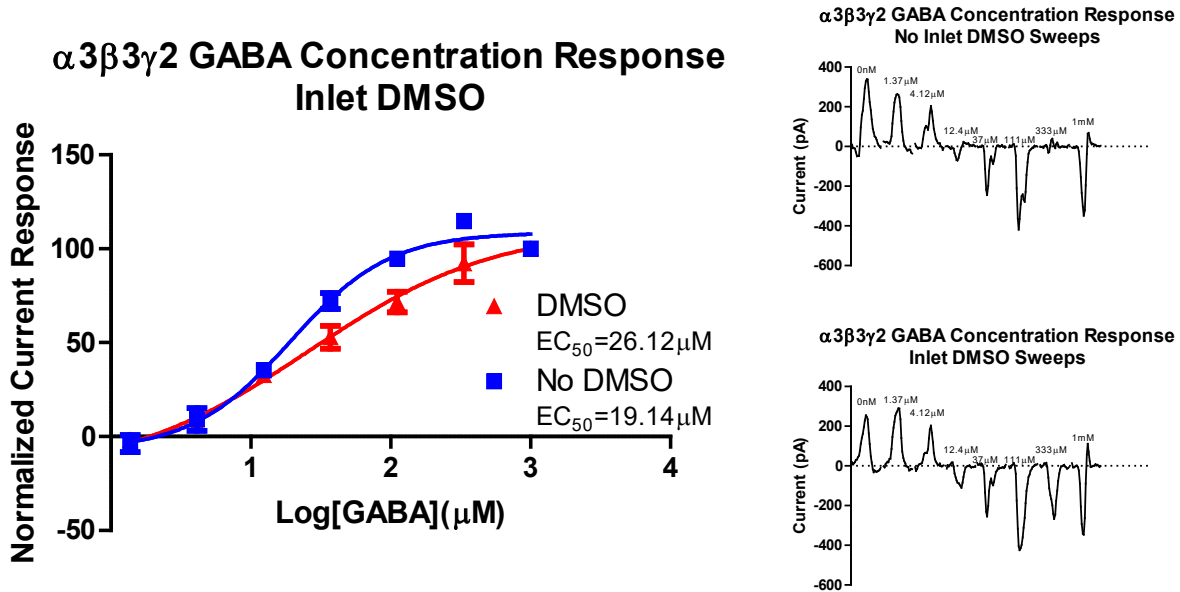


Figure 34. Addition of Inlet DMSO Patch clamp readings were taken with and without 0.1% DMSO added to inlet wells. The results were normalized such that 0% represented the response to ECS alone and 100% was the maximum response to GABA. Sweeps corresponding to the concentration curve (left) are shown on the right.

Another potential reason for the lack of response to initial applications of GABA was that as concentrations increased during the concentration response experiments, the cells became sensitized. If true, a higher concentration would be required to generate the same response if not preceded by other GABA applications. Therefore, the initial concentration of GABA applied before the introduction of modulators was increased beyond the EC₂₀.

Even though the concentration of GABA doubled, positive currents were still seen with the GABA only application (**Figure 35**). A response of approximately -500 pA was expected based on the concentration response seen in **Figure 15**. Increased GABA concentrations were used with multiple cell lines, all with the same lack of success.

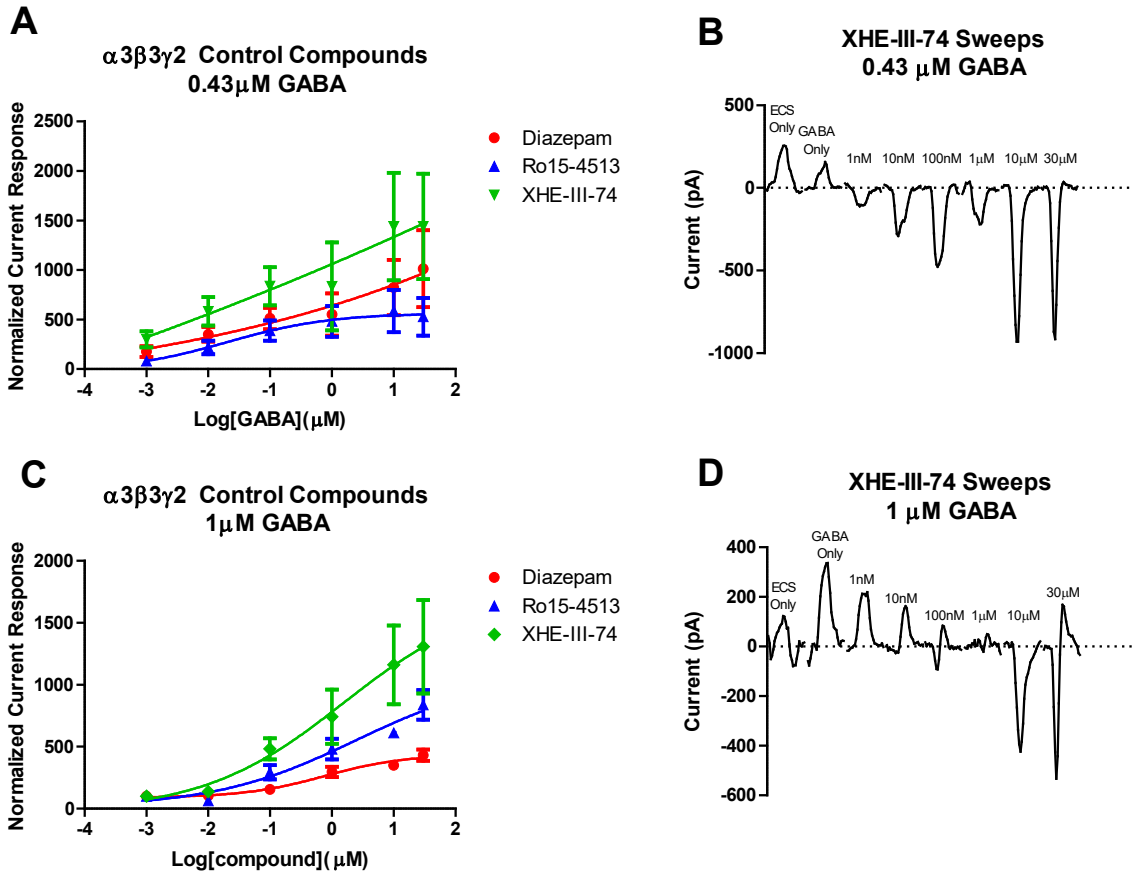


Figure 35. Increased Concentration of Initial GABA Application Initial concentration of GABA was increased from 0.43 μM (A-B) to 1 μM (C-D). Responses were normalized such that the response to GABA alone was 100% (A,C) and representative sweeps are displayed for XHE-III-74 (B,D).

Assay Format Modifications (Compound Additions)

In a final attempt to overcome issues encountered in patch clamp experiments, the compound addition schedule was modified. The standard protocol called for six applications of the C1 solution (typically ECS alone or GABA alone), and two applications of the remaining seven compound solutions (6X2X protocol). The six initial applications were thought to be necessary to provide a good baseline from which the normalization could be calculated.

However, over the course of many experiments and endless troubleshooting, that was determined to be false. It was hypothesized that the cells may simply be too stressed and the assay too long, causing the cells to stop responding towards the end of the assay that would account for the

occasional lack of response in the highest concentrations. The standard protocol was amended to two applications from all wells, which reduced the overall experiment time by approximately 2 minutes.

As seen in **Figure 36**, the protocol change did result in an approximately 50% increase in the current amplitudes, however the concentration response curves did not change as the EC_{50} values are nearly identical. The 2X protocol was deemed the better option moving forward, though by the time these data were generated, the project was nearing its end and this protocol was only used for a few failed experiments.

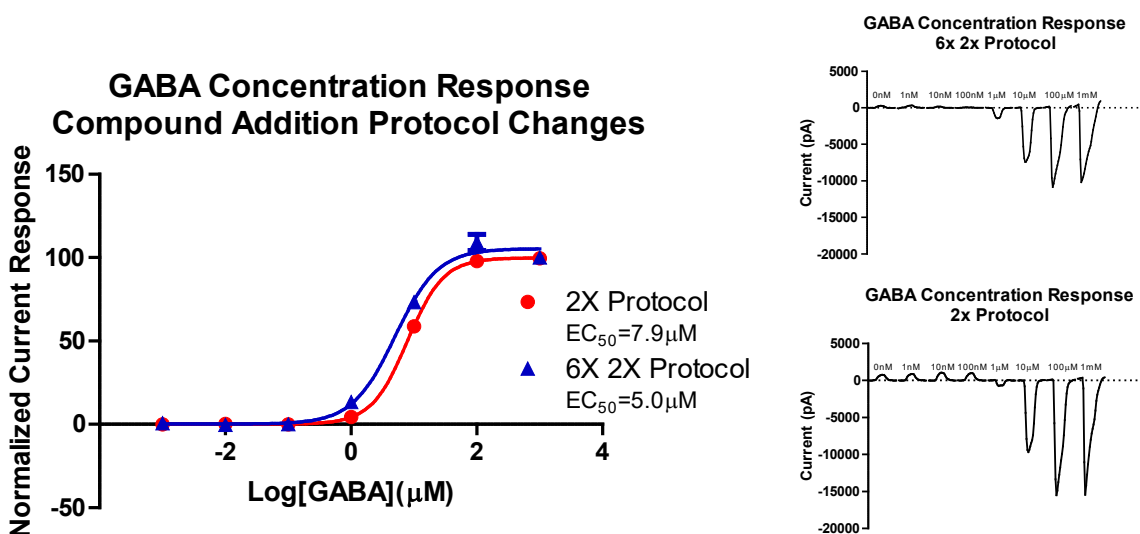


Figure 36. Compound Protocol Changes to Shorten Assay Time The $\alpha 1\beta 3\gamma 2$ cell line was tested in GABA concentration response with the 2X protocol, which applied two rounds of each compound solution and the 6X2X protocol, which applied six applications of the first compound solution and two applications of the remaining solutions. The results were normalized such that 0% represented the response to ECS alone and 100% was the maximum response to GABA. Sweeps corresponding to the concentration curve (left) are shown on the right.

A 3X3X2X protocol was also tested prior to the 2X protocol. The hypothesis included the observation that there were smaller positive currents in the GABA concentration response experiments, where the first compound well contained ECS buffer only. Therefore, if ECS buffer was the first solution exposed in modulator experiments followed by GABA only and then compounds, perhaps it would allow the cells to adapt to the new environment. However, it did not yield any benefits over the standard 6X2X protocol (data not shown).

2.3.5 Discussion

Five stable cell lines were developed and briefly characterized by Nina Yuan, a previous graduate student in the Arnold Lab.⁸⁴ The goal of this project was to expand upon that initial characterization and use the stable cells lines in conjunction with automated patch clamp to generate subtype selectivity data for novel imidazodiazepines, chiefly those developed by the Cook Lab (UWM).

GABA concentration curves were established for the α 1-5 β 3 γ 2 cell lines by applying increasing concentrations of GABA ranging from 1 nM to 1 mM. Each cell line tested had comparable EC₅₀ values with previously published results, and similar maximum potentiations. It was noted that positive currents were unexpectedly appearing in the ECS only applications and lower concentrations of GABA in the α 2-5 β 3 γ 2 stable cell lines. Though these positive currents were inconsistent with previous results, the EC₅₀ and maximum current were similar, thus experimentation with control compounds began in parallel with troubleshooting.

Control compounds were chosen based on published literature describing the binding and efficacy of each compound at specific receptor types (i.e. α 1 containing receptors). Positive controls represented compounds that had previously shown high potentiation for each specific receptor subtype and included Zolpidem (α 1 containing receptors), Diazepam (α 2 and α 3 containing receptors), XHE-III-74 (α 4 containing receptors) and SH053-2'F-R-CH₃ (α 5 containing receptors).^{87,75} Ro15-4513 was utilized as a negative control for α 1, α 2, α 3, and α 5 containing receptors as it is a highly selective modulator for α 4 containing receptors but has comparatively low efficacy in comparison to XHE-III-74.⁷⁶ Compounds other than the previously stated positive and negative controls were also tested to determine if moderate responses were similar to reported literature values.

The α 1 β 3 γ 2 stable cell line was tested with Zolpidem (positive control), Diazepam, XHE-III-74, and Ro15-4513 (negative control). As expected, the highest response was seen with Zolpidem, moderate responses were seen with diazepam, and low responses were seen with XHE-III-74 and Ro15-4513.

Positive currents appeared in the ECS only applications, however the GABA applications produced a negative current as expected. Over the course of the experiment, the cells inconsistently stopped responding to the increasing concentrations of modulator; some traps would respond to an application and others would not. This led to a reduced average current in the sweeps (**Figure 18**) and high standard deviations for the concentration response curves. This problem was observed across all cell lines and compounds and was a key issue addressed in the troubleshooting process. Though there were certain assay optimizations carried out, the $\alpha 1\beta 3\gamma 2$ stable cell line appeared to be functioning as expected and was used in subtype selectivity determination.

Numerous attempts to eliminate positive currents were made. First, the holding voltage was changed from -80mV to -70mV however the concentration response curves lost all differentiation between the compounds.

Next it was hypothesized that the extended periods at room temperature may affect the cells' normal function, so the instrument was set physiological temperature (37°C) for the duration of the experiment. Again, this abolished the difference in response between the compounds seen at room temperature. Neither the holding voltage nor temperature changes were implemented for any other experiments.

Other assay changes included modified compound addition. The standard protocol applied six replicates from the first concentration well (ECS only for GABA concentration response experiments, and GABA only for modulator response experiments) and two replicates from the remaining seven concentration wells (increasing concentrations of GABA or modulator). It was hypothesized that twenty separate compound applications could influence the integrity for the cell wall. While current responses did increase with the shorter protocol, the GABA concentration response curve remained unchanged, and nearly identical EC_{50} values were calculated.

Many buffer changes were made throughout troubleshooting, and the $\alpha 1\beta 3\gamma 2$ stable cell line was used to identify changes between the standard buffers and buffers published in Yuan.⁸⁴ The normalized GABA concentration response curve did not change, and therefore the EC_{50} value remained the same, however the currents nearly doubled in the buffer system that utilized magnesium free ECS. This improved buffer system was discovered towards the end of the project, and was not able to be tested in other cell lines.

Diazepam and Ro15-4513 were used as positive and negative controls for the $\alpha 2\beta 3\gamma 2$ and $\alpha 3\beta 3\gamma 2$ stable cell lines, along with XHE-III-74, which induced a moderate response for these GABA_ARs. Both cell lines responded with positive currents to GABA only applications, even when the GABA concentration was increased beyond the EC_{20} concentration. Because both cell lines utilized the same control compounds and responded similarly, the $\alpha 3\beta 3\gamma 2$ stable cell line was used for troubleshooting in assumption to use the optimized protocol for the $\alpha 2\beta 3\gamma 2$ stable cell line.

The brand of culture flasks did not influence the GABA concentration response curves. The cell preparation for the patch clamp experiment that included three washes in serum free media and three washes in ECS buffer was investigated as well. The serum free media washes were eliminated, which reduced the total number of washes to three. No difference was seen in the concentration response curves, and the currents were not significantly different from each other. Thus, the shorter three wash protocol was adopted for all further experiments.

Using the IonFlux buffers generated very jagged-looking current responses and therefore many electrophysiological artifacts. These buffers did not reverse the positive currents seen in GABA only applications or applications of low concentration of modulators and were therefore not adopted.

The GABA_AR modulators are solubilized in DMSO before being added to the ECS buffer at a final concentration of 0.1% DMSO. Cells have previously been shown to respond electrophysiologically to DMSO at high enough concentrations, however the stable cell lines were shown to respond equivalently

when the DMSO concentration was 0.3% and 1%.⁸⁴ However, it was thought that the positive currents may be a result of the initial DMSO exposure from the first concentration well. DMSO was added to the inlet to eliminate the introduction of DMSO concurrently with the first compound addition. However, nearly identical current sweeps and concentration response graphs were obtained.

Next it was hypothesized that over the course of the GABA concentration curve generation the multiple exposures to GABA may sensitize the cells to respond more than they would have been at the same concentration without prior contact. The concentration of GABA was doubled, however the positive currents in response to the GABA only application remained. Further increases in GABA were also tested, but were also unsuccessful.

Many of the troubleshooting efforts with the $\alpha 1\beta 3\gamma 2$ stable cell line that were detailed earlier in this section, and those with the $\alpha 5\beta 3\gamma 2$ stable cell line that will be discussed subsequently had also been applied to the $\alpha 3\beta 3\gamma 2$ stable cell line with no success. It was determined that the $\alpha 2\beta 3\gamma 2$ and $\alpha 3\beta 3\gamma 2$ stable cell lines could not be used to test for subtype selectivity and were discontinued.

Initial results with the $\alpha 4\beta 3\gamma 2$ stable cell line showed high potentiation with diazepam, a compound that is widely known to generate no effects through $\alpha 4$ and $\alpha 6$ containing receptors. The established cell line was clone 1 (CL1), so three other clones with high expression of the GABA_AR subunits were chosen: CL5, CL13, and CL17. All four of these clones responded similarly in the GABA concentration responses, though the curve shape was decidedly more sigmoidal for the CL13 and CL17. Only CL13 and CL17 had low levels of potentiation with diazepam, so these two clones were then tested separately with XHE-III-74 as the high-efficacy positive control, Ro15-4513 the moderately potent $\alpha 4$ -selective agonist, and diazepam. Again, CL13 and CL17 behaved almost equally, however CL17 had a slightly lower response to diazepam so it was selected for further testing. Additional runs confirmed these results though slight positive currents remained in the ECS only applications. Nevertheless, the $\alpha 4\beta 3\gamma 2$ stable cell line was deemed acceptable for subtype selective testing of novel imidazodiazepines.

Lastly, the $\alpha 5\beta 3\gamma 2$ stable cell line was tested with SH053-2'F-R-CH₃ as a positive control and zolpidem and Ro15-4513 as negative controls, and diazepam, which should have a moderately low response. Initial results were not promising, and after making many of the same changes described previously the response to SH053-2'F-R-053 was still very low and significant positive currents were still seen in GABA only applications and low concentrations of modulators.

Hygromycin B is a key component to the cell culture media for these stable cell lines as it acts as the selection antibiotic. A hygromycin B resistance gene is coded on the same plasmid as the three GABA_AR subunit genes, and therefore only cells that have high expression of the plasmid are able to survive in culture containing the antibiotic. Initially 100 $\mu\text{g}/\text{mL}$ was used for maintaining the culture, however it was hypothesized that this concentration may not be high enough and the cell population may not be homogenous. The concentration was increased to 300 $\mu\text{g}/\text{mL}$. In light of this increased antibiotic concentration, non-essential amino acids and Matrigel-coated culture media flasks were used. These culture changes resulted in a diazepam response that was decreased to reasonable levels, however Ro15-4513 continued giving exceedingly high responses and SH053-2'F-R-CH₃ barely responded at all.

Prior to the successful buffer change identified with the $\alpha 1\beta 3\gamma 2$ line, a different buffer system was designed and tested with the $\alpha 5\beta 3\gamma 2$ stable cell line. The standard buffers contained an excess of chloride ions in the ECS compared to the concentration in the ICS. The new buffer system reversed that relationship, placing a higher concentration of chloride ions within the cell in an attempt to reverse the directionality of the currents from buffer only applications. The new buffers did help decrease the response to the negative control Zolpidem, however the response from SH053-2'F-R-CH₃ was still barely above baseline. In light of the extensive troubleshooting with continued failure, the $\alpha 5\beta 3\gamma 2$ stable cell line was not utilized for further experiments.

There exist two other cell lines that were generated alongside the $\alpha 1\text{-}5\beta 3\gamma 2$, the $\alpha 6\beta 3\gamma 2$ and the $\beta 3\gamma 2$ that would function as a negative control. Due to the failure of the other five lines to produce quality data, these additional lines were not tested.

2.4 Novel Imidazodiazepine Testing

2.4.1 Experimental

See 2.3.1 Experimental.

2.4.2 Results

The $\alpha 1\beta 3\gamma 2$ and $\alpha 4\beta 3\gamma 2$ stable cell lines were deemed acceptable based on the responses with the control compounds, so they were used to screen novel imidazodiazepines developed by Dr. James Cook. RJ-02-50 (**Figure 37**) was determined to be a lead compound through other *in vivo* and *in vitro* assays, so subtype selectivity data were sought.²³

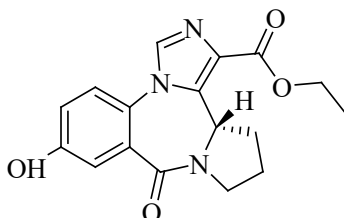


Figure 37. Structure of RJ-02-50 that combines the ethyl ester functionality of XHE-III-74 Ethyl Ester with the increased hydrophilicity of XHE-III-74 Acid to generate a new lead compound. RJ-02-50 was synthesized by Rajwana Jahan of the James Cook Lab.²³

RJ-02-50 showed preferential activity through the $\alpha 4\beta 3\gamma 2$ cell line (873% potentiation) compared to the $\alpha 1\beta 3\gamma 2$ cell line (309% potentiation) (**Figure 38**). It should be noted that ECS only applications did produce positive currents in both cell lines, as well as the GABA only application in the $\alpha 4\beta 3\gamma 2$ cell line. This is despite increasing the concentration of GABA beyond the EC_{20} value typically used with modulators. These positive currents in the GABA only applications also make the standard normalization impossible, forcing normalization to be based on the lowest concentration of modulator and making the assumption that no potentiation has occurred at low compounds concentrations.

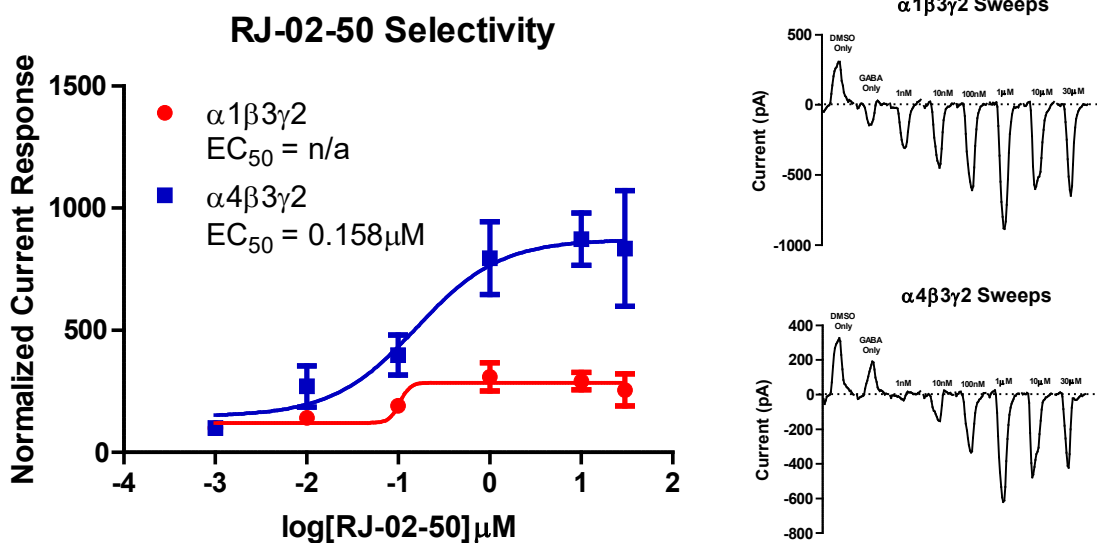


Figure 38. Subtype Selectivity of RJ-02-50 Compound was co-applied with 400 nM with the $\alpha 1\beta 3\gamma 2$ cell line and 600nM with the $\alpha 4\beta 3\gamma 2$ cell line. Left: Responses were normalized such that 100% represented the response to GABA alone. Right: Sweeps graphs depict the current responses to 3 second applications of the respective concentrations.

MRS-01-66 (**Figure 39**) was another lead compound identified through extensive *in vitro* and *in vivo* testing, thereby prompting the need for GABA_AR subtype selectivity data.⁷²

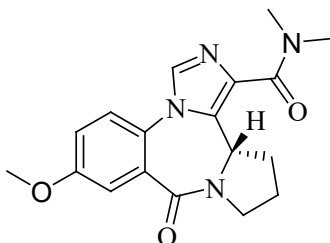


Figure 39. Structure of MRS-01-66 which was synthesized through published routes by Michael Rajesh Stephen of the James Cook Lab.⁷²

MRS-01-66 also showed selectivity towards $\alpha 4$ -containing receptors with a maximum potentiation of 712% for the $\alpha 4\beta 3\gamma 2$ stable cell line in comparison to 290% maximum potentiation in the $\alpha 1\beta 3\gamma 2$ stable cell line (**Figure 40**). Again positive currents showed up in ECS only applications in the $\alpha 4\beta 3\gamma 2$ stable cell line though despite increasing the GABA concentration beyond the EC₂₀ value. Out of necessity, the normalization for the results with the $\alpha 4\beta 3\gamma 2$ cell line needed to be normalized against the

0.12 μ M MRS-01-66 application instead of the GABA only application with the assumption that no modulation occurred at that concentration.

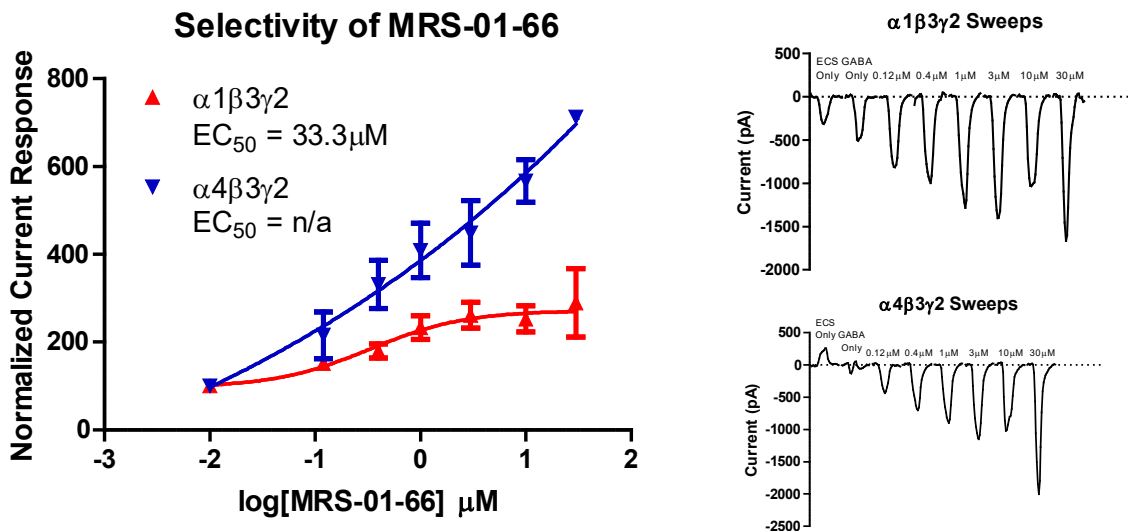


Figure 40. Subtype Selectivity of MRS-01-66 Compound was co-applied with 400 nM with the $\alpha 1\beta 3\gamma 2$ cell line and 800 nM with the $\alpha 4\beta 3\gamma 2$ cell line. Left: Responses were normalized such that 100% represented the response to GABA alone. Right: Sweeps graphs depict the current responses to 3 second applications of the respective concentrations.

MIDD0301 (Figure 41) was developed together with RJ-02-50 as lead compound for asthma.²⁴

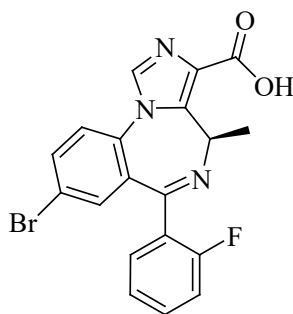


Figure 41. Structure of MIDD0301 which was synthesized by Guanguan Li of the James Cook lab according to a published procedure.²⁴

Subtype selectivity data were already available from a collaborator, however the $\alpha 4$ subunit containing receptors were not tested. Therefore, MIDD0301 was only tested in the $\alpha 4\beta 3\gamma 2$ stable cell line at the time and showed 570% potentiation (Figure 42). It was again necessary to normalize the current against a low concentration of modulator rather than GABA alone due to the positive currents under the

assumption that no true modulation had occurred at that concentration. In order for these results to be trusted, MIDD0301 should be tested in established subtype-selectivity assays for comparison.

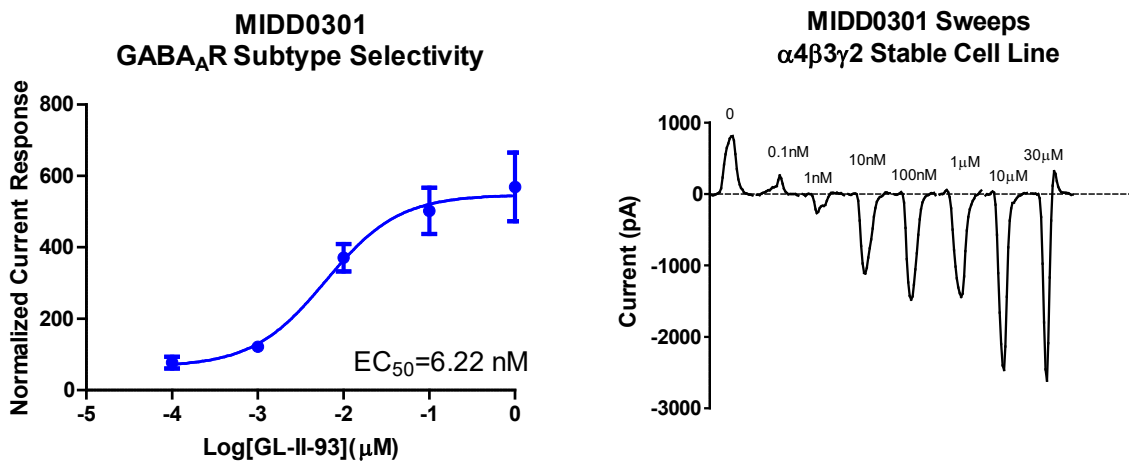


Figure 42. MIDD0301 Response in the $\alpha 4\beta 3\gamma 2$ Stable Cell Line Compound was co-applied with 600nM. Left: Responses were normalized such that 100% represented the response to GABA alone. Right: Sweeps graphs depict the current responses to 3 second applications of the respective concentrations.

The final set of compounds tested in collaboration with Prof. Cook were designed to treat anxiety and depression and therefore were expected to be $\alpha 5$ subtype selective compounds (**Figure 43**). However, since the $\alpha 5\beta 3\gamma 2$ cell line was not functional, these compounds were only tested in the $\alpha 1\beta 3\gamma 2$ stable cell line.

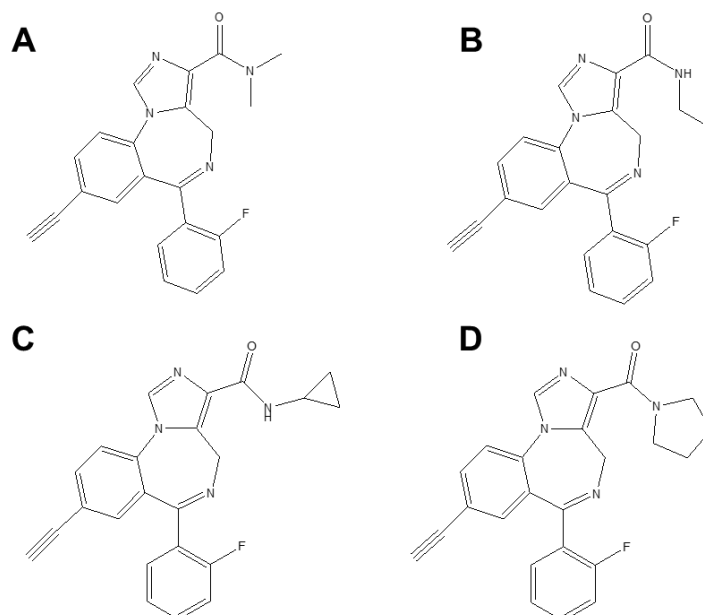


Figure 43. Compounds Designed to be α_2 Selective to Treat Depression and Anxiety Compounds were synthesized according to published routes by Guanguan Li.⁶⁸ (A) GL-II-74 (B) GL-II-74 (C) GL-II-75 (D) GL-II-76

GL-II-75 showed the highest potentiation at 240%, followed by GL-II-74 and GL-II-75 at 204% and 17% respectively. GL-II-76 responded very little with a potentiation of 142% at 30 μM (**Figure 44**). Only very minor positive currents were seen in ECS only applications for this experiment, and the cell line responded very well to the GABA alone application (data not shown). This made normalizing to the GABA response possible.

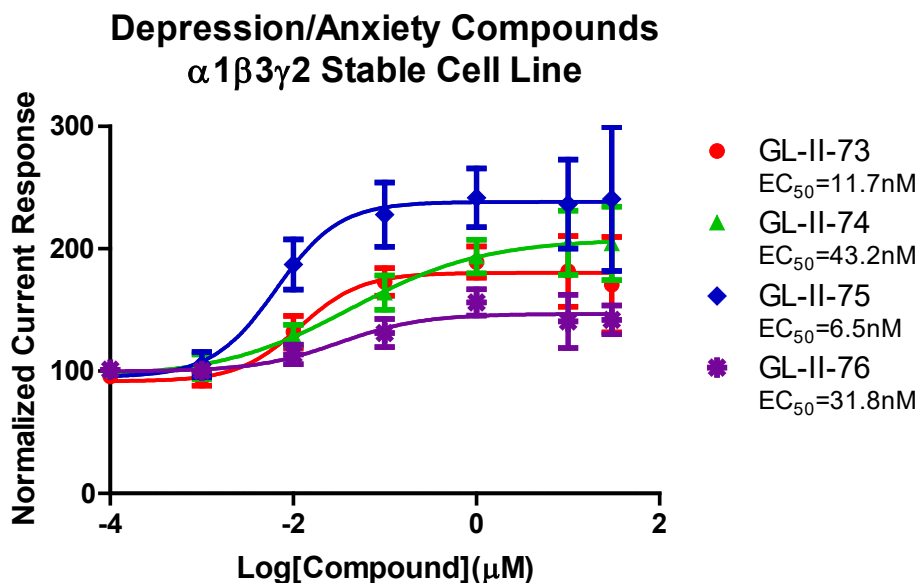


Figure 44. Electrophysiological Response of Depression/Anxiety Compounds in $\alpha 1\beta 3\gamma 2$ Stable Cell Line Compounds were co-applied with 600 nM GABA in three second applications.

2.4.3 Discussion

RJ-02-50 was developed based on the success of XHE-III-74 Ethyl Ester and XHE-III-74 Acid, which were both determined to be $\alpha 4$ subtype selective compounds.⁷¹ RJ-02-50 combined the ethyl ester functionality of the XHE-III-74 Ethyl Ester, which yielded favorable airway hyperresponsiveness results with the increased hydrophilicity of the XHE-III-74 Acid that prevented CNS effects by the lack of BBB permeation.

RJ-02-50 showed potentiation that was nearly three time higher in the $\alpha 4\beta 3\gamma 2$ stable cell line compared to the $\alpha 1\beta 3\gamma 2$ stable cell line. These results support that RJ-02-50 is an $\alpha 4$ -selective compound, however full characterization with all six α subunit-containing receptors is still missing. Additionally, there are no subtype selectivity results for RJ-02-50 generated by well-established methods to compare these results.

MRS-01-66 was unique among the other amide-containing imidazodiazepines for not generating negative CNS effects as determined by Rotarod studies (**3.4.2 Results**). The limited subtype selectivity results also suggest $\alpha 4$ -subtype selectivity, as the maximum potentiation in the $\alpha 4\beta 3\gamma 2$ stable cell line

was nearly three times that in the $\alpha 1\beta 3\gamma 2$ stable cell line. As mentioned above though, these results only provide an incomplete picture of the subtype selectivity and testing with the four remaining α subtypes is necessary.

MIDD0301 is currently the asthma lead compound. It is structurally different than previously tested imidazodiazepines for asthma as it is based on the scaffold typically seen in $\alpha 5$ subtype selective compounds. However, it was another combination of multiple compounds that had proved somewhat effective, including the $\alpha 5$ selective compound SH053-2'F-R-053 Acid.

Subtype selectivity for MIDD0301 was completed by a collaborator, however $\alpha 4$ or $\alpha 6$ containing receptors were not tested. High responses in the $\alpha 1$, $\alpha 2$, $\alpha 3$, and $\alpha 5$ containing receptors however confirm that this compound is not subtype selective.²⁴ Our results also show activity in the $\alpha 4$ containing receptors, adding to the lack of specificity of this compound. Because two different methods were used to come to this conclusion, it would be beneficial to test MIDD0301 in the collaborator's assay to confirm results for a better direct comparison.

The final group of compounds tested were developed to treat depression and pain. The compounds that target the $\alpha 5$ subunit are known to moderate these conditions.⁸ Because of the failure of the $\alpha 5\beta 3\gamma 2$ to function properly, only the response for $\alpha 1$ containing receptors was able to be tested. This is still important because of the role of the $\alpha 1$ containing receptors is important for amnesia and addiction.⁸

The results showed that GL-II-75 showed the highest efficacy for $\alpha 1$ containing receptors, GL-II-74 and GL-II-73 had moderate efficacy, and GL-II-76 showed very little efficacy. The results obtained here at 1 μM closely mirror those reported by the authors at the same concentration, with the exception of a slightly higher response for GL-II-75 in the authors' assay. Having this direct comparison confirms that the $\alpha 1\beta 3\gamma 2$ cell line is capable of producing reliable results.

2.5 Alternative Methods

There exist chloride sensitive dyes that could be used to monitor the chloride concentration in the presence of GABA_AR modulators as opposed to monitoring the current effects from the modulators as shown above. One such dye, MQ-DS, is a fluorescent ratiometric dye that contains a chloride insensitive dansyl group that fluoresces in the red region and a chloride sensitive methoxyquinolinium group that fluoresces blue in the absence of chloride (**Figure 45**).⁸⁹

Attempts were made to develop a high throughput screening assay with MQ-DS, however fluorescence above baseline was never able to be measured. It was postulated that the dye leaked from the cells during wash steps, despite the introduction of probenecid. Probenecid inhibits organic anion transporters, and is used alongside many intracellular dyes to prevent sequestration in organelles and secretion.⁹⁰

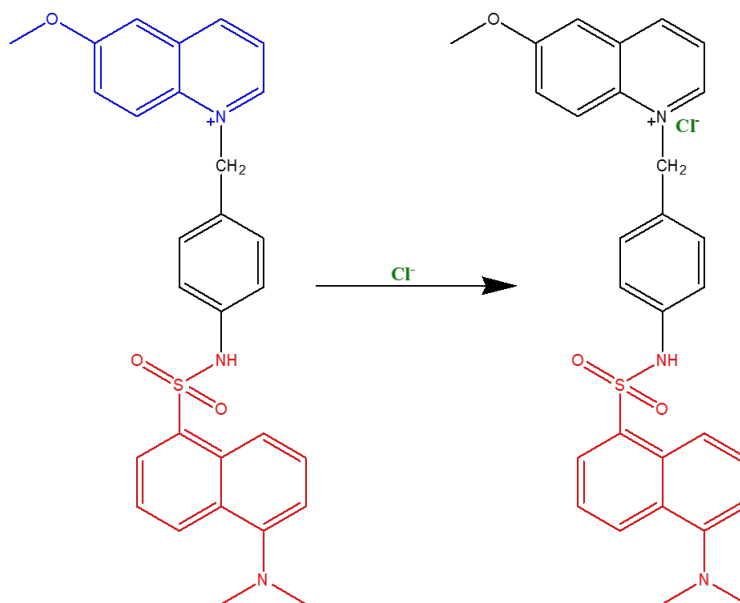


Figure 45. Structure of MQ-DS This ratiometric dye produces dual fluorescence emissions with a single excitation at 405 nm. The methoxyquinolinium group (blue) emits at 440 nm and decreases in signal as chloride concentration increases. The dansyl group (red) emits at 560 nm and is insensitive to chloride ions, providing a baseline on which to normalize the response of the methoxyquinolinium group (F_{560}/F_{440}).

CHAPTER 3

Determining Sensorimotor Coordination Effects of Drug Candidates via Rotarod

3.1 Background

Due to their unmatched efficacy and high level of safety, benzodiazepines are the most widely prescribed sedative and anxiolytic drugs.⁷ However, there are other known clinical effects such as muscle relaxation and epileptic seizure control.⁸ For patients that are prescribed benzodiazepines such as diazepam, unwelcome side effects such as anxiety, sedation and muscle relaxation can occur. Rational drug design can tailor compounds to target specific GABA_A receptor subtypes to circumvent these side effects⁸, however this strategy is not always successful. Therefore, it is crucial to investigate any potential adverse effects of all novel drug candidates.

The first RotaRod device was described in 1957 by N.W. Dunham and T.S. Miya.¹² They described a roller from a window shade controlled by a motor shaft and roller skate wheel, which was divided by cardboard disks to create separate intervals for individual mice. The height of the apparatus was set such that it discouraged the mice from jumping off, but not so high that they would be injured if they fell. There were also cages placed under each interval to catch the mice that fell during the test. Because of this test's capability to detect neurological deficits, the authors suggested its use for muscle relaxants, convulsants, and CNS depressants.¹²

Over time, the RotaRod device has been adapted to include many options such as fixed-speed vs. accelerating rod. Accelerating rod is beneficial when training time is limited. However, insufficient training will affect performance and quality of data. Fixed-speed RotaRod requires longer training periods, however it is significantly more sensitive. Fatigue can also confound data from fixed-speed assays if the appropriate speed is not determined. The speed needs to be slow enough to avoid false positives from excessive physical demands, though quick enough that the affected mice fall relatively early and the assay is not needlessly prolonged.⁹¹

Since its inception, the RotaRod has been used to assess the pharmacological effect of many compounds and is frequently an initial screening assay for benzodiazepines in particular due to well-

documented motor impairment across the drug class. Its wide-spread use is attributed to its simple set up and minimal animal training compared to other behavioral assays.

3.2 Instrumentation

The AccuRotor 4-Channel RotaRod (Omnitech Electronics, Inc., Columbus, OH) can be adapted for either mouse or rat, depending on the diameter of the rod (30mm for mouse, 70mm for rat). The speed of the rod can be set at a constant rate or accelerating rate from 0-100 RPM. The instrument is equipped with fall detection in each individual chamber that stops a timer when a mouse falls from the rod. The directionality of the rod can also be changed so that the mice can face towards or away from the experimenter during the assay.⁹²



Figure 46. Mice running on the RotaRod Apparatus The RotaRod apparatus has individual compartments for each mouse to maintain the animal's focus. The area beneath the rod is enclosed to contain the animals if they fall. The rod is high enough to encourage the animals to stay on the rod, but not so high as to cause injury if they do fall.

3.3 Initial Protocol

3.3.1 Experimental

6 week old, male BALB/c mice were purchased from Charles River (Wilmington, MA). They were trained to run on the RotaRod apparatus (**Figure 46**) for 3 minutes at a constant speed of 15 RPM. When a mouse completed three consecutive trials on different days without falling, the training was completed. Training typically took two weeks.

After training was complete, compound testing was started using groups of eight animals. Compounds were administered via 100 μ L intraperitoneal injection (i.p.) unless otherwise noted, using a vehicle consisting of 10% DMSO (Fisher Scientific, D128-500), 40% propylene glycol (Spectrum, P1440), and 50% PBS (Hyclone, SH30256.01). Compound was first dissolved in DMSO for solubility purposes before propylene glycol and finally PBS were added. 1mL 25G syringes were used for delivery (BD, 309626).

Mice were placed on the RotaRod 10 minutes post-injection, the approximate t_{max} as determined by pharmacokinetic studies. If a mouse fell before the three minutes were completed, the run was considered a fail and the mouse was assigned a 0. If the mouse successfully completed the run, the mouse was assigned a 1.

3.3.2 Results

As expected, the vehicle did not produce any adverse effects on RotaRod performance. Diazepam was used as a positive control due to its known sedative effects at higher dose. 1 mg/kg of Diazepam did not produce statistically significant sedation, however, 5 mg/kg was sedative and impaired the animal's balance on the rotating rod (**Figure 47**). The initial compounds investigated, XHE-III-74 Acid and XHE-III-74 Ethyl Ester (EE), were tested at different concentrations ranging from 1 mg/kg to 20 mg/kg. XHE-III-74 EE induced visual sedative effects but did not statistically reduce RotaRod performance, so an

additional dose was investigated. At 40mg/kg EE, solubility issues arose and 200µL injections were necessary. A statistically reduced performance was observed at this dose (**Figure 47**). XHE-III-74 Acid did not induce any adverse effects at all investigated doses.

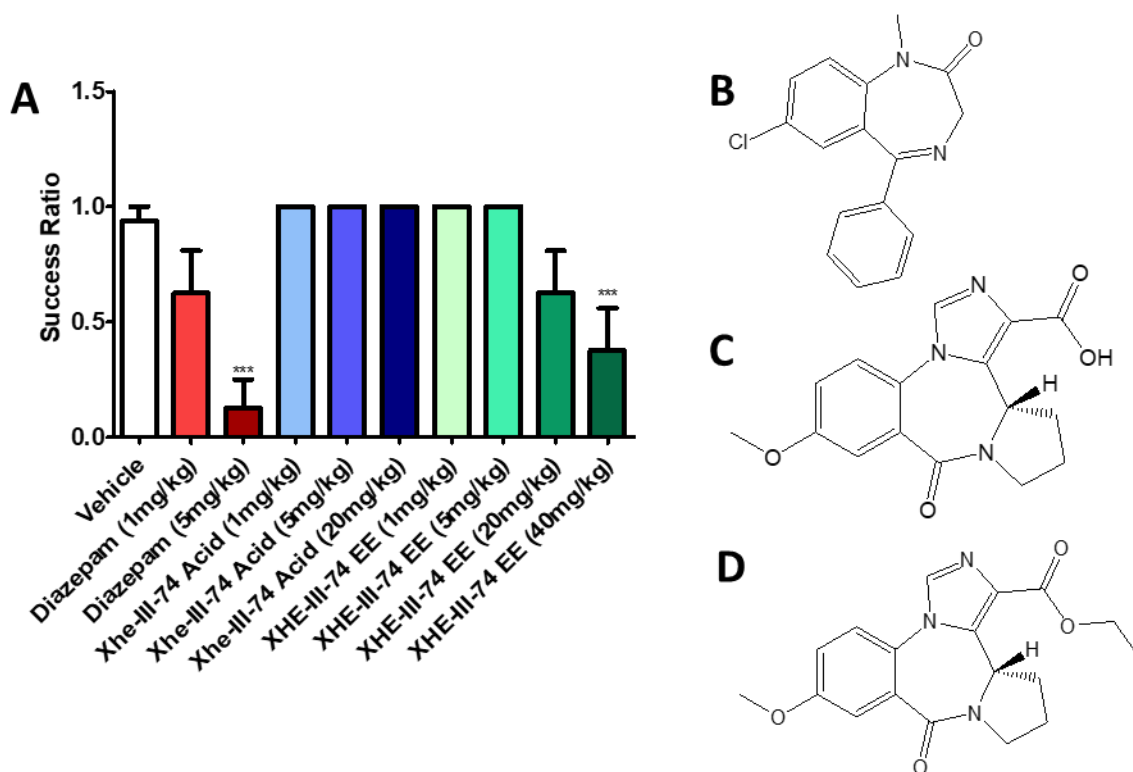


Figure 47. Initial RotaRod Studies with Male BALB/c Mice (A) Trained mice ($n = 8$) were placed on the RotaRod set at a constant speed of 15 RPM. Results are presented as the percent success rate. (B) Structure of Diazepam (Valium®), which was used as a positive control. (C) Structure of XHE-III-74 Acid (D) Structure of XHE-III-74 Ethyl Ester (EE).

3.3.3 Discussion

After approximately two weeks of training was successfully completed, the vehicle used induced no visual effects and 3 minute RotaRod runs were completed without fall by all mice. Diazepam at 5 mg/kg produce statistically significant results in comparison to the negative control (vehicle) and was used as the positive control.

Initial studies with XHE-III-74 Ethyl Ester (EE) and XHE-III-74 Acid at different doses demonstrated significantly different effects in respect to sensorimotor inhibition. XHE-III-74 Acid did not yield adverse effects, however XHE-III-74 EE showed dose dependent effects that became significant at 40 mg/kg.

Because sensorimotor inhibition is mediated by the CNS, it can be hypothesized that XHE-III-74 Acid, in contrast to XHE-III-74 EE is not able to cross the blood-brain barrier. Subsequent pharmacokinetic studies confirmed this hypothesis.⁷¹

However, over the course of a few weeks, the RotaRod performance of the male mice decreased and aggressive behaviors was observed. Therefore, female mice were suggested for subsequent protocols because they are known to have less aggression. Changing mouse strains to Swiss Webster (CFW) instead of BALB/c was also recommended. As outbred mice, CFW better represent genetic diversity in contrast to inbred BALB/c. To maintain statistical significance with the greater genetic diversity, increasing the group size from 8 to 10 mice was proposed.

It was also thought that testing the same mice over the course of time rather than at different doses could provide valuable information on compound metabolism/elimination and estimate the compound t_{max} when pharmacokinetic data were not yet generated. A 40 mg/kg dose was suggested because a significant number of compounds induced sensorimotor inhibition at that dose. Finally, it was observed that after 60 minutes post-injection the majority of compounds did not induce adverse side effects. Therefore, a 40 mg/kg dose and evaluation 10, 30, and 60 minutes post-injection was the recommended new protocol.

While making additional adjustments leading up to the second protocol, it was also noted that a mouse would occasionally fail due to distraction, and not as a result of compound administration. A fail was redefined to represent two falls with the first being forgiven, assuming that a compound with true adverse effects would cause subsequent falls. The time of the second fail was also recorded, instead of a basic pass/fail system to better represent the extent of the effects.

3.4 Improved Protocol

3.4.1 Experimental

6 week old, female CFW mice were purchased from Charles River (Wilmington, MA). They were trained to run on the RotaRod apparatus (**Figure 46**) for 3 minutes at a constant speed of 15 RPM. When a mouse completed three consecutive trials on different days without falling, the training was completed. Training typically took two weeks.

After training was complete, compound testing was started using groups of ten animals. Compounds were administered via 100 μ L intraperitoneal injection (i.p.) using a vehicle consisting of 10% DMSO (Fisher Scientific, D128-500), 40% propylene glycol (Spectrum, P1440), and 50% PBS (Hyclone, SH30256.01). Compound was first dissolved in DMSO for solubility purposes before propylene glycol and finally PBS were added. 1mL 25G syringes were used for delivery (BD, 309626). 5mg/kg Diazepam was used for a positive control.

Mice were placed on the rod 10, 30, and 60 minutes post-injection. If a mouse fell before the three minutes were completed, it was placed on the rod again. If a mouse fell for the second time the time of the fall was recorded.

3.4.2 Results

Figure 48 shows the vehicle and diazepam as controls with the new assay format. Vehicle-treated mice showed no visual effects and all animals completed the three minute run without failure even after three runs within an hour. 5 mg/kg diazepam statistically induced impairment at 10 and 30 minutes, however the effects were not significantly different from the negative control at 60 minutes post-injection.

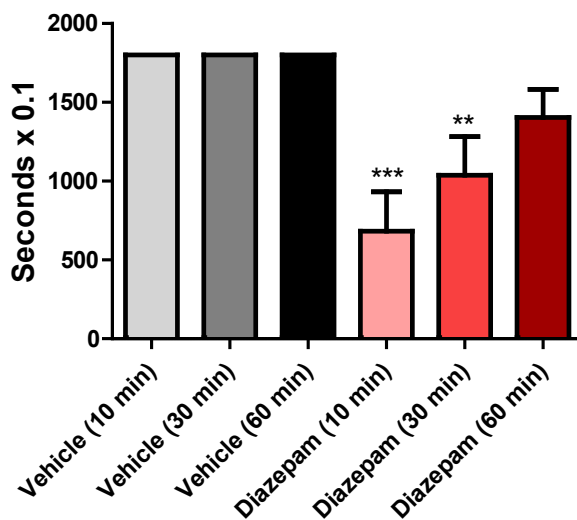


Figure 48. RotaRod Controls with Female Swiss Webster Mice Trained mice ($n = 10$) were placed on the RotaRod set at a constant speed of 15 RPM at various time points post-injection. Vehicle only was used as a negative control, and 5 mg/kg diazepam was used as a positive control. All compounds were administered *i.p.*

Compounds of interest (**Figure 49**) were synthesized by Rajwana Jahan (RJ) and Michael Rajesh Stephen (MRS), who were members of the Cook Group.⁷² All compounds were investigated at a dose of 40 mg/kg (**Figure 50**).

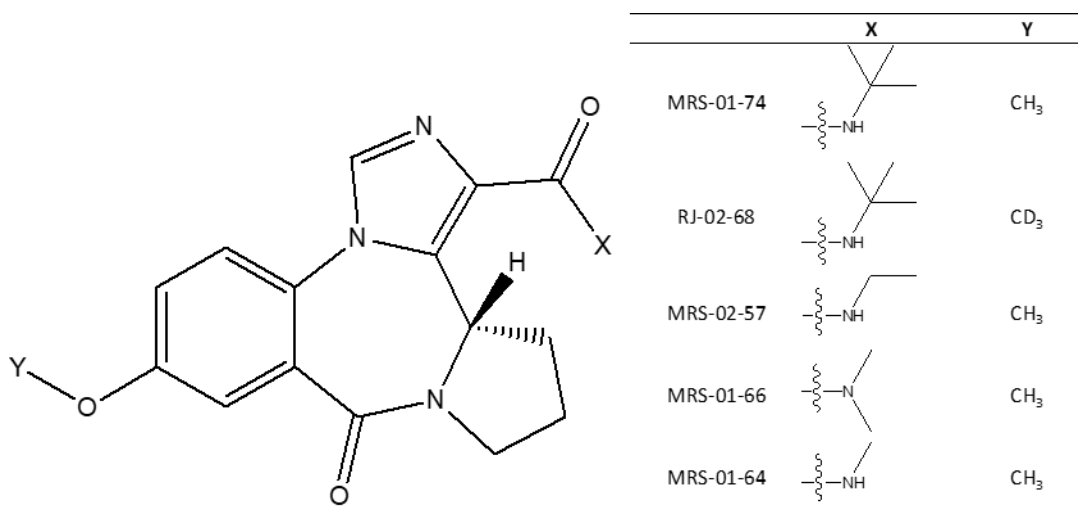


Figure 49. Asthma Compounds with Amide Functionality Compounds were synthesized according to a published procedure by Jahan et al.⁷² The table indicates the X and Y groups of the scaffold.

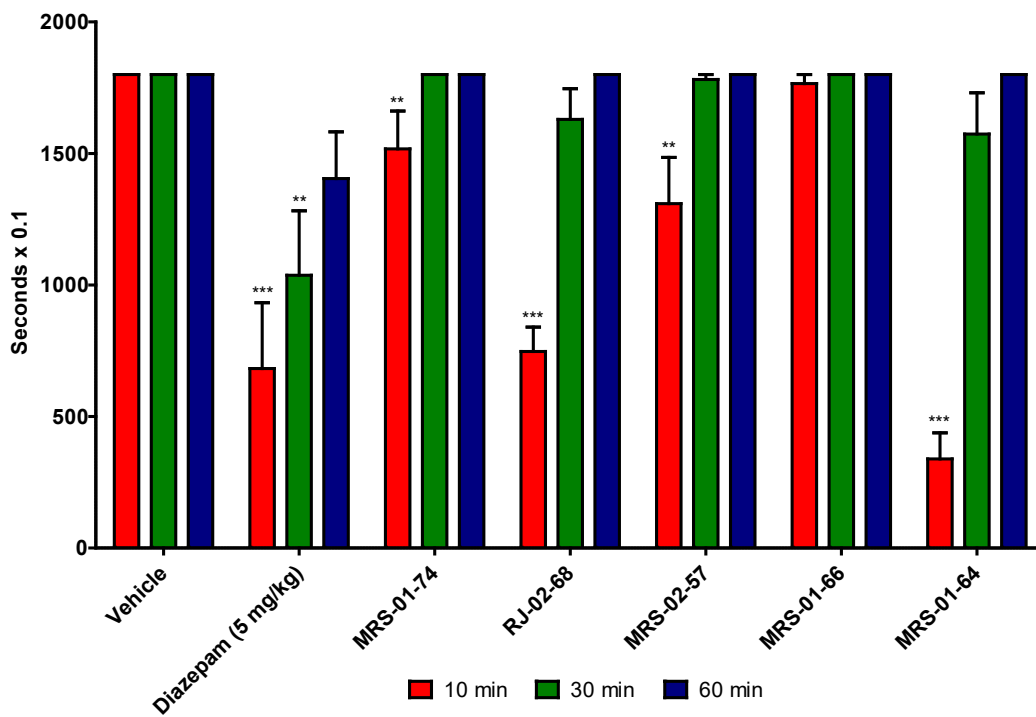


Figure 50. Rotarod Study of Imidazobenzodiazepines with Non-Amide Functionalities Trained mice ($n = 10$) were placed on the RotaRod set at a constant speed of 15 RPM at various time points. Vehicle only was used as a negative control, and 5 mg/kg diazepam was used as a positive control. All compounds were administered i.p. at 40 mg/kg.

The amides investigated in this study induced inhibition of sensorimotor coordination at 40 mg/kg. Compounds MRS-01-74, RJ-02-68, MRS-02-57, and MRS-01-64 reduced the ability of the animal to balance on the rotating rod 10 minutes post-injection (**Figure 50**). At 30 and 60 minutes however, no statistical difference was observed for these compounds in comparison with the vehicle control. MRS-01-66 was the only compound that did not induce sensorimotor inhibition at 10 minutes post injection in addition to the 30 and 60 minute time points.

Additional compounds were investigated that did not contain an amide functionality (**Figure 51**).

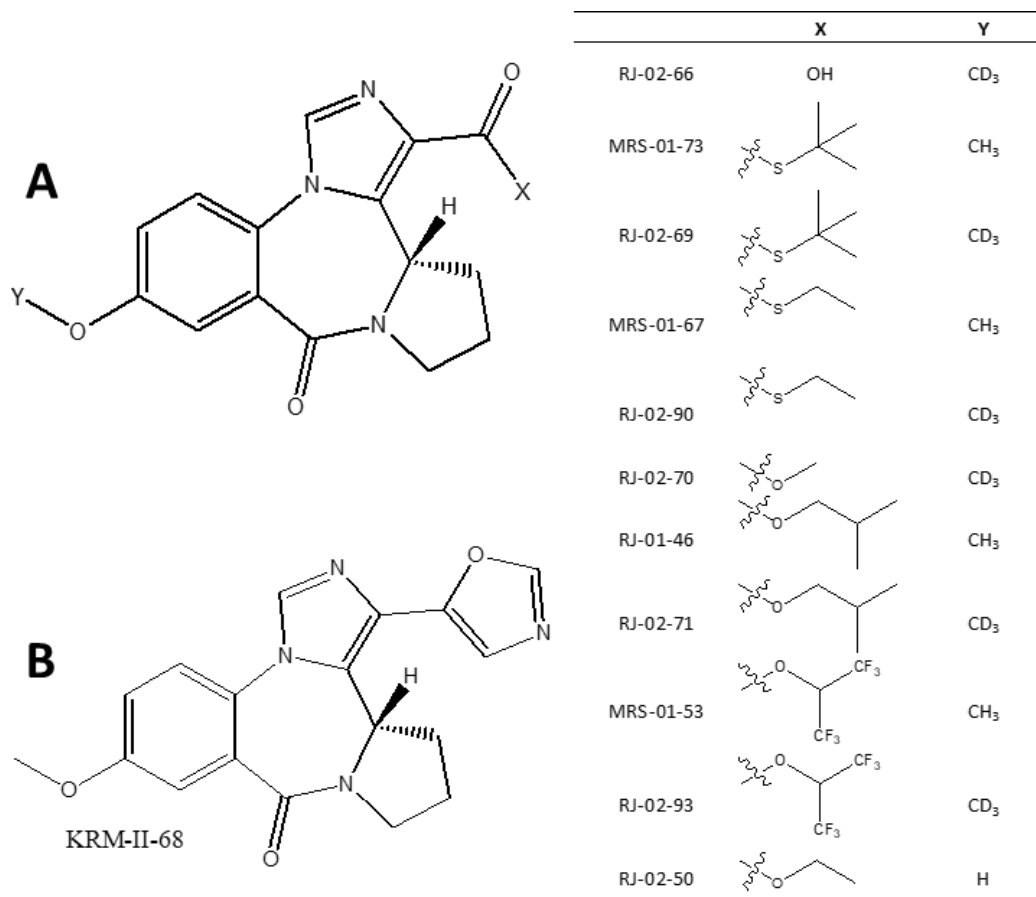


Figure 51. Imidazobenzodiazepines with Non-Amide Functionalities Compounds were synthesized according to published routes by Jahan et al.⁷² (A) Structure of scaffold with indicated X and Y substituents in table to right. (B) Structure of KRM-II-68.

This included RJ-02-66, an acid bearing a deuterated methoxy functionality and deuterated and non-deuterated thioesters MRS-01-73 & RJ-02-69 and MRS-01-67 & RJ-02-90. Furthermore, we investigated deuterated and non-deuterated esters RJ-01-46 & RJ-02-71 and MRS-01-53 & RJ-02-93. Finally, we investigated deuterated methyl ester RJ-02-70, phenolic compound RJ-02-50 and KRM-II-68, an imidazobenzodiazepine with an oxazole functionality. The RotaRod evaluation is depicted in **Figure 52**.

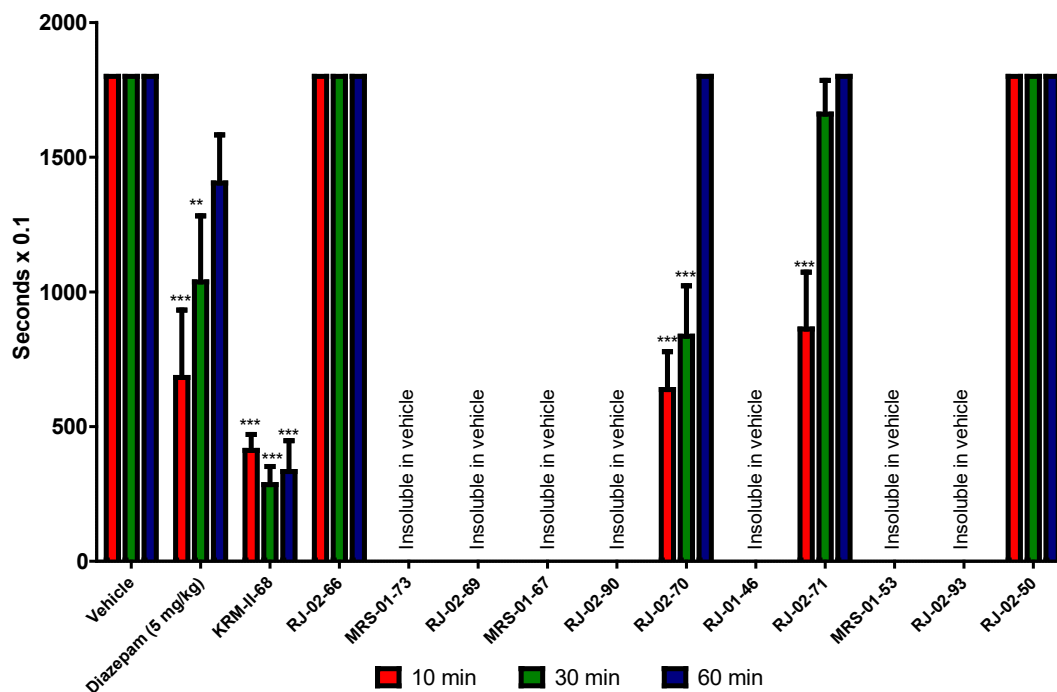


Figure 52. RotaRod of Additional Asthma Compounds Trained mice ($n = 10$) were placed on the RotaRod set at a constant speed of 15 RPM. Vehicle only was used as a negative control, and 5 mg/kg diazepam was used as a positive control. All compounds were administered i.p.. Compounds that were not soluble at an initial concentration of 500 μ M in DMSO were excluded from testing because the resulting suspension was not injectable.

Compounds MRS-01-73, RJ-02-69, MRS-01-67, RJ-02-90, RJ-01-46, MRS-01-53, and RJ-02-93 were not investigated because efforts to dissolve these compounds in DMSO to create an injectable solution were not successful due to low solubility in this vehicle (**Figure 52**). However, acid RJ-02-66 and phenolic compound RJ-02-50 were soluble in the vehicle and induced no measurable sensorimotor inhibition. RJ-02-70 and RJ-02-71 showed adverse effects after 10 and 30 minutes post injection. However, all injected mice successfully balanced on the RotaRod after 60 minutes for both compounds. KRM-II-68 injected mice exhibited very strong sedation and a significant number of them were not able to successfully pass the RotaRod test after 10, 30, and 60 minutes post injection.

3.4.3 Discussion

The improved protocol, which utilized outbred CFW mice tested at various time points after compound administration, was used to investigate imidazobenzodiazepines synthesized by the group of Professor Cook, which were of mutual interest for our collaborative Asthma Project.

Among the amides, MRS-01-66 was selected for further investigation because it was the only compound in the group with no observable CNS effects. Microsomal stability studies confirmed that the lack of CNS effects was not due to rapid metabolism, as 82% of the compound was still remaining after one hour incubation with mouse microsomes.⁷² Among the second group of compounds, RJ-02-66 and RJ-02-50 induced no sensorimotor inhibition at all time points. Even though it did not show any CNS effects, RJ-02-66 was not further investigated because it's the deuterated version of XHE-III-74 Acid, which was already extensively tested *in vitro* and *in vivo*.⁷¹ RJ-02-50 was further investigated due to lack of CNS effects.²³ Again the lack of adverse effects were not a result of rapid metabolism, as microsomal stability studies showed there was 91% of the compound remaining after one hour incubation with mouse microsomes.⁷² RJ-02-50 contains a hydroxyl group instead of a methyl ester that causes partial ionization and hydrogen bonding in water, increasing the hydrophilicity and reduced blood-brain barrier penetration. Pharmacokinetic studies confirmed this hypothesis.²³ KRM-II-68 induced severed CNS effects and will be investigated at a lower dose in the future.

3.5 Conclusion

After many procedural adjustments, the final protocol for the RotaRod assay represents a robust assay that is capable of identifying compounds that do not affect sensorimotor control. Additionally, the data also provide crude information about compound metabolism/elimination in the brain without a full pharmacokinetic study.

Two compounds, MRS-01-66 and RJ-02-50, were identified as potential drug candidates by the rotarod assay due to the lack of adverse CNS effects seen after administration.

The RotaRod assay is still performed by the Arnold Group. Additional changes have been implemented by Nicolas Zahn that include changing the i.p. injection to oral gavage injections to investigate the potential of these compounds to be developed as oral medications.

CHAPTER 4

Using Novel Imidazodiazepines to Reduce Inflammation in Asthma

4.1 Background

Asthma is an increasingly prevalent disease that currently affects approximately 8% of Americans.⁹³⁻⁹⁵ Typically patients present with chest tightness, shortness of breath, wheezing, and/or cough, however symptoms vary widely due to the various genotypes and environmental factors that are not currently well understood.⁹⁴ Most of those patients find relief through inhaled corticosteroids (ICS) for long term control and long-acting β 2-adrenergic agonists (LABAs) to control acute attacks or when ICS are not sufficient.⁹⁶ Generally these treatments are successful, however there are some major drawbacks to extended use. Symptoms can still progress under this course of treatment requiring increased dosages of ICS.⁹⁷ Additionally, up to 5% of cases are steroid resistant.⁹⁷⁻⁹⁸ High doses of steroids are linked to numerous secondary diseases, including osteoporosis and cataracts and growth delay in children.⁹⁹ Due to these factors, there is an unmet need for new categories of asthma treatments.

Inflammation, bronchoconstriction, and increased mucus production are the three hallmark pathophysiological characteristics of asthma.¹³ Many types of immune cells play a role in this pathophysiology, including mast cells, B-cells, neutrophils, epithelial cells, eosinophils, macrophages, and T-lymphocytes.¹³

There are two main classes of T-lymphocytes: CD8⁺ cytotoxic cells and CD4⁺ helper cells (T-helper), which are characterized based on their surface expression of CD8 or CD4¹⁰⁰, which form co-receptors with the T cell receptor to promote T-cell activation.¹⁰⁰⁻¹⁰¹ Antigen activation the T-cell receptor (TCR) triggers many pathways and stimulates calcium to be released from intracellular stores, which further promotes calcium entry through membrane bound store-operated calcium channels.²² This increase in intracellular calcium provides the foundation for a vast majority of inflammatory process mediated by T-cells, such as stabilizing antigen presentation in the short term and inducing pathways that lead to genetic changes, such as induction of cytokine transcription.²²

Functionally, CD8⁺ cells are responsible for cytotoxicity, and have a lesser understood role in asthma pathogenesis.²⁰ While they have been shown to suppress asthma phenotypes such as antigen specific IgE production, other studies have shown CD8⁺ cells increase inflammation and airway hyperresponsiveness.¹⁰²

CD4⁺ T-cells have a better understood role in asthma, and are known to be responsible for perpetuating the inflammatory response by infiltrating the airway and secreting inflammatory mediators, such as cytokines.²⁰ When these cytokines are released, they direct other cell types to mediate many of the diagnostic features of asthma, including increased blood eosinophilia, heightened IgE production by B-cells, and immune cell proliferation.⁹⁴ This wide-ranging inflammatory reaction can be broken down into Th1 and Th2 responses. Th1 responses are characterized by cytokines such as interferon γ (IFN γ), interleukin-2 (IL-2), and lymphotoxin (LT), which promote the cell-mediated immune response.¹⁰³ The Th2 immune response is characterized by production of multiple cytokines: IL-4, IL-5, IL-10, and IL-13, among others.¹⁰³ This response promotes strong antibody responses and eosinophil activation.¹⁰³ Some believe asthma to be an imbalance between Th1 and Th2 responses.¹⁰⁴ There is overwhelming evidence that Th2 cytokines are the main class of cytokines that lead to asthma pathology, however there is some evidence of Th1 cytokines, such as IL-2, are present in bronchoalveolar lavage fluid (BALF) and serum during asthma exacerbations.²¹

Upon activation by an antigen, Th2 cytokine producing T-cells begin recruitment of eosinophils from the bone marrow to the blood and finally to the lung tissues, driven by IL-5.¹⁶ While excessive eosinophilia in the lung correlates with atopy, there is a significant range of blood eosinophil counts among asthmatic patients.¹⁰⁵ During the asthmatic allergic response, matured eosinophils migrate from bone marrow to the lung tissue, are stimulated, and release numerous cytotoxic mediators in a process called degranulation.¹⁶⁻¹⁷ These mediators include Major Basic Protein (MBP) and eosinophil peroxidase, which have both been shown to cause airway hyperresponsiveness (AHR).¹⁶⁻¹⁷ MBP has also been

implicated in the release of histamine through triggering mast cells and basophils, which leads to bronchial hyperreactivity.¹⁷ Eosinophils produce additional cytokines, such as IL-13, which stimulates mucus production from goblet cells.¹⁷

Macrophages are another key immune cell type involved in the asthmatic response. There are three main classes of macrophage in the lung, including bronchial macrophages from sputum, interstitial macrophages in the interstitium, and alveolar macrophages that reside in the alveoli lumen.¹⁰⁶ These classes of macrophages, and many other types throughout the body, can be characterized as M1 or M2 macrophages depending on their role in the inflammatory process. M1 macrophages are polarized by IFN γ and lipopolysaccharide (LPS) and are responsible for the response to intracellular pathogens. On the other hand, M2 macrophages are responsible for phagocytosis of foreign pathogens and apoptotic cells and are polarized by IL-4 and IL-13.¹⁰⁶ M1 macrophages are thought to be more active in non-eosinophilic asthma, however it is not clear which subpopulation is more prevalent in general asthmatics.¹⁰⁶

Macrophages are involved in spreading the inflammatory response.^{18, 106} To promote the inflammatory response, macrophages produce a number of factors that affect numerous other cells types. For example, asthmatic alveolar macrophages are known to have increased NO production compared to their healthy counterparts.¹⁰⁶ The upregulated nitric oxide synthase dependent pathway is responsible for the regulation of T-lymphocyte proliferation and excess NO can reduce the production of inflammatory cytokines from alveolar macrophages as a coping mechanism.¹⁰⁶ However, excess NO can cause vasodilation¹⁸, increase in mucus secretion¹⁸, recruit eosinophils¹⁸, cause cell injury and airway remodeling¹⁹, and eventual steroid resistance.¹⁹ Increased levels of exhaled NO were associated with severe, difficult to treat asthma with accelerated decline in lung function.¹⁹

GABA_ARs have been recently characterized on many cell types related to asthma, including airway smooth muscle cells (ASM)¹⁰⁷ and immune cells such as lymphocytes and macrophages.¹⁴⁻¹⁵ Lymphocytes showed membrane currents and reduced proliferation in the presence of GABA_AR agonists, supporting

the idea that targeting the GABA_AR on macrophages could be anti-inflammatory.¹⁴ Peritoneal macrophages showed reduced levels of cytokine production when treated with GABA, an effect that was reversed by the GABA_AR channel blocker picrotoxin.¹⁵ GABA_AR-mediated signaling has also proven essential in macrophage differentiation.¹⁰⁸

Other Arnold Group members' studies have shown that novel imidazodiazepines are present at high levels in the lung and low levels in the brain after both I.P. administration and oral gavage and can target the GABA_AR subtypes present on ASM and immune cells.^{23-24, 71-72} These compounds are also proven to reduce clinical asthma phenotypes in an ovalbumin-induced murine model of asthma resulting in airway hyperresponsiveness and leukocyte recruitment to the lung.^{23-24, 71-72} In addition to being the most efficacious asthma treatment developed by the group to date²⁴, MIDD0301 was shown to have no adverse immunotoxicological effects over a 28 day period of twice daily dosing.¹⁰⁹

4.2 Targeting GABA_AR on Lymphocytes

4.2.1 Experimental

Cell Culture

Jurkat T-Lymphocytes (ATCC, TIB-152) were maintained in RPMI-1640 (Hyclone, SH30027.01) and supplemented with 10% heat-inactivated FBS (Corning, 35011CV) and 100 U/mL penicillin/100 µg/mL streptomycin (Hyclone, SV30010). Cultures were maintained at 37°C and 5% CO₂. Cultures were passaged when they reached a density of approximately 3x10⁶ cells/mL and resuspended no lower than 100,000 cells/mL.

qPCR

mRNA was collected from 5x10⁶ Jurkat cells using QIAshredder (Qiagen, 79654) and RNeasy Mini Kit (Qiagen, 74104). 20 ng of mRNA per reaction was analyzed using the QuantiFast SYBR Green RT-PCR

kit (Qiagen, 204154) along with the primers listed in **Table 7** according to manual specifications. Data were analyzed by the Delta C_t method.

Table 7. Human GABA_AR Subunit qPCR Primers

GABA _A R Subunit	Forward	Reverse	Size	Ref
GAPDH	ACC ACA GTC CAT GCC ATC AC	TCC ACC ACC CTG TTG CTG TA	452	⁸¹
α1	GGA TTG GGA GAG CGT GTA ACC	TGA AAC GGG TCC GAA ACT G	66	⁸¹
α2	GTT CAA GCT GAA TGC CCA AT	ACC TAG AGC CAT CAG GAG CA	160	⁸¹
α3	CAA CTT GTT TCA GTT CAT TCA TCC TT	CTT GTT TGT GTG ATT ATC ATC TTC TTA GG	102	⁸¹
α4	TTG GGG GTC CTG TTA CAG AAG	TCT GCC TGA AGA ACA CAT CCA	105	⁸¹
α5	CTT CTC GGC GCT GAT AGA GT	CGC TTT TTC TTG ATC TTG GC	105	⁸¹
α6	CTG AAC CTT TGG AAG CTG AGA	TTA TTG GCC TCG GAA GAT GA	109	¹¹⁰
β3	CCG TTC AAA GAG CGA AAG CAA CCG	TCG CCA ATG CCG CCT GAG AC	105	⁸¹
γ2	CAC AGA AAA TGA CGG TGT GG	TCA CCC TCA GGA ACT TTT GG	91	⁸¹

ELISA

10,000 Jurkat cells were plated per well in 200 μL of media in 96 well optical bottom plates (Nunc, 265302) and 0.2 μL of imidazodiazepine compounds in DMSO were added with the Tecan Liquid Handler. After 15 minutes of incubation, cells were activated with a mixture of phytohemagglutinin (1000 μg/mL) (MP Biomedical, 0215188401) and phorbol myristate acetate (50 μg/mL) (Tocris, 1201/1) to a final concentration of 1 μg/mL and 50 ng/mL respectively and incubated for 24 hours at 37°C. Supernatant was analyzed with the BD Human IL-2 ELISA Kit II (BD Biosciences, 550611) following manual instructions.

Intracellular Calcium

Intracellular calcium levels were analyzed with the Fluo-4 NW Calcium Assay Kit (Molecular Probes, F36206). Jurkat cells were collected, resuspended in assay buffer to a density of 5x10⁶ cells/mL, and 25 μL was dispensed per well in 384 well optical bottom plates (Nunc, 142761). It was incubated for 1 hour at 37°C. 25 μL of 2X Fluo-4 NW dye was added to each well and incubated for 30 minutes at 37°C followed by 15 minutes at room temperature. 1 μL Imidazodiazepine solubilized in DMSO and/or 1 μL GABA solubilized in water was added and incubated 15 minutes at room temperature. Immediately

before reading, cells were activated with 2 μ L of a mixture containing phytohemagglutinin (25 μ g/mL) and phorbol myristate acetate (1.25 μ g/mL) for a final concentration in the assay well of 1 μ g/mL and 50 ng/mL respectively. Fluorescence (ex: 494 nm, em: 516 nm) readings were recorded every 10 seconds for 3 minutes.

Primary Murine CD4⁺ T-Lymphocyte Isolation

Animals were housed in specific pathogen free conditions with a 12 hour light and dark cycle and free access to food and water according to UWM IACUC protocols. Spleens were harvested from male BALB/c mice and immediately placed in ice cold PBS and transferred to a biological safety cabinet. Spleens were pressed through 40 μ m cell strainers (Fisher, 22-363-547) with a syringe plunger into 50 mL conical tubes. Sterile PBS (Hyclone, SH30256.01) was used to wash the strainer mesh and collected in the same conical tube. The resulting cell suspension was centrifuged for 5 minutes at 1600 RPM. CD4⁺ T-lymphocytes were separated using the MagniSort Mouse CD4 T cell Enrichment Kit (ThermoFisher, 8804-6821-74) and used immediately following isolation without characterization.

Automated Patch Clamp

All buffers (**Table 2**) were made with the following chemicals: NaCl (Fisher, BP358-1), KCl (Fisher, BP366-1), MgCl₂ (Sigma, M8266), CaCl₂ (Acros Org, 123350025), CsCl (Sigma, 203025), Glucose (Sigma, G0350500), HEPES (Fisher, BP410-500), and EGTA (Sigma, E4378). Buffers were filter sterilized before being stored in autoclaved glass bottles.

Table 8. Automated Patch Clamp Buffer Components

	ECS (M)	ICS (M)
NaCl	0.14	
KCl	0.005	
MgCl ₂	0.001	0.001
CaCl ₂	0.002	0.001
Glucose	0.005	
HEPES	0.01	0.01
KF		
EGTA		0.011
CsCl		0.14
pH	7.4	7.2

The instrumental electrodes were prepared through chlorination before experimentation. 300 μ L of bleach was dispensed into the solid bottom plate in columns 1, 2, 7, and 8. The preset ‘chloride’ protocol was run. After completion, the solid bottom plate was rinsed with deionized water and the same wells were filled with 300 μ L of calcium and magnesium free PBS (Hyclone, SH30256.01). The ‘hydrate’ protocol was run.

The IonFlux plate was gently rinsed three times with deionized water to remove any storage solution from the wells. 250 μ L of MilliQ water was dispensed into every well except the outlet, which received 50 μ L to allow space in the well to collect waste. The ‘water rinse’ protocol was run to ensure the storage solution was removed from the microfluidics. The water was emptied from the plate and dried well by lightly tapping the plate on a paper towel.

Experimental solutions were then distributed into the plate. 250 μ L of ICS was dispensed into each trap, 250 μ L of ECS into the inlet, and 50 μ L of ECS into the outlet to ensure the microfluidics remained wet. Imidazodiazepines were first serially diluted in DMSO, then diluted into ECS to achieve the desired concentration with 0.1% DMSO. 250 μ L of each solution was dispensed into corresponding concentration wells. The ‘prime’ protocol was run.

Primary murine CD4⁺ T-lymphocytes were suspended in ECS at a final density of 5x10⁶ cells/mL and 250 µL was dispensed into each of the eight inlets. The plate was inserted into the instrument and the experiment protocol begun. Voltages and pressures for each phase of the experiment are detailed in

Table 3. Details regarding data analysis can be found in Section 2.3.1.

Table 9. Instrumental Settings for Patch Clamp Experiments

		Pressure	Voltage
Prime	Main Channel	1 PSI, 45 s 0.4 PSI, 10 s	-80 mV, 50 ms -90 mV, 50 ms -80 mV, 50 ms
	Traps	6 PSI, 40 s 1.5 PSI, 15 s 2 PSI, 5 s	
	Compound Wells	6 PSI, 40 s 1.5 PSI, 15 s	
Trap	Main Channel	0.2 PSI, 2 s 0 PSI, 4.2 s 0.35 PSI, 0.8 s (repeat 12 times) 0.2 PSI, 8 s	-80 mV, 20 ms -100 mV, 30 ms
	Traps	5 PSI, 70 s	
	Compound Wells		
Break	Main Channel	0.05 PSI, 25 s	-80 mV, 50 ms -90 mV, 50 ms -80 mV, 50 ms
	Traps	5 PSI, 5 s 10 PSI, 15 s 5 PSI, 5 s	
	Compound Wells		
Data Acquisition	Main Channel	0.15 PSI for duration of experiment	-80 mV, 200 ms -80 mV, 200 ms -90 mV, 200 ms -80 mV, 9850 ms
	Traps	5 PSI for duration of experiment	
	Compound Wells		

Primary Murine Splenocytes

Animals were housed in specific pathogen free conditions with a 12 hour light and dark cycle and free access to food and water according to UWM IACUC protocols. 5 week old male BALB/c mice were sensitized with 1 mg/mL ovalbumin (Sigma, S5253) in PBS (Hyclone, SH30256.01) diluted 1:1 with Imject Alum Adjuvant (Thermo Scientific, 77161) via 100 μ L I.P. injection on days 0 and 7. On days 14 and 16 mice were intranasally challenged with 20 μ L of 2 mg/mL ovalbumin in PBS before euthanasia on day 17.

Spleens were harvested and immediately placed in ice cold PBS, transferred to the biological safety cabinet, and pressed through 40 μ m cell strainers (Fisher, 22-363-547) with a syringe plunger into 50 mL conical tubes. Sterile PBS was used to wash the strainer mesh and collected in the same conical tube. The resulting cell suspension was centrifuged for 5 minutes at 1600 RPM. 2 mL of warmed RBC lysis buffer (0.15 M NH_4Cl , 10 mM KHCO_3 , 0.1 mM Na_2EDTA) was used to resuspend the pellet and was incubated at 37°C for 2 minutes. A minimum of 30 mL of PBS was added and centrifuged at 1600 RPM for 5 minutes. Cells were resuspended in RPMI-1640 (Hyclone, SH30027.01) supplemented with 10% heat-inactivated FBS (Corning, 35011CV), 100 U/mL penicillin/100 μ g/mL streptomycin (Hyclone, SV30010), and 10 μ M 2 β -mercaptoethanol (Sigma Aldrich, M6250). Cultures were maintained at 37°C and 5% CO_2 .

Proliferation Assay

A 1×10^6 cells/mL suspension of primary splenocytes was dispensed at 100 μ L per well in 96 well optical bottom plates (Nunc, 265302) into wells representing non-treated samples. The remaining culture was activated with 100 μ g/mL ovalbumin and dispensed into treated plates. 0.2 μ L of compounds of interest was added with the Tecan Liquid Handler. Plates were incubated for 48 hours then analyzed using Cell Titer Glo (Promega, G7572).

Imidazodiazepine Synthesis

Imidazodiazepines were synthesized by the Prof. James Cook Lab according to established routes.^{23-24, 71-72} The structures of lead compounds are shown in **Figure 53**, and other structures can be found in **Appendix A – Asthma Compound Structures**.

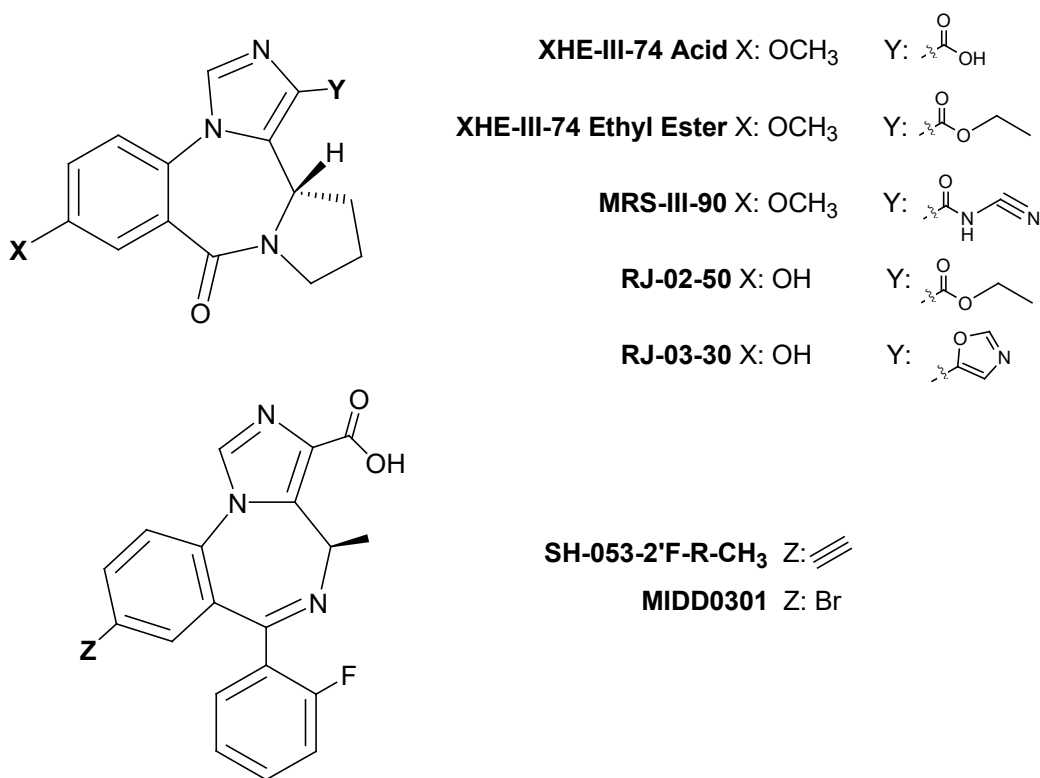


Figure 53. Structures of Novel Imidazodiazepines Identified as Lead Compounds for Potential Asthma Treatments Two different scaffolds were utilized based on previously tested compounds that were determined to be $\alpha 4$ (top) or $\alpha 5$ (bottom) subtype selective GABA_AR modulators.^{111,112}

4.2.2 Results

Lymphocytes Contain GABA_ARs

Jurkat T-lymphocytes have previously been investigated in respect to GABA_AR expression.^{81, 113} Herein, we recapitulated this study and our results are shown in **Figure 54**. Among the alpha subunits, $\alpha 1$ and $\alpha 3$ were most prevalent, with a slightly lower expression of $\alpha 5$ and $\alpha 6$. $\alpha 2$ and $\alpha 4$ had the lowest levels of expression of the alpha subunits. $\beta 3$ was expressed more than $\gamma 2$. While the $\gamma 2$ expression was low, there were all necessary components present to form a functional receptor. Additionally, these results compared well to reported literature values.^{81, 113}

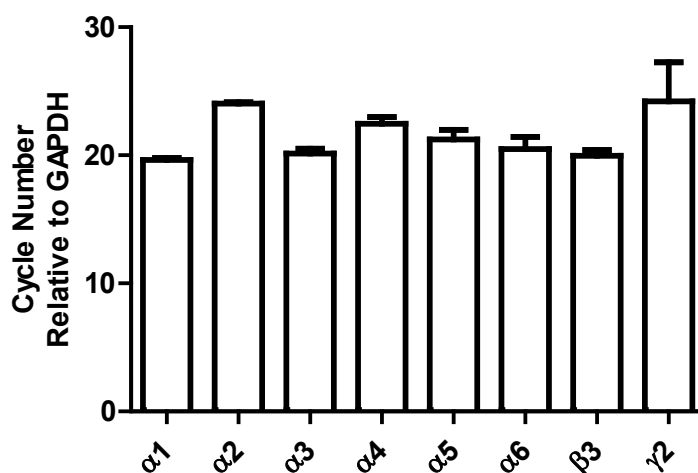


Figure 54. T-Lymphocytes contain GABA_AR mRNA was isolated from Jurkat T-lymphocytes and analyzed via RT-qPCR. Quantification was completed using QuantiFast SYBR green RT-qPCR kit. Cycle numbers from each subunit were normalized to GAPDH using the ΔC_t method.

Functional GABA_AR on Lymphocytes

Primary lymphocytes have also been characterized in terms of GABA_AR subunit composition.⁸¹ To test the functionality of these receptors on lymphocytes, we employed imidazodiazepines that are known to bind GABA_AR. Lymphocytes were isolated from spleens of untreated mice and utilized in the patch clamp assay. Increasing concentrations of GABA resulted in increasing transmembrane currents (**Figure 55**). Normalization of these data to generate the concentration response curve was very difficult however, as the responses in the ECS only and 1 nM GABA applications were too noisy to be used for normalization. Therefore, it was assumed that no true response was occurring through the receptor at GABA concentrations lower than 10 nM, which was then used as the 0% for normalization purposes.

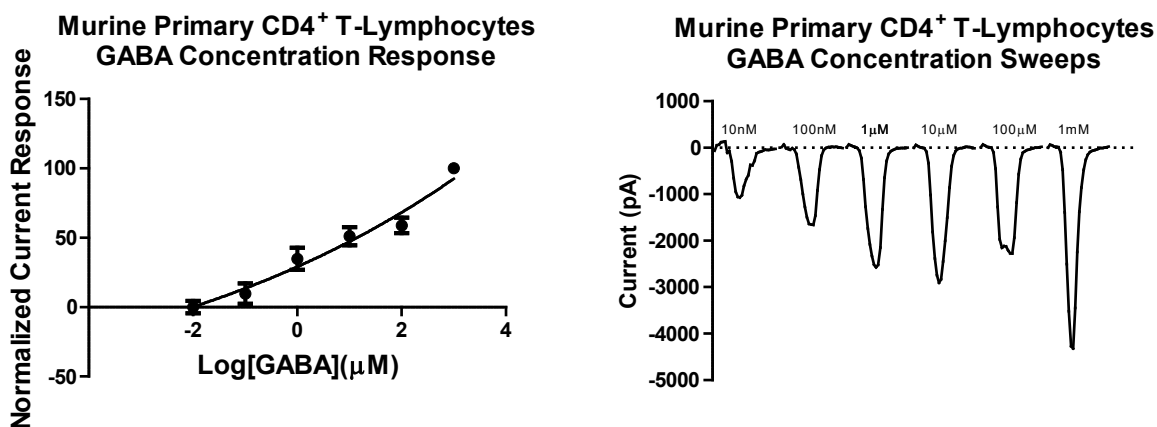


Figure 55. GABA_AR on Lymphocytes are Functional Primary CD4⁺ T-Lymphocytes were isolated from spleens of male BALB/c mice via magnetic negative selection and utilized in the automated patch clamp assay. GABA was applied in concentrations ranging from 10nM to 1mM. Data were normalized such that 0 represents the response to 10nM GABA and 100 represents the response to 1mM GABA.

From the GABA concentration curve shown in **Figure 55**, the EC₂₀ value was determined to be approximately 600 nM. This concentration was used in conjunction with four novel Imidazodiazepines of particular interest, MIDD0301, RJ-03-30, SH-053-2'F-R-CH₃ Acid, and RJ-02-50 (**Figure 56**). Of these compounds, MIDD0301 and RJ-03-30 showed the greatest maximum potentiation at approximately 460% and 400% respectively and similar potency with EC₅₀ values around 10 nM. SH-053-2'F-R-CH₃ and RJ-02-50 were much less efficacious, only eliciting maximum potentiations of 160% and 170% respectively.

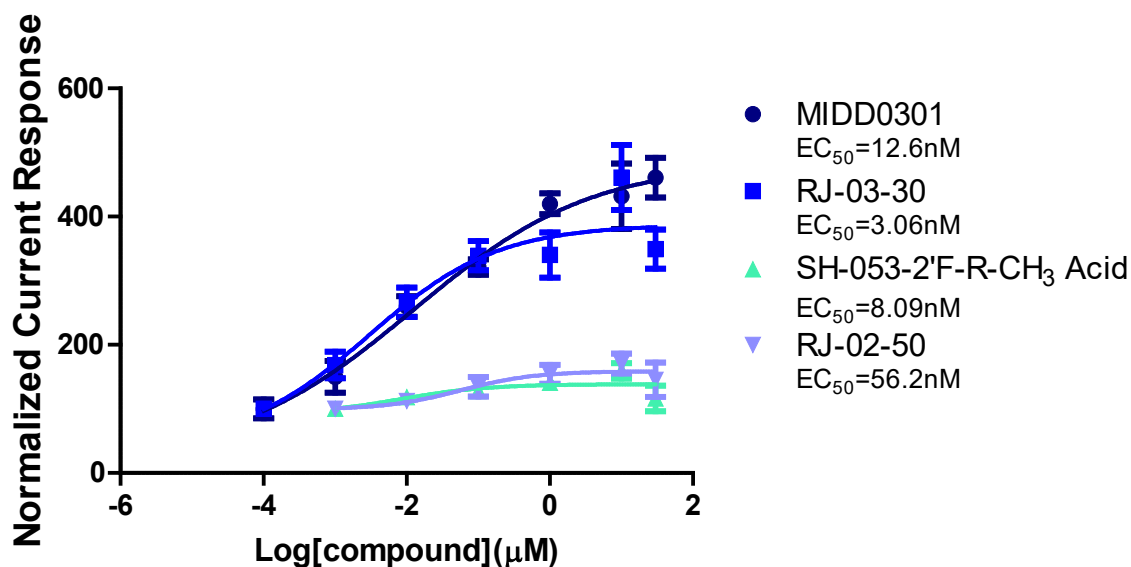


Figure 56. GABA_AR on Lymphocytes can be Modulated by Imidazodiazepines CD4⁺ T-Lymphocytes were isolated from male BALB/c mice via magnetic negative selection. The purified cells were utilized in the patch clamp assay, which tested concentrations of four novel imidazodiazepines ranging from 100nM to 30μM in combination with 600 nM GABA. Responses were normalized such that 100% represented the response to GABA alone.

Both RJ-03-30 and MIDD0301 were dosed for a period of 5 days in the ova S/C murine model of asthma. T-lymphocytes were isolated from spleens of compound treated and untreated mice to compare the sensitivity of the receptors to the compound after chronic treatment. **Figure 57** shows the concentration response curves and transmembrane currents. The difference in the concentration response is mainly due to the noisy baseline making normalization very difficult and inconsistent responses between compound applications, similar to the GABA concentration response. Buffers optimized for lymphocytes may improve the signal to noise ratio and support cell health through the assay.

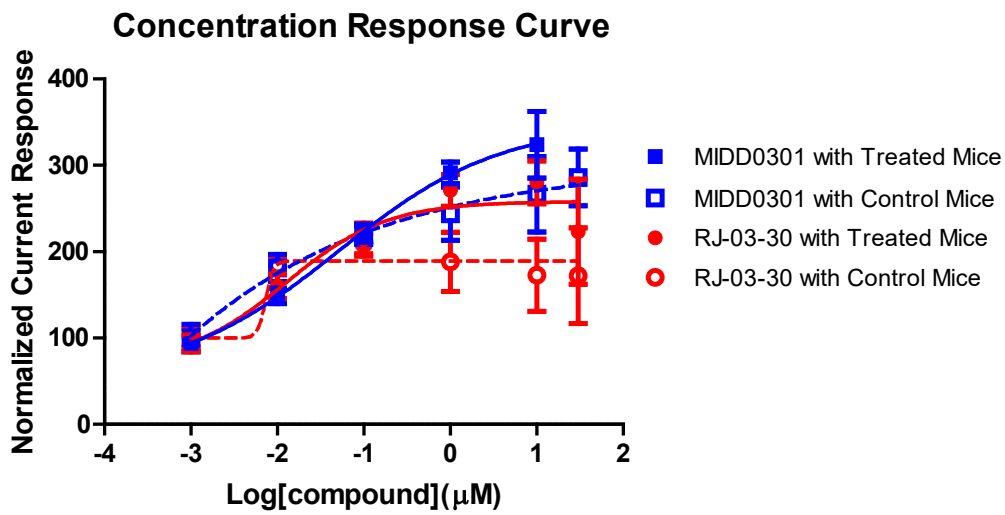
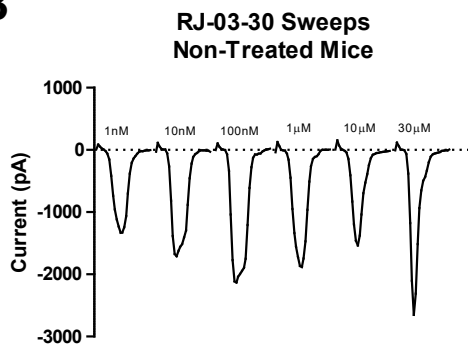
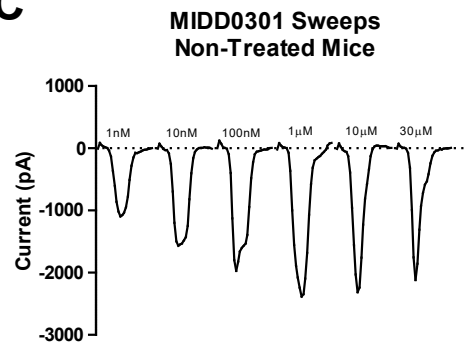
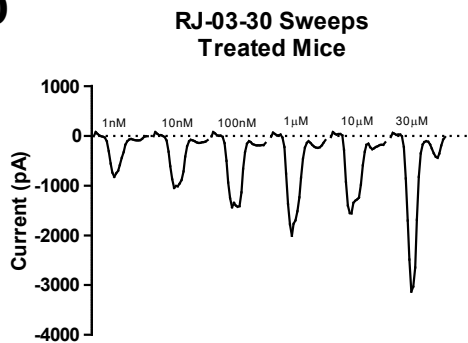
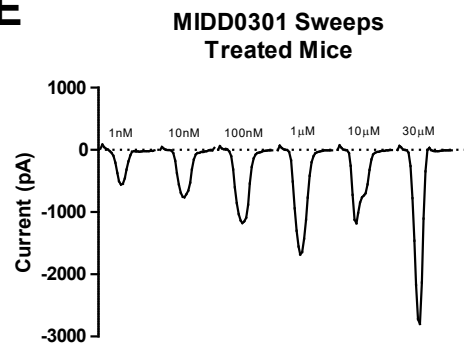
A**B****C****D****E**

Figure 57. Receptors are Still Activated by Modulators after Repeated In Vivo Dosing $CD4^+$ T-Lymphocytes were isolated from male BALB/c mice via magnetic negative selection. The purified cells were utilized in the patch clamp assay, which tested concentrations of four novel imidazodiazepines ranging from 100nM to 30 μM in combination with 600 nM GABA. Responses were normalized such that 100% represented the response to GABA alone.

Targeting GABA_AR on Lymphocytes Generates Anti-Inflammatory Effects

After demonstrating the expression and functionality of GABA_AR, GABA_AR ligands were used to investigate anti-inflammatory effects. Increase of intracellular calcium triggered by PMA and PHA was investigated with increasing concentrations of GABA. Concentrations of more than 1 mM GABA reduced intracellular calcium levels and 100 mM GABA eliminating the acute release of calcium (**Figure 58**).

Calcium Response in Jurkat Cells

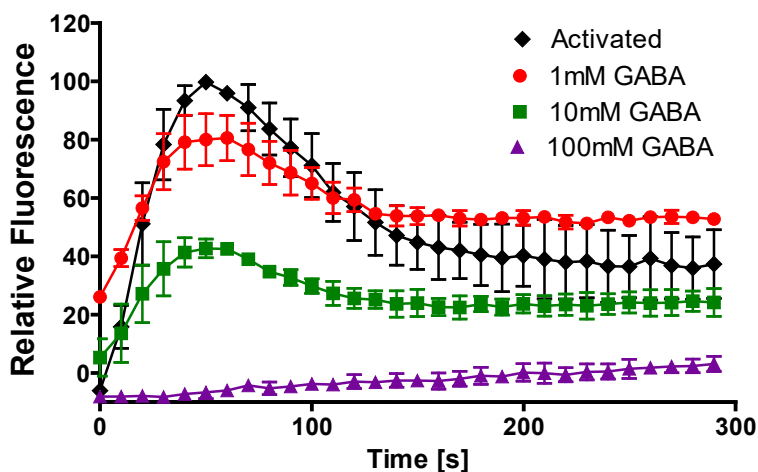


Figure 58. Intracellular Calcium Levels are Reduced by Targeting GABA_AR Intracellular calcium levels were investigated with the Fluo-4 NW Calcium Assay. Jurkat T-lymphocytes were plated, treated 30 minutes prior to reading, and activated immediately before reading with 50ng/mL PMA and 1µg/mL PHA. Fluorescence (ex: 494 nm, em: 516 nm) was recorded over 5 minutes at 10 second intervals. Results were normalized such that 100% represents the maximum response in the activated cells.

Imidazodiazepines XHE-III-74 Acid and XHE-III-74 Ethyl Ester were tested in regard to intracellular calcium reduction. Both compounds were capable of reducing the calcium release in a concentration dependent manner. XHE-III-74 Acid was less potent with an IC₅₀ value of 332.5 nM compared to 25 nM for XHE-III-74 Ethyl Ester. However XHE-III-74 Acid had slightly better efficacy with 76% reduction of intracellular calcium release compared to a 70% reduction with XHE-III-74 Ethyl Ester.

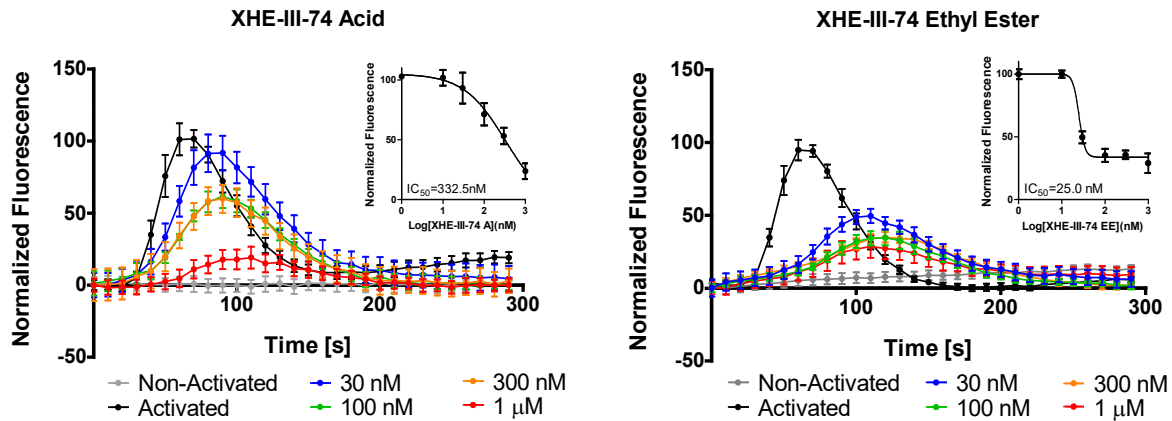


Figure 59. Intracellular Calcium Response in the Presence of Imidazodiazepines Intracellular calcium levels were investigated with the Fluo-4 NW Calcium Assay. Jurkat T-lymphocytes were plated, treated 30 minutes prior to reading, and activated immediately before reading with 50ng/mL PMA and 1μg/mL PHA. Fluorescence (ex: 494 nm, em: 516 nm) was recorded over 5 minutes at 10 second intervals. Results were normalized such that 100% represents the maximum response in the activated cells.

Calcium-dependent cytokine release from lymphocytes is a hallmark sign of inflammation, and IL-2 is implicated in the wide-spread promotion of inflammation across immune cell types.¹¹⁴⁻¹¹⁵ It is also commonly found in exhaled breath condensates in symptomatic asthmatic patients.¹¹⁵ Targeting the GABA_AR with the endogenous ligand GABA did not reduce cytokine production, even at concentrations one hundred times higher than the native GABA concentration in blood of approximately 1 mM¹¹⁶ (Figure 60).

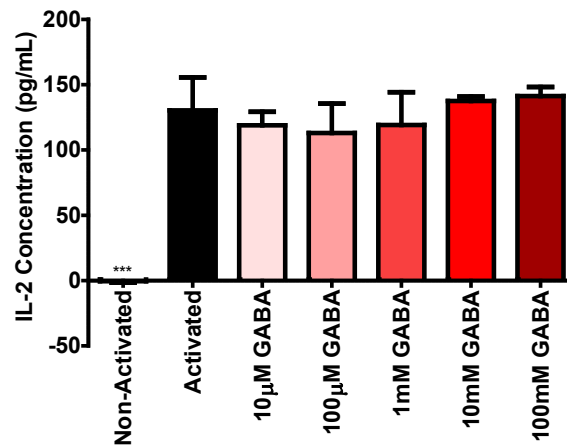


Figure 60. IL-2 Production in the Presence of GABA Jurkat T-lymphocytes were activated with 50 ng/mL PMA and 1 μg/mL PHA, and treated with increasing concentrations of γ-aminobutyric acid (GABA) and incubated for 24 hours. Supernatant was analyzed with the BD Biosciences Human IL-2 ELISA kit.

However, treatment with the imidazodiazepines XHE-III-74 Ethyl Ester (EE) and XHE-III-74 Acid (Acid) reduced the secretion of IL-2 into the supernatant measured by ELISA (**Figure 61**). It was interesting to note that an identical reduction was seen without the co-application of 1mM GABA, which will be discussed further in *4.2.3 Discussion*.

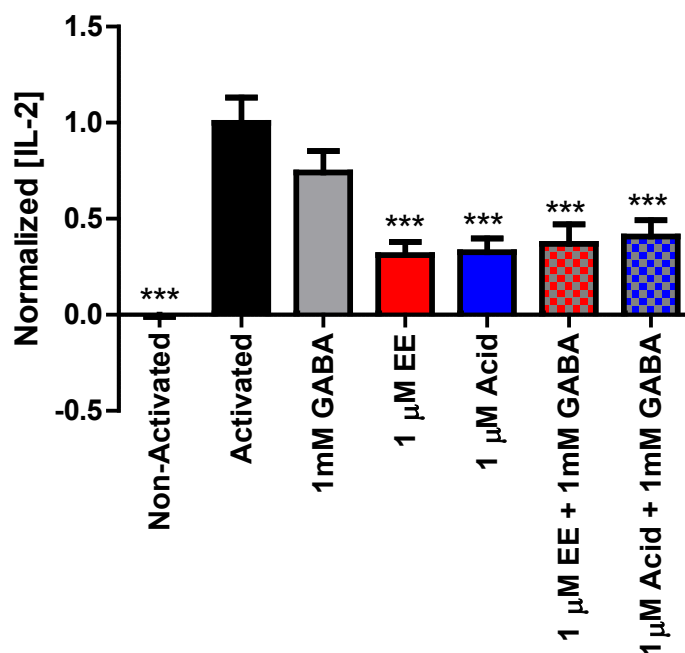


Figure 61. Novel Imidazodiazepines Reduce Cytokine Production Jurkat T-lymphocytes were activated with 50ng/mL PMA and 1 μ g/mL PHA, and treated with XHE-III-74 Ethyl Ester (EE) and XHE-III-74 Acid (Acid) with and without 1mM GABA for 24 hours. Supernatant was analyzed with the BD Biosciences Human IL-2 ELISA kit.

Proliferation of multiple different immune cell types is one of many effects stimulated by IL-2 release. Splenocytes were isolated from spleens from Ova S/C (asthmatic) mice, activated in culture with ovalbumin, and treated with 1 μ M of various imidazodiazepines of interest. Only one compound, MRS-01-64 was capable of reducing proliferation of activated splenocytes measured by the Cell Titer Glo assay. As a control, splenocytes from the same spleens were cultured in parallel, but not activated with ovalbumin to stimulate proliferation. MRS-01-64 showed similar levels of reduction of ATP levels measured by the Cell Titer Glo assay, so it can be determined that toxicity is the cause of the reduction in the activated cells as well.

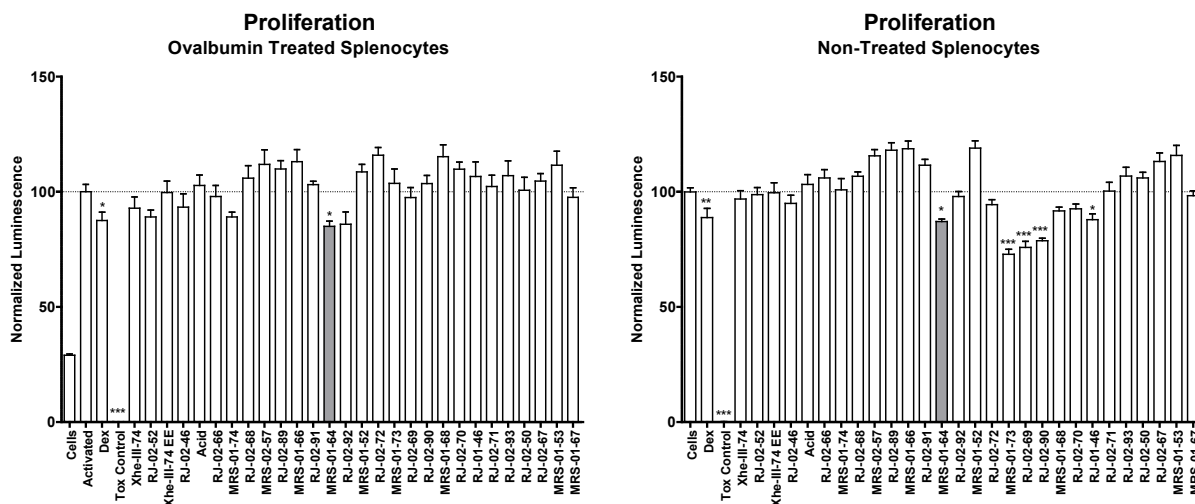


Figure 62. Imidazodiazepines Do Not Reduce Inflammatory Cell Proliferation Splenocytes were isolated from asthmatic mice and cultured with 100 $\mu\text{g}/\text{mL}$ of the allergen ovalbumin (A) or without the allergic stimulus to control for toxicity (B). Cells were incubated in the presence of compounds (1 μM) for 48 hours. ATP levels were quantified by the Cell Titer Glo kit as a measure of proliferation.

4.2.3 Discussion

Previous studies reported the presence of GABA_AR on both primary murine T-lymphocytes and immortalized human T-lymphocyte line Jurkat.⁸¹ The above results agree that the most prevalent subunits in Jurkat T-lymphocytes are the $\alpha 1$, $\alpha 3$, and $\beta 3$ (Figure 54). Though little $\gamma 2$ subunit expression was observed, additional tertiary subunits were reported in the literature.⁸¹

Endogenously expressed GABA_AR were confirmed functional as demonstrated by manual and automated patch clamp. Transmembrane current responses of up to 300 pA after applications of 10 mM GABA and 50 μM of the GABA_AR agonist muscimol were elicited from individual lymphocytes using traditional, manual patch clamp.¹⁴ The current responses from the automated patch clamp experiments with primary murine lymphocytes also support the functionality of GABA_AR on lymphocytes through activation with the native agonist GABA (Figure 55) and with imidazodiazepines (Figure 56), which are positive allosteric modulators that are known to bind to GABA_AR. These novel results show that GABA_AR do not become desensitized after prolonged exposure to these novel imidazodiazepines, as they

continued to respond similarly *in vitro* after one month of repeated *in vivo* treatment (**Figure 57**). Functionally, this suggests that tolerance to these imidazodiazepines is not an expected adverse effect.

Prior to this collaborative project, GABA_AR on immune cells were not being investigated as novel targets for imidazodiazepines to treat asthma, though interest in GABAergic asthma treatments is now growing.¹¹⁷ To investigate whether imidazodiazepines could be anti-inflammatory, intracellular calcium levels were measured as one of the immediate effects of T-cell activation.²² The hypothesis was that depolarizing the cell through GABA_AR would decrease the amount of calcium that would pass into the cell during T-cell activation.^{14, 118} Targeting the GABA_AR with both GABA (**Figure 58**) and novel imidazodiazepines (**Figure 59**) reduced intracellular calcium levels in a dose dependent manner. While the mechanism of this reduction was not investigated, it was hypothesized that the calcium release from the endoplasmic reticulum was inhibited because the reduction was seen in the initial increase in calcium. To determine what aspect of calcium increase was affected, an inhibitor for calcium release-activated channels (CRAC) could be employed to block influx of extracellular calcium.¹¹⁹

Downstream of intracellular calcium increases are multiple genetic changes, such as the onset of cytokine transcription.²² IL-2 was investigated because of its relevance in human asthma²¹ and steroid-resistance¹²⁰. This cytokine was found at reduced levels with the application of novel imidazodiazepines, however it was interesting to note that the same reduction was achieved without the addition of GABA, which is required to be bound to the receptor in order for the modulator to have an effect (**Figure 61**). This suggested either that there was sufficient native GABA to activate GABA_AR or that the compounds triggered a different pathway. Subsequent experiments by Margaret Guthrie determined that 0.847 μM of GABA was present in culture supernatant, therefore negating the need to supplement compound application with GABA.¹²¹ This supports the conclusion that cytokine production can be reduced by targeting GABA_AR with imidazodiazepines.

Another inflammatory effect is the proliferation of immune cells.¹⁰⁰ IL-2 is responsible for the stimulating T-lymphocyte proliferation¹²², and the blockage of intracellular calcium signals has been shown to inhibit proliferation.¹¹⁹ Dionisio *et al* demonstrated that activating the GABA_AR on primary human peripheral lymphocytes with GABA and muscimol decreased PHA-invoked proliferation.¹⁴ Others have shown that diazepam-treated peripheral blood mononuclear cells (which include T-lymphocytes) show reduced IL-2 production and proliferation.¹²³

However, treatment of primary murine splenocytes sensitized *in vivo* and activated *in vitro* with ovalbumin did not result in an increase in proliferation (**Figure 62**). Approximately 21-25% of splenocytes are CD4⁺ T-lymphocytes and an additional 5-14% are CD8⁺ lymphocytes¹²⁴, so a decrease in lymphocyte expansion alone would be expected show a notable difference. However, only one concentration was tested for screening purposes, and the corresponding IL-2 reduction was not confirmed in the primary lymphocytes. A follow-up study was performed *in vivo* by Gloria Forkuo with MIDD0301, which did show reduced proliferation of total inflammatory cells, CD4⁺ T-cells, macrophages, and eosinophils without statistically decreased IL-2 levels or cytotoxicity by flow cytometry.²⁴

4.3 Targeting GABA_AR on Other Immune Cell Types

4.3.1 Experimental

Expression of GABA_AR on Eosinophils

Pure human eosinophils were isolated from approximately 40 mL of whole human blood using the MACSxpress Whole Blood Eosinophil Isolation Kit (Miltenyi Biotec, 130-104-46), which yielded 2.4x10⁶ cells total, purity not determined. mRNA was collected using QIAshredder (Qiagen, 79654) and RNeasy Mini Kit (Qiagen, 74104). 38 ng/rxn of mRNA was analyzed using the QuantiFast SYBR Green RT-PCR kit

(Qiagen, 204154) along with the primers listed in **Table 7** according to manual specifications. Data were analyzed by the Delta C_t method.

Griess Assay

RAW264.7 Murine Macrophages (ATCC, TIB-71) were cultured in non-treated flasks (CellStar, 658195) with DMEM/High Glucose media (Hyclone, SH30243.01) supplemented with 10% heat-inactivated FBS (Corning, 35011CV) and 100 U/mL penicillin/100µg/mL streptomycin (Hyclone, SV30010). Cultures were maintained at 37°C and 5% CO₂. Cultures were passaged when they reached a density of approximately 3x10⁶ cells/mL using cell scrapers (VWR, 10062-906) to lift cells from flask surface and resuspended at densities of approximately 500,000 cells/mL.

80 µL of cell solution was dispensed per well in 384 well optical bottom plates (Nunc, 142761) at a density of 1x10⁶ cells/mL. Cells were activated with 50 ng/mL LPS (Invivogen, NC9836) and 150U/mL IFNγ (R&D Systems, 485MI100). GABA (0.1 µL of 800 µM solution) and compounds (0.1 µL of 16 mM solution in DMSO) were added with the Tecan Liquid Handler. Plates were incubated for 24 hours. Supernatant was removed and analyzed with the Griess Reagent System (Promega, G2930).

4.3.2 Results: Eosinophils

mRNA was collected from primary human eosinophils and examined via RT-qPCR to determine alpha GABA_AR subunit expression. **Figure 63** shows that the α1 and α5 subunits were the most prevalent compared to the other three alpha subunits investigated. α4 and α6 showed particularly low levels. The α3 subunit was not investigated so unfortunately a clear picture of the alpha subtypes could not be determined.

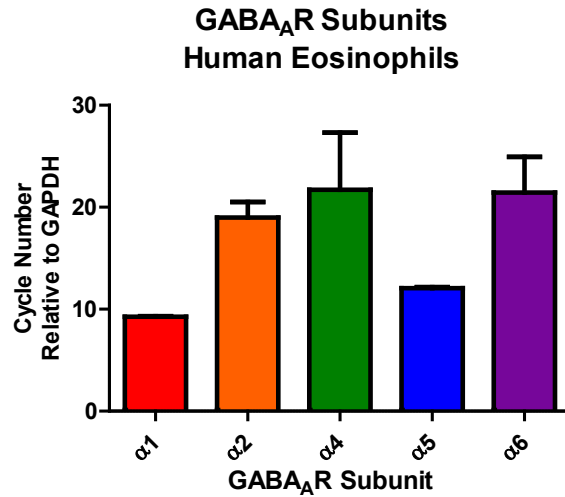


Figure 63. GABA_AR Subunits in Primary Human Eosinophils Eosinophils were isolated from human blood using magnetic negative selection. mRNA was isolated and analyzed using RT-qPCR to identify GABA_AR subunits.

4.3.3 Results: Macrophages

Nitric oxide is one of many mediators secreted by macrophages during an inflammatory response. RAW264.7 mouse macrophages were activated with interferon gamma (IFN γ) and lipopolysaccharide (LPS) and treated with 20 μ M of imidazodiazepines of interest co-applied with 1 μ M GABA. MRS-III-90 showed a 25% reduction in nitric oxide production (**Figure 64**).

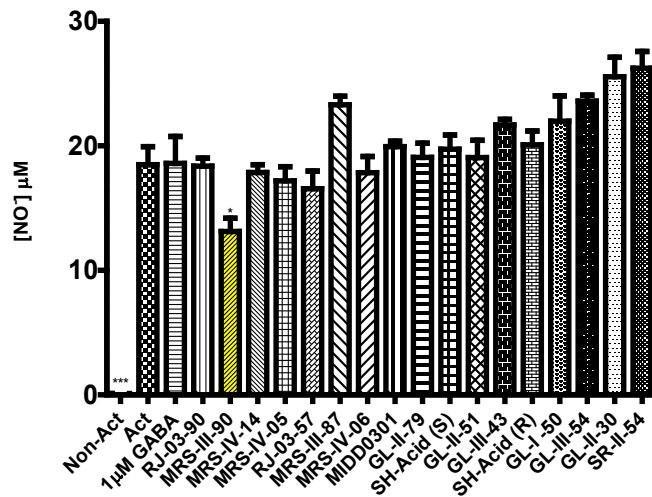


Figure 64. Nitric Oxide Production in Response to Imidazodiazepines RAW264.7 Mouse Macrophages were activated with interferon γ (IFN γ) and lipopolysaccharide (LPS) and treated with 20 μ M of each compound for 24 hours. Supernatant was analyzed with the Griess Assay.

At the time of this screening however, the assay had not yet been combined with the Cell Titer Glo assay to control for toxicity. Studies performed by Michael Rajesh Stephen had not shown toxicity at this concentration in HEK293 cells (data not shown). MRS-III-90 was then tested in concentration response using the RAW264.7 mouse macrophages in both the Griess Assay for nitric oxide production and the Cell Titer Glo assay for cytotoxicity. MRS-III-90 reduced nitric oxide production at 50 μM to similar levels 20 μM . Additionally, no toxicity was observed through the Cell Titer Glo assay, which measures cytotoxicity as a function of ATP production.

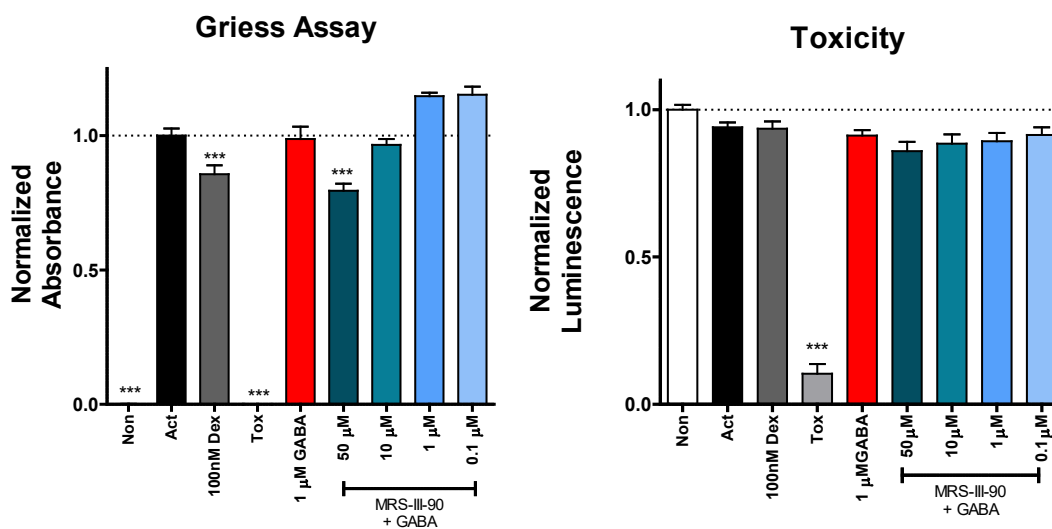


Figure 65. Reduction of Nitric Oxide with MRS-III-90 RAW264.7 Mouse Macrophages were activated with interferon γ (IFN γ) and lipopolysaccharide (LPS) and treated with varying concentrations of MRS-III-90 in combination with 1 μM GABA for 24 hours. Half of the supernatant was removed and analyzed with the Griess Assay. ATP levels were quantified by the Cell Titer Glo kit as a measure of proliferation using the cells and remaining supernatant.

4.3.4 Discussion

Eosinophils and macrophages both play important roles in the asthmatic response. Eosinophils are becoming popular pharmaceutical targets given their key role in asthma pathology, however treatments have been limited to various anti-IL-5 biologics.¹⁷ In terms of GABA $_A$ R immunological research, eosinophils have been greatly overlooked especially given their diagnostic role in asthma. There is

currently no literature describing GABA_AR on eosinophils or attempts to target their GABA_AR. The limited results shown here demonstrate that GABA_AR subunits are present and that the α 1 or α 5 subtype selective compounds could effectively target eosinophils after a full characterization confirms the presence of functional receptors.

Macrophages have received more attention in respect to GABA_AR research. GABA_AR^{108, 125-126} and glutamate decarboxylase (GAD), the enzyme responsible for synthesis of GABA,¹⁰⁸ have been reported on lung macrophages. Monocytes¹²⁷ and peritoneal macrophages¹²⁸ have both shown transmembrane current changes with the application of GABA and other GABA_AR agonists, supporting the idea that the GABA_AR on alveolar macrophages are similarly functional.

However, targeting the GABA_AR on macrophages with novel imidazodiazepines has not been investigated regarding reduction of nitric oxide production, which would in turn affect multiple facets of the inflammatory aspect of asthma. MRS-III-90 was the only compound tested capable of reducing nitric oxide production at a fairly high concentration, though toxicity was not a factor in the reduction. This assay may not be the screening tool to identify new lead compounds, as many of the compounds that showed promising *in vivo* effects, such as SH053-2'-F-R-CH₃ and MIDD0301 had no effect at the relatively high screening concentration of 20 μ M. Changing the assay from LPS/IFN γ stimulated M1-type macrophages to IL-4/IL-13 stimulated M2-type macrophages may also show more promising results due to the uncertainty of the subclass of macrophage that is responsible for asthma resolution.

4.4 Conclusion

Asthma is a disease in which many cells play a role, and effective treatments should be capable of targeting a majority of these players. Imidazodiazepines appear to be a promising new class of asthma therapeutic that can effectively target lymphocytes and cause reductions in intracellular calcium levels and cytokines. Macrophages are also possible targets for imidazodiazepines because one novel

compound MRS-III-90 was capable of reducing nitric oxide output. Further studies need to be done to determine the full mechanism of action in lymphocytes, and the effects imidazodiazepines have on macrophages and eosinophils.

CHAPTER 5

Using Novel Imidazodiazepines to Reduce
Inflammation in Neuropathic Pain

5.1 Background

Neuropathic Pain (NP) is a difficult to treat type of chronic pain occurring in about 7% of the US population¹²⁹. This chronic pain can arise without overt stimulation of associated peripheral sensory endings, and is commonly associated with diabetic neuropathy, HIV infection, post-herpetic neuralgia, chemotherapy treatment for cancer.¹³⁰ Opioids are currently one of the leading NP therapeutic choices, but their use is controversial¹³¹. Additional treatments include tricyclic antidepressants, serotonin-norepinephrine reuptake inhibitors, and anti-epileptics, which are often followed by second-line opioids and topical drugs or third-line strong opioids¹³¹. Patients often see minimal benefit from these drugs however, as less than one-fourth of patients experiencing significant pain relief with these options¹³².

While previously thought to simply function as a scaffold for the neuronal networks, more recent evidence suggests glia contribute to neurological disorders, such as Alzheimer's disease, autism, and chronic pain.²⁶⁻²⁷ Glial have emerged as major target for neurological diseases because they represent 33-66% of the brain by mass.²⁷ There exist three main types of glial cells: microglia, astrocytes, and oligodendrocytes.²⁷

Oligodendrocytes are responsible for myelination of neuronal axons.¹³³ As an example of just how misunderstood glia have historically been, it was not until the 1950's that oligodendrocytes' role in myelination was acknowledged, which had previously been attributed to the axons themselves.¹³³ It was not until the 2010's that oligodendrocytes were credited with additional roles in neuronal maintenance, survival, and adaptation.¹³³ Oligodendrocytes are increasingly being linked to diseases caused by demyelination, such as multiple sclerosis, Alzheimer's disease, and Huntington's disease.¹³⁴

The primary line of defense in the CNS are microglia, the resident macrophages. Because of their role as the CNS immune system, microglia have been implicated in many neuro-inflammatory diseases such as Alzheimer's disease, Parkinson's disease, and multiple sclerosis and neuropathic pain.¹³⁵

Phosphodiesterase inhibitors pentoxifylline and ibudilast and antibiotic minocycline reduce secretion of cytokines and reduce NP in animal and human studies, confirming the role of microglia in NP.³⁰

Upon nerve injury, microglia are activated by extracellular ATP released from damaged cells.²⁸ ATP binds to purigenic receptors, particularly P2X4Rs, which are calcium permeable and promotes calcium entry into the cell.²⁹ This increase in intracellular calcium promotes neuro-inflammation via the release of mediators, such as cytokines, various chemokines, and cytotoxic compounds; substances known to contribute to allodynia, hyperalgesia, and nociception.³⁰⁻³²

One such cytotoxic compound is nitric oxide (NO), synthesized by nitric oxide synthase (NOS) through the conversion of L-arginine to L-citrulline.^{33, 136} During inflammation high amounts of NO are released into the spinal cord, which sensitizes the neurons, reduces firing thresholds, and increases neuronal firing leading to painful sensations.¹³⁶ Confirming the role NO plays in pain, direct injection of NO causes pain, and NOS inhibitors have proven analgesic.¹³⁶

Three different forms of NOS exist: neuronal or nNOS, endothelial or eNOS, and inducible or iNOS. eNOS is mainly expressed in endothelial cells and serves to reduce inflammation, control vascular smooth muscle proliferation, and promote angiogenesis.³³ nNOS is constitutively expressed in certain neurons and plays a role in regulating functions such as learning and memory in the brain.³³ In the spinal cord, nNOS is also constitutively expressed by dorsal horn neurons, and the number of neurons expressing nNOS are greatly increased during inflammation.¹³⁶

iNOS is expressed in immune cells such as macrophages, and it is the only form of NOS to be reported in microglia.³⁴ Activated microglia induce the expression of iNOS that in turn produces large cytotoxic quantities of NO. NO can inhibit many iron-containing enzymes involved in mitochondrial electron transport and DNA replication.³³ Direct contact between DNA and NO can cause DNA damage and cell death.³³ Additional cytotoxic effects can occur when NO reacts with $O_2^{\cdot-}$ and forms peroxynitrite.³³

Among glial cells, astrocytes are the most abundant subset representing up to 50% of the population.¹³⁷ The main role of astrocytes in the healthy CNS is to support and nourish the neural network, providing the link between the neurons and the blood supply.¹³⁷ Once activated however, astrocytes become hypertrophic and produce large amounts of glial fibrillary acidic protein (GFAP), which is a key factor in mitosis, cell-cell communication, and cellular repair after CNS injury.¹³⁸ Interestingly, GFAP upregulation has been linked to nitric oxide signaling, which is one of the many pathways primary-responding microglia activate and recruit astrocytes to aid in the immune response.¹³⁸

Functional γ -aminobutyric acid type A receptors (GABA_AR), which are well-characterized in neurons, have recently been discovered on glial cells. Currently only α 1, α 3, and β 1 subunits have been described in mouse microglia¹¹, however it has been established that GABA_AR in microglia can mediate immune suppressive signaling.¹³⁹ The role of glial GABAergic signaling has been better studied in astrocytes. Astrocytes contain an isoform of the enzyme responsible for synthesizing GABA, glutamic acid decarboxylase (GAD67)¹¹ and GABA_AR subunits.^{11, 140} One group further showed that expression is not uniform across individual cells.¹⁴⁰ The most commonly found GABA_AR subunits in freshly isolated murine astrocytes included α 2 and α 5, β 1, and γ 1 and γ 3.¹⁴⁰ In contrast, primary human astrocytes express α 1 along with high levels of α 3 and β 1.¹¹ This suggests that GABA_AR subunit expression is highly variable, both between and within species.

Astrocyte GABA_AR have also been shown to be functional via manual patch clamp. Primary murine astrocytes produced large inward currents when treated with muscimol, a GABA agonist, which were blocked by bicuculline, a GABA binding site antagonist.¹⁴⁰ Additional studies in rat primary astrocytes confirmed functioning GABA_AR with agonists GABA and muscimol and antagonists bicuculline and picrotoxin.¹⁴¹ GABA elicited currents were potentiated by diazepam¹⁴¹, indicating that targeting the benzodiazepine site can also modulate astrocytes.

Previous anti-inflammatory studies with novel imidazodiazepines have shown that these compounds are capable of reducing alveolar macrophage populations.²³⁻²⁴ There is evidence that resident macrophage populations, including alveolar macrophages and microglia, arise early in development from common progenitors in the yolk sack distinct from circulating macrophage precursors.²⁵ Additionally, previous research with $\alpha 2/\alpha 3$ -subtype GABA_AR positive allosteric modulators has shown these novel imidazodiazepines are analgesic.^{142,70} Taken together, these research results suggest that novel imidazodiazepines are capable of reducing inflammation by targeting microglia, which in turn have shown to mediate neuropathic pain.

5.2 Targeting GABA_AR on Astrocytes

5.2.1 Experimental

Cell Culture

DI TNC1 cells (ATCC, CRL-2005) were cultured in cell culture treated flasks (Nunc, 156472) with DMEM/High Glucose media (Hyclone, SH30243.01) supplemented with 10% heat-inactivated FBS (Corning, 35011CV) and 100 U/mL penicillin/100 μ g/mL streptomycin (Hyclone, SV30010), and Normocin (Invivogen, ant-nr). Cultures were maintained at 37°C and 5% CO₂. Cultures were passaged when they reached a density of approximately 750,000 cells/mL and resuspended at densities no lower than 100,000 cells/mL.

qPCR

mRNA was collected from 5x10⁶ cells using QIAshredder (Qiagen, 79654) and RNeasy Mini Kit (Qiagen, 74104). 50 ng/rxn of Astrocyte mRNA and 10 ng/rxn of Whole Brain mRNA (BioChain, R1434035-50) was analyzed using the QuantiFast SYBR Green RT-PCR kit (Qiagen, 204154) along with the primers listed in **Table 10** according to manual specifications. Data were analyzed by the Delta C_t method.

Table 10. Rat GABA_AR Subunit RT-qPCR Primers

GABA _A R Subunit	Forward	Reverse	Size	Ref
α1	CTCCTACAGCAACCAAGCTATACCC	GCGGTTTTGTCTCAGGCTTGAC	115	84
α2	AAG AGA AAG GCT CCG TCA TG	GCT TCT TGT TTG GTT CTG GAG TAG	135	84
α3	ACAAGCCACCACCTTCAACATAG	AGGTCTTGGTCTCAGCAGGA	176	84
α4	GATGTCAACAGCAGAACTGAGGTG	TTGTGCCAGATCCAGAAGGTGGTG	346	84
α5	GCCTTGAAGCAGCTAAAATC	GAAGTCTTCTCCTCAGATGCTCT	179	84
α6	CACTCTGACTCCAAGTACCATCTG	GTACACAAGGTTGAATCCTG	222	84
β1	ACAACAGGGGCATATCCACG	CAGTGTGGAGGGCATGTAGG	93	143
β2	TGTCAACAAGATGGACCCACA	ATGCTGGAGGCATCATAGGC	135	143
β3	CCTACTAGCACCGATGGATGTT	GATGCTTCTGTCTCCCATGTAC	163	84
γ1	AAACATGGGTCTTGGCACCT	ATTACTGTGGGTCTCACGCC	118	143
γ2	CGCTCTACCCAGGCTTCACTAGC	TCGGGCCGAAGTTTGTGTCGT	157	84
γ3	GAGGCTCACTGGATCACCAC	GGGGTAGCCATAGCTAGAGA	168	143
δ	GCGCCAGAGCAATGAATGAC	GCGTAGCCCTCCATTAGTCC	94	143
GAPDH	CAAGTTCAACGGCACAGTCAAG	ACATACTCAGCACCAGCATCAC	123	144

Imidazodiazepine Synthesis

MP-III-080 was synthesized by the Prof. James Cook Lab according to established routes.¹⁴⁵

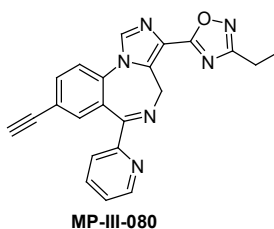


Figure 66. Structure of MP-III-080 MP-III-080 was synthesized by Mike Poe of the Prof. Cook Lab according to established routes.¹⁴⁵

Automated Patch Clamp

All buffers (**Table 2**) were made with the following chemicals: NaCl (Fisher, BP358-1), KCl (Fisher, BP366-1), MgCl₂ (Sigma, M8266), CaCl₂ (Acros Org, 123350025), CsCl (Sigma, 203025), Glucose (Sigma, G0350500), HEPES (Fisher, BP410-500), and EGTA (Sigma, E4378). Buffers were filter sterilized before being stored in autoclaved glass bottles.

Table 11. Automated Patch Clamp Buffer Components

	ECS (M)	ICS (M)
NaCl	0.14	
KCl	0.005	
MgCl ₂	0.001	0.001
CaCl ₂	0.002	0.001
Glucose	0.005	
HEPES	0.01	0.01
EGTA		0.011
CsCl		0.14
pH	7.4	7.2

The instrumental electrodes were prepared through chlorination before experimentation. 300 μ L of bleach was dispensed into the solid bottom plate in columns 1, 2, 7, and 8. The preset ‘chloride’ protocol was run. After completion, the solid bottom plate was rinsed with deionized water and the same wells were filled with 300 μ L of calcium and magnesium free PBS (Hyclone, SH30256.01). The ‘hydrate’ protocol was run.

The IonFlux plate was gently rinsed three times with deionized water to remove any storage solution from the wells. 250 μ L of MilliQ water was dispensed into every well except the outlet, which received 50 μ L to allow space in the well to collect waste. The ‘water rinse’ protocol was run to ensure the storage solution was removed from the microfluidics. The water was emptied from the plate and dried well by lightly tapping the plate on a paper towel.

Experimental solutions were then distributed into the plate. 250 μ L of ICS was dispensed into each trap, 250 μ L of ECS into the inlet, and 50 μ L of ECS into the outlet to ensure the microfluidics remained wet. Imidazodiazepines were first serially diluted in DMSO, then into ECS to achieve the desired concentration with 0.1% DMSO. 250 μ L of each solution was dispensed into corresponding concentration wells. The ‘prime’ protocol was run.

Astrocytes were suspended in ECS at a final density of 5×10^6 cells/mL and 250 μ L was dispensed into each of the eight inlets. The plate was inserted into the instrument and the experiment protocol

begun. Voltages and pressures for each phase of the experiment are detailed in **Table 3**. Details regarding data analysis can be found in Section 2.3.1.

Table 12. Instrumental Settings for Patch Clamp Experiments

		Pressure	Voltage
Prime	Main Channel	1 PSI, 45 s 0.4 PSI, 10 s	-80 mV, 50 ms -90 mV, 50 ms -80 mV, 50 ms
	Traps	6 PSI, 40 s 1.5 PSI, 15 s 2 PSI, 5 s	
	Compound Wells	6 PSI, 40 s 1.5 PSI, 15 s	
Trap	Main Channel	0.2 PSI, 2 s 0 PSI, 4.2 s 0.35 PSI, 0.8 s (repeat 12 times) 0.2 PSI, 8 s	-80 mV, 20 ms -100 mV, 30 ms
	Traps	5 PSI, 70 s	
Break	Main Channel	0.05 PSI, 25 s	-80 mV, 50 ms -90 mV, 50 ms -80 mV, 50 ms
	Traps	5 PSI, 5 s 10 PSI, 15 s 5 PSI, 5 s	
Data Acquisition	Main Channel	0.15 PSI for duration of experiment	-80 mV, 200 ms -80 mV, 200 ms -90 mV, 200 ms -80 mV, 9850 ms
	Traps	5 PSI for duration of experiment	

5.2.2 Results

RT-qPCR was employed to investigate whether or not the rat astrocyte line DI-TNC1 contained sufficient GABA_AR subunits to form a functional receptor. Whole rat brain RNA was used for comparison. The results can be seen in **Figure 67**. Overall, astrocytes showed a lower expression of GABA_AR than the whole brain as expected, however adequate subunits were found to form a functional receptor. All α subunits were present, with the exception of $\alpha 4$. $\beta 2$ and $\beta 3$ were found as well as all three γ subunits and

δ to complete the receptor. There appeared to be fairly uniform expression of the α subunits, though the $\alpha 5$ showed slightly lower expression than the others.

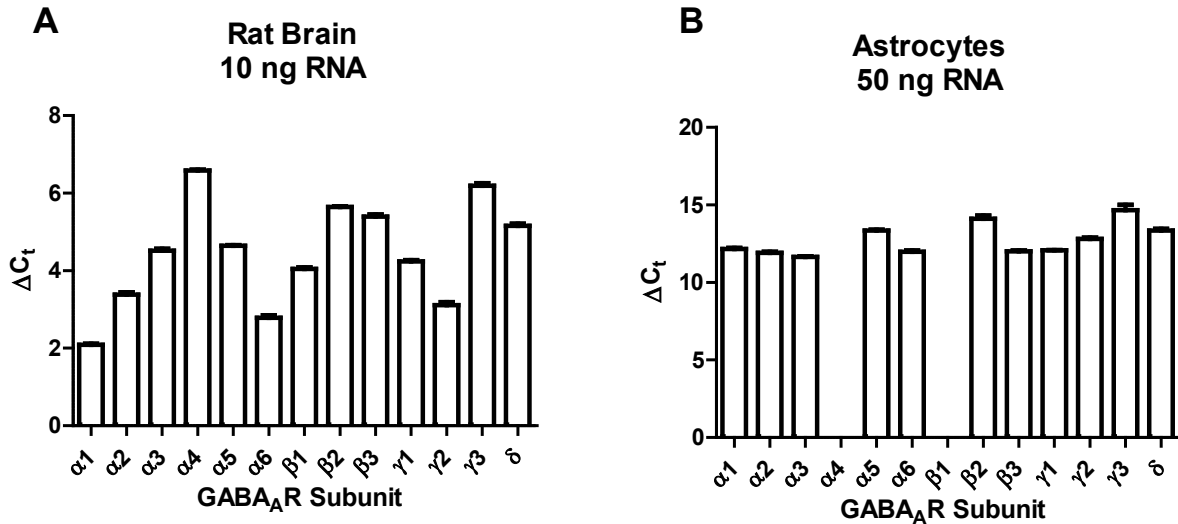


Figure 67. Rat Astrocytes Contain GABA_AR mRNA was isolated from DI TNC1 Rat Astrocytes and whole rat brain. 10 ng of mRNA was used to assess GABA_AR subunits in whole rat brain due to the expected high expression. 50 ng of mRNA was used for rat astrocytes due to unknown expression. Quantification was completed using QuantiFast SYBR green RT-qPCR kit. Cycle numbers for each subunit were normalized to GAPDH using the ΔC_t method.

Because there was sufficient transcription of GABA_AR subunit mRNA, automated patch clamp was utilized to determine if the receptors were functional. Concentrations of GABA ranging from 1 nM to 1 mM were applied to the astrocytes, which resulted in a concentration response curve with an EC₅₀ of 70.3 nM and an approximate maximum potentiation of -1000pA (**Figure 68**).

As with previous patch clamp experiments, positive currents were seen in buffer only applications and low concentrations of GABA. Extensive troubleshooting (detailed in Section 2.3.4) was performed to address this problem in other cell lines with little success. However, the increasing currents with increasing GABA concentration confirms that the GABA_AR are functional.

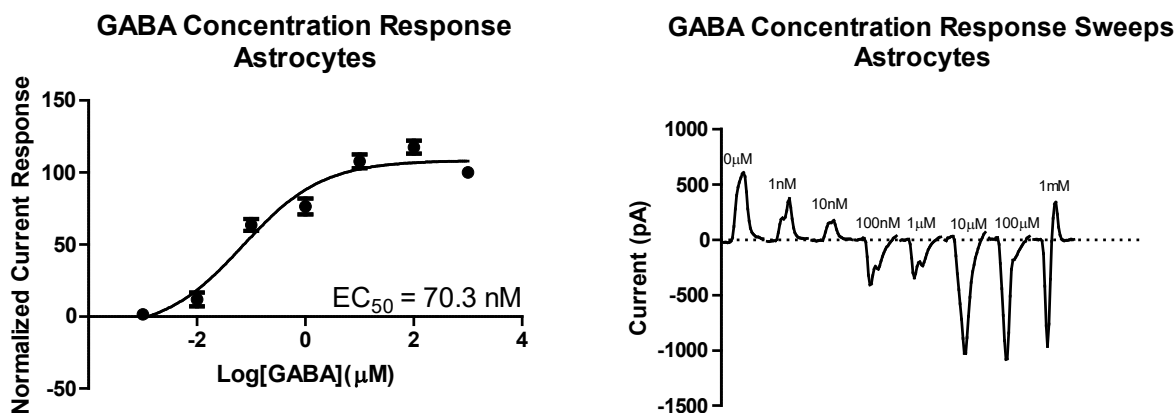


Figure 68. GABA_AR on Rat Astrocytes are Functional Astrocytes were analyzed in the patch clamp assay with increasing concentrations of GABA ranging from 1 nM to 1 mM. Data were normalized such that 0 represented the response to ECS buffer only applications and 100 represents the response to 1 mM GABA.

Currents through GABA_AR generated by the endogenous ligand can be further potentiated with imidazodiazepines. MP-III-080 was developed as an $\alpha 2/3$ selective compound for neuropathic pain¹⁴⁶ that could also effectively target the receptors shown to be present in astrocytes. **Figure 69** shows that MP-III-080 potentiates the transmembrane current elicited by 10 nM GABA to a maximum current of -1100pA and an EC₅₀ of 0.29 μ M.

The positive currents made normalization of the concentration response difficult. It was assumed that the response to 0.1 nM MP-III-080 did not represent any potentiation beyond that of GABA alone for normalization purposes, however the lack of negative currents seen in this application also hindered proper normalization. Increasing currents were seen with increasing concentrations that confirmed that the receptor could be allosterically modulated by $\alpha 2/\alpha 3$ subtype selective imidazodiazepines.

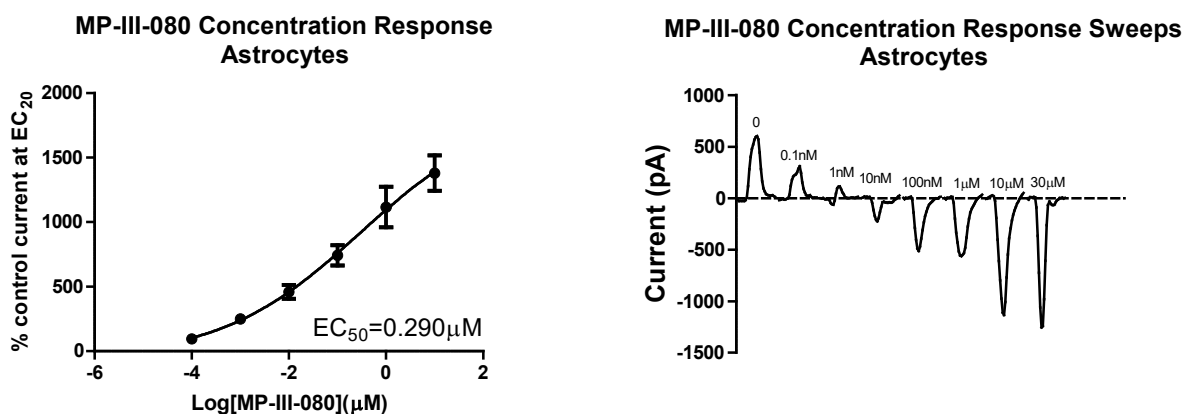


Figure 69. Imidazodiazepines can Potentiate GABA-induced Currents in Rat Astrocytes MP-III-080 was co-applied with 10 nM GABA in concentrations ranging from 0.1 nM to 30 μM. Responses were normalized such that 100 represented the response to 0.1 nM MP-III-080.

5.2.3 Discussion

GABA_AR expression has been reported to be highly variable within and between species^{11, 140}, with no subunits standing out as the most common. The findings in **Figure 67** show that there are sufficient GABA_AR subunits expressed to assemble a functional GABA_AR. Interestingly, the β1 subunit was not identified but reported in the literature.^{11, 140}

The induction of transmembrane current with the endogenous ligand was also consistent with literature reports¹⁴⁰⁻¹⁴¹, however modulating GABA-induced currents with novel benzodiazepines had not previously been reported. MP-III-080 was capable of significantly potentiating GABA-induced currents in rat astrocytes, however EC₅₀ calculations were less reliable due to occurring positive currents.

Additionally, current responses to 10 nM GABA were not consistent, which further complicated the measurement of MP-III-080. The inconsistency was observed using identical conditions for the same IonFlux plate. Even though the current sweeps confirm that the response returns to baseline during the washout period after a GABA application, it is hypothesized that repeated applications sensitize the cells and results in more negative responses compared to initial applications of the same concentration.

To overcome this problem, troubleshooting independent of the stable cell line project needs to be completed for glial patch clamp experiments to address the positive currents seen in applications of buffer only, GABA, and low modulator concentrations. This should most likely include buffer changes and assay format changes.

5.3 Targeting GABA_AR on Microglia

5.3.1 Experimental

Cell Culture

HMC3 Microglia (CRL-3304) were maintained in cell culture treated flasks (Nunc, 156472) with EMEM (Corning, 10010CV) supplemented with 10% heat-inactivated FBS (Corning, 35011CV) and 100 U/mL penicillin/100µg/mL streptomycin (Hyclone, SV30010). Cultures were maintained at 37°C and 5% CO₂. When they reached a cell density of 7x10⁴ cells/mL, cultures were passaged with 0.25% Trypsin (Corning, 25-053-CI) and resuspended to a density no lower than 1x10⁴ cells/mL.

Human and mouse microglia cell lines were a gift from Dr. David Alvarez-Carbonell at Case Western Reserve University.¹⁴⁷ Microglia were cultured in cell culture treated flasks (Nunc, 156472) with DME/F12 media (Hyclone, SH30023.01) supplemented with 10% heat-inactivated FBS (Corning, 35011CV), 100 U/mL penicillin/100µg/mL streptomycin (Hyclone, SV30010), and Normocin (Invivogen, ant-nr). Cultures were maintained at 37°C and 5% CO₂. Cultures were passaged with 0.25% Trypsin (Corning, 25-053-CI) when they reached a density of approximately 500,000 cells/mL and resuspended at densities no lower than 50,000 cells/mL.

RAW264.7 Murine Macrophages (ATCC, TIB-71) were cultured in non-treated flasks (CellStar, 658195) with DMEM/High Glucose media (Hyclone, SH30243.01) supplemented with supplemented with 10% heat-inactivated FBS (Corning, 35011CV), 100 U/mL penicillin/100µg/mL streptomycin (Hyclone,

SV30010), and Normocin (Invivogen, ant-nr). Cultures were maintained at 37°C and 5% CO₂. Cells were passaged when they reached a density of approximately 3x10⁶ cells/mL using cell scrapers (VWR, 10062-906) to lift cells from flask surface and resuspended at densities of approximately 500,000 cells/mL.

GABA_AR Subunit RT-qPCR

mRNA was collected from 5x10⁶ microglia cells or 23.5 mg of brain tissue from female CFW mice (Charles River, 024CFW) using QIAshredder (Qiagen, 79654) and RNeasy Mini Kit (Qiagen, 74104). Human whole brain RNA was purchased (BioChain, R1434035-50). 50 ng/rxn of Microglial mRNA and 10 ng/rxn of whole brain mRNA was analyzed using the QuantiFast SYBR Green RT-PCR kit (Qiagen, 204154) along with the primers listed in **Table 13** and **Table 14** according to manual specifications. Data were analyzed by the Delta C_t method.

Table 13. Human GABA_AR Subunit qPCR Primers

GABA _A R Subunit	Forward	Reverse	Size	Ref
GAPDH	ACC ACA GTC CAT GCC ATC AC	TCC ACC ACC CTG TTG CTG TA	452	81
α1	GGA TTG GGA GAG CGT GTA ACC	TGA AAC GGG TCC GAA ACT G	66	81
α2	GTT CAA GCT GAA TGC CCA AT	ACC TAG AGC CAT CAG GAG CA	160	81
α3	CAA CTT GTT TCA GTT CAT TCA TCC TT	CTT GTT TGT GTG ATT ATC ATC TTC TTA GG	102	81
α4	TTG GGG GTC CTG TTA CAG AAG	TCT GCC TGA AGA ACA CAT CCA	105	81
α5	CTT CTC GGC GCT GAT AGA GT	CGC TTT TTC TTG ATC TTG GC	105	81
α6	CTG AAC CTT TGG AAG CTG AGA	TTA TTG GCC TCG GAA GAT GA	109	110
β1	CCA GGT CGA CGC CCA CGG TA	GTG GCC TTG GGG TCG CTC AC	102	81
β2	GCA GAG TGT CAA TGA CCC TAG T	GGC AAT GTC AAT GTT CAT CCC	137	81
β3	CCG TTC AAA GAG CGA AAG CAA CCG	TCG CCA ATG CCG CCT GAG AC	105	81
γ1	CCT TTT CTT CTG CGG AGT CAA	CAT CTG CCT TAT CAA CAC AGT TTC C	91	81
γ2	CAC AGA AAA TGA CGG TGT GG	TCA CCC TCA GGA ACT TTT GG	136	81
γ3	AAC CAA CCA CCA CGA AGA AGA	CCT CAT GTC CAG GAG GGA AT	113/131	81
δ	GAG GCC AAC ATG GAG TAC AC	TTC ACG ATG AAG GTG TCG G	145	113

Table 14. Mouse GABA_AR Subunit RT-qPCR Primers

GABA _A R Subunit	Forward	Reverse	Size	Ref
α1	CAA GAG CAG AAG TTG TCT ATG AGT	GCA CGG CAG ATA TGT TTG AAT AAC	215	148
α2	GCT ACG CTT ACA CAA CCT CAG A	GAC TGG CCC AGC AAA TCA TAC T	115	148
α3	GCC GTC TGT TAT GCC TTT GTA TTT	TTC TTC ATC TCC AGG GCC TCT	119	149
α4	AGA ACT CAA AGG ACG AGA AAT TGT	TTC ACT TCT GTA ACA GGA CCC C	118	81
α5	AAG TTC GCT CCG GCA GTA TG	TGT TCT TGC CTC CAA CTT GAT CT	209/149	149
α6	CTT GCT GGA AGG CTA TGA CAA C	AAG TCT GGC GGA AGA AAA CAT C	146	149
β1	GGT TTG TTG TGC ACA CAG CTC C	ATG CTG GCG ACA TCG ATC CGC	153	81
β2	GCT GGT GAG GAA ATC TCG GTC CC	CAT GCG CAC GGC GTA CCA AA	70	81
β3	CTT TGC GGG AGG AAG GCT TT	GGG GTC GTT TAC GCT CTG AG	85	149
γ1	ATC CAC TCT CAT TCC CAT GAA CAG C	ACA GAA AAA GCT AGT ACA GTC TTT GC	100	81
γ2	ACT TCT GGT GAC TAT GTG GTG AT	GGC AGG AAC AGC ATC CTT ATT G	147	148
γ3	ATT ACA TCC AGA TTC CAC AAG ATG	CAC AGG TGT CCT CAA ATT CCT	149	81
δ	TCA AAT CGG CTG GCC AGT TCC C	GCA CGG CTG CCT GGC TAA TCC	147	150
GAPDH	AAC ACA GTC CAT GCC ATC AC	CAC CAC CCT GTT GCT GTA GCC	450	81

Imidazodiazepine Synthesis

Imidazodiazepines were synthesized by the Prof. James Cook Lab according to established routes.^{145, 151} The structures of lead compounds are shown in **Figure 70**, and other structures can be found in Appendix B.

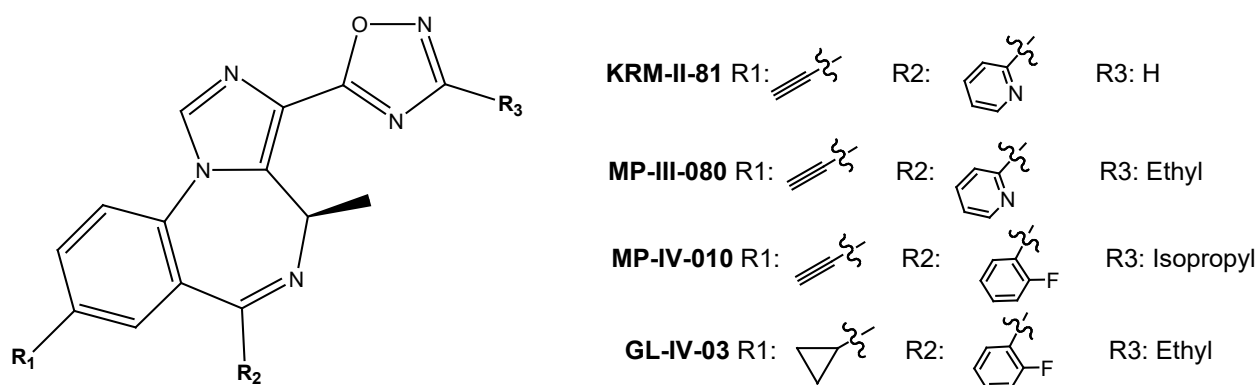


Figure 70. Structure of Lead Compounds for Neuropathic Pain Compounds were synthesized by Mike Poe and Guanguan Li of the Prof. Cook Lab according to established routes.^{145, 151}

Automated Patch Clamp

All buffers (**Table 15**) were made with the following chemicals: NaCl (Fisher, BP358-1), KCl (Fisher, BP366-1), MgCl₂ (Sigma, M8266), CaCl₂ (Acros Org, 123350025), CsCl (Sigma, 203025), Glucose (Sigma,

G0350500), HEPES (Fisher, BP410-500), and EGTA (Sigma, E4378). Buffers were filter sterilized before being stored in autoclaved glass bottles. α 4 buffers were used for all experiments except where noted.

Table 15. Automated Patch Clamp Buffer Components

	α 4 Buffers		IonFlux Buffers	
	ECS (M)	ICS (M)	ECS (M)	ICS (M)
NaCl	0.14		0.138	0.015
KCl	0.005		0.004	0.06
MgCl ₂	0.001	0.001	0.001	
CaCl ₂	0.002	0.001	0.0018	
Glucose	0.005		0.0056	0.005
HEPES	0.01	0.01	0.01	0.005
EGTA		0.011		
CsCl		0.14		
KF				0.07
pH	7.4	7.2	7.4	7.25

The instrumental electrodes were prepared through chlorination before experimentation. 300 μ L of bleach was dispensed into the solid bottom plate in columns 1, 2, 7, and 8. The preset ‘chloride’ protocol was run. After completion, the solid bottom plate was rinsed with deionized water and the same wells were filled with 300 μ L of calcium and magnesium free PBS (Hyclone, SH30256.01). The ‘hydrate’ protocol was run.

The IonFlux plate was gently rinsed three times with deionized water to remove any storage solution from the wells. 250 μ L of MilliQ water was dispensed into every well except the outlet, which received 50 μ L to allow space in the well to collect waste. The ‘water rinse’ protocol was run to ensure the storage solution was removed from the microfluidics. The water was emptied from the plate and dried well by lightly tapping the plate on a paper towel.

Experimental solutions were then distributed into the plate. 250 μ L of ICS was dispensed into each trap, 250 μ L of ECS into the inlet, and 50 μ L of ECS into the outlet to ensure the microfluidics remained wet. Imidazodiazepines were first serial diluted in DMSO, then into ECS to achieve the desired

concentration with 0.1% DMSO. 250 μ L of each solution was dispensed into corresponding concentration wells. The 'prime' protocol was run.

Microglia were suspended in ECS at a final density of 5×10^6 cells/mL and 250 μ L was dispensed into each of the eight inlets. The plate was inserted into the instrument and the experiment protocol begun. Voltages and pressures for each phase of the experiment are detailed in **Table 3**. Details regarding data analysis can be found in Section 2.3.1.

Rotarod

6 week old, female CFW mice were purchased from Charles River (Wilmington, MA). They were trained to run on the RotaRod apparatus for 3 minutes at a constant speed of 15 RPM. When a mouse completed three consecutive trials on different days without falling, the training was completed. Training typically took two weeks.

After training was complete, compound testing was started using groups of ten animals. 40 mg/kg was used as an initial dose. If no sensorimotor effects were seen the dosage was increased. Compounds were administered via 100 μ L oral gavage using a vehicle consisting of 2% hydroxypropyl methycellulose (Sigma Aldrich, H9262-25G) and 2.5% polyethylene glycol (Sigma Aldrich, 06855). Mice were placed on the rod at various times post-injection. If a mouse fell before the three minutes were completed, it was placed on the rod again. If a mouse fell for the second time the time of the fall was recorded. Mice were allowed a minimum of two days between compounds or dosages to ensure complete clearance of the compound.

Psychoactive Drug Screening Program

Detailed protocols for the primary and secondary radioligand binding assays can be found in the National Institute of Mental Health's Psychoactive Drug Screening Program (NIMH PDSP) Assay Protocol Book.¹⁵²

Briefly, compounds are submitted to the PDSP. Primary radioligand binding assays are run at 10 μ M in quadruplicate screening against approximately 50 receptors. Compounds that show greater than 50% inhibition of radioligand binding (greater than 50% binding of compound) at a certain receptor are tagged for secondary assays.

Secondary binding assays are run for each receptor identified in the primary screen. Eleven concentrations ranging from 0.1 nM to 10 μ M are tested in triplicate alongside a known reference compound. The total amount of radioligand bound after incubation is quantified and graphed in a concentration response. The lower the amount of radioactive ligand bound, the higher the amount of compound is bound.

Intracellular Calcium Assay

Cells were collected, spun down, and resuspended in culture media at a concentration of 400,000 cells/mL. 50 μ L of culture was dispensed per well in a 96 well optical bottom plate and cells were allowed to attach overnight. The following day, the Fluo-4 Calcium Kit (Invitrogen, Carlsbad, CA) was used to analyze calcium response following the non-adherent cell line protocol to avoid media exchange. Briefly, 50 μ L of dye mix was added to all wells and incubated for 1 hour at 37°C, then for 45 minutes at room temperature. 500 μ M GABA in MilliQ water and appropriate concentrations of compounds of interest in DMSO were added to the plate via TECAN automated liquid handling robot (0.2 μ L transferred) and incubated for 15 minutes at room temperature for a total room temperature incubation of 1 hour. Individual rows were activated with 2 μ L of 2.5 mM ATP (50 μ M final concentration), immediately placed

in TECAN Infinite M1000 plate reader. Fluorescence (ex: 494 nm, em: 516 nm) was tracked every 10 seconds for 5 minutes.

Nitric Oxide Production (Griess Assay) and Toxicity

80 μ L of mouse microglia culture (1×10^6 cells/mL) was plated in sterile 384 well plates representing non-activated wells. The remaining culture was activated with 50 ng/mL LPS (Invivogen, NC9836) and 150 U/mL IFN γ (R&D Systems, 485MI100) and distributed into the 384 well plate. 0.1 μ L of 800 μ M GABA diluted in MilliQ water (final concentration of 1 μ M) and appropriate concentrations of compounds of interest diluted in DMSO were added via TECAN automated liquid handling robot. Assay plate was incubated for approximately 24 hours (unless otherwise noted) at 37°C, spun down, and 40 μ L of supernatant was removed to a new plate for analysis by the Griess Assay (Promega, Madison, WI). Absorbance at 530 nm was measured using a TECAN Infinite M1000 plate reader. The remaining 40 μ L containing cells was analyzed for toxicity by the Cell Titer-Glo Assay (Promega, Madison, WI). Luminescence was read using a TECAN Infinite M1000 plate reader.

Cell Titer Blue Cytotoxicity

25 μ L of mouse microglia culture (1×10^6 cells/mL) was plated in sterile 384 well plates representing non-activated wells. Compound was solubilized in DMSO to a final concentration of 50 mM and diluted appropriately with DMSO into the drug plate. Compounds were added to the assay plate with the TECAN automated liquid handling robot with a final DMSO concentration of 0.4%. Assay plate was incubated for 24 hours at 37°C. 20 μ L of Cell Titer Blue reagent was added to each well, briefly shaken, and incubated for 3 hours. Fluorescence (ex: 560 nm/em: 590 nm) was read using a TECAN Infinite M1000 plate reader.

iNOS RT-qPCR

1x10⁶ mouse microglia cells were plated in 6 well plates (VWR, 10062-892) in 1-2 mL of media, activated with 50 ng/mL LPS (Invivogen, NC9836) and 150 U/mL IFN γ (R&D Systems, 485MI100), and treated with compounds of interest. Final DMSO concentration did not exceed 0.1%. Plates were incubated for stated times at 37°C and 5% CO₂. mRNA was collected using QIAshredder (Qiagen, 79654) and RNeasy Mini Kit (Qiagen, 74104). mRNA was analyzed using the QuantiFast SYBR Green RT-PCR kit (Qiagen, 204154) along with iNOS primers (F: 5' – ACA TCA GGT CGG CCA TCA CT – 3', R: 5' – CGT ACC GGA TGA GCT GTG AAT – 3'). Expected product size was 87 bp.

iNOS Activity Assay

Cells were activated with 50 ng/mL LPS (Invivogen, NC9836) and 150 U/mL IFN γ (R&D Systems, 485MI100), and treated with compounds of interest in 6 well plates for 2 or 24 hours. Final DMSO concentration did not exceed 0.1%. Protein was collected, quantified, and analyzed with the Nitric Oxide Synthase Activity kit (Abcam, ab211083) with minor alterations to the established protocol. Briefly, protein was incubated with cofactors and substrates in 96 well plates for 2.5 hours at 37°C and 5% CO₂. Enhancer was added to each well and incubated for 10 minutes before Griess reagents were added and incubated. Absorbance (λ : 540nm) was measured using a TECAN Infinite M1000 plate reader.

iNOS ELISA

Mouse microglia (2 mL of 500,000 cells/mL cell solution) were activated with 50 ng/mL LPS (Invivogen, NC9836) and 150 U/mL IFN γ (R&D Systems, 485MI100), and treated with compounds of interest in 6 well plates (VWR, 10062-892) for 24 hours. Final DMSO concentration did not exceed 0.1%. Protein was collected, quantified with the Pierce Rapid Gold BCA Protein Assay Kit (Thermo Scientific,

A53227) and 50 $\mu\text{g}/\text{mL}$ was analyzed with the Mouse iNOS ELISA kit (ABCAM, ab253219). Absorbance (λ : 450 nm) was measured using a TECAN Infinite M1000 plate reader.

5.3.2 Results

Human Microglia Contain Functional GABA_AR

HMC3 human microglia cells were utilized with the automated patch clamp assay to determine if GABA could generate transmembrane current, which would suggest functional receptors present. While the same positive currents appeared in buffer only and 1 nM GABA applications, increasing transmembrane current was observed (**Figure 71**). The maximum current achieved in the presence of 1 mM GABA was approximately -800 pA, and an EC_{50} of 0.31 μM was observed.

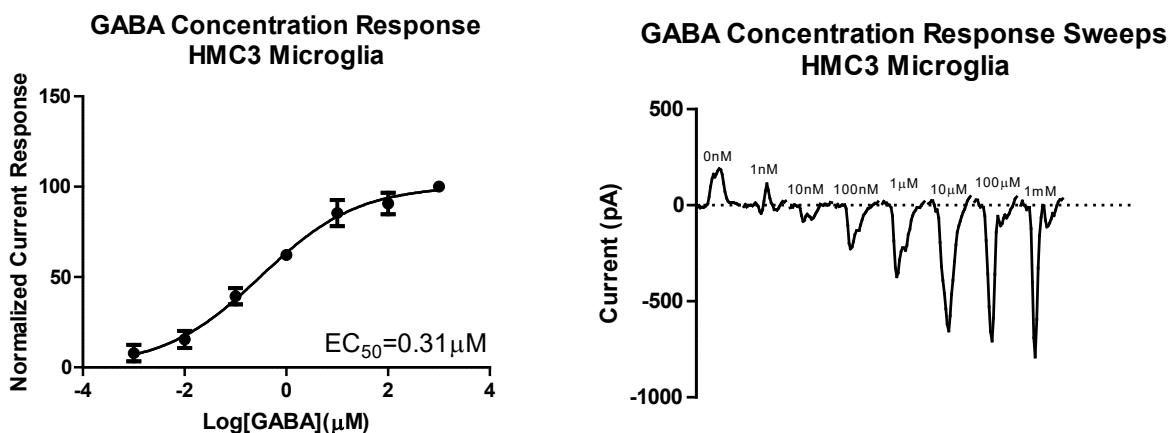


Figure 71. GABA_AR on Human Microglia are Functional HMC3 Microglia were analyzed in the patch clamp assay with increasing concentrations of GABA ranging from 1 nM to 1 mM in IonFlux Buffers. Data were normalized such that 0 represented the response to 1 nM GABA applications and 100 represents the response to 1 mM GABA.

Because the microglia responded to GABA, KRM-II-81, a modulator known to attenuate chronic pain⁷⁰, was co-applied with GABA. The GABA induced current was potentiated 650% reaching a maximum current of approximately -650 pA (**Figure 72**). This confirms that microglia can be modulated with imidazodiazepines, and suggests that there are GABA_AR present in microglia.

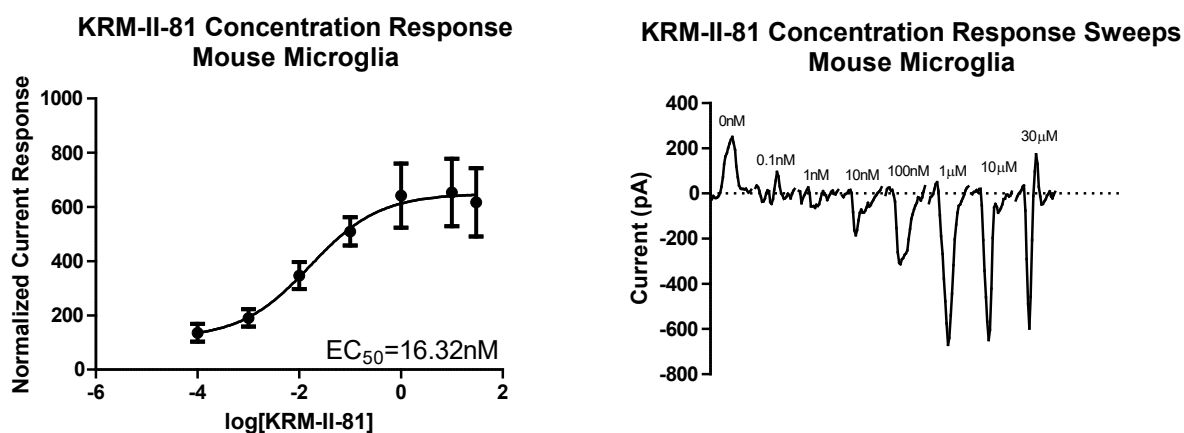


Figure 72. Imidazodiazepines can Potentiate GABA-induced Currents in HMC3 Human Microglia KRM-II-81 was co-applied with 100 nM GABA in concentrations ranging from 0.1 nM to 30 μ M in IonFlux Buffers. Responses were normalized such that 100 represented the response to 1 nM MP-III-080 applications.

However, evidence in the literature called into question that HMC3 cells (Also called CHME-5 cells) are of human origin, so a group at Case Western Reserve University immortalized human and mouse microglia.¹⁴⁷ Before testing novel imidazodiazepines with these cells, characterization of the GABA_AR present needed to be completed, shown in **Figure 73**. Human microglia contained all α subunits but the $\alpha 3$ subunit was by far the most prevalent. $\beta 1$ was present along with the tertiary subunits $\gamma 2$ and δ needed to complete the receptor. In contrast, the $\alpha 1$ is the most prevalent and $\alpha 3$ represented the second lowest expression of the α subunits in the entire brain together with β , γ , and δ subunits. Thus, human microglia express a much more distinct subset of GABA_AR subunits than neurons.

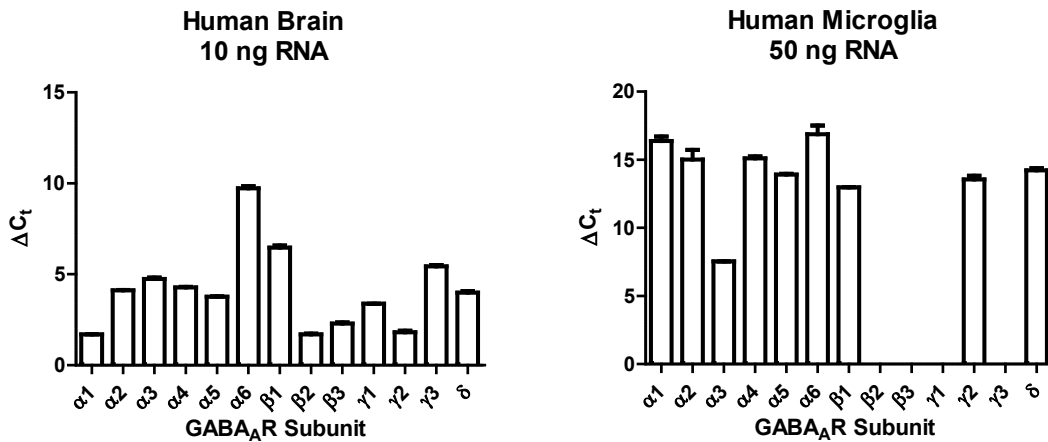


Figure 73. Immortalized Human Microglia Contain GABA_AR mRNA was isolated from human microglia immortalized at Case Western University¹⁴⁷ and whole human brain. 10 ng of mRNA was used to assess GABA_AR subunits in whole brain due to the expected high expression. 50 ng of mRNA was used for microglia due to unknown expression. Quantification was completed using QuantiFast SYBR green RT-qPCR kit. Cycle numbers for each subunit were normalized to GAPDH using the ΔC_t method.

The GABA_AR expressed in microglia were tested for functionality using automated patch clamp. Again, positive currents appeared in low concentration applications and a very noisy baseline (**Figure 74**). The noisy baseline is most likely due to non-optimized buffers and might be improved with ion concentration changes. Increasing concentrations of GABA did increase transmembrane currents, with the maximum current reaching -1200 pA and a calculated EC₅₀ of 15.74 μ M.

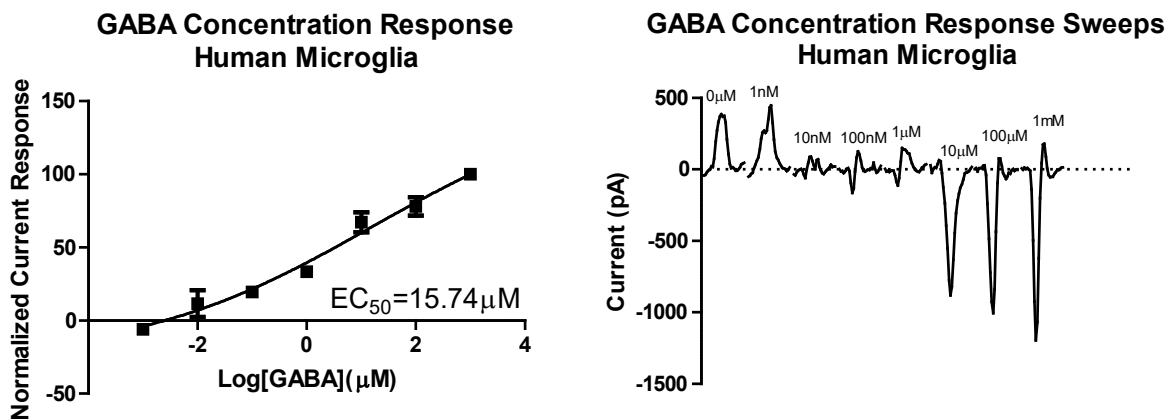


Figure 74. GABA_AR on Human Microglia are Functional Microglia were analyzed in the patch clamp assay with increasing concentrations of GABA ranging from 1 nM to 1 mM. Data were normalized such that 0 represented the response to ECS buffer only applications and 100 represents the response to 1 mM GABA.

Mouse Microglia Contain Functional GABA_AR

The same studies were completed for the immortalized mouse microglia. The mouse microglia did not contain $\alpha 4$ or $\alpha 6$ subunits, however there was similar expression of $\alpha 2$, $\alpha 3$, and $\alpha 5$ (**Figure 73**). All of the β , γ , and δ subunits were present as well. In comparison to the whole brain, the most notable difference is the low expression of $\alpha 1$ receptors on microglia and the very high expression of this subunit in the whole brain. Interestingly, the $\alpha 6$ showed very high expression in the mouse brain, which contrasts with the literature showing lower expression than the $\alpha 1$ and $\alpha 3$ subunits, but high expression localized to the cerebellum.¹⁵³ Because the mRNA was isolated from a small piece removed from the brain and not the whole brain, perhaps the cerebellum was utilized, accounting for the surprising amount of $\alpha 6$ subunit present.

Contrasting the mouse microglia with the human microglia (**Figure 73**), the mouse microglia express more diverse expression of subunits than human microglia. However, both microglia lines share the high expression of $\alpha 3$ subunit, which further supports using $\alpha 2/3$ selective imidazodiazepines to target neuropathic pain both on neurons and microglia.

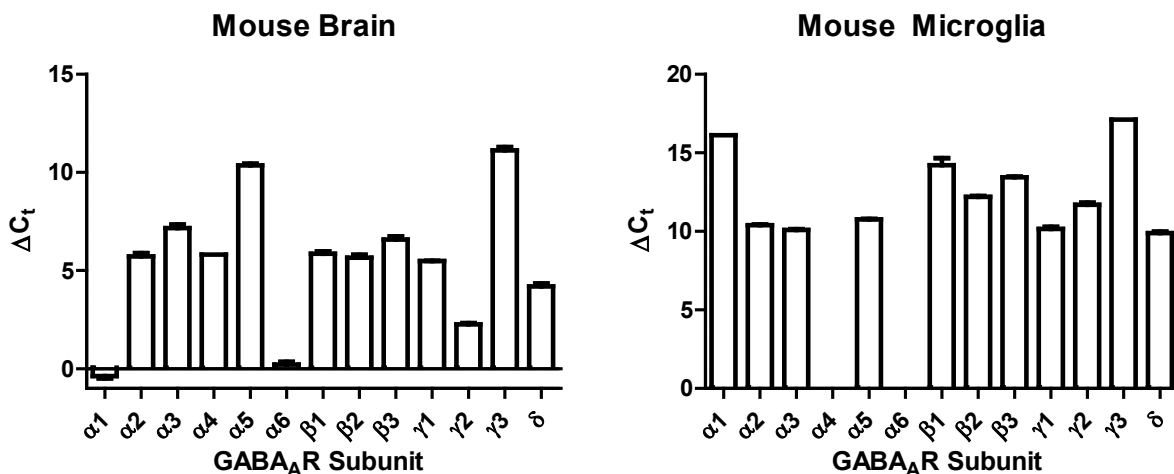


Figure 75. Immortalized Mouse Microglia Contain GABA_AR mRNA was isolated from microglia immortalized at Case Western University¹⁴⁷ and whole mouse brain. 10 ng of mRNA was used to assess GABA_AR subunits in whole mouse brain due to the expected high expression. 50 ng of mRNA was used for microglia due to unknown expression. Quantification was completed using QuantiFast SYBR green RT-qPCR kit. Cycle numbers for each subunit were normalized to GAPDH using the ΔC_t method.

Mouse microglia were also subjected to automated patch clamp to determine if GABA could produce transmembrane currents. Similar problems arose, such as positive currents appeared in low concentration applications and a very noisy baseline (**Figure 76**). Increasing concentrations of GABA did increase transmembrane currents though, with the maximum current reaching -1500 pA and a calculated EC_{50} of 286.4 nM.

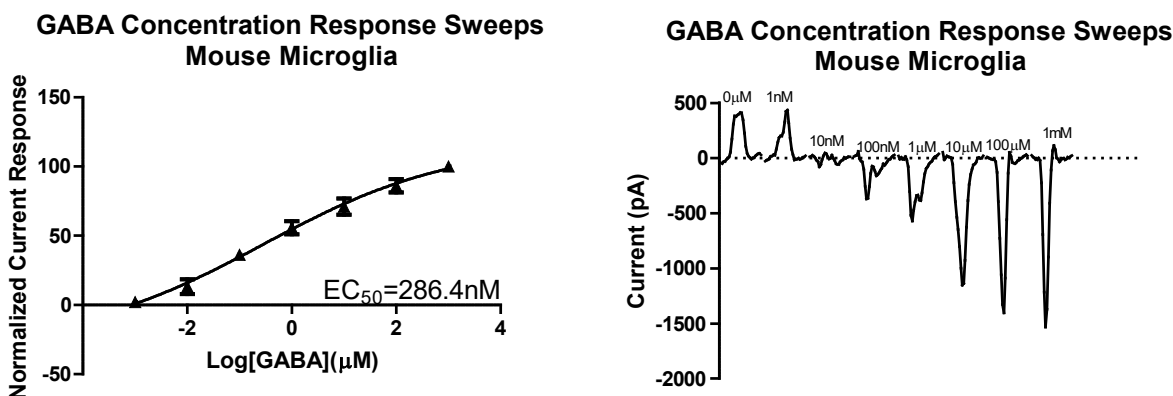


Figure 76. $GABA_A$ R on Mouse Microglia are Functional Microglia were analyzed in the patch clamp assay with increasing concentrations of GABA ranging from 1 nM to 1 mM. Data were normalized such that 0 represented the response to ECS buffer only applications and 100 represents the response to 1 mM GABA.

First Lead Compound: MP-III-080

In vivo testing had shown KRM-II-81 to be a less suitable drug candidate (data not published), so the analog MP-III-080 was developed in response. To first determine if MP-III-080 had potential as a lead compound, it was tested in automated patch clamp with both human and mouse microglia to see if GABA-induced currents could be further potentiated (**Figure 77**). The same problems continued with early applications of GABA and low concentrations of MP-III-080, so 1 nM MP-III-080 was used for normalization assuming that no true current modulation was taking place at that concentration. While an EC_{50} concentration was unable to be calculated from the concentration response, it is true that MP-III-080 generated increasing transmembrane currents with increasing concentrations in both human and mouse

microglia. In human microglia, the maximum current reached -1100 pA, whereas in mouse the maximum current was nearly double at -2200 pA. This can be attributed to the more diverse subset of α subunits present in mouse microglia, as MP-III-080 is known to have high efficacy at not only $\alpha 3$, but $\alpha 2$ and $\alpha 5$ containing receptors as well.¹⁴⁶

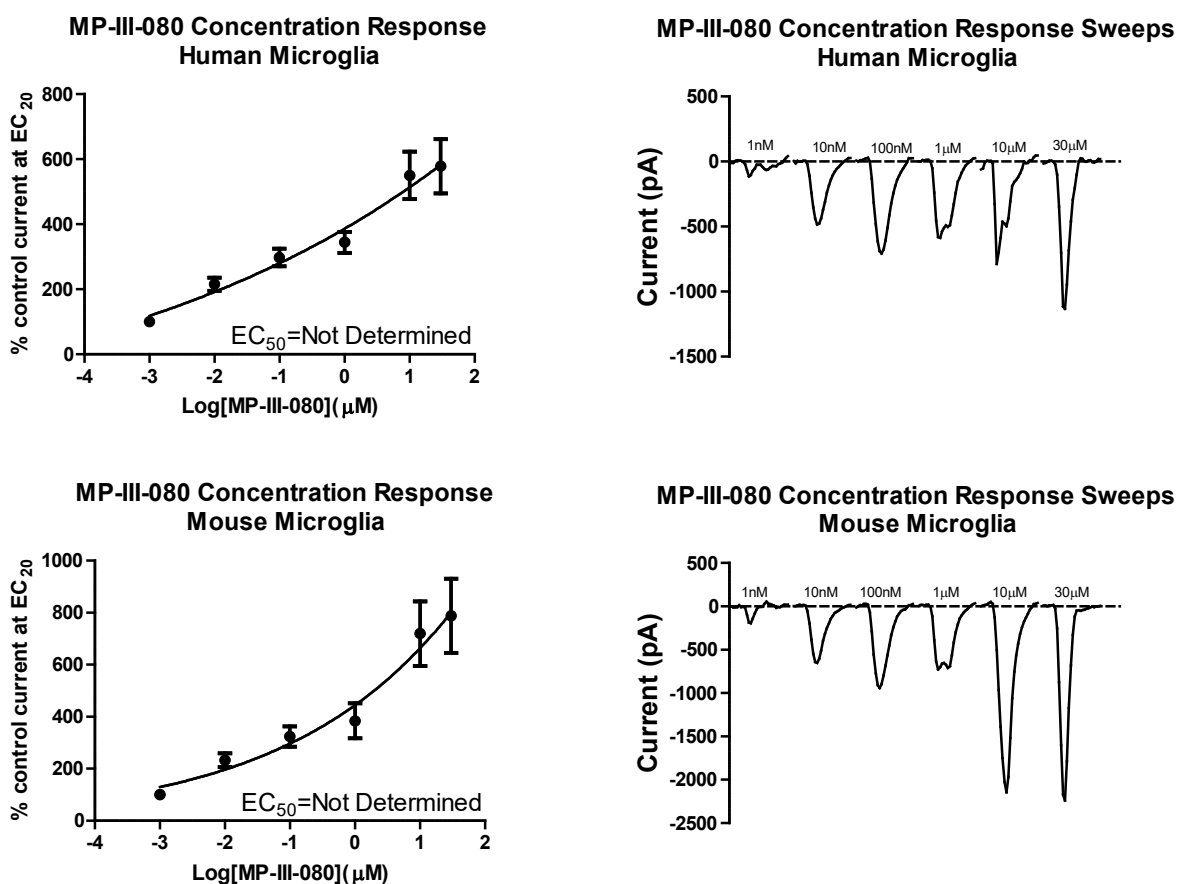


Figure 77. Imidazodiazepines can Potentiate GABA-induced Currents in Microglia MP-III-080 was co-applied with 50 nM GABA in concentrations ranging from 0.1 nM to 30 μ M. Responses were normalized such that 100 represented the response to 1 nM MP-III-080 applications.

Because KRM-II-81 showed adverse *in vivo* side effects, the safety of MP-III-080 needed to be established before it could be considered a lead compound. Rotarod was used to demonstrate that MP-III-080 generated no adverse sensorimotor effects at oral dosages up to 150 mg/kg (**Figure 78**).

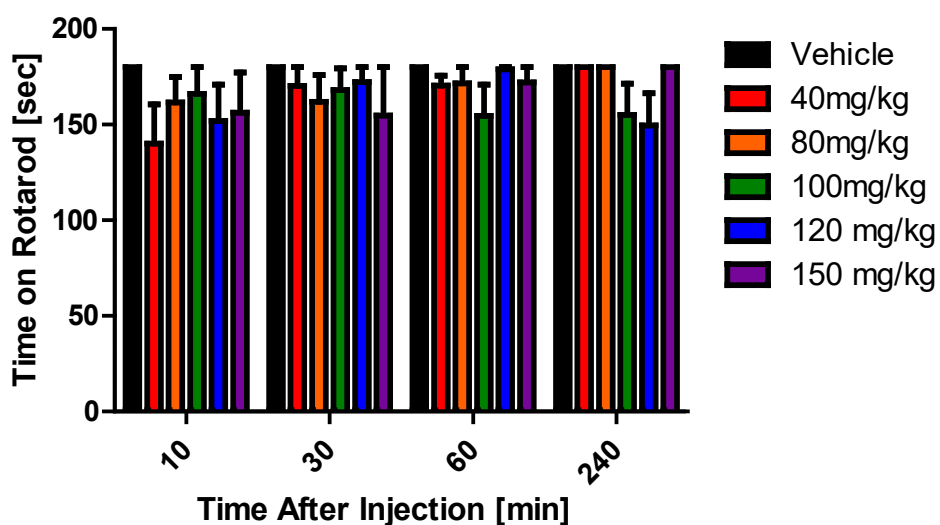


Figure 78. Rotarod Performance of Mice Treated with MP-III-080 Mice were orally dosed with MP-III-080 at 40, 80, 100, 120, and 150 mg/kg and placed on the Rotarod apparatus at various time post-treatment to determine if MP-III-080 caused any detrimental sensorimotor effects. Data Courtesy of Alex Kehoe and Ian Luecke.

Potential adverse neurological effects can also be gleaned from screening data provided by National Institute of Mental Health’s Psychoactive Drug Screening Program (NIMH PDSP), which analyzes any compounds submitted against a collection of receptors known to induce adverse effects. At 10 μ M, any compound with more than 50% competition of the corresponding radioligand for a particular receptor is considered active. The summary of the primary radioligand screening data is depicted in **Table 16**. MP-III-080 binds to the 5-HT_{2C}, H₁, and PBR in addition to the BZP rat brain site (benzodiazepine receptor). The Peripheral Benzodiazepine Receptor (PBR) is located in the mitochondria and is implicated in cholesterol transport for steroid formation, associated with aggressive phenotypes of various cancers and Alzheimer’s disease.¹⁵⁴⁻¹⁵⁵ Agonists of the 5-HT_{2C} are largely hallucinogenic.¹⁵⁶⁻¹⁵⁷ The H₁ receptor is targeted by antihistamines and is implicated in the sleep-wake cycle.¹⁵⁸⁻¹⁵⁹ Binding does not necessarily equal efficacy at those receptors however, so further studies would be necessary to confirm possible CNS effects.

Table 16. PDSP Primary Screening Data for MP-III-080

Receptor	Percent Competition	Receptor	Percent Competition	Receptor	Percent Competition
5-HT1A	19	SERT	-13	Alpha2C	1
5-HT1B	11	NET	-3	Beta1	-20
5-HT1D	-3	DAT	-6	Beta2	8
5-HT1E	2	MOR	-1	M1	4
5-HT2A	-12	DOR	0	M2	26
5-HT2B	1	KOR	47	M3	8
5-HT2C	96	GABAA	-0.6	M4	27
5-HT3	-11	H1	89	M5	12
5-HT5A	12	H2	3	Beta3	15
5-HT6	-18	H3	8	BZP Rat Brain Site	88
5-HT7	19	H4	7	PBR	85
D1	11	Calcium Channel	-11	Alpha1D	-10
D2	-6	Alpha1A	11	HERG binding	5
D3	12	Alpha1B	3	Sigma 1 GP	36
D4	-0.3	Alpha2A	23	Sigma 2 PC12	24
D5	12	Alpha2B	35		

To begin investigating anti-inflammatory effects of MP-III-080, intracellular calcium levels were measured as increased calcium leads to numerous inflammatory processes. MP-III-080 appeared to reduce intracellular calcium in a dose dependent manner, however the high standard deviation did not allow for statistical significance (**Figure 58**). More replicates of this assay would need to be completed and some further troubleshooting. Attempts to replicate the reported increase in purigenic receptors with fibronectin and IFN γ that lead to prolonged increased intracellular calcium were unsuccessful (data not shown).

Additionally, the initial increase in calcium stimulated with ATP application was highly variable between 30-60 seconds. In a few instances, the maximum response was recorded immediately. The highly variable response could be improved using a plate reader with injectors. This would allow a baseline reading to be taken before ATP activated the calcium channels and readings immediately after. In the

absence of injectors, time differences are caused by inserting and removing the plate from the plate reader.

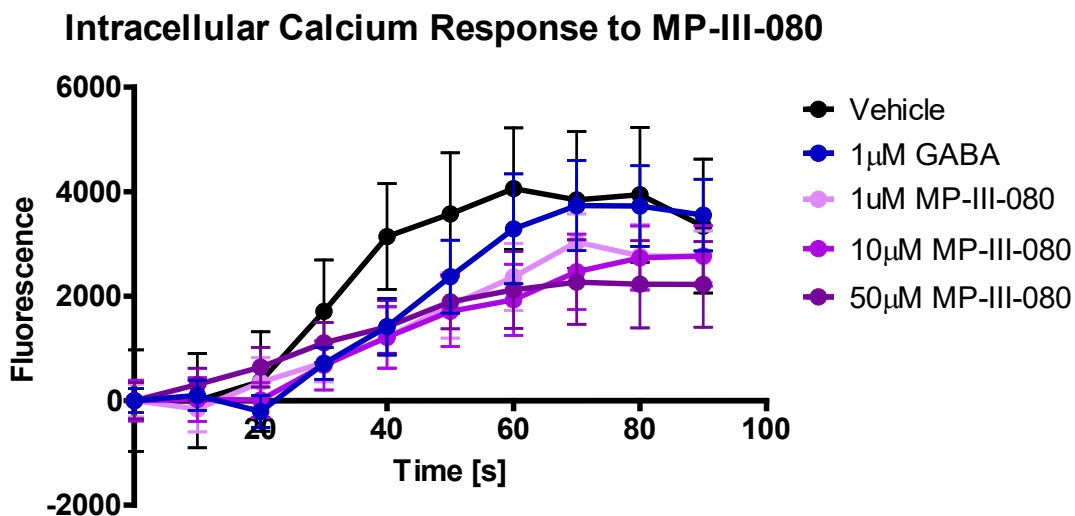


Figure 79. Intracellular Calcium Levels are Reduced by Targeting $GABA_A$ R with MP-III-080 Intracellular calcium levels were investigated with the Fluo-4 NW Calcium Assay. Mouse Microglia were plated, treated 30 minutes prior to reading, and purigenic calcium channels were activated immediately before reading with 100 μ M ATP. Fluorescence (ex: 494 nm, em: 516 nm) was recorded over 3 minutes at 10 second intervals.

One hallmark inflammatory export of microglia is nitric oxide. Nitric oxide can be easily measured through the Griess Assay, which utilizes anilines that react with NO to generate an Azo dye. MP-III-080 concentrations of up to 100 μ M were not toxic to microglia cells, however it was also not capable of reducing the production of nitric oxide (**Figure 80**). Therefore, MP-III-080 was removed from consideration as a potential therapeutic compound.

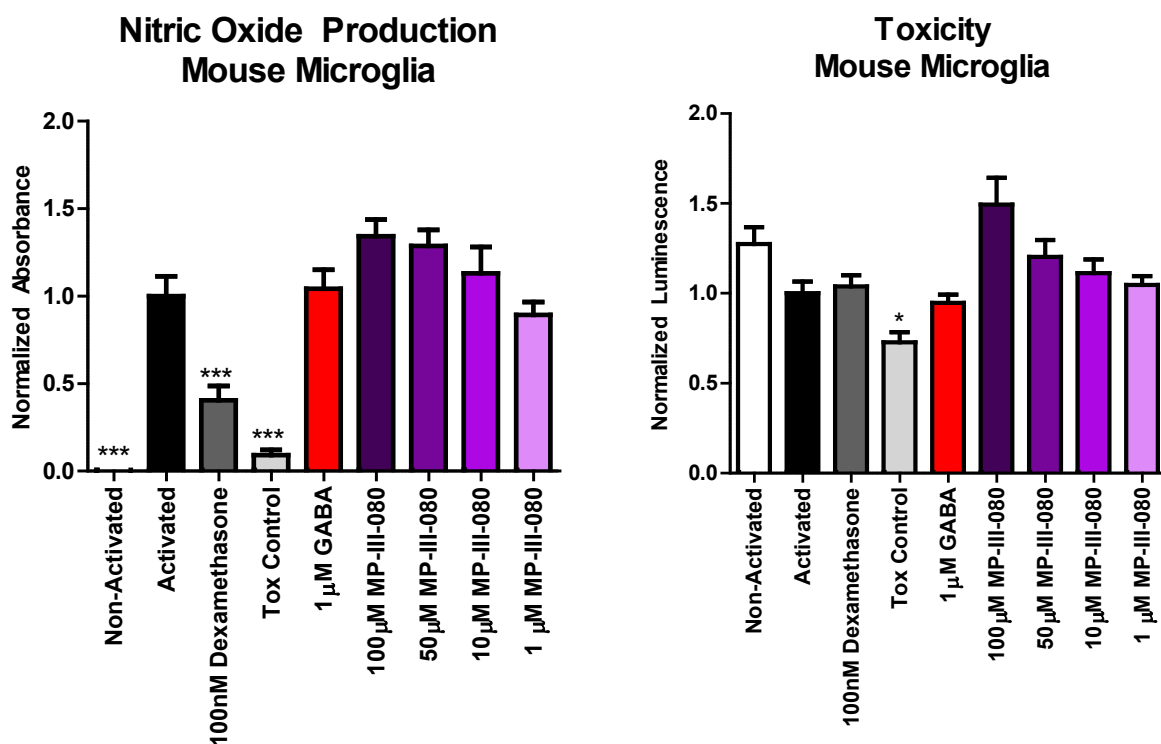


Figure 80. MP-III-080 has no Effect on Nitric Oxide Production Mouse Microglia were activated with interferon γ (IFN γ) and lipopolysaccharide (LPS) and treated with 1 – 100 μ M of MP-III-080 for 24 hours. Supernatant was analyzed with the Griess Assay.

First Round Screening & Lead Compound Determination

A small library of 19 compounds was curated by the Cook Group that included MP-III-080 and KRM-II-81 as controls. All compounds were screened at 50 μ M using the Griess Assay and the corresponding toxicity assay. Of these compounds GL-I-66, GL-I-81, MP-IV-004, GL-III-60, GL-III-63, MP-IV-005, MP-IV-010, and GL-III-36 reduced nitric oxide production approximately 50% or more. GL-I-66 showed slight toxicity, but not to the same degree as the decrease of nitric oxide.

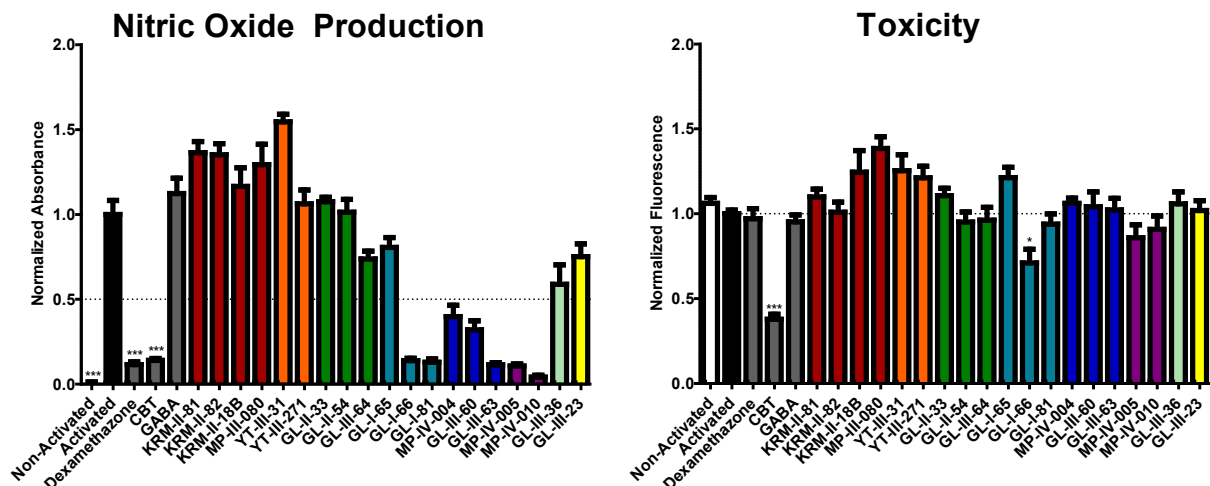


Figure 81. First Round of Compound Screening Mouse Microglia were activated with LPS and IFN γ and treated with 1 μ M GABA co-applied with 50 μ M of compounds of interest for 24 hours. Half of the supernatant was removed and analyzed with the Griess Assay. ATP levels were quantified by the Cell Titer Glo kit as a measure of toxicity using the cells and remaining supernatant. Data courtesy of Brandon Mikulsky.

These eight compounds were further screened in concentration response from 1 nM to 50 μ M.

All compounds, except for GL-III-36, were structurally related (**Figure 82**) and reduced nitric oxide (**Figure 83**).

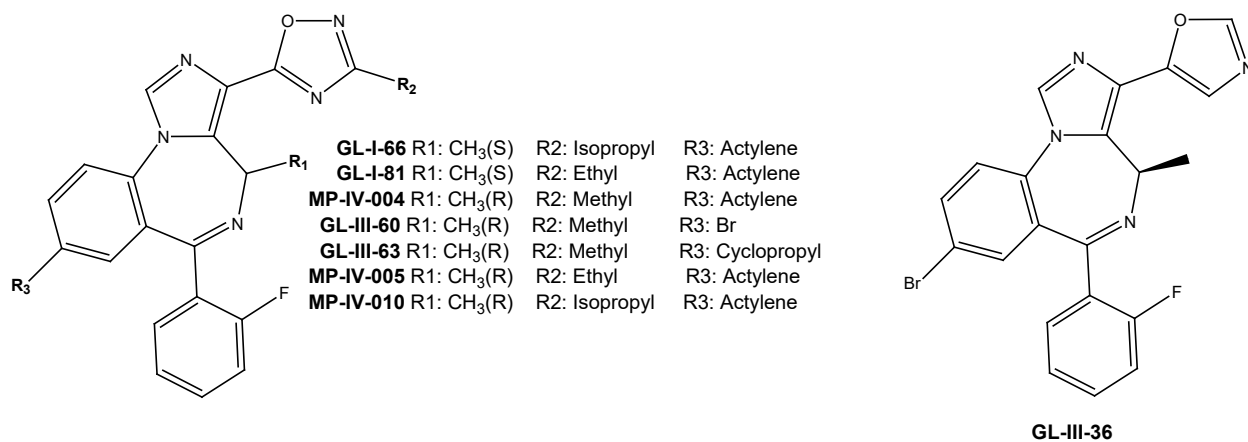


Figure 82. Structures of Compounds that Reduced Nitric Oxide Compounds were synthesized by Mike Poe and Guanguan Li of the Prof. Cook Group according to established routes.^{145, 151}

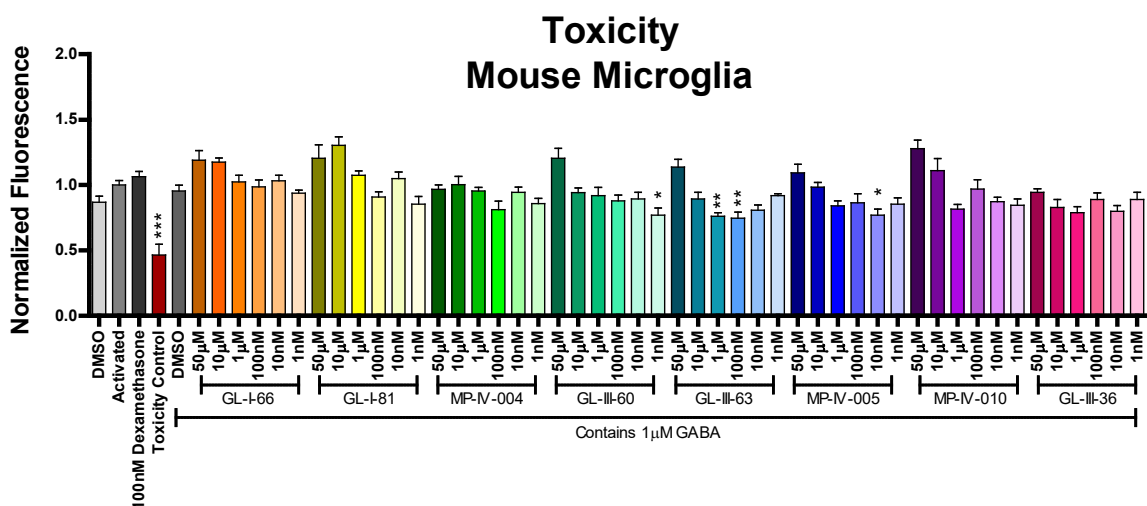
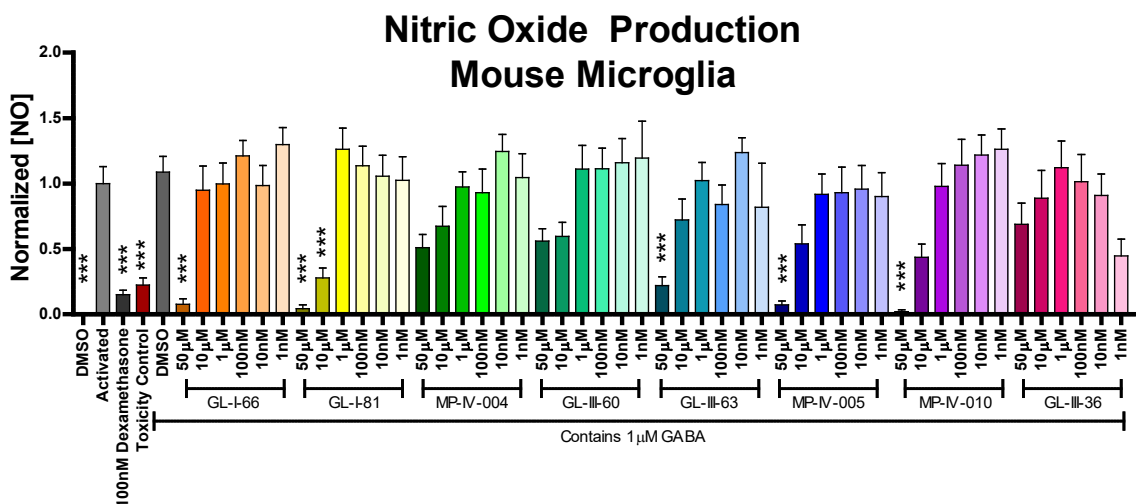


Figure 83. Concentration Response of Compounds that Showed NO Reduction in Screening Assay Mouse Microglia were activated with LPS and IFN γ and treated with 1 μ M GABA co-applied with 1 nM - 50 μ M of compounds of interest for 24 hours. Half of the supernatant was removed and analyzed with the Griess Assay. ATP levels were quantified by the Cell Titer Glo kit as a measure of toxicity using the cells and remaining supernatant. Data courtesy of Brandon Mikulsky.

To confirm the activity of these compounds towards macrophages, the mouse macrophage line RAW264.7 was used. Again, these compounds were able to reduce nitric oxide production (**Figure 84**). Because of the structural similarity, MP-IV-010 was chosen to represent the class in further experiments because it had the highest efficacy in the initial screening assay.

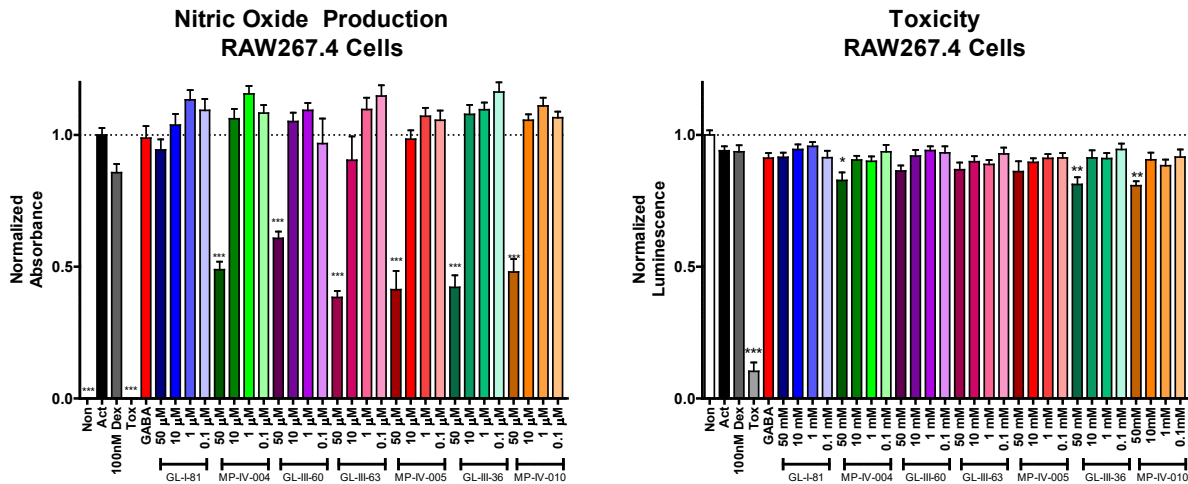


Figure 84. Concentration Response of Compounds that Showed NO Reduction in Screening Assay in Mouse Macrophages RAW264.7 Mouse Macrophages were activated with LPS and IFN γ and treated with 1 μ M GABA co-applied with 100 nM - 50 μ M of compounds of interest for 24 hours. Half of the supernatant was removed and analyzed with the Griess Assay. ATP levels were quantified by the Cell Titer Glo kit as a measure of toxicity using the cells and remaining supernatant.

Second Lead Compound: MP-IV-010

As the new lead compound, MP-IV-010 had to be assessed for safety. *In vitro* cytotoxicity was assessed with the Cell Titer Blue assay with concentrations ranging from 1nM to 200 μ M. MP-IV-010 did not cause any cytotoxicity at even the highest concentration, confirming that it would be suitable for further *in vitro* testing (Figure 85).

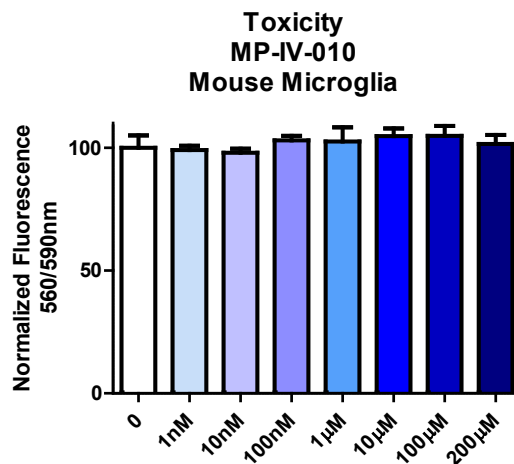


Figure 85. Cytotoxicity of MP-IV-010 Mouse Microglia were treated with 1 nM – 200 μ M of MP-IV-010 for 24 hours. Cytotoxicity was measured based on the cells' metabolic reduction capabilities with the Cell Titer Blue Assay.

The rotarod assay was employed to show that MP-IV-010 would cause no adverse effects when used *in vivo*. No impairment of sensorimotor coordination was seen after oral dosing with MP-IV-010 at dosages of up to 120 mg/kg (Figure 86).

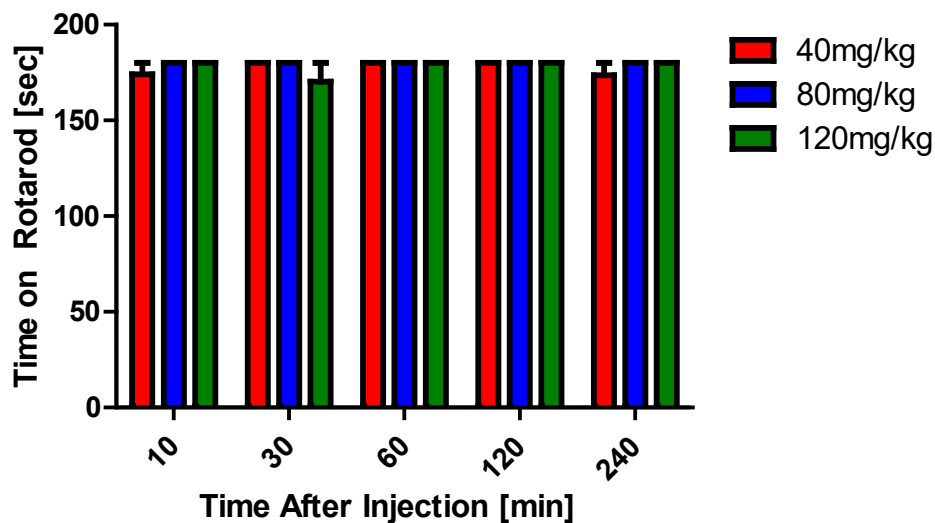


Figure 86. Rotarod Performance of Mice Treated with MP-IV-010 Mice were orally dosed with MP-IV-010 at 40, 80, and 120 mg/kg and placed on the Rotarod apparatus at various time post-treatment to determine if MP-IV-010 caused any detrimental sensorimotor effects. Data Courtesy of Alex Kehoe and Ian Luecke.

In addition to rotarod screening, MP-IV-010 was submitted to the NIMH PDSP for screening. The results of the primary screen are summarized in **Table 17**. Other than the Rat Brain BZP receptor, MP-IV-010 bound to the KOR and the Sigma2 receptor. The κ Opioid Receptor (KOR) can be stimulated by drugs of abuse, endogenous ligands, and stress, which leads to addiction and despair-like responses.¹⁶⁰ Sigma2 receptors are less well understood, but they can modulate intracellular calcium and cytokine expression in microglia.¹⁶¹ Antagonists of Sigma2 are also being investigated to treat addiction, anxiety, and depression.¹⁶¹

Table 17. PDSP Primary Screening Data for MP-IV-010

Receptor	Percent Competition	Receptor	Percent Competition	Receptor	Percent Competition
5-HT1A	19	D5	29	Alpha2A	14
5-HT1B	29	SERT	22	Alpha2B	29
5-HT1D	6	NET	-2	Alpha2C	31
5-HT1E	-7	DAT	14	Beta1	6
5-HT2A	-1	MOR	33	Beta2	20
5-HT2B	0	DOR	5	M1	-11
5-HT2C	-2	KOR	94	M2	10
5-HT3	13	GABAA	-8	M3	0
5-HT5A	11	H1	19	M4	8
5-HT6	21	H2	28	M5	26
5-HT7	-5	H3	-18	Beta3	38
D1	28	H4	6	BZP Rat Brain Site	64
D2	25	Calcium Channel	15	PBR	28
D3	15	Alpha1A	2	Alpha1D	9
D4	5	Alpha1B	15	HERG binding	29
				Sigma 2	64

Because MP-IV-010 interacted with the KOR, BZP Rat Brain Site, and Sigma2 receptor in the primary screen, the PDSP completed secondary screening using 11 different concentrations to generate a concentration response curve. MP-IV-010 bound to the KOR, BZP, and Sigma2 with an EC₅₀ of 409 nM, 2.5 μM, and 3.0 μM respectively (**Figure 87**).

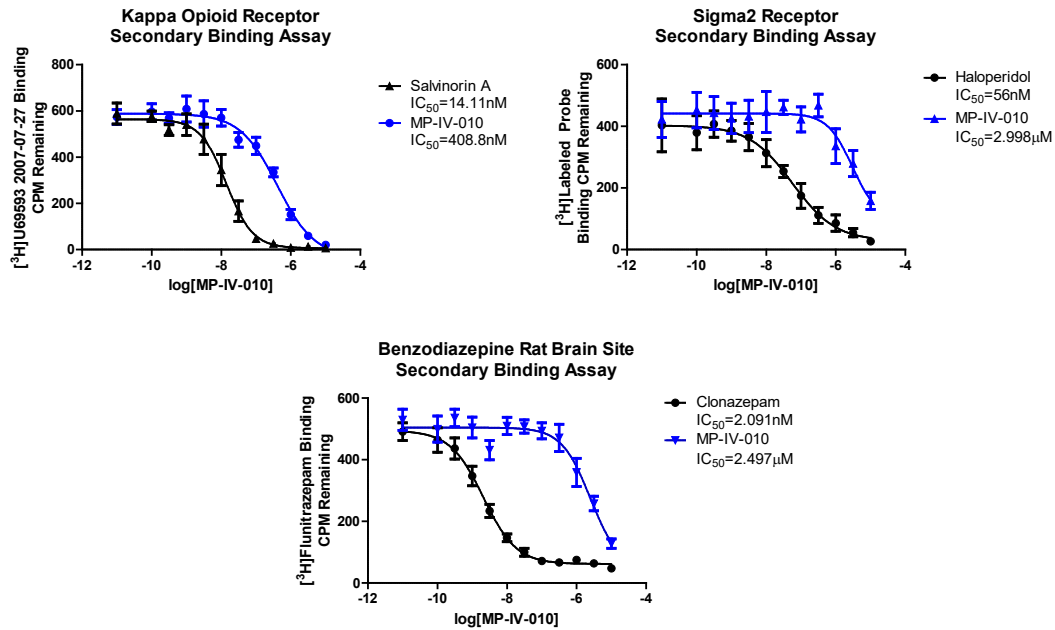


Figure 87. PDSP Secondary Screening Data Dose dependent binding was determined for the κ Opioid receptor, the Sigma2 receptor, and the rat brain benzodiazepine site utilizing, Salvinorin A, Haloperidol, and Clonazepam respectively as positive controls.

To determine the receptor that was responsible to the reduction of NO when MP-IV-010 is bound, GABA_AR antagonists were enlisted to confirm that MP-IV-010 was working through the GABA_AR. Picrotoxin binds within the chloride pore of the receptor, blocking the chloride flux.³ Bicuculline binds competitively at the GABA site, preventing the endogenous activation of the receptor.³ Flumazenil binds at the benzodiazepine site, theoretically competing with MP-IV-010.³ However, maximum concentrations of all of these antagonists were not capable of reversing the reduction of nitric oxide by MP-IV-010. This suggests that reduction of NO by MP-IV-010 is not mediated by the GABA_AR.

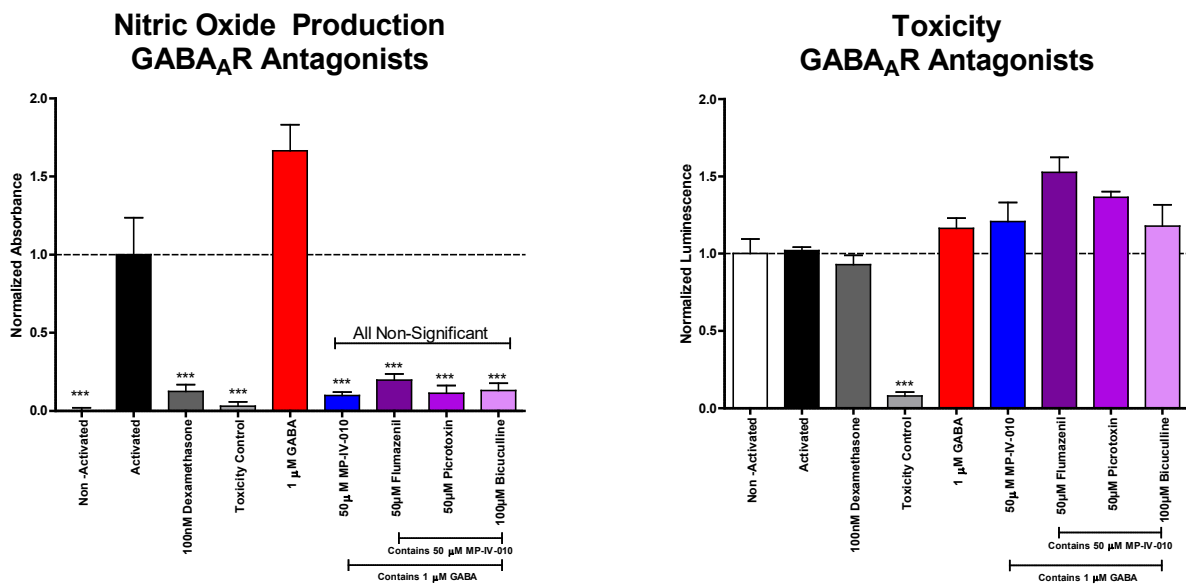


Figure 88. Antagonizing the GABA_AR to Reverse NO Reduction Mouse Microglia were incubated for 24 hours with LPS and IFN γ , 1 μ M GABA, 50 μ M MP-IV-010, and maximum concentrations of antagonists determined by solubility in DMSO. Flumazenil was used to antagonize the benzodiazepine binding site on the GABA_AR, Picrotoxin was used to block the chloride channel of the GABA_AR, and Bicuculline inhibits the binding of GABA. Half of the supernatant was removed and analyzed with the Griess Assay. ATP levels were quantified by the Cell Titer Glo kit as a measure of toxicity using the cells and remaining supernatant. Data courtesy of Brandon Mikulsky.

To investigate other possible targets, norbinaltorphimine was used as a selective KOR antagonist¹⁶² and PK11195¹⁵⁵ was used to antagonize PBR. As **Figure 89** shows, norbinaltorphimine did not reverse the nitric oxide reduction induced by MP-IV-010, although the concentrations used were not sufficient to completely reverse the effect. Thus, there might be the possibility that other receptors may be working in conjunction with the KOR to reduce nitric oxide production. 50 μ M of PK11195 was not capable of returning nitric oxide levels reduced by MP-IV-010 back to the untreated levels, however toxicity of PK11195 at that concentration was too pronounced.

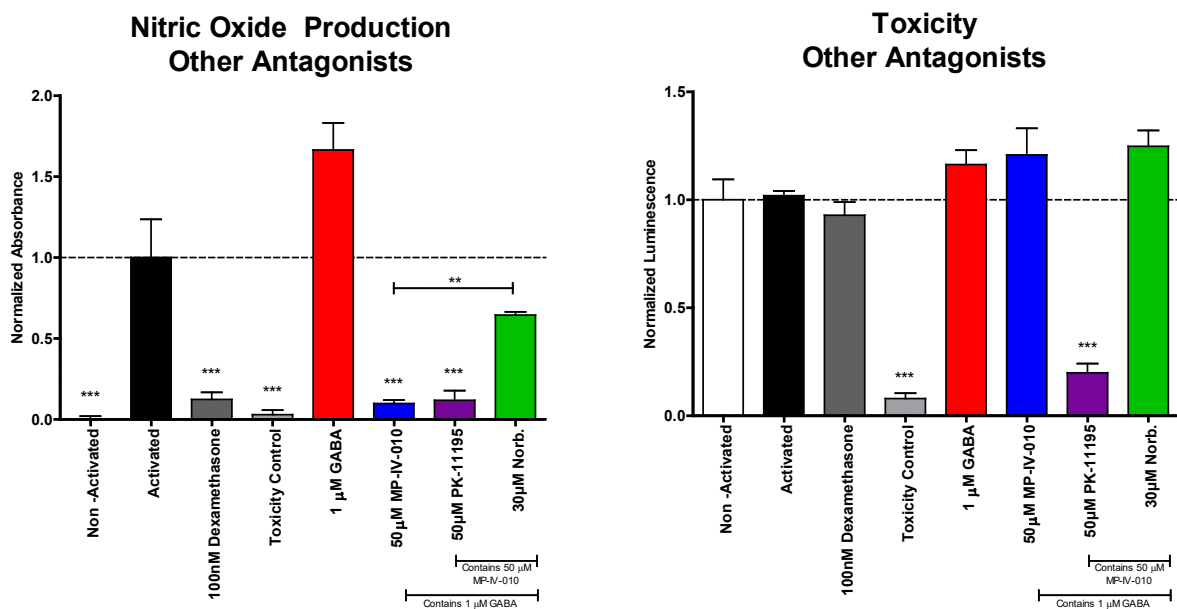


Figure 89. Antagonizing Other Receptors to Reverse NO Reduction Mouse Microglia were incubated for 24 hours with LPS and IFN γ , 1 μ M GABA, 50 μ M MP-IV-010, and maximum concentrations of antagonists determined by solubility in DMSO. PK-11195 antagonizes the peripheral benzodiazepine receptor (PBR) and Norbinaltorphimine antagonizes the κ Opioid Receptor (KOR). Half of the supernatant was removed and analyzed with the Griess Assay. ATP levels were quantified by the Cell Titer Glo kit as a measure of toxicity using the cells and remaining supernatant. Data courtesy of Brandon Mikulsky.

Additionally, some reports have shown that activating the PBR with small molecule agonists reduced inflammation.¹⁵⁴ Therefore, we employed 4-chlorodiazepam, a known PBR agonist, and showed that at a concentration of 100 μ M nitric oxide was reduced to similar levels as those achieved with 50 μ M MP-IV-010 (**Figure 90**). While this suggests that the PBR may be the other receptor responsible for the MP-IV-010 reduction of nitric oxide, alternative antagonist studies are needed to confirm. Additionally, the Sigma2 receptor was implicated in the PDSP screening, but was not tested here. Because of the many links suggested in the literature between the Sigma2 receptor and microglial activation, additional studies are necessary to completely tease out the mechanism of action of MP-IV-010.

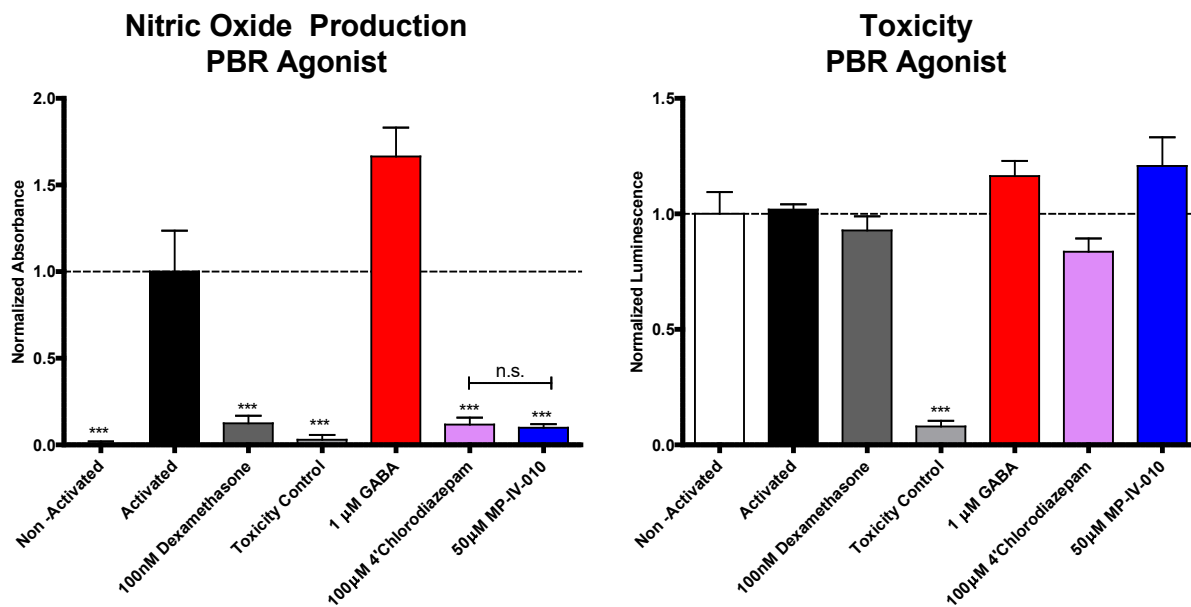


Figure 90. Reducing Nitric Oxide Production through the Peripheral Benzodiazepine Receptor (PBR) Mouse Microglia were incubated for 24 hours with LPS and IFN γ . Cells were either treated with the PBR agonist 100 μ M 4'Chlorodiazepam or 1 μ M GABA with and without 50 μ M MP-IV-010, and. Half of the supernatant was removed and analyzed with the Griess Assay. ATP levels were quantified by the Cell Titer Glo kit as a measure of toxicity using the cells and remaining supernatant. Data courtesy of Brandon Mikulsky.

Regardless of the fact that the receptor for MP-IV-010 is still unclear, it is clear that MP-IV-010 produces anti-inflammatory effects. The mechanism by which nitric oxide was being reduced by MP-IV-010 was investigated next. Increased intercellular calcium is an integral part of many inflammatory processes. As shown in **Figure 91**, MP-IV-010 reduced intracellular calcium at 10 μ M and higher. However, similar problems that affected the results with MP-III-080 (**Figure 58**) were still observed for this assay. To generate this graph, any wells that had immediately reached peak calcium response were excluded. Thus, as pointed out the application of injectors would greatly improve the accuracy of this assay.

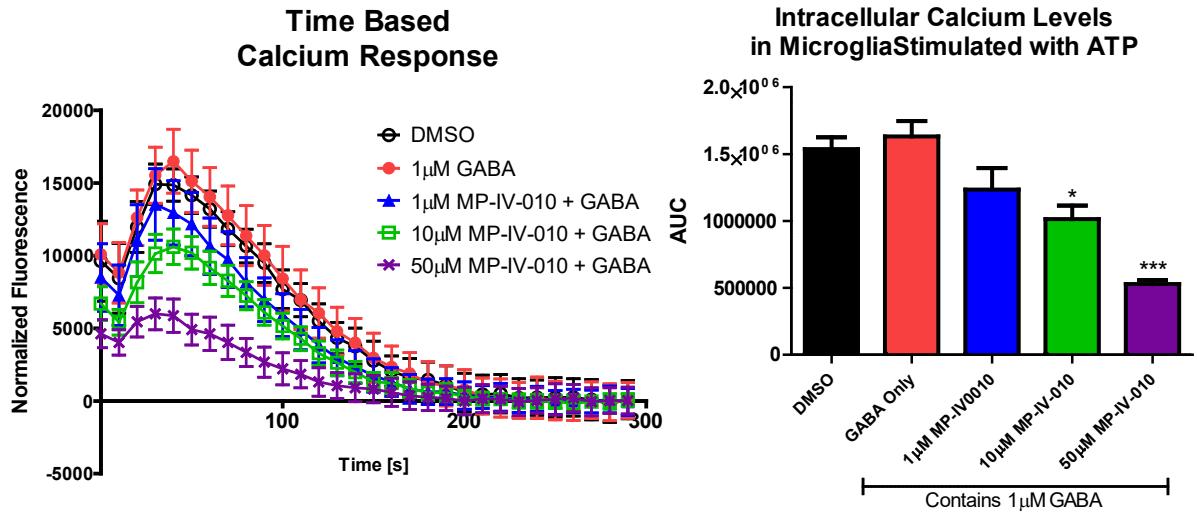


Figure 91. Intracellular Calcium Levels are Reduced by Targeting GABA_AR with MP-IV-010 Intracellular calcium levels were investigated with the Fluo-4 NW Calcium Assay. Mouse Microglia were plated, treated 30 minutes prior to reading, and purigenic calcium channels were activated immediately before reading with 100 µM ATP. Fluorescence (ex: 494 nm, em: 516 nm) was recorded over 3 minutes at 10 second intervals.

Inducible nitric oxide synthase (iNOS) is the enzyme responsible for generating nitric oxide through the conversion of arginine to citrulline.³³ Transcription of iNOS can be affected by calcium, which binds calmodulin and activates calcium/calmodulin protein kinase.¹⁶³ Microglia were activated with LPS and IFN γ and treated with 50 µM MP-IV-010 for 24 hours, at which time RT-qPCR was used to analyze the transcription of iNOS. A large upregulation was seen upon activation of the microglia as expected, however MP-IV-010 did not decrease iNOS transcription 24 hours after treatment (**Figure 92**).

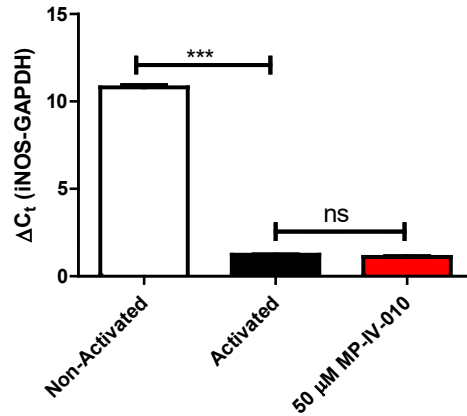


Figure 92. 24 Hour MP-IV-010 Treatment Does Not Reduce iNOS Transcription Mouse Microglia were activated for 24 hours with IFN γ and LPS and treated with 50 μ M MP-IV-010. mRNA was isolated and quantified using QuantiFast SYBR green RT-qPCR kit. Cycle numbers for each sample were normalized to GAPDH using the ΔC_t method.

Since inhibition of nitric oxide production by MP-IV-010 did not appear to be transcriptionally controlled, potential enzyme inhibition was investigated next. The iNOS activity assay utilizes isolated proteins from cell culture or tissue to generate nitric oxide. The process removes any preexisting nitric oxide. Microglia were treated for 24 hours, consistent with the Griess assay results, before proteins were isolated. At the end of the assay incubation, there was a significant difference between the activity of proteins from non-activated microglia and microglia activated with IFN γ and LPS (**Figure 93**). MP-IV-010 treatment reduced iNOS activity down to baseline levels.

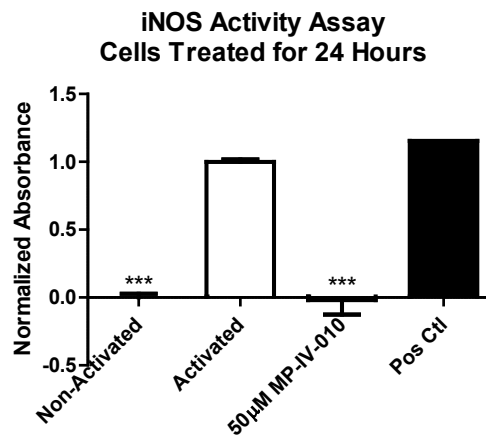


Figure 93. iNOS Activity after 24 Hour Treatment with MP-IV-010 Mouse Microglia were treated for 24 hours with IFN γ , LPS, and 50 μ M MP-IV-010. Protein was harvested and 100 μ g was incubated with cofactors and substrates from the Abcam iNOS Activity Assay kit to determine nitric oxide production by isolated iNOS.

To investigate whether MP-IV-010 directly inhibits iNOS, protein was isolated from non-activated and activated microglia. Protein from activated microglia was treated with MP-IV-010 for 2 hours. No activity difference was observed for non-treated and MP-IV-010 treated protein. Thus, MP-IV-010 is not a direct inhibitor of iNOS (**Figure 94**).

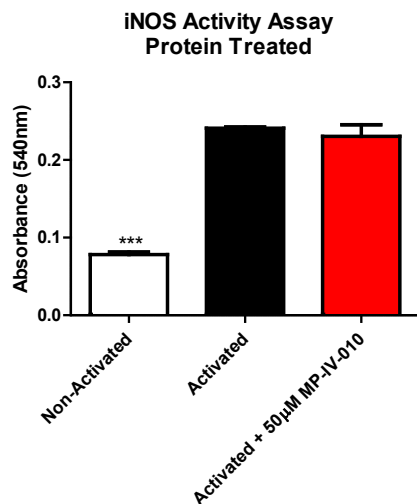


Figure 94. Nitric Oxide Production from MP-IV-010 Treated Protein Protein was isolated from Mouse Microglia activated with IFN γ and LPS. 100 μ g of protein was incubated with 50 μ M MP-IV-010 and cofactors and substrates from the Abcam iNOS Activity Assay kit for 2 hours before measurement.

Second Round Screening & Lead Compound Determination

Concurrent with the MP-IV-010 studies, additional compounds were investigated to identify more potent compounds. 54 compounds were provided by Guanguan Li of the Prof. James Cook Group. For the initial screen, compounds were tested at 10 μ M to identify compounds more potent than MP-IV-010. 12 compounds showed a reduction of more than 50% at that concentration (**Figure 95**). Among those hit compounds were a significant number of imidazodiazepines with an oxadiazole function. The structures are depicted in **Figure 96**. Interestingly, some members of this compound class were already identified in the previous screening (**Figure 82**).

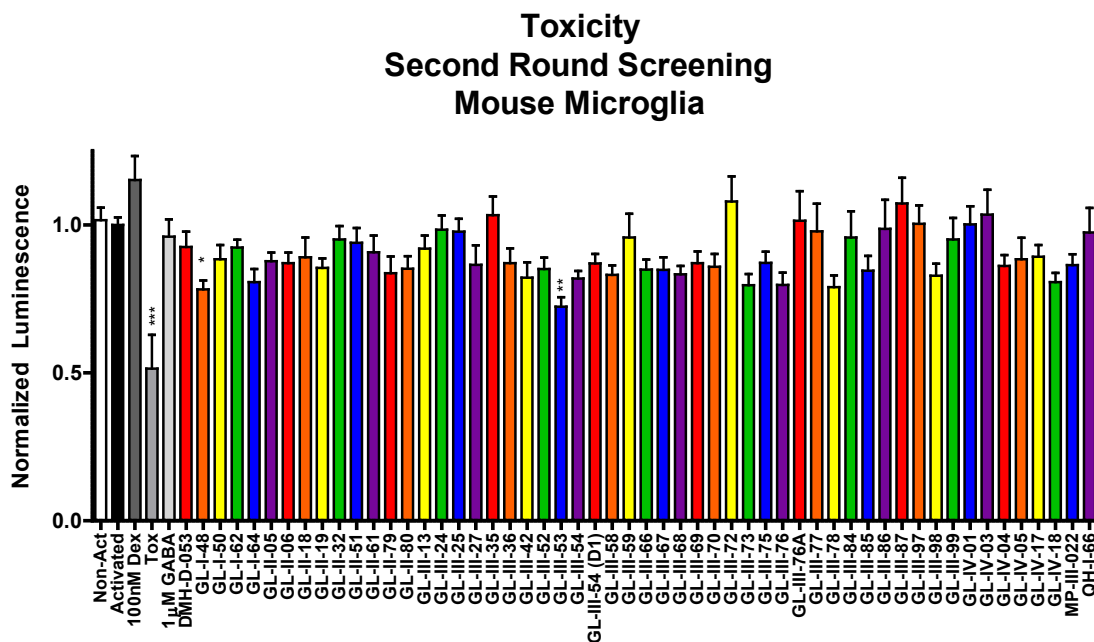
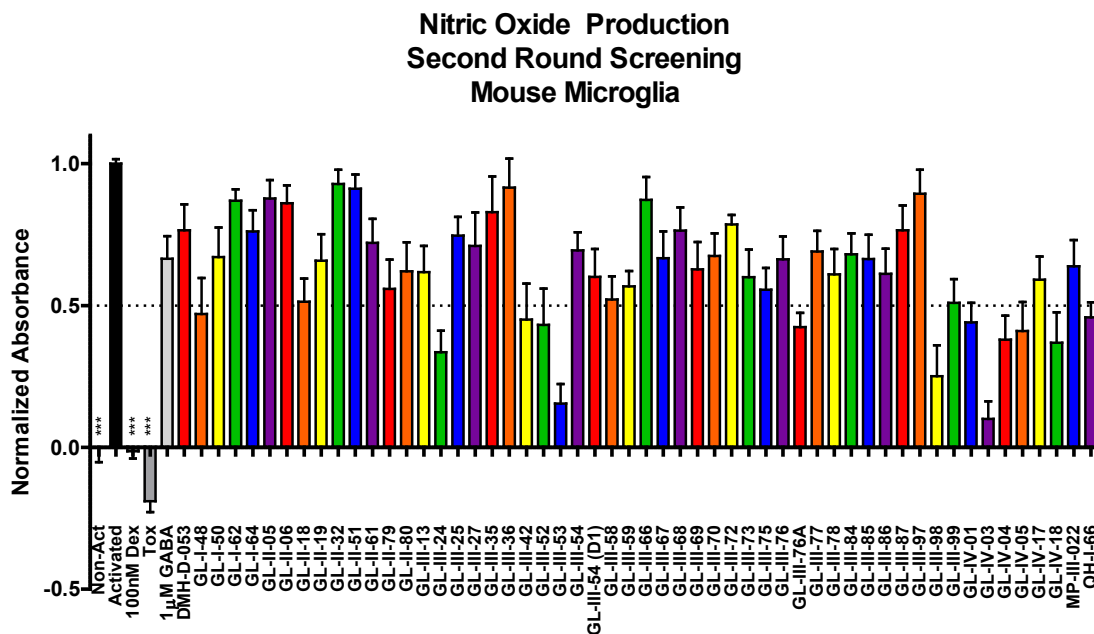


Figure 95. Second Round of Compound Screening Mouse Microglia were activated with LPS and IFN γ and treated with 1 μ M GABA co-applied with 10 μ M of compounds of interest for 24 hours. Half of the supernatant was removed and analyzed with the Griess Assay. ATP levels were quantified by the Cell Titer Glo kit as a measure of toxicity using the cells and remaining supernatant.

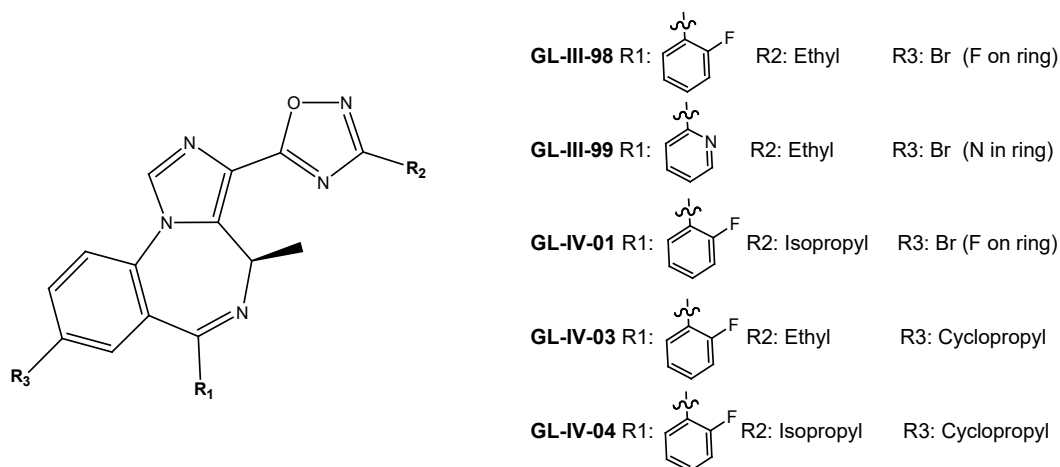


Figure 96. Structures of Compounds that Reduced Nitric Oxide Compounds were synthesized by Mike Poe and Guanguan Li of the Prof. Cook Lab according to established routes.^{145, 151}

These compounds were then tested in concentration response (**Figure 97**). Most compounds showed NO reduction at concentrations lower than 10 μM , especially GL-IV-01 and GL-IV-04, which showed reduction at 100 nM. GL-IV-03 appeared the most efficacious however, with near complete inhibition of NO production at 30 μM .

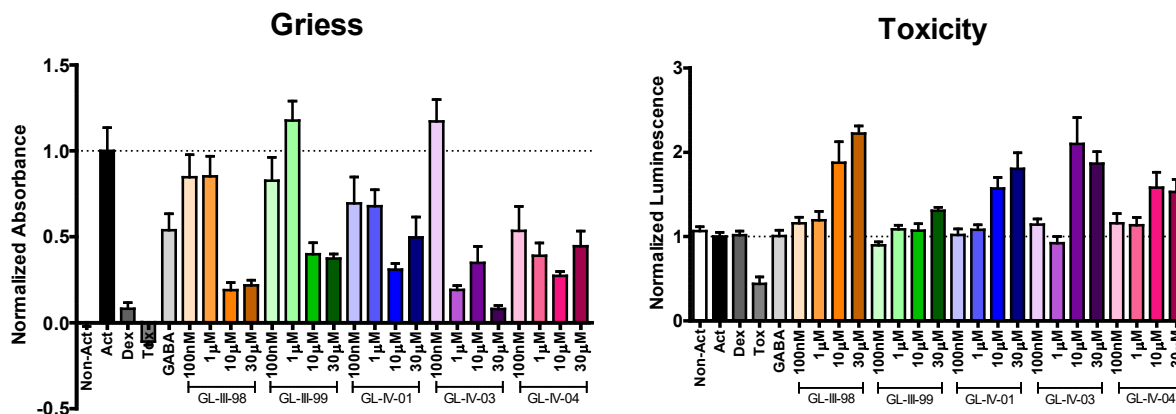


Figure 97. Concentration Response of Compounds from Second Screening Assay in Mouse Microglia Mouse Microglia were activated with LPS and IFN γ and treated with 1 μM GABA co-applied with 100 nM - 30 μM of compounds of interest for 24 hours. Half of the supernatant was removed and analyzed with the Griess Assay. ATP levels were quantified by the Cell Titer Glo kit as a measure of toxicity using the cells and remaining supernatant.

The same compounds were investigated with RAW264.7 mouse macrophages (**Figure 98**). Interestingly only 2 compounds GL-IV-03 and GL-III-72 reduced the NO levels more than 50%. GL-III-72, however, showed some cytotoxic effects.

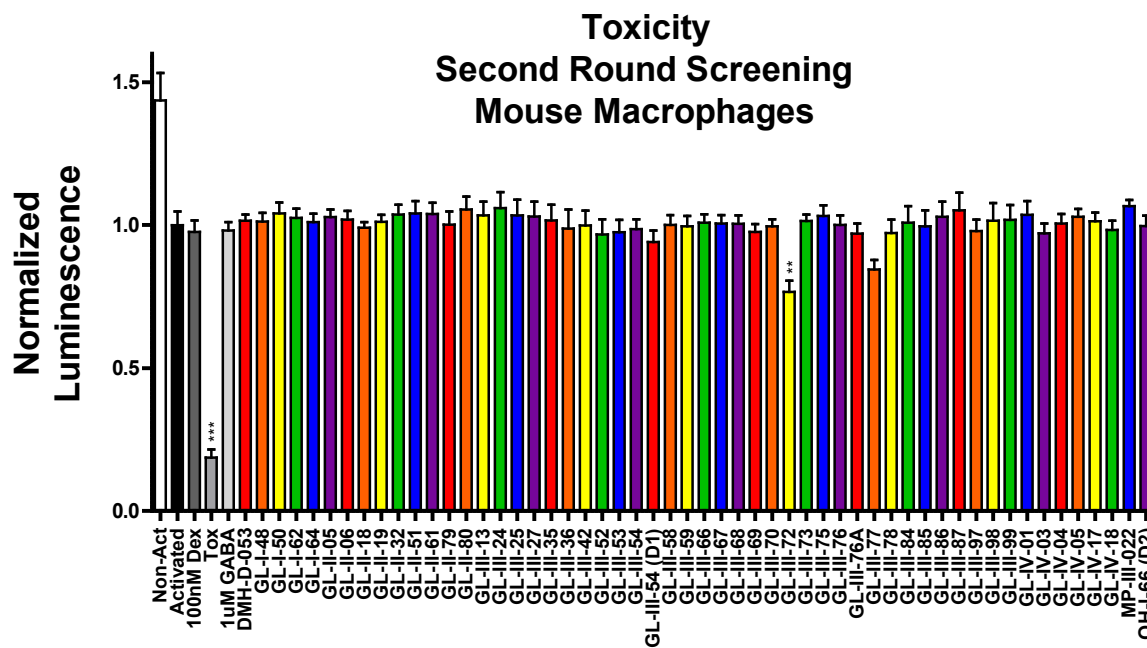
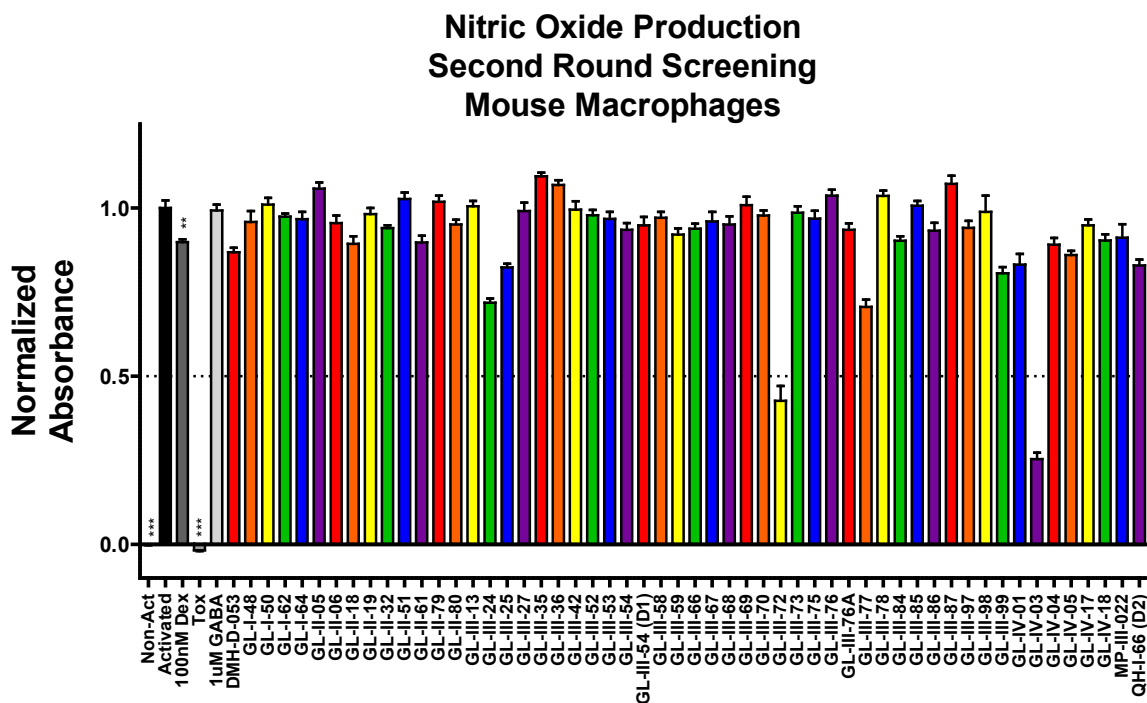


Figure 98. Second Round of Compound Screening in Mouse Macrophages RAW264.7 Mouse Macrophages were activated with LPS and IFN γ and treated with 1 μ M GABA co-applied with 10 μ M of compounds of interest for 24 hours. Half of the supernatant was removed and analyzed with the Griess Assay. ATP levels were quantified by the Cell Titer Glo kit as a measure of toxicity using the cells and remaining supernatant.

GL-IV-03 and the two related compounds GL-III-24 and GL-III-25 were tested at different concentrations. GL-IV-03 did not show nitric oxide reduction at concentrations lower than the initial 10 μM from the screening assay, however GL-III-24 and GL-III-25 showed some activity at 1 μM . For structural continuity purposes, GL-IV-03 was chosen as the third lead compound.

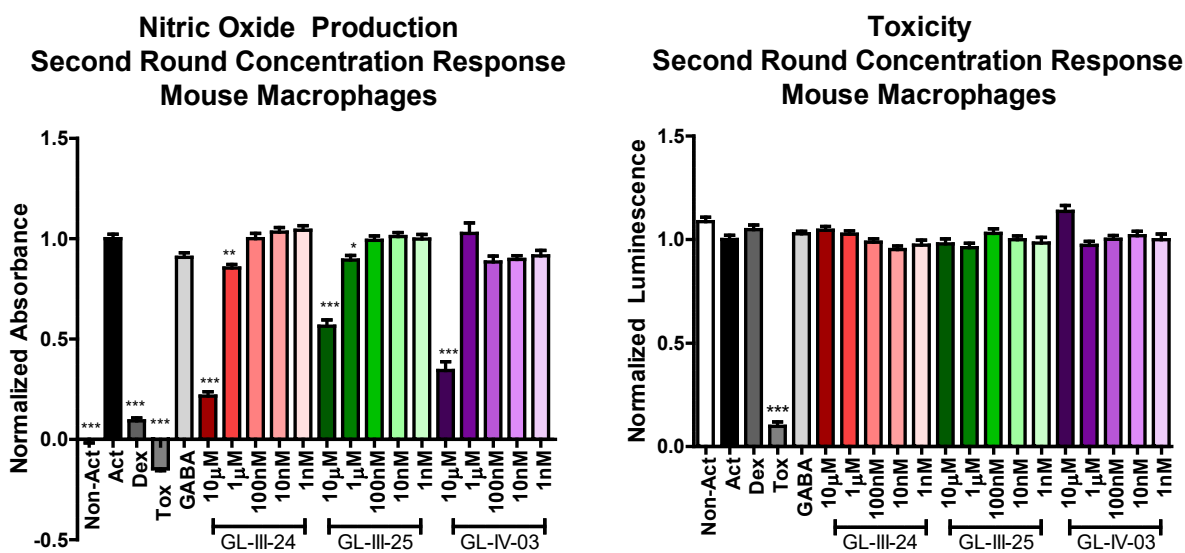


Figure 99. Concentration Response of Compounds from Second Screening Assay in Mouse Macrophages RWA264.7 Mouse Macrophages were activated with LPS and $\text{IFN}\gamma$ and treated with 1 μM GABA co-applied with 1 nM - 10 μM of compounds of interest for 24 hours. Half of the supernatant was removed and analyzed with the Griess Assay. ATP levels were quantified by the Cell Titer Glo kit as a measure of toxicity using the cells and remaining supernatant.

Third Lead Compound: GL-IV-03

As with the previous lead compounds, GL-IV-03 was assessed for safety purposes. Oral doses at 40 mg/kg did not show any adverse sensorimotor effects in mice (**Figure 100**). Assessing GL-IV-03 with IP dosing is also planned but has yet to be completed.

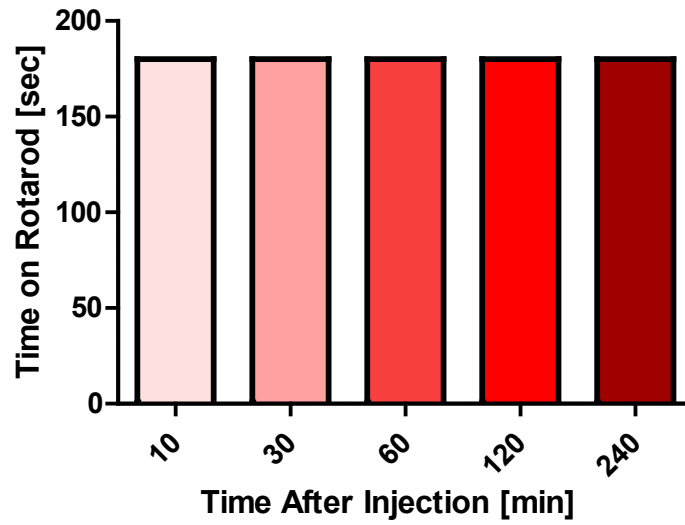


Figure 100. Rotarod Performance of Mice Treated with GL-IV-03 Mice were orally dosed with 40 mg/kg GL-IV-03 and placed on the Rotarod apparatus at various time post-treatment to determine if GL-IV-03 caused any detrimental sensorimotor effects. Data Courtesy of Alex Kehoe and Ian Luecke.

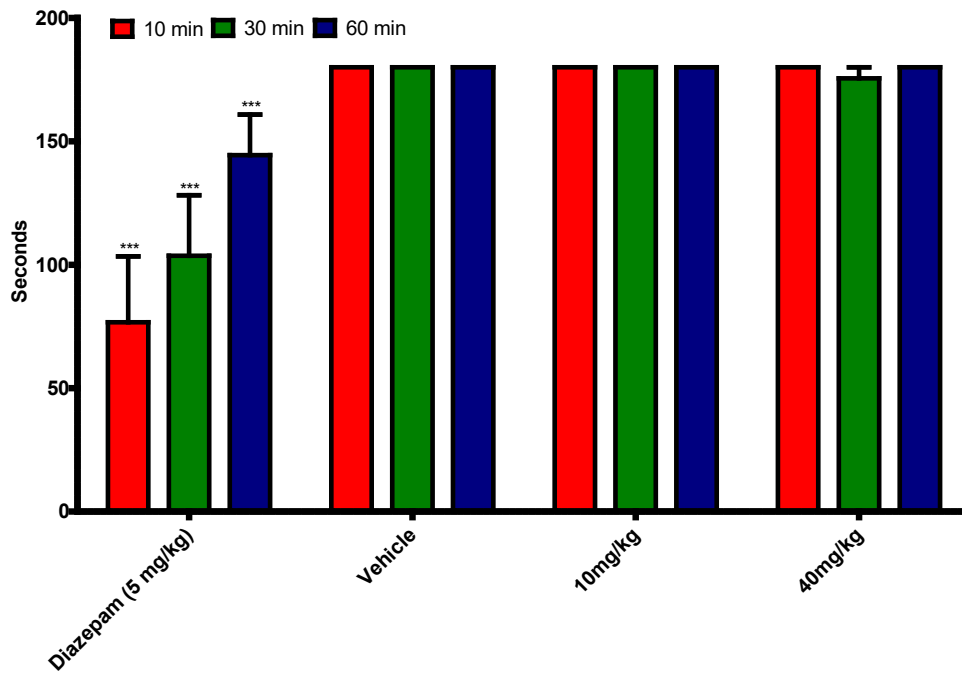


Figure 101. Rotarod Performance of Mice Treated with GL-IV-03 Mice were dosed I.P. with 10 or 40 mg/kg GL-IV-03 and placed on the Rotarod apparatus at various time post-treatment to determine if GL-IV-03 caused any detrimental sensorimotor effects. Data Courtesy of Nicolas Zahn.

GL-IV-03 was used to continue the investigations into the mechanism by which imidazodiazepines inhibit nitric oxide production. Based on the inability of MP-IV-010 to reduce iNOS mRNA after 24 hours (Figure 92), it was hypothesized that iNOS transcription might be inhibited at earlier time points. Therefore, iNOS mRNA levels were quantified after 3, 6, 12, 18, and 24 hours by RT-qPCR (Figure 102).

Time Based Activation of iNOS Transcription

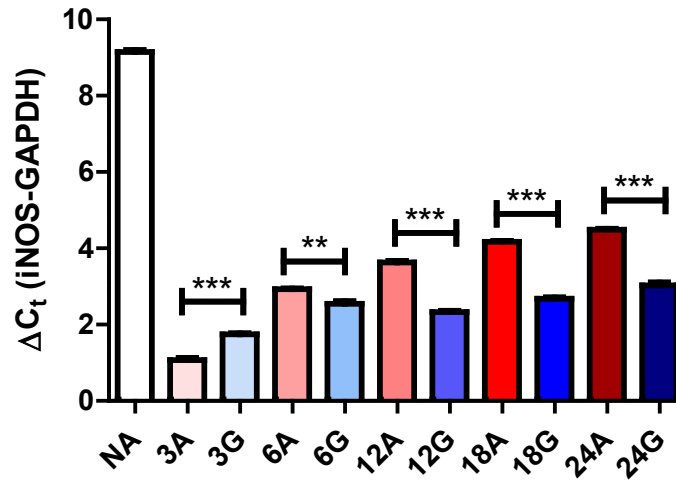


Figure 102. GL-IV-03 Regulates iNOS Transcription Mouse Microglia were activated with IFN γ and LPS (A) and treated with 10 μ M GL-IV-03 (G) for 3, 6, 12, 18, and 24 hours. mRNA was isolated and quantified using QuantiFast SYBR green RT-qPCR kit. Cycle numbers for each sample were normalized to GAPDH using the ΔC_t method.

GL-IV-03 reduced iNOS transcription at 3 hours. At 6 hours, however, higher iNOS mRNA levels were observed for the GL-IV-03 treated cells implying that GL-IV-03 induces the transcription of iNOS. Additional early time points were investigated to confirm these results and are presented in Figure 103.

Time Based Activation of iNOS Transcription

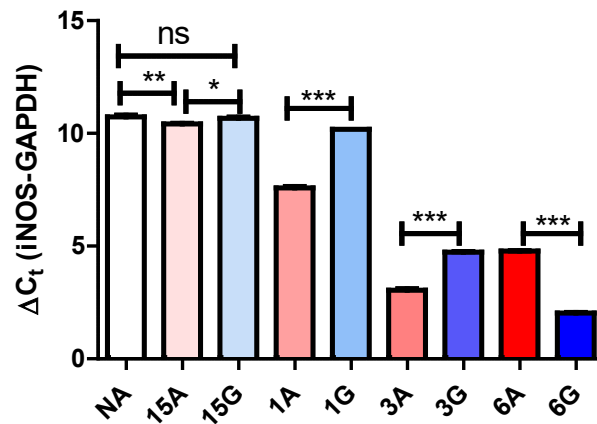


Figure 103. GL-IV-03 Regulates iNOS Transcription at Early Time Points Mouse Microglia were activated with IFN γ and LPS (A) and treated with 10 μ M GL-IV-03 (G) for 15 minutes, 1, 3, and 6 hours. mRNA was isolated and quantified using QuantiFast SYBR green RT-qPCR kit. Cycle numbers for each sample were normalized to GAPDH using the Δ Ct method.

The second experiment confirmed that early transcription of iNOS (1 and 3 hours after activation) is inhibited by GL-IV-03. At 6 hours after activation, the effects of GL-IV-03 is the opposite. To investigate the effect on protein iNOS protein production, iNOS protein levels were assessed by ELISA after 24 hour treatment with GL-IV-03 (Figure 104). GL-IV-03 reduced protein levels of iNOS by about 60%.

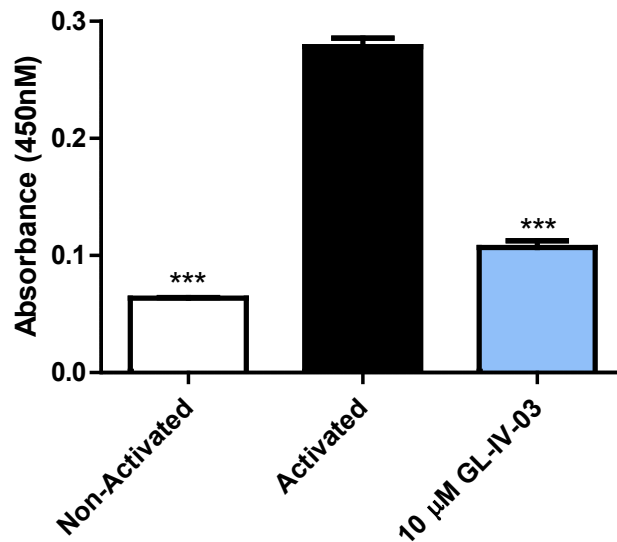


Figure 104. iNOS Protein Levels after 24 Hour Treatment with GL-IV-03 Mouse microglia were activated with IFN γ and LPS and treated with 10 μ M GL-IV-03 for 24 hours. Protein was extracted and analyzed with the Mouse iNOS ELISA kit from ABCAM.

5.3.3 Discussion

The GABAergic system has not been well studied in microglia. The above results represent the initial characterization of functional human microglial GABA_AR, showing that $\alpha 3$ is the most prevalent alpha subunit, and only $\beta 1$, $\gamma 2$, and δ were found in addition to alpha subunits (**Figure 73**). Although there is limited diversity among the GABA_AR, there are sufficient subunits to form functional receptors as shown by patch clamp (**Figure 71**, **Figure 74**). Additional results support this identification of functional GABA_AR because microglial transmembrane current was modulated by imidazodiazepines (**Figure 72**).

Only one group, Lee *et al* described $\alpha 1$, $\alpha 3$, and $\beta 1$ subunits in primary mouse microglia.¹¹ The results above agree with and expand on this characterization using immortalized mouse microglia. A much more diverse set of GABA_AR subunits was identified for mouse microglia than human microglia, although $\alpha 3$, $\beta 1$, $\gamma 2$, and δ expression was consistent in both species (**Figure 75**). Primary mouse microglia have previously been patched, however GABA_AR agonist muscimol did not generate current flow.¹⁶⁴ Neither GABA nor imidazodiazepines have been previously investigated for their effects on GABA_AR-mediated transmembrane currents, and are shown here to have a significant transmembrane effect (**Figure 76**, **Figure 77**).

KRM-II-81 has shown to have antinociceptive effects⁷⁰ and modulate GABA_AR-mediated currents in microglia (**Figure 72**), however it produced adverse effects *in vivo* (data not published). MP-III-080 was developed in response and modulated microglial transmembrane currents (**Figure 77**). *In vivo* behavioral studies suggest that the slight structure change eliminated the adverse *in vivo* effects (**Figure 78**), and PDSP data suggests limited off target binding (**Table 16**).

In vitro, MP-III-080 did not reduce nitric oxide (**Figure 80**), despite the reduction of intracellular calcium that mediates a majority of inflammatory processes (**Figure 58**).³⁰⁻³² Because of its lack of anti-inflammatory properties, MP-III-080 was eliminated from consideration.

MP-IV-010 was identified after screening additional compounds for significant nitric oxide reduction (**Figure 81, Figure 84**) and for lack of adverse *in vitro* and *in vivo* effects (**Figure 85, Figure 86, Table 17**). The secondary PDSP screening showed tightest binding to the κ Opioid receptor (KOR), which is known for eliciting sensorimotor effects¹⁶⁵⁻¹⁶⁶ when agonized (**Figure 87**), however the rotarod assay did not show any adverse effects, even at doses as high as 120 mg/kg (**Figure 86**). Therefore, three GABA_AR antagonists were employed to show that MP-IV-010 was working through the GABA_AR.

Neither flumazenil, picrotoxin, nor bicuculline was able to reverse the nitric oxide reduction seen with MP-IV-010 treatment, indicating that nitric oxide reduction was not mediated by the GABA_AR (**Figure 88**). KOR antagonist norbinaltorphimine was capable of partially reversing the reduction, suggesting that MP-IV-010 is at least partially acting through the KOR to reduce NO production.

The peripheral benzodiazepine receptor (PBR) did not qualify as a hit in the primary PDSP screening, however the screen was completed at 10 μ M, whereas effects with MP-IV-010 were not seen until the concentration reached 50 μ M. Interestingly, the PBR agonist 4'Chlorodiazepam was capable of reducing nitric oxide production to similar levels as MP-IV-010 (**Figure 90**). This is consistent with numerous reports that the PBR plays a role in microglia activation, many of which are summarized in Venneti *et al.*¹⁶⁷ The PBR antagonist PK11195 has been shown to reduce calcium responses in human microglia¹⁶⁸ and iNOS expression in the rat striatum.¹⁶⁹ However, it cannot be determined if PK11195 reversed nitric oxide production achieved with MP-IV-010 as significant toxicity was recorded (**Figure 89**).

The Sigma2 receptor was also identified by the PDSP screen, however this receptor was not further investigated due to time constraints. This receptor would be an excellent point of investigation because sigma receptors are known to have a role in microglia activation and stimulation of these receptors suppressed calcium signaling.¹⁷⁰

Though iNOS is calcium-independent once expressed,³³ there is evidence that iNOS expression and nitric oxide production can be reduced by blocking extracellular calcium entry through calcium

release-activated calcium (CRAC) channels.¹⁶³ As MP-IV-010 also reduced intracellular calcium levels (**Figure 91**), iNOS transcription was investigated. However, after 24 hours of MP-IV-010 treatment, iNOS mRNA levels were not significantly different (**Figure 92**). This suggested that MP-IV-010 may act directly on iNOS or causes changes during post-translational modifications.

iNOS activity was reduced after 24 hours of MP-IV-010 treatment (**Figure 93**), however it was unclear if this effect related to direct inhibition of the enzyme or changes in post-translational modifications. Incubating MP-IV-010 with the isolated proteins for a short period, however, did not reduce iNOS activity (**Figure 94**), confirming that MP-IV-010 is not an inhibitor of iNOS.

Concurrently with these studies, screening of additional compounds was completed, identifying GL-IV-03 as a more potent reducer of nitric oxide production from microglia (**Figure 95**) and macrophages (**Figure 98**). GL-IV-03 is structurally related to MP-IV-010. PDSP data is not yet available for this compound, however rotarod studies showed no sensorimotor inhibition at oral and I.P. doses of 40 mg/kg.

Investigations into the mechanism of NO reduction continued with GL-IV-03. Reports showed upregulation of iNOS after LPS stimulus can be seen on the protein level as early as 6 hours after treatment.¹⁷¹ Once iNOS is produced and activated, it is long lived and yields high amounts of nitric oxide.¹⁷² Therefore, it was hypothesized that iNOS transcription may be transiently controlled so earlier time points were investigated.

GL-IV-03 was capable of reducing iNOS transcription soon after treatment, however that trend reversed at 6 hours (**Figure 102, Figure 103**) and GL-IV-03 treatment began contributing to iNOS mRNA production. Though it appeared that iNOS was being transcribed at higher than expected levels up to 24 hours post-treatment, protein levels were significantly reduced approximately 60% (**Figure 104**). However, nitric oxide levels were reduced almost 90% and previous experiments with MP-IV-010 revealed that iNOS activity was back to baseline during that same timeframe but not directly inhibited by the compound.

Because NO has a very short half-life (estimated to be less than two seconds in extravascular tissue¹⁷³) and gene expression changes can be seen on the protein level within a few hours, the low levels of nitric oxide are not solely due to the low amounts of iNOS transcription early after treatment. Therefore, it is hypothesized that control of nitric oxide production through iNOS is controlled in part through early reduction of transcription, reduced translation or post-translational modifications, and potentially through reduction of iNOS cofactors or substrates.

5.4 Conclusion

Neuropathic pain has thus far been a difficult to treat type of chronic pain, but imidazodiazepines show potential as new treatments. These compounds have been used for decades to target and reduce neuronal firing that leads to pain. Additionally, tuning them to be anti-inflammatory presents a very promising, multi-faceted treatment option that could change the way chronic pain is managed. Though this work is in its infancy, safe imidazodiazepines have been developed that are capable of reducing intracellular calcium and nitric oxide.

Many additional studies need to be conducted, including fully elucidating the mechanism behind the nitric oxide reduction. This most likely includes transcription factors and common signaling molecules such as MAP Kinases. Further *in vitro* studies are required to determine the effects of these compounds on microglial inflammatory outputs such as cytokines and chemokines, and safety profiles. *In vitro* studies should also be carried out in neurons and astrocytes, as astrocytes act as immunomodulators during an inflammatory response. Additional *in vivo* anti-nociceptive studies are currently underway with GL-IV-03.

REFERENCES

1. Richter, L.; de Graaf, C.; Sieghart, W.; Varagic, Z.; Morzinger, M.; de Esch, I. J.; Ecker, G. F.; Ernst, M., Diazepam-bound GABAA receptor models identify new benzodiazepine binding-site ligands. *Nature chemical biology* **2012**, *8* (5), 455-64.
2. Olsen, R. W.; Sieghart, W., GABA A receptors: subtypes provide diversity of function and pharmacology. *Neuropharmacology* **2009**, *56* (1), 141-8.
3. Olsen, R. W.; Sieghart, W., International Union of Pharmacology. LXX. Subtypes of gamma-aminobutyric acid(A) receptors: classification on the basis of subunit composition, pharmacology, and function. Update. *Pharmacological reviews* **2008**, *60* (3), 243-60.
4. Siegel, G. J., *Basic neurochemistry : molecular, cellular, and medical aspects*. 6th ed.; Lippincott Williams & Wilkins: Philadelphia, 1999; p xxi, 1183.
5. Sieghart, W., Structure and pharmacology of gamma-aminobutyric acidA receptor subtypes. *Pharmacological reviews* **1995**, *47* (2), 181-234.
6. Griffin, C. E., 3rd; Kaye, A. M.; Bueno, F. R.; Kaye, A. D., Benzodiazepine pharmacology and central nervous system-mediated effects. *The Ochsner journal* **2013**, *13* (2), 214-23.
7. Donaldson, M.; Gizzarelli, G.; Chanpong, B., Oral sedation: a primer on anxiolysis for the adult patient. *Anesthesia progress* **2007**, *54* (3), 118-28; quiz 129.
8. Tan, K. R.; Rudolph, U.; Luscher, C., Hooked on benzodiazepines: GABAA receptor subtypes and addiction. *Trends in neurosciences* **2011**, *34* (4), 188-97.
9. Yocum, G. T.; Turner, D. L.; Danielsson, J.; Barajas, M. B.; Zhang, Y.; Xu, D.; Harrison, N. L.; Homanics, G. E.; Farber, D. L.; Emala, C. W., GABAA receptor alpha4-subunit knockout enhances lung inflammation and airway reactivity in a murine asthma model. *American journal of physiology. Lung cellular and molecular physiology* **2017**, *313* (2), L406-L415.
10. Mizuta, K.; Xu, D.; Pan, Y.; Comas, G.; Sonett, J. R.; Zhang, Y.; Panettieri, R. A., Jr.; Yang, J.; Emala, C. W., Sr., GABAA receptors are expressed and facilitate relaxation in airway smooth muscle. *American journal of physiology. Lung cellular and molecular physiology* **2008**, *294* (6), L1206-16.
11. Lee, M.; Schwab, C.; McGeer, P. L., Astrocytes are GABAergic cells that modulate microglial activity. *Glia* **2011**, *59* (1), 152-65.
12. Dunham, N. W.; Miya, T. S., A note on a simple apparatus for detecting neurological deficit in rats and mice. *Journal of the American Pharmaceutical Association. American Pharmaceutical Association* **1957**, *46* (3), 208-9.
13. Kudo, M.; Ishigatsubo, Y.; Aoki, I., Pathology of asthma. *Frontiers in microbiology* **2013**, *4*, 263.
14. Dionisio, L.; Jose De Rosa, M.; Bouzat, C.; Esandi Mdel, C., An intrinsic GABAergic system in human lymphocytes. *Neuropharmacology* **2011**, *60* (2-3), 513-9.
15. Reyes-Garcia, M. G.; Hernandez-Hernandez, F.; Hernandez-Tellez, B.; Garcia-Tamayo, F., GABA (A) receptor subunits RNA expression in mice peritoneal macrophages modulate their IL-6/IL-12 production. *Journal of neuroimmunology* **2007**, *188* (1-2), 64-8.
16. Possa, S. S.; Leick, E. A.; Prado, C. M.; Martins, M. A.; Tiberio, I. F., Eosinophilic inflammation in allergic asthma. *Frontiers in pharmacology* **2013**, *4*, 46.
17. McBrien, C. N.; Menzies-Gow, A., The Biology of Eosinophils and Their Role in Asthma. *Frontiers in medicine* **2017**, *4*, 93.

18. Prado, C. M.; Martins, M. A.; Tiberio, I. F., Nitric oxide in asthma physiopathology. *ISRN allergy* **2011**, *2011*, 832560.
19. van Veen, I. H.; Ten Brinke, A.; Sterk, P. J.; Sont, J. K.; Gauw, S. A.; Rabe, K. F.; Bel, E. H., Exhaled nitric oxide predicts lung function decline in difficult-to-treat asthma. *The European respiratory journal* **2008**, *32* (2), 344-9.
20. Koretzky, G. A., Multiple roles of CD4 and CD8 in T cell activation. *Journal of immunology* **2010**, *185* (5), 2643-4.
21. Larche, M.; Robinson, D. S.; Kay, A. B., The role of T lymphocytes in the pathogenesis of asthma. *The Journal of allergy and clinical immunology* **2003**, *111* (3), 450-63; quiz 464.
22. Lewis, R. S., Calcium signaling mechanisms in T lymphocytes. *Annual review of immunology* **2001**, *19*, 497-521.
23. Forkuo, G. S.; Nieman, A. N.; Yuan, N. Y.; Kodali, R.; Yu, O. B.; Zahn, N. M.; Jahan, R.; Li, G.; Stephen, M. R.; Guthrie, M. L.; Poe, M. M.; Hartzler, B. D.; Harris, T. W.; Yocum, G. T.; Emala, C. W.; Steeber, D. A.; Stafford, D. C.; Cook, J. M.; Arnold, L. A., Alleviation of Multiple Asthmatic Pathologic Features with Orally Available and Subtype Selective GABAA Receptor Modulators. *Molecular pharmaceutics* **2017**, *14* (6), 2088-2098.
24. Forkuo, G. S.; Nieman, A. N.; Kodali, R.; Zahn, N. M.; Li, G.; Rashid Roni, M. S.; Stephen, M. R.; Harris, T. W.; Jahan, R.; Guthrie, M. L.; Yu, O. B.; Fisher, J. L.; Yocum, G. T.; Emala, C. W.; Steeber, D. A.; Stafford, D. C.; Cook, J. M.; Arnold, L. A., A Novel Orally Available Asthma Drug Candidate That Reduces Smooth Muscle Constriction and Inflammation by Targeting GABAA Receptors in the Lung. *Molecular pharmaceutics* **2018**.
25. Hoeffel, G.; Ginhoux, F., Ontogeny of Tissue-Resident Macrophages. *Frontiers in immunology* **2015**, *6*, 486.
26. Rock, R. B.; Gekker, G.; Hu, S.; Sheng, W. S.; Cheeran, M.; Lokensgard, J. R.; Peterson, P. K., Role of microglia in central nervous system infections. *Clinical microbiology reviews* **2004**, *17* (4), 942-64, table of contents.
27. Jakel, S.; Dimou, L., Glial Cells and Their Function in the Adult Brain: A Journey through the History of Their Ablation. *Frontiers in cellular neuroscience* **2017**, *11*, 24.
28. Shinozaki, Y.; Nomura, M.; Iwatsuki, K.; Moriyama, Y.; Gachet, C.; Koizumi, S., Microglia trigger astrocyte-mediated neuroprotection via purinergic gliotransmission. *Scientific reports* **2014**, *4*, 4329.
29. Moller, T., Calcium signaling in microglial cells. *Glia* **2002**, *40* (2), 184-94.
30. Mika, J.; Zychowska, M.; Popiolek-Barczyk, K.; Rojewska, E.; Przewlocka, B., Importance of glial activation in neuropathic pain. *European journal of pharmacology* **2013**, *716* (1-3), 106-19.
31. Inoue, K., Purinergic signaling in microglia in the pathogenesis of neuropathic pain. *Proceedings of the Japan Academy. Series B, Physical and biological sciences* **2017**, *93* (4), 174-182.
32. Donnelly-Roberts, D.; McGaraughty, S.; Shieh, C. C.; Honore, P.; Jarvis, M. F., Painful purinergic receptors. *The Journal of pharmacology and experimental therapeutics* **2008**, *324* (2), 409-15.
33. Forstermann, U.; Sessa, W. C., Nitric oxide synthases: regulation and function. *European heart journal* **2012**, *33* (7), 829-37, 837a-837d.
34. Sierra, A.; Navascues, J.; Cuadros, M. A.; Calvente, R.; Martin-Oliva, D.; Ferrer-Martin, R. M.; Martin-Estebane, M.; Carrasco, M. C.; Marin-Teva, J. L., Expression of inducible nitric oxide synthase (iNOS) in microglia of the developing quail retina. *PLoS one* **2014**, *9* (8), e106048.
35. Cooper, J. R.; Bloom, F. E.; Roth, R. H., *The biochemical basis of neuropharmacology*. 8th ed.; Oxford University Press: Oxford ; New York, 2003; p vii, 405 p.
36. Spiering, M. J., The discovery of GABA in the brain. *The Journal of biological chemistry* **2018**, *293* (49), 19159-19160.
37. Roberts, E.; Frankel, S., gamma-Aminobutyric acid in brain: its formation from glutamic acid. *The Journal of biological chemistry* **1950**, *187* (1), 55-63.

38. Florey, E., An inhibitory and an excitatory factor of mammalian central nervous system, and their action of a single sensory neuron. *Archives internationales de physiologie* **1954**, 62 (1), 33-53.
39. Florey, E.; Mc, L. H., The effects of factor I and of gamma-aminobutyric acid on smooth muscle preparations. *The Journal of physiology* **1959**, 145 (1), 66-76.
40. Edwards, D. H.; Heitler, W. J.; Krasne, F. B., Fifty years of a command neuron: the neurobiology of escape behavior in the crayfish. *Trends in neurosciences* **1999**, 22 (4), 153-61.
41. Hayashi, T., Inhibition and excitation due to gamma-aminobutyric acid in the central nervous system. *Nature* **1958**, 182 (4642), 1076-7.
42. Iversen, L. L.; Neal, M. J., The uptake of [3H]GABA by slices of rat cerebral cortex. *Journal of neurochemistry* **1968**, 15 (10), 1141-9.
43. Krnjevic, K.; Schwartz, S., The action of gamma-aminobutyric acid on cortical neurones. *Experimental brain research* **1967**, 3 (4), 320-36.
44. Fenalti, G.; Law, R. H.; Buckle, A. M.; Langendorf, C.; Tuck, K.; Rosado, C. J.; Faux, N. G.; Mahmood, K.; Hampe, C. S.; Banga, J. P.; Wilce, M.; Schmidberger, J.; Rossjohn, J.; El-Kabbani, O.; Pike, R. N.; Smith, A. I.; Mackay, I. R.; Rowley, M. J.; Whisstock, J. C., GABA production by glutamic acid decarboxylase is regulated by a dynamic catalytic loop. *Nature structural & molecular biology* **2007**, 14 (4), 280-6.
45. Jin, X. T.; Galvan, A.; Wichmann, T.; Smith, Y., Localization and Function of GABA Transporters GAT-1 and GAT-3 in the Basal Ganglia. *Frontiers in systems neuroscience* **2011**, 5, 63.
46. Olsen, R. W.; Tobin, A. J., Molecular biology of GABA_A receptors. *FASEB journal : official publication of the Federation of American Societies for Experimental Biology* **1990**, 4, 1469-1480.
47. Bowery, N. G.; Smart, T. G., GABA and glycine as neurotransmitters: a brief history. *British journal of pharmacology* **2006**, 147 Suppl 1, S109-19.
48. Schofield, P. R.; Darlison, M. G.; Fujita, N.; Burt, D. R.; Stephenson, F. A.; Rodriguez, H.; Rhee, L. M.; Ramachandran, J.; Reale, V.; Glencorse, T. A.; et al., Sequence and functional expression of the GABA A receptor shows a ligand-gated receptor super-family. *Nature* **1987**, 328 (6127), 221-7.
49. Zhu, S.; Noviello, C. M.; Teng, J.; Walsh, R. M., Jr.; Kim, J. J.; Hibbs, R. E., Structure of a human synaptic GABA_A receptor. *Nature* **2018**, 559 (7712), 67-72.
50. Miller, P. S.; Aricescu, A. R., Crystal structure of a human GABA_A receptor. *Nature* **2014**, 512 (7514), 270-5.
51. Sieghart, W.; Savic, M. M., International Union of Basic and Clinical Pharmacology. CVI: GABA_A Receptor Subtype- and Function-selective Ligands: Key Issues in Translation to Humans. *Pharmacological reviews* **2018**, 70 (4), 836-878.
52. Krall, J., Balle, T., Krogsgaard-Larsen, N., Sorensen, T., Frolund, B., Chapter 8 - GABA_A Receptor Partial Agonists and Antagonists: Structure, Binding Mode, and Pharmacology. In *Diversity and functions of GABA receptors : a tribute to Hanns Möhler, Part A*, Rudolph, U., Ed. Els: 2015; pp 201-227.
53. Johnston, G. A., Muscimol as an ionotropic GABA receptor agonist. *Neurochemical research* **2014**, 39 (10), 1942-7.
54. Wafford, K. A.; Ebert, B., Gaboxadol--a new awakening in sleep. *Current opinion in pharmacology* **2006**, 6 (1), 30-6.
55. Lankford, D. A.; Corser, B. C.; Zheng, Y. P.; Li, Z.; Snavely, D. B.; Lines, C. R.; Deacon, S., Effect of gaboxadol on sleep in adult and elderly patients with primary insomnia: results from two randomized, placebo-controlled, 30-night polysomnography studies. *Sleep* **2008**, 31 (10), 1359-70.
56. Skerritt, J. H.; Johnston, G. A., Diazepam stimulates the binding of GABA and muscimol but not THIP to rat brain membranes. *Neuroscience letters* **1983**, 38 (3), 315-20.
57. Johnston, G. A., Advantages of an antagonist: bicuculline and other GABA antagonists. *British journal of pharmacology* **2013**, 169 (2), 328-36.
58. Krishek, B. J.; Moss, S. J.; Smart, T. G., A functional comparison of the antagonists bicuculline and picrotoxin at recombinant GABA_A receptors. *Neuropharmacology* **1996**, 35 (9-10), 1289-98.

59. Massey, S. C.; Linn, D. M.; Kittila, C. A.; Mirza, W., Contributions of GABAA receptors and GABAC receptors to acetylcholine release and directional selectivity in the rabbit retina. *Visual neuroscience* **1997**, *14* (5), 939-48.
60. Ueno, S.; Bracamontes, J.; Zorumski, C.; Weiss, D. S.; Steinbach, J. H., Bicuculline and gabazine are allosteric inhibitors of channel opening of the GABAA receptor. *The Journal of neuroscience : the official journal of the Society for Neuroscience* **1997**, *17* (2), 625-34.
61. Olsen, R. W., Picrotoxin-like channel blockers of GABAA receptors. *Proceedings of the National Academy of Sciences of the United States of America* **2006**, *103* (16), 6081-2.
62. Olsen, R. W., GABAA receptor: Positive and negative allosteric modulators. *Neuropharmacology* **2018**, *136* (Pt A), 10-22.
63. Wang, D. S.; Buckinx, R.; Lecorronc, H.; Mangin, J. M.; Rigo, J. M.; Legendre, P., Mechanisms for picrotoxinin and picrotin blocks of alpha2 homomeric glycine receptors. *The Journal of biological chemistry* **2007**, *282* (22), 16016-35.
64. Xu, M.; Covey, D. F.; Akabas, M. H., Interaction of picrotoxin with GABAA receptor channel-lining residues probed in cysteine mutants. *Biophysical journal* **1995**, *69* (5), 1858-67.
65. Sternbach, L. H., The benzodiazepine story. *Journal of medicinal chemistry* **1979**, *22* (1), 1-7.
66. Fuentes, A. V.; Pineda, M. D.; Venkata, K. C. N., Comprehension of Top 200 Prescribed Drugs in the US as a Resource for Pharmacy Teaching, Training and Practice. *Pharmacy* **2018**, *6* (2).
67. Clayton, T.; Chen, J. L.; Ernst, M.; Richter, L.; Cromer, B. A.; Morton, C. J.; Ng, H.; Kaczorowski, C. C.; Helmstetter, F. J.; Furtmuller, R.; Ecker, G.; Parker, M. W.; Sieghart, W.; Cook, J. M., An updated unified pharmacophore model of the benzodiazepine binding site on gamma-aminobutyric acid(a) receptors: correlation with comparative models. *Current medicinal chemistry* **2007**, *14* (26), 2755-75.
68. Prevot, T. D.; Li, G.; Vidojevic, A.; Misquitta, K. A.; Fee, C.; Santrac, A.; Knutson, D. E.; Stephen, M. R.; Kodali, R.; Zahn, N. M.; Arnold, L. A.; Scholze, P.; Fisher, J. L.; Markovic, B. D.; Banasr, M.; Cook, J. M.; Savic, M.; Sibille, E., Novel Benzodiazepine-Like Ligands with Various Anxiolytic, Antidepressant, or Pro-Cognitive Profiles. *Molecular neuropsychiatry* **2019**, *5* (2), 84-97.
69. Gill, K. M.; Lodge, D. J.; Cook, J. M.; Aras, S.; Grace, A. A., A novel alpha5GABA(A)R-positive allosteric modulator reverses hyperactivation of the dopamine system in the MAM model of schizophrenia. *Neuropsychopharmacology : official publication of the American College of Neuropsychopharmacology* **2011**, *36* (9), 1903-11.
70. Lewter, L. A.; Fisher, J. L.; Siemian, J. N.; Methuku, K. R.; Poe, M. M.; Cook, J. M.; Li, J. X., Antinociceptive Effects of a Novel alpha2/alpha3-Subtype Selective GABAA Receptor Positive Allosteric Modulator. *ACS chemical neuroscience* **2017**, *8* (6), 1305-1312.
71. Forkuo, G. S.; Guthrie, M. L.; Yuan, N. Y.; Nieman, A. N.; Kodali, R.; Jahan, R.; Stephen, M. R.; Yocum, G. T.; Treven, M.; Poe, M. M.; Li, G.; Yu, O. B.; Hartzler, B. D.; Zahn, N. M.; Ernst, M.; Emala, C. W.; Stafford, D. C.; Cook, J. M.; Arnold, L. A., Development of GABAA Receptor Subtype-Selective Imidazobenzodiazepines as Novel Asthma Treatments. *Molecular pharmaceuticals* **2016**, *13* (6), 2026-38.
72. Jahan, R.; Stephen, M. R.; Forkuo, G. S.; Kodali, R.; Guthrie, M. L.; Nieman, A. N.; Yuan, N. Y.; Zahn, N. M.; Poe, M. M.; Li, G.; Yu, O. B.; Yocum, G. T.; Emala, C. W.; Stafford, D. C.; Cook, J. M.; Arnold, L. A., Optimization of substituted imidazobenzodiazepines as novel asthma treatments. *European journal of medicinal chemistry* **2017**, *126*, 550-560.
73. Whitwam, J. G.; Amrein, R., Pharmacology of flumazenil. *Acta anaesthesiologica Scandinavica. Supplementum* **1995**, *108*, 3-14.
74. Hadingham, K. L.; Garrett, E. M.; Wafford, K. A.; Bain, C.; Heavens, R. P.; Sirinathsinghji, D. J.; Whiting, P. J., Cloning of cDNAs encoding the human gamma-aminobutyric acid type A receptor alpha 6 subunit and characterization of the pharmacology of alpha 6-containing receptors. *Molecular pharmacology* **1996**, *49* (2), 253-9.

75. Clayton, T.; Poe, M. M.; Rallapalli, S.; Biawat, P.; Savic, M. M.; Rowlett, J. K.; Gallos, G.; Emala, C. W.; Kaczorowski, C. C.; Stafford, D. C.; Arnold, L. A.; Cook, J. M., A Review of the Updated Pharmacophore for the Alpha 5 GABA(A) Benzodiazepine Receptor Model. *International journal of medicinal chemistry* **2015**, *2015*, 430248.
76. Hanchar, H. J.; Chutsrinopkun, P.; Meera, P.; Supavilai, P.; Sieghart, W.; Wallner, M.; Olsen, R. W., Ethanol potently and competitively inhibits binding of the alcohol antagonist Ro15-4513 to alpha4/6beta3delta GABAA receptors. *Proceedings of the National Academy of Sciences of the United States of America* **2006**, *103* (22), 8546-51.
77. Uhlen, M.; Zhang, C.; Lee, S.; Sjostedt, E.; Fagerberg, L.; Bidkhor, G.; Benfeitas, R.; Arif, M.; Liu, Z.; Edfors, F.; Sanli, K.; von Feilitzen, K.; Oksvold, P.; Lundberg, E.; Hober, S.; Nilsson, P.; Mattsson, J.; Schwenk, J. M.; Brunnstrom, H.; Glimelius, B.; Sjoblom, T.; Edqvist, P. H.; Djureinovic, D.; Micke, P.; Lindskog, C.; Mardinoglu, A.; Ponten, F., A pathology atlas of the human cancer transcriptome. *Science* **2017**, *357* (6352).
78. Uhlen, M.; Fagerberg, L.; Hallstrom, B. M.; Lindskog, C.; Oksvold, P.; Mardinoglu, A.; Sivertsson, A.; Kampf, C.; Sjostedt, E.; Asplund, A.; Olsson, I.; Edlund, K.; Lundberg, E.; Navani, S.; Szgyarto, C. A.; Odeberg, J.; Djureinovic, D.; Takanen, J. O.; Hober, S.; Alm, T.; Edqvist, P. H.; Berling, H.; Tegel, H.; Mulder, J.; Rockberg, J.; Nilsson, P.; Schwenk, J. M.; Hamsten, M.; von Feilitzen, K.; Forsberg, M.; Persson, L.; Johansson, F.; Zwahlen, M.; von Heijne, G.; Nielsen, J.; Ponten, F., Proteomics. Tissue-based map of the human proteome. *Science* **2015**, *347* (6220), 1260419.
79. Thul, P. J.; Akesson, L.; Wiking, M.; Mahdessian, D.; Geladaki, A.; Ait Blal, H.; Alm, T.; Asplund, A.; Bjork, L.; Breckels, L. M.; Backstrom, A.; Danielsson, F.; Fagerberg, L.; Fall, J.; Gatto, L.; Gnann, C.; Hober, S.; Hjelmare, M.; Johansson, F.; Lee, S.; Lindskog, C.; Mulder, J.; Mulvey, C. M.; Nilsson, P.; Oksvold, P.; Rockberg, J.; Schutten, R.; Schwenk, J. M.; Sivertsson, A.; Sjostedt, E.; Skogs, M.; Stadler, C.; Sullivan, D. P.; Tegel, H.; Winsnes, C.; Zhang, C.; Zwahlen, M.; Mardinoglu, A.; Ponten, F.; von Feilitzen, K.; Lilley, K. S.; Uhlen, M.; Lundberg, E., A subcellular map of the human proteome. *Science* **2017**, *356* (6340).
80. Nutt, D., GABAA receptors: subtypes, regional distribution, and function. *Journal of clinical sleep medicine : JCSM : official publication of the American Academy of Sleep Medicine* **2006**, *2* (2), S7-11.
81. Mendu, S. K.; Bhandage, A.; Jin, Z.; Birnir, B., Different subtypes of GABA-A receptors are expressed in human, mouse and rat T lymphocytes. *PLoS one* **2012**, *7* (8), e42959.
82. Fisher, J. L.; Zhang, J.; Macdonald, R. L., The role of alpha1 and alpha6 subtype amino-terminal domains in allosteric regulation of gamma-aminobutyric acid receptors. *Molecular pharmacology* **1997**, *52* (4), 714-24.
83. Neher, E.; Sakmann, B., Single-channel currents recorded from membrane of denervated frog muscle fibres. *Nature* **1976**, *260* (5554), 799-802.
84. Yuan, N. Y. Development of Cellular High Throughput Assays to Determine the Electrophysiological Profile of GABA_A Receptor Modulators for Neurology and Immunology. University of Wisconsin - Milwaukee, 2016.
85. Molleman, A., *Patch Clamping: An Introductory Guide To Patch Clamp Electrophysiology*. John Wiley & Sons Ltd: New York, 2003.
86. Ionescu-Zanetti, C., Ligand-Gated Ion-Channel Target Screening. *Genetic Engineering & Biotechnology News* **2010**, *30* (1).
87. Savic, M. M.; Majumder, S.; Huang, S.; Edwankar, R. V.; Furtmuller, R.; Joksimovic, S.; Clayton, T., Sr.; Ramerstorfer, J.; Milinkovic, M. M.; Roth, B. L.; Sieghart, W.; Cook, J. M., Novel positive allosteric modulators of GABAA receptors: do subtle differences in activity at alpha1 plus alpha5 versus alpha2 plus alpha3 subunits account for dissimilarities in behavioral effects in rats? *Progress in neuro-psychopharmacology & biological psychiatry* **2010**, *34* (2), 376-86.

88. Adelman, W. J., Jr.; Senft, J. P., Voltage clamp studies on the effect of internal cesium ion on sodium and potassium currents in the squid giant axon. *The Journal of general physiology* **1966**, *50* (2), 279-93.
89. Li, P.; Zhang, S.; Fan, N.; Xiao, H.; Zhang, W.; Zhang, W.; Wang, H.; Tang, B., Quantitative fluorescence ratio imaging of intralysosomal chloride ions with single excitation/dual maximum emission. *Chemistry* **2014**, *20* (37), 11760-7.
90. Di Virgilio, F.; Steinberg, T. H.; Silverstein, S. C., Inhibition of Fura-2 sequestration and secretion with organic anion transport blockers. *Cell calcium* **1990**, *11* (2-3), 57-62.
91. Brooks, S. P.; Dunnett, S. B., Tests to assess motor phenotype in mice: a user's guide. *Nature reviews. Neuroscience* **2009**, *10* (7), 519-29.
92. OmniTech Electronics, I. Multi (Four Animal) Accelerating RotaRod. (accessed June 18).
93. To, T.; Stanojevic, S.; Moores, G.; Gershon, A. S.; Bateman, E. D.; Cruz, A. A.; Boulet, L. P., Global asthma prevalence in adults: findings from the cross-sectional world health survey. *BMC public health* **2012**, *12*, 204.
94. Maslan, J.; Mims, J. W., What is asthma? Pathophysiology, demographics, and health care costs. *Otolaryngologic clinics of North America* **2014**, *47* (1), 13-22.
95. Akinbami, L. J.; Moorman, J. E.; Liu, X.; National Center for Health Statistics (U.S.), *Asthma prevalence, health care use, and mortality : United States, 2005-2009*. U.S. Dept. of Health and Human Services, Centers for Disease Control and Prevention, National Center for Health Statistics: Hyattsville, MD, 2011; p 16 p.
96. National Asthma Education and Prevention Program (National Heart Lung and Blood Institute). Third Expert Panel on the Management of Asthma., *Guidelines for the diagnosis and management of asthma : full report 2007*. U.S Dept. of Health and Human Services, National Institutes of Health, National Heart, Lung, and Blood Institute: Bethesda, Md., 2010; p xxii, 326 p.
97. Barnes, P. J., Corticosteroid resistance in patients with asthma and chronic obstructive pulmonary disease. *The Journal of allergy and clinical immunology* **2013**, *131* (3), 636-45.
98. National Asthma, E.; Prevention, P., Expert Panel Report 3 (EPR-3): Guidelines for the Diagnosis and Management of Asthma-Summary Report 2007. *The Journal of allergy and clinical immunology* **2007**, *120* (5 Suppl), S94-138.
99. Xu, J.; Sabarinath, S. N.; Derendorf, H., Cortisol suppression as a surrogate marker for inhaled corticosteroid-induced growth retardation in children. *European journal of pharmaceutical sciences : official journal of the European Federation for Pharmaceutical Sciences* **2009**, *36* (1), 110-21.
100. Abbas, A. K.; Lichtman, A. H.; Pillai, S., *Cellular and molecular immunology*. 7th ed.; Elsevier/Saunders: Philadelphia, 2012; p x, 545 p.
101. Miceli, M. C.; Parnes, J. R., The roles of CD4 and CD8 in T cell activation. *Seminars in immunology* **1991**, *3* (3), 133-41.
102. Betts, R. J.; Kemeny, D. M., CD8+ T cells in asthma: friend or foe? *Pharmacology & therapeutics* **2009**, *121* (2), 123-31.
103. Romagnani, S., T-cell subsets (Th1 versus Th2). *Annals of allergy, asthma & immunology : official publication of the American College of Allergy, Asthma, & Immunology* **2000**, *85* (1), 9-18; quiz 18, 21.
104. Kidd, P., Th1/Th2 balance: the hypothesis, its limitations, and implications for health and disease. *Alternative medicine review : a journal of clinical therapeutic* **2003**, *8* (3), 223-46.
105. Mathur, S. K.; Fichtinger, P. S.; Evans, M. D.; Schwantes, E. A.; Jarjour, N. N., Variability of blood eosinophil count as an asthma biomarker. *Annals of allergy, asthma & immunology : official publication of the American College of Allergy, Asthma, & Immunology* **2016**, *117* (5), 551-553.
106. Balhara, J.; Gounni, A. S., The alveolar macrophages in asthma: a double-edged sword. *Mucosal immunology* **2012**, *5* (6), 605-9.

107. Gallos, G.; Yim, P.; Chang, S.; Zhang, Y.; Xu, D.; Cook, J. M.; Gerthoffer, W. T.; Emala, C. W., Sr., Targeting the restricted alpha-subunit repertoire of airway smooth muscle GABAA receptors augments airway smooth muscle relaxation. *American journal of physiology. Lung cellular and molecular physiology* **2012**, *302* (2), L248-56.
108. Januzi, L.; Poirier, J. W.; Maksoud, M. J. E.; Xiang, Y. Y.; Veldhuizen, R. A. W.; Gill, S. E.; Cregan, S. P.; Zhang, H.; Dekaban, G. A.; Lu, W. Y., Autocrine GABA signaling distinctively regulates phenotypic activation of mouse pulmonary macrophages. *Cellular immunology* **2018**, *332*, 7-23.
109. Zahn, N. M.; Huber, A. T.; Mikulsky, B. N.; Stepanski, M. E.; Kehoe, A. S.; Li, G.; Schussman, M.; Rashid Roni, M. S.; Kodali, R.; Cook, J. M.; Stafford, D. C.; Steeber, D. A.; Arnold, L. A., MIDD0301 - A first-in-class anti-inflammatory asthma drug targets GABAA receptors without causing systemic immune suppression. *Basic & clinical pharmacology & toxicology* **2019**, *125* (1), 75-84.
110. Braun, M.; Ramracheya, R.; Bengtsson, M.; Clark, A.; Walker, J. N.; Johnson, P. R.; Rorsman, P., Gamma-aminobutyric acid (GABA) is an autocrine excitatory transmitter in human pancreatic beta-cells. *Diabetes* **2010**, *59* (7), 1694-701.
111. Yocum, G. T.; Gallos, G.; Zhang, Y.; Jahan, R.; Stephen, M. R.; Varagic, Z.; Puthenkalam, R.; Ernst, M.; Cook, J. M.; Emala, C. W., Targeting the gamma-Aminobutyric Acid A Receptor alpha4 Subunit in Airway Smooth Muscle to Alleviate Bronchoconstriction. *American journal of respiratory cell and molecular biology* **2016**, *54* (4), 546-53.
112. Savic, M. M.; Huang, S.; Furtmuller, R.; Clayton, T.; Huck, S.; Obradovic, D. I.; Ugresic, N. D.; Sieghart, W.; Bokonjic, D. R.; Cook, J. M., Are GABAA receptors containing alpha5 subunits contributing to the sedative properties of benzodiazepine site agonists? *Neuropsychopharmacology : official publication of the American College of Neuropsychopharmacology* **2008**, *33* (2), 332-9.
113. Dionisio, L.; Arias, V.; Bouzat, C.; Esandi Mdel, C., GABAA receptor plasticity in Jurkat T cells. *Biochimie* **2013**, *95* (12), 2376-84.
114. Hoyer, K. K.; Dooms, H.; Barron, L.; Abbas, A. K., Interleukin-2 in the development and control of inflammatory disease. *Immunological reviews* **2008**, *226*, 19-28.
115. Broide, D. H.; Lotz, M.; Cuomo, A. J.; Coburn, D. A.; Federman, E. C.; Wasserman, S. I., Cytokines in symptomatic asthma airways. *The Journal of allergy and clinical immunology* **1992**, *89* (5), 958-67.
116. Ferkany, J. W.; Smith, L. A.; Seifert, W. E.; Caprioli, R. M.; Enna, S. J., Measurement of gamma-aminobutyric acid (GABA) in blood. *Life sciences* **1978**, *22* (23), 2121-8.
117. Shen, M. L.; Wang, C. H.; Lin, C. H.; Zhou, N.; Kao, S. T.; Wu, D. C., Luteolin Attenuates Airway Mucus Overproduction via Inhibition of the GABAergic System. *Scientific reports* **2016**, *6*, 32756.
118. Bjurstrom, H.; Wang, J.; Ericsson, I.; Bengtsson, M.; Liu, Y.; Kumar-Mendru, S.; Issazadeh-Navikas, S.; Birnir, B., GABA, a natural immunomodulator of T lymphocytes. *Journal of neuroimmunology* **2008**, *205* (1-2), 44-50.
119. Chen, G.; Panicker, S.; Lau, K. Y.; Apparsundaram, S.; Patel, V. A.; Chen, S. L.; Soto, R.; Jung, J. K.; Ravindran, P.; Okuhara, D.; Bohnert, G.; Che, Q.; Rao, P. E.; Allard, J. D.; Badi, L.; Bitter, H. M.; Nunn, P. A.; Narula, S. K.; DeMartino, J. A., Characterization of a novel CRAC inhibitor that potently blocks human T cell activation and effector functions. *Molecular immunology* **2013**, *54* (3-4), 355-67.
120. Kam, J. C.; Szeffler, S. J.; Surs, W.; Sher, E. R.; Leung, D. Y., Combination IL-2 and IL-4 reduces glucocorticoid receptor-binding affinity and T cell response to glucocorticoids. *Journal of immunology* **1993**, *151* (7), 3460-6.
121. Guthrie, M. L. Development of Pre-Clinical Assays Based on Tandem Mass Spectrometry to Investigate GABA_A Receptor Modulators. University of Wisconsin - Milwaukee, Milwaukee, WI, 2017.
122. Heckford, S. E.; Gelmann, E. P.; Agnor, C. L.; Jacobson, S.; Zinn, S.; Matis, L. A., Distinct signals are required for proliferation and lymphokine gene expression in murine T cell clones. *Journal of immunology* **1986**, *137* (11), 3652-63.

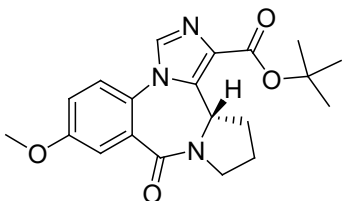
123. Bessler, H.; Weizman, R.; Gavish, M.; Notti, I.; Djaldetti, M., Immunomodulatory effect of peripheral benzodiazepine receptor ligands on human mononuclear cells. *Journal of neuroimmunology* **1992**, *38* (1-2), 19-25.
124. Cell concentrations in human and mouse samples. https://assets.thermofisher.com/TFS-Assets/LSG/brochures/I-076357%20cell%20count%20table%20topp_WEB.pdf (accessed September 23).
125. Sanders, R. D.; Grover, V.; Goulding, J.; Godlee, A.; Gurney, S.; Snelgrove, R.; Ma, D.; Singh, S.; Maze, M.; Hussell, T., Immune cell expression of GABAA receptors and the effects of diazepam on influenza infection. *Journal of neuroimmunology* **2015**, *282*, 97-103.
126. Sanders, R. D.; Godlee, A.; Fujimori, T.; Goulding, J.; Xin, G.; Salek-Ardakani, S.; Snelgrove, R. J.; Ma, D.; Maze, M.; Hussell, T., Benzodiazepine augmented gamma-amino-butyric acid signaling increases mortality from pneumonia in mice. *Critical care medicine* **2013**, *41* (7), 1627-36.
127. Wheeler, D. W.; Thompson, A. J.; Corletto, F.; Reckless, J.; Loke, J. C.; Lapaque, N.; Grant, A. J.; Mastroeni, P.; Grainger, D. J.; Padgett, C. L.; O'Brien, J. A.; Miller, N. G.; Trowsdale, J.; Lummis, S. C.; Menon, D. K.; Beech, J. S., Anaesthetic impairment of immune function is mediated via GABA(A) receptors. *PLoS one* **2011**, *6* (2), e17152.
128. Bhat, R.; Axtell, R.; Mitra, A.; Miranda, M.; Lock, C.; Tsien, R. W.; Steinman, L., Inhibitory role for GABA in autoimmune inflammation. *Proceedings of the National Academy of Sciences of the United States of America* **2010**, *107* (6), 2580-5.
129. Hedegaard, H.; Warner, M.; Minino, A. M., Drug Overdose Deaths in the United States, 1999-2016. *NCHS data brief* **2017**, (294), 1-8.
130. van Hecke, O.; Austin, S. K.; Khan, R. A.; Smith, B. H.; Torrance, N., Neuropathic pain in the general population: a systematic review of epidemiological studies. *Pain* **2014**, *155* (4), 654-62.
131. Colloca, L.; Ludman, T.; Bouhassira, D.; Baron, R.; Dickenson, A. H.; Yarnitsky, D.; Freeman, R.; Truini, A.; Attal, N.; Finnerup, N. B.; Eccleston, C.; Kalso, E.; Bennett, D. L.; Dworkin, R. H.; Raja, S. N., Neuropathic pain. *Nature reviews. Disease primers* **2017**, *3*, 17002.
132. Nightingale, S., The neuropathic pain market. *Nature reviews. Drug discovery* **2012**, *11* (2), 101-2.
133. Michalski, J. P.; Kothary, R., Oligodendrocytes in a Nutshell. *Frontiers in cellular neuroscience* **2015**, *9*, 340.
134. Etle, B.; Schlachetzki, J. C. M.; Winkler, J., Oligodendroglia and Myelin in Neurodegenerative Diseases: More Than Just Bystanders? *Molecular neurobiology* **2016**, *53* (5), 3046-3062.
135. Salter, M. W.; Stevens, B., Microglia emerge as central players in brain disease. *Nature medicine* **2017**, *23* (9), 1018-1027.
136. Levy, D.; Zochodne, D. W., NO pain: potential roles of nitric oxide in neuropathic pain. *Pain practice : the official journal of World Institute of Pain* **2004**, *4* (1), 11-8.
137. Gao, Y. J.; Ji, R. R., Targeting astrocyte signaling for chronic pain. *Neurotherapeutics : the journal of the American Society for Experimental NeuroTherapeutics* **2010**, *7* (4), 482-93.
138. Brahmachari, S.; Fung, Y. K.; Pahan, K., Induction of glial fibrillary acidic protein expression in astrocytes by nitric oxide. *The Journal of neuroscience : the official journal of the Society for Neuroscience* **2006**, *26* (18), 4930-9.
139. Wu, C.; Qin, X.; Du, H.; Li, N.; Ren, W.; Peng, Y., The immunological function of GABAergic system. *Frontiers in bioscience* **2017**, *22*, 1162-1172.
140. Hoft, S.; Griemsmann, S.; Seifert, G.; Steinhauser, C., Heterogeneity in expression of functional ionotropic glutamate and GABA receptors in astrocytes across brain regions: insights from the thalamus. *Philosophical transactions of the Royal Society of London. Series B, Biological sciences* **2014**, *369* (1654), 20130602.
141. Fraser, D. D.; Duffy, S.; Angelides, K. J.; Perez-Velazquez, J. L.; Kettenmann, H.; MacVicar, B. A., GABAA/benzodiazepine receptors in acutely isolated hippocampal astrocytes. *The Journal of neuroscience : the official journal of the Society for Neuroscience* **1995**, *15* (4), 2720-32.

142. Di Lio, A.; Benke, D.; Besson, M.; Desmeules, J.; Daali, Y.; Wang, Z. J.; Edwankar, R.; Cook, J. M.; Zeilhofer, H. U., HZ166, a novel GABAA receptor subtype-selective benzodiazepine site ligand, is antihyperalgesic in mouse models of inflammatory and neuropathic pain. *Neuropharmacology* **2011**, *60* (4), 626-32.
143. Iwata, H.; Yamamuro, Y., Subregional Expression of Hippocampal Glutamatergic and GABAergic Genes in F344 Rats with Social Isolation after Weaning. *Comparative medicine* **2016**, *66* (1), 4-9.
144. Kim, I.; Yang, D.; Tang, X.; Carroll, J. L., Reference gene validation for qPCR in rat carotid body during postnatal development. *BMC research notes* **2011**, *4*, 440.
145. Poe, M. M. Synthesis of Subtype Selective Bz/GABA_A Receptor Ligands for the Treatment of Anxiety, Epilepsy and Neuropathic Pain, as well as Schizophrenia and Asthma. University of Wisconsin - Milwaukee, Milwaukee, WI, 2016.
146. Witkin, J. M.; Cerne, R.; Wakulchik, M.; S, J.; Gleason, S. D.; Jones, T. M.; Li, G.; Arnold, L. A.; Li, J. X.; Schkeryantz, J. M.; Methuku, K. R.; Cook, J. M.; Poe, M. M., Further evaluation of the potential anxiolytic activity of imidazo[1,5-a][1,4]diazepin agents selective for alpha2/3-containing GABAA receptors. *Pharmacology, biochemistry, and behavior* **2017**, *157*, 35-40.
147. Garcia-Mesa, Y.; Jay, T. R.; Checkley, M. A.; Luttgge, B.; Dobrowolski, C.; Valadkhan, S.; Landreth, G. E.; Karn, J.; Alvarez-Carbonell, D., Immortalization of primary microglia: a new platform to study HIV regulation in the central nervous system. *Journal of neurovirology* **2017**, *23* (1), 47-66.
148. Nakai, T.; Nagai, T.; Wang, R.; Yamada, S.; Kuroda, K.; Kaibuchi, K.; Yamada, K., Alterations of GABAergic and dopaminergic systems in mutant mice with disruption of exons 2 and 3 of the Disc1 gene. *Neurochemistry international* **2014**, *74*, 74-83.
149. Gangisetty, O.; Reddy, D. S., The optimization of TaqMan real-time RT-PCR assay for transcriptional profiling of GABA-A receptor subunit plasticity. *Journal of neuroscience methods* **2009**, *181* (1), 58-66.
150. Masocha, W., Comprehensive analysis of the GABAergic system gene expression profile in the anterior cingulate cortex of mice with Paclitaxel-induced neuropathic pain. *Gene expression* **2015**, *16* (3), 145-53.
151. Li, G. Design and Synthesis of Achiral and Chiral Imidazodiazepine (IMDZ) GABA(A)R Subtype Selective Ligands for the Treatment of CNS Disorders, as well as Asthma. University of Wisconsin - Milwaukee, Milwaukee, WI, 2019.
152. Roth, B., National Institute of Mental Health Psychoactive Drug Screening Program. In *Assay Protocol Book* [Online] Department of Pharmacology: University of North Carolina at Chapel Hill, 2018; p. 359.
153. Hortnagl, H.; Tasan, R. O.; Wieselthaler, A.; Kirchmair, E.; Sieghart, W.; Sperk, G., Patterns of mRNA and protein expression for 12 GABAA receptor subunits in the mouse brain. *Neuroscience* **2013**, *236*, 345-72.
154. Papadopoulos, V., Peripheral benzodiazepine receptor: structure and function in health and disease. *Annales pharmaceutiques francaises* **2003**, *61* (1), 30-50.
155. Casellas, P.; Galiegue, S.; Basile, A. S., Peripheral benzodiazepine receptors and mitochondrial function. *Neurochemistry international* **2002**, *40* (6), 475-86.
156. Peng, Y.; McCorvy, J. D.; Harpoe, K.; Lansu, K.; Yuan, S.; Popov, P.; Qu, L.; Pu, M.; Che, T.; Nikolajsen, L. F.; Huang, X. P.; Wu, Y.; Shen, L.; Bjorn-Yoshimoto, W. E.; Ding, K.; Wacker, D.; Han, G. W.; Cheng, J.; Katritch, V.; Jensen, A. A.; Hanson, M. A.; Zhao, S.; Gloriam, D. E.; Roth, B. L.; Stevens, R. C.; Liu, Z. J., 5-HT_{2C} Receptor Structures Reveal the Structural Basis of GPCR Polypharmacology. *Cell* **2018**, *172* (4), 719-730 e14.
157. Canal, C. E.; Murnane, K. S., The serotonin 5-HT_{2C} receptor and the non-addictive nature of classic hallucinogens. *Journal of psychopharmacology* **2017**, *31* (1), 127-143.

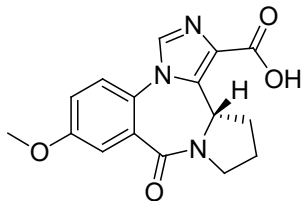
158. Monti, J. M.; Pellejero, T.; Jantos, H., Effects of H1- and H2-histamine receptor agonists and antagonists on sleep and wakefulness in the rat. *Journal of neural transmission* **1986**, *66* (1), 1-11.
159. Parsons, M. E.; Ganellin, C. R., Histamine and its receptors. *British journal of pharmacology* **2006**, *147 Suppl 1*, S127-35.
160. Lalanne, L.; Ayranci, G.; Kieffer, B. L.; Lutz, P. E., The kappa opioid receptor: from addiction to depression, and back. *Frontiers in psychiatry* **2014**, *5*, 170.
161. Guo, L.; Zhen, X., Sigma-2 receptor ligands: neurobiological effects. *Current medicinal chemistry* **2015**, *22* (8), 989-1003.
162. Kamei, J.; Nagase, H., Norbinaltorphimine, a selective kappa-opioid receptor antagonist, induces an itch-associated response in mice. *European journal of pharmacology* **2001**, *418* (1-2), 141-5.
163. Mizuma, A.; Kim, J. Y.; Kacimi, R.; Stauderman, K.; Dunn, M.; Hebbar, S.; Yenari, M. A., Microglial Calcium Release-Activated Calcium Channel Inhibition Improves Outcome from Experimental Traumatic Brain Injury and Microglia-Induced Neuronal Death. *Journal of neurotrauma* **2019**, *36* (7), 996-1007.
164. Cheung, G.; Kann, O.; Kohsaka, S.; Faerber, K.; Kettenmann, H., GABAergic activities enhance macrophage inflammatory protein-1 α release from microglia (brain macrophages) in postnatal mouse brain. *The Journal of physiology* **2009**, *587* (Pt 4), 753-68.
165. Gallantine, E. L.; Meert, T. F., Antinociceptive and adverse effects of mu- and kappa-opioid receptor agonists: a comparison of morphine and U50488-H. *Basic & clinical pharmacology & toxicology* **2008**, *103* (5), 419-27.
166. White, K. L.; Robinson, J. E.; Zhu, H.; DiBerto, J. F.; Polepally, P. R.; Zjawiony, J. K.; Nichols, D. E.; Malanga, C. J.; Roth, B. L., The G protein-biased kappa-opioid receptor agonist RB-64 is analgesic with a unique spectrum of activities in vivo. *The Journal of pharmacology and experimental therapeutics* **2015**, *352* (1), 98-109.
167. Venneti, S.; Lopresti, B. J.; Wiley, C. A., The peripheral benzodiazepine receptor (Translocator protein 18kDa) in microglia: from pathology to imaging. *Progress in neurobiology* **2006**, *80* (6), 308-22.
168. Choi, H. B.; Khoo, C.; Ryu, J. K.; van Breemen, E.; Kim, S. U.; McLarnon, J. G., Inhibition of lipopolysaccharide-induced cyclooxygenase-2, tumor necrosis factor- α and [Ca²⁺]_i responses in human microglia by the peripheral benzodiazepine receptor ligand PK11195. *Journal of neurochemistry* **2002**, *83* (3), 546-55.
169. Ryu, J. K.; Choi, H. B.; McLarnon, J. G., Peripheral benzodiazepine receptor ligand PK11195 reduces microglial activation and neuronal death in quinolinic acid-injected rat striatum. *Neurobiology of disease* **2005**, *20* (2), 550-61.
170. Hall, A. A.; Herrera, Y.; Ajmo, C. T., Jr.; Cuevas, J.; Pennypacker, K. R., Sigma receptors suppress multiple aspects of microglial activation. *Glia* **2009**, *57* (7), 744-54.
171. Hwang, J. S.; Kwon, M. Y.; Kim, K. H.; Lee, Y.; Lyoo, I. K.; Kim, J. E.; Oh, E. S.; Han, I. O., Lipopolysaccharide (LPS)-stimulated iNOS Induction Is Increased by Glucosamine under Normal Glucose Conditions but Is Inhibited by Glucosamine under High Glucose Conditions in Macrophage Cells. *The Journal of biological chemistry* **2017**, *292* (5), 1724-1736.
172. Saha, R. N.; Pahan, K., Regulation of inducible nitric oxide synthase gene in glial cells. *Antioxidants & redox signaling* **2006**, *8* (5-6), 929-47.
173. Thomas, D. D.; Liu, X.; Kantrow, S. P.; Lancaster, J. R., Jr., The biological lifetime of nitric oxide: implications for the perivascular dynamics of NO and O₂. *Proceedings of the National Academy of Sciences of the United States of America* **2001**, *98* (1), 355-60.

APPENDICES

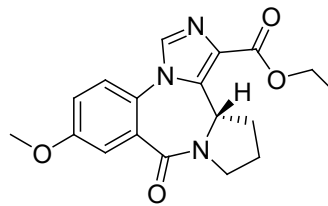
Appendix A – Asthma Compound Structures



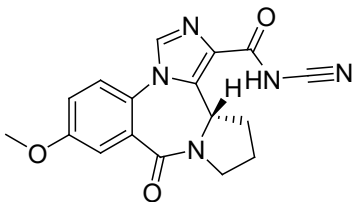
XHE-III-74



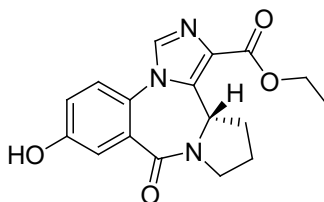
XHE-III-74 Acid



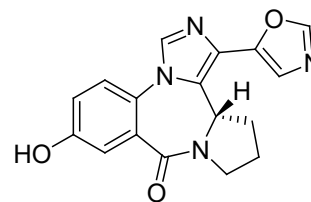
XHE-III-74 Ethyl Ester



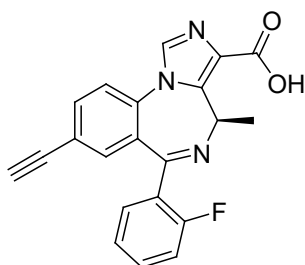
MRS-III-90



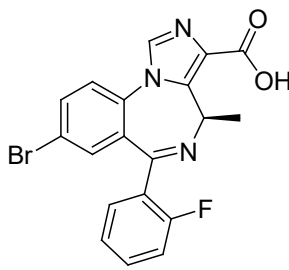
RJ-02-50



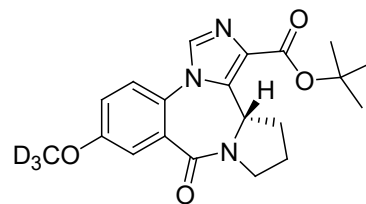
RJ-03-30



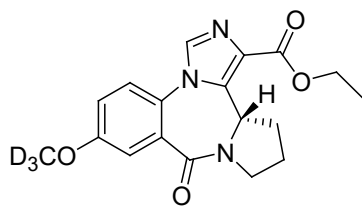
SH-053-2'F-R-CH₃ Acid



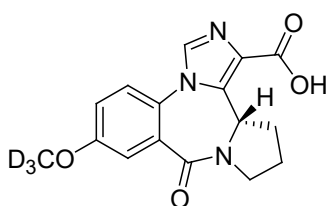
MIDD0301



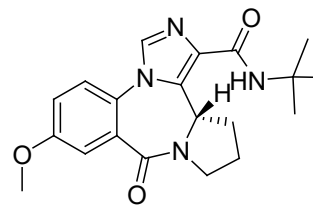
RJ-02-52



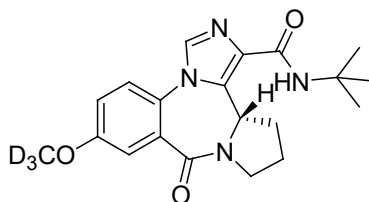
RJ-02-46



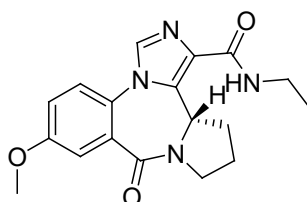
RJ-02-66



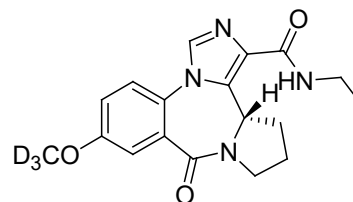
MRS-01-74



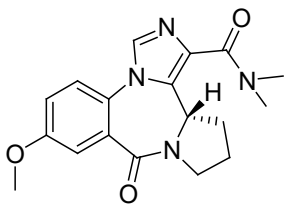
RJ-02-68



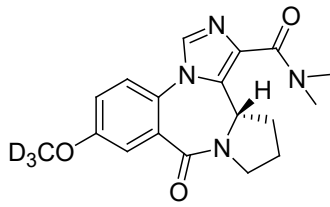
MRS-02-57



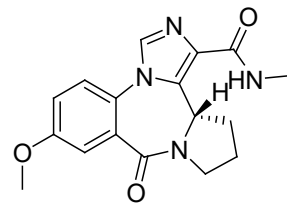
RJ-02-89



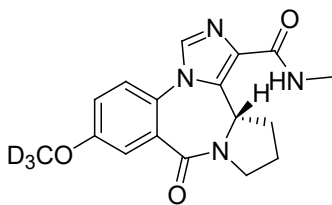
MRS-01-66



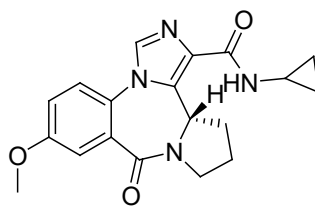
RJ-02-91



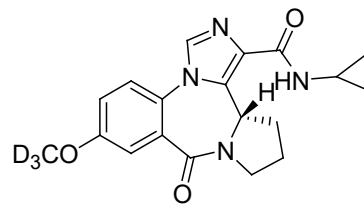
MRS-01-64



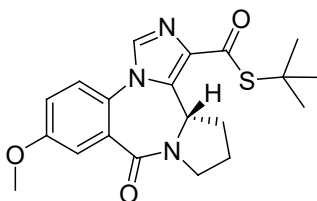
RJ-02-92



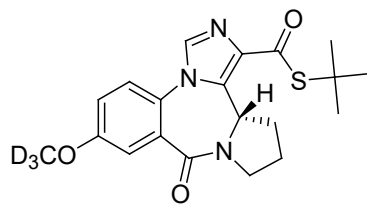
MRS-01-52



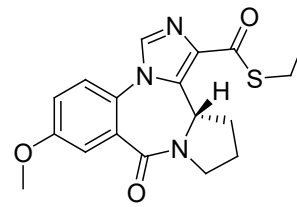
RJ-02-72



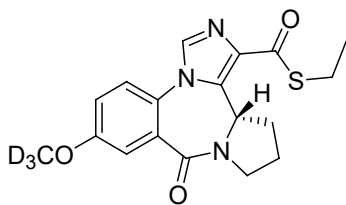
MRS-01-73



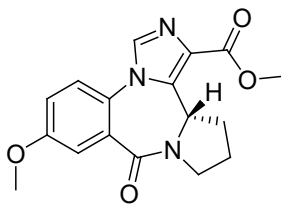
RJ-02-69



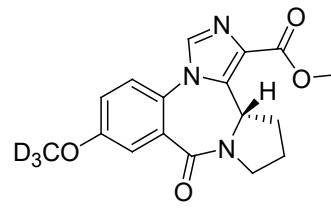
MRS-01-67



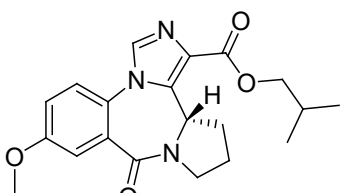
RJ-02-90



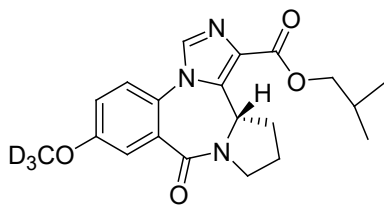
MRS-01-68



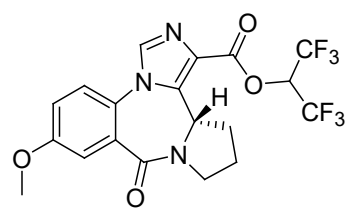
RJ-02-70



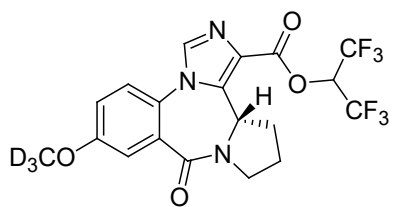
RJ-01-46



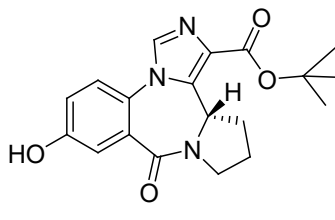
RJ-02-71



MRS-01-53

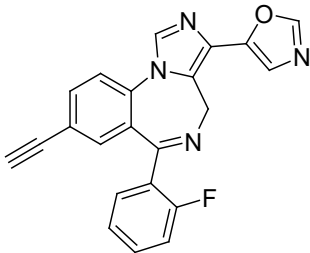


RJ-02-93

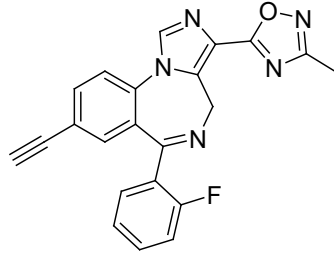


RJ-02-67

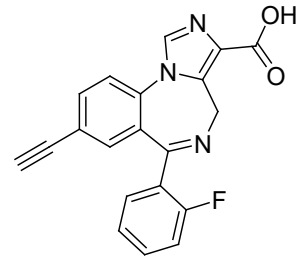
Appendix B – Pain Compound Structures



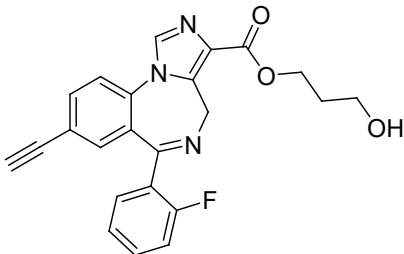
KRM-II-18B



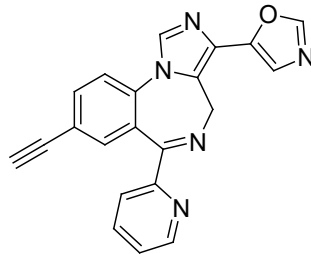
GL-III-23



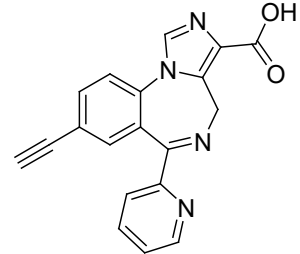
GL-III-79



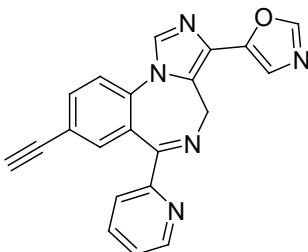
GL-II-80



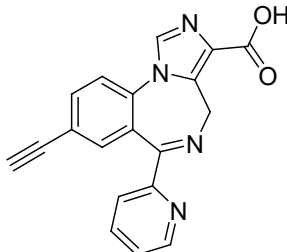
KRM-II-81



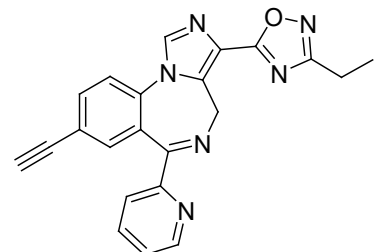
GL-III-13



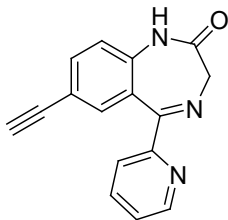
KRM-II-81



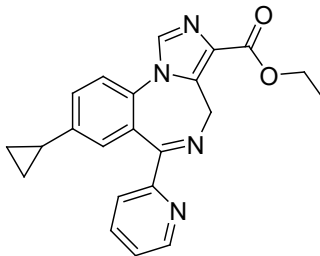
GL-III-13



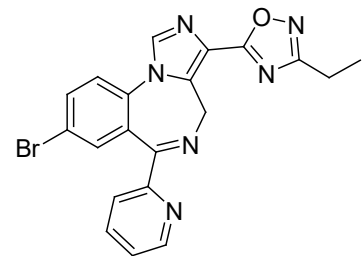
MP-III-80



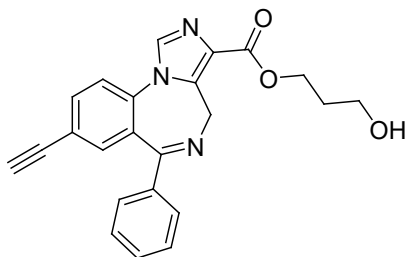
GL-III-58



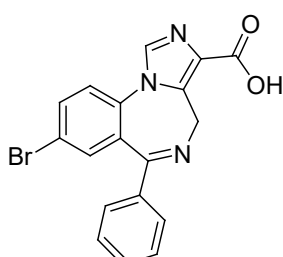
GL-IV-05



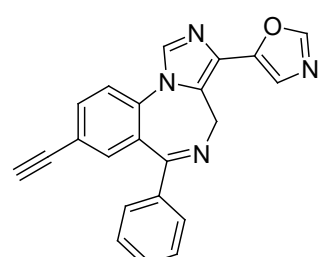
GL-III-99



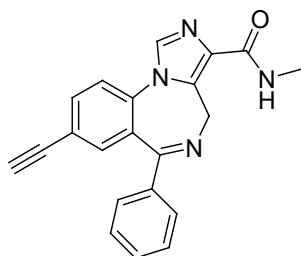
GL-I-48



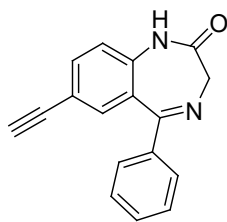
GL-I-50



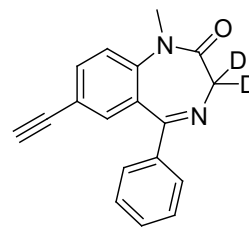
KRM-II-82



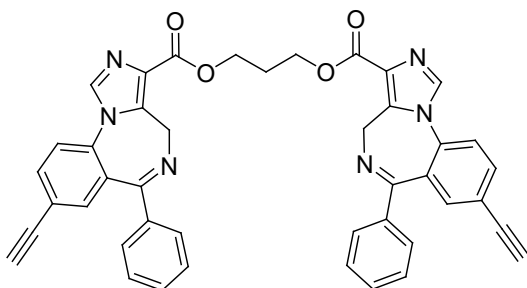
YT-III-31



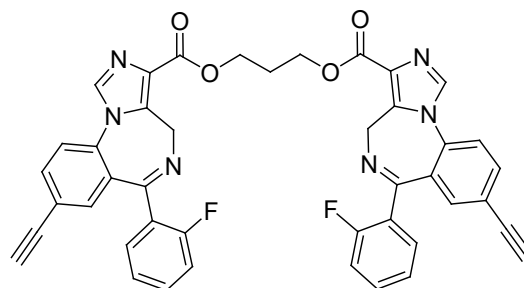
GL-III-59



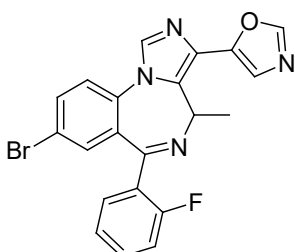
D2-QH-II-66



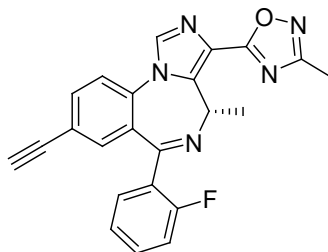
DMH-D-053



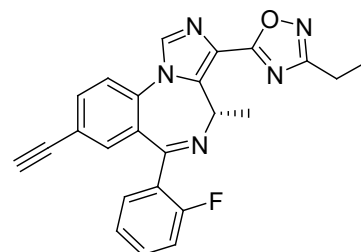
YT-III-271



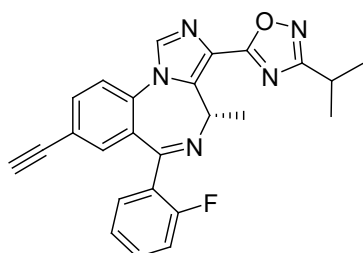
GL-III-76A



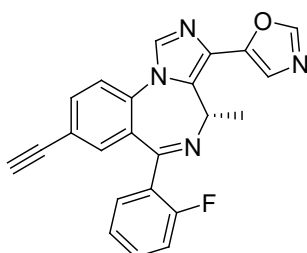
GL-I-65



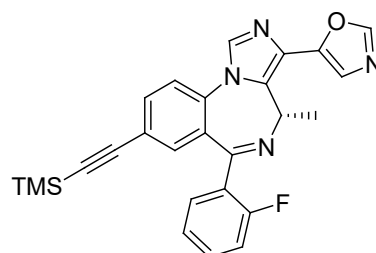
GL-I-66



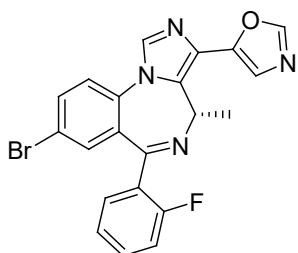
GL-I-81



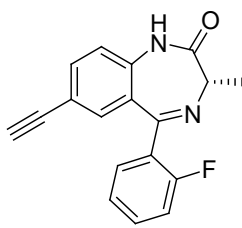
GL-III-78



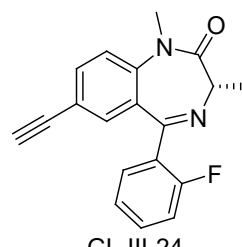
GL-III-77



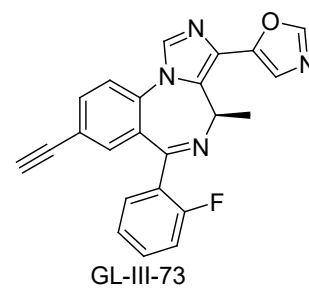
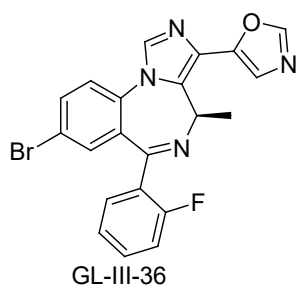
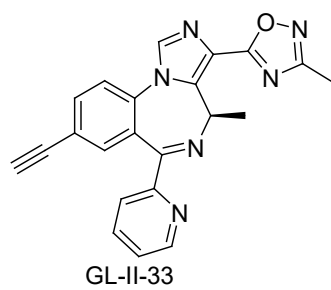
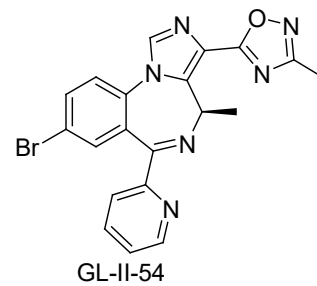
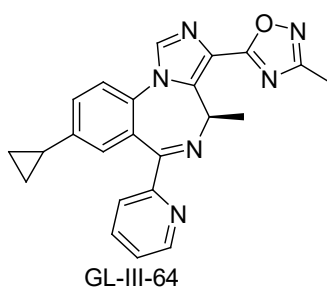
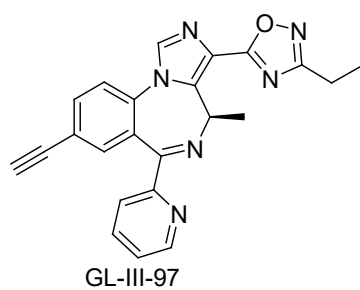
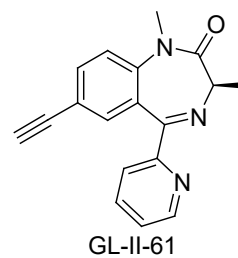
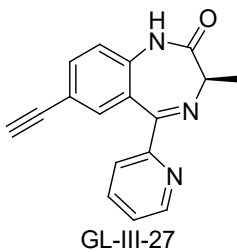
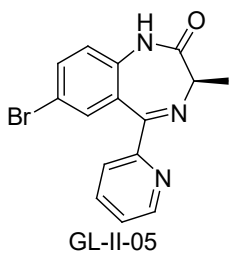
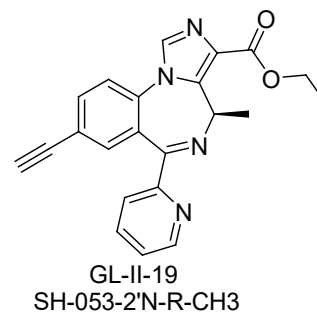
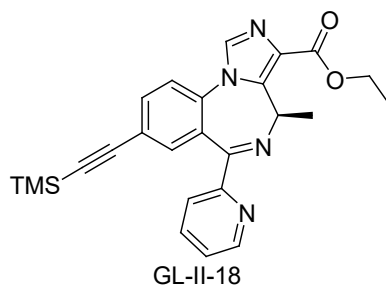
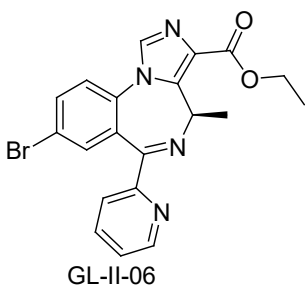
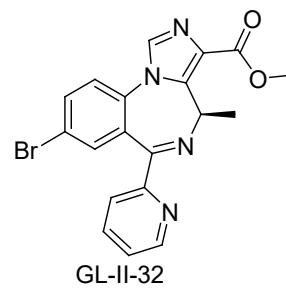
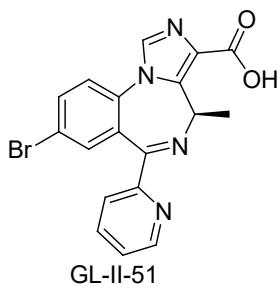
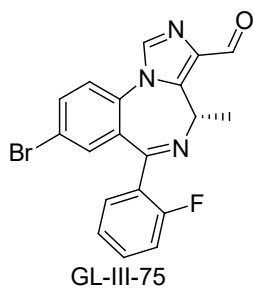
GL-III-76

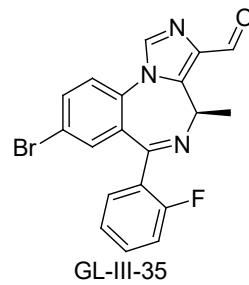
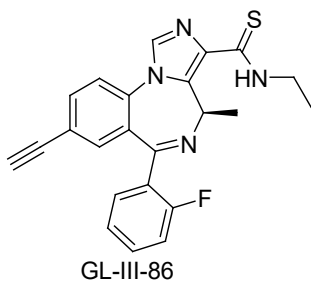
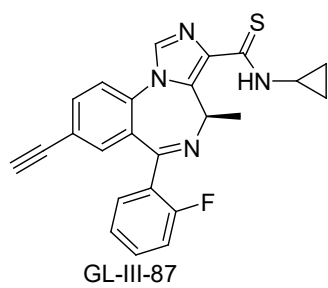
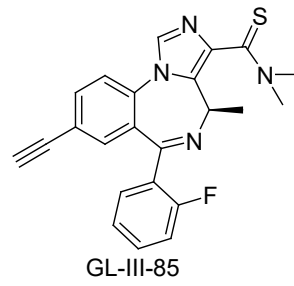
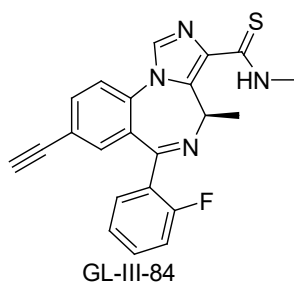
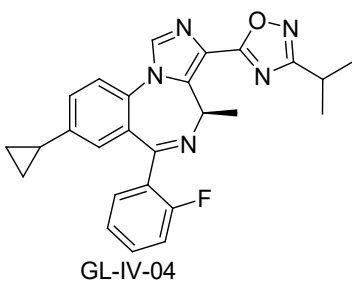
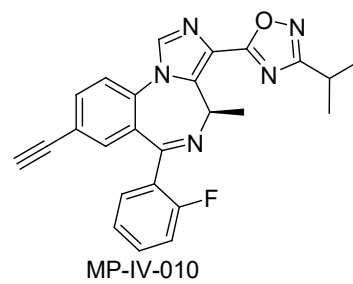
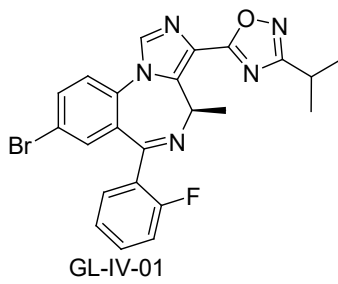
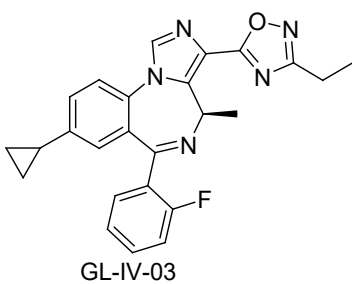
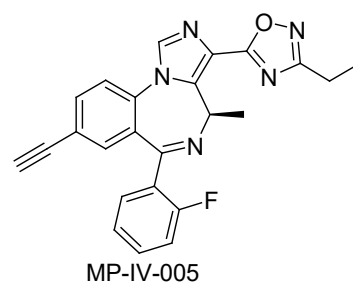
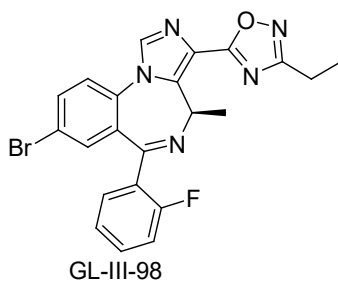
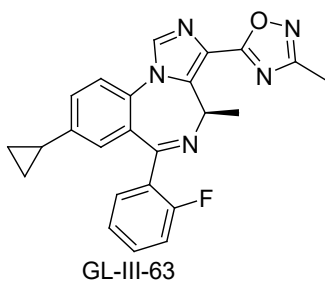
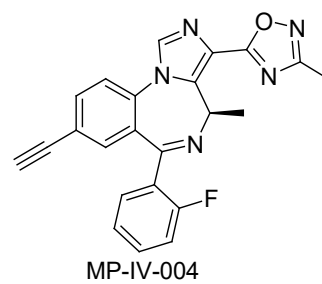
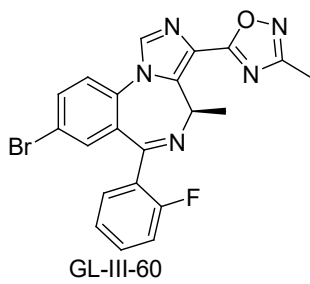
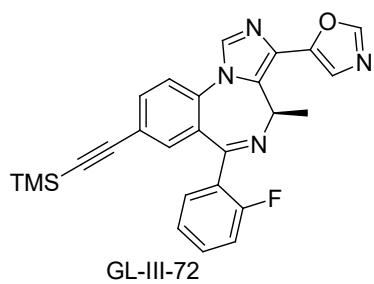


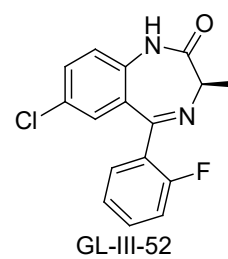
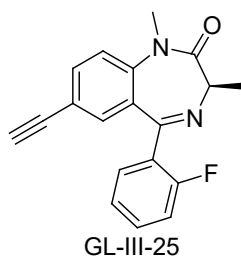
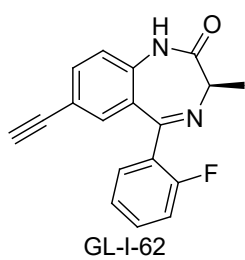
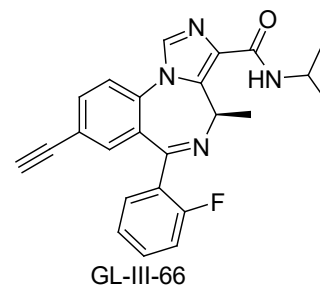
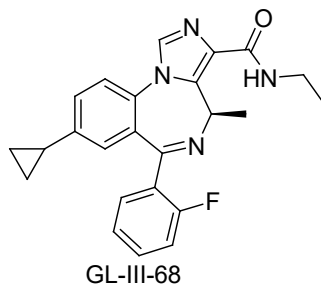
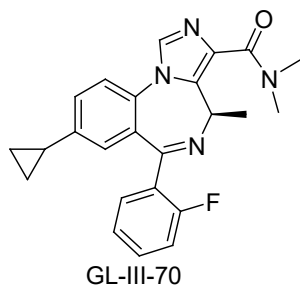
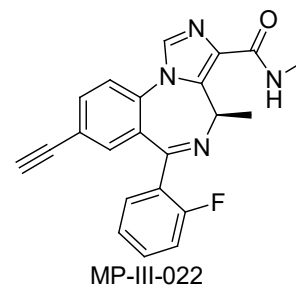
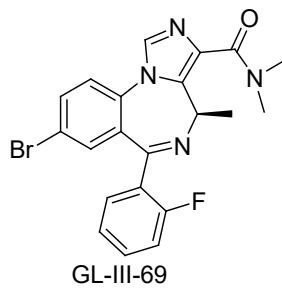
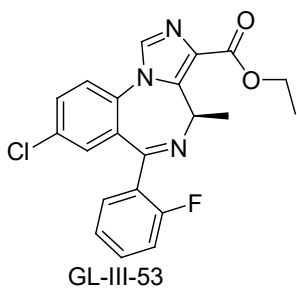
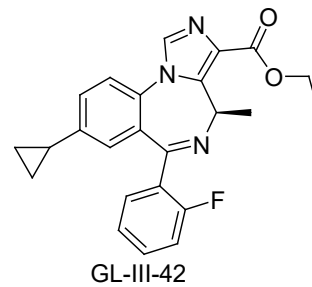
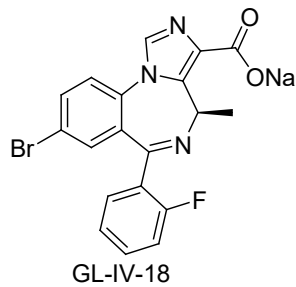
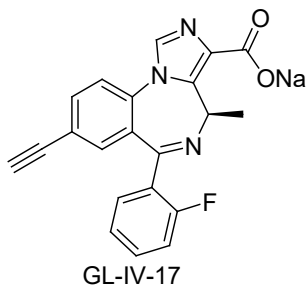
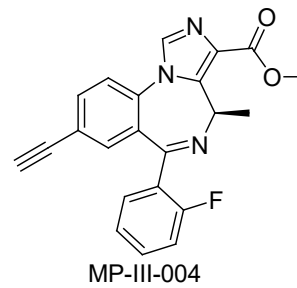
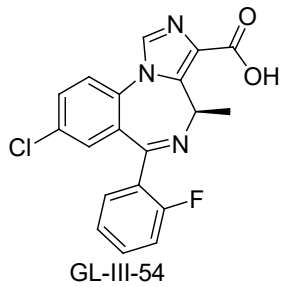
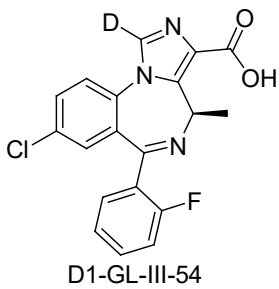
GL-I-64



GL-III-24







CURRICULUM VITAE

EDUCATION

University of Wisconsin – Milwaukee, Milwaukee, WI

Ph.D. in Biochemistry

August 2014 - December 2019

Dissertation: Targeting the γ -Aminobutyric Acid A Receptor to Alleviate Inflammation for Asthma and Neuropathic Pain

PI: Alexander (Leggy) Arnold

Milwaukee School of Engineering, Milwaukee, WI

B.S. in BioMolecular Engineering

September 2010 - May 2014

Minors in Chemistry and Mathematics

AWARDS

AAI Trainee Abstract Award

2018

UW-Milwaukee Graduate Student Travel Award

2018

Graduate Research Assistantship

2015 – 2019

Chancellor's Fellowship

2014-2016, 2018-2019

RESEARCH EXPERIENCE

University of Wisconsin – Milwaukee, Milwaukee, WI

Targeting the GABA_AR to Alleviate Inflammation for Asthma and Neuropathic Pain

2014-2019

Department: Chemistry, PI: Alexander Arnold

- Maintained multiple mammalian cell lines and cultured primary murine cells
- Performed *in vitro* assays including automated patch clamp, RT-qPCR, Western Blotting, ELISA, and fluorescence and luminescence based assays
- Screened compound libraries using high-throughput cell-based assays
- Executed *in vivo* murine studies using disease models and behavioral assays
- Mentored new scientists including undergraduate and graduate students

Marquette University, Milwaukee, WI

Possible Gene Interactions with *drop-dead* (*drd*) in *D. melanogaster*

Summer 2013

Department: Biological Sciences, PI: Edward Blumenthal

- NSF – REU: Interdisciplinary Undergraduate Research Program
- Maintained *D. melanogaster* stocks, including experimental crosses
- Collected immature eggs from decapitated flies, isolated mRNA, and utilized RT-qPCR to quantify gene expression

TEACHING EXPERIENCE

University of Wisconsin – Milwaukee, Milwaukee, WI

Teaching Assistant – CHEM 105 (General Chemistry for Engineering)

2016, 2018-2019

- Coordinated learning outcomes with course instructors
- Generated lesson plans and quizzes

- Managed laboratories of up to 18 students
- Provided tutoring for students department wide

University of Wisconsin – Milwaukee, Milwaukee, WI

Teaching Assistant – CHEM 104 (General Chemistry and Qualitative Analysis)

2014-2015

Coordinated learning outcomes with course instructors

- Managed discussions and laboratories of up to 18 students
- Provided tutoring for students department wide

OTHER RELATED EXPERIENCE

Johnson Level & Tool, Mequon, WI

Engineering Intern

2011 – 2014

- Generated Playbooks detailing processes, components, and quality standards for all work centers in assembly, fabrication, molding, and silk screen departments to satisfy Lean Manufacturing requirements
- Developed internal labor tracking program using MS Access
- Redesigned plant-wide scheduling program in MS Excel to improve ease of use for both management and production team members
- Worked with Quality Assurance Team to assess domestic and imported products to ensure quality standards were met

PUBLICATIONS AND PRESENTATIONS

Amanda N. Nieman, G. Li, B. Mikulsky, A.S. Kehoe, I.W. Leuke, M.M. Poe, D. C. Stafford, J. M. Cook, and L. A. Arnold. (2019, May). Targeting Microglia with Novel Benzodiazepines for the Treatment of Neuropathic Pain. Poster presented at Chemistry and Biochemistry Research Symposium, Milwaukee.

Amanda N. Nieman, G. S. Forkuo, N. M. Zahn, R. Kodali, G. Li, M. S. R. Roni, M. R. Stephen, T. W. Harris, R. Jahan, M. L. Guthrie, O. B. Yu, J. L. Fisher, G. T. Yocum, C. W. Emala, D. A. Steeber, D. C. Stafford, J. M. Cook, and L. A. Arnold. (2018, May). Reducing airway constriction and inflammation through GABAA receptors in the lung with a novel, orally available drug candidate. Poster presented at Chemistry and Biochemistry Research Symposium, Milwaukee.

Amanda N. Nieman, G. S. Forkuo, N. M. Zahn, R. Kodali, G. Li, M. S. R. Roni, M. R. Stephen, T. W. Harris, R. Jahan, M. L. Guthrie, O. B. Yu, J. L. Fisher, G. T. Yocum, C. W. Emala, D. A. Steeber, D. C. Stafford, J. M. Cook, and L. A. Arnold. (2018, May). Reducing airway constriction and inflammation through GABAA receptors in the lung with a novel, orally available drug candidate. Poster presented at Immunology, Austin, TX.

Amanda N. Nieman, G. S. Forkuo, N. M. Zahn, R. Kodali, G. Li, M. S. R. Roni, M. R. Stephen, T. W. Harris, R. Jahan, M. L. Guthrie, O. B. Yu, J. L. Fisher, G. T. Yocum, C. W. Emala, D. A. Steeber, D. C. Stafford, J. M. Cook, and L. A. Arnold. (2018, May). Reducing airway constriction and inflammation through GABA_A receptors in the lung with a novel, orally available drug candidate. In Mitchell Grayson & Nicola Heller (Chair), *Asthma, Lung Inflammation, and Immunity*. Symposium conducted at Immunology, Austin TX

Forkuo, G. S., **Nieman, A. N.**, Kodali, R., Zahn, N. M., Li, G., Rashid Roni, M. S., . . . Arnold, L. A. (2018). A Novel Orally Available Asthma Drug Candidate That Reduces Smooth Muscle Constriction and Inflammation by Targeting GABAA Receptors in the Lung. *Mol Pharm*. doi: 10.1021/acs.molpharmaceut.7b01013

Forkuo, G. S., **Nieman, A. N.**, Yuan, N. Y., Kodali, R., Yu, O. B., Zahn, N. M., . . . Arnold, L. A. (2017). Alleviation of Multiple Asthmatic Pathologic Features with Orally Available and Subtype Selective GABAA Receptor Modulators. *Mol Pharm*, 14(6), 2088-2098. doi: 10.1021/acs.molpharmaceut.7b00183

Amanda N. Nieman (2017, September). Gamma-Aminobutyric Acid A Receptor (GABA_AR), A New Way to Target Inflammation? In Alexander Arnold (Chair), *Nobel Graduate Student Symposium*. Symposium conducted at University of Wisconsin-Milwaukee

Amanda N. Nieman, G. S. Forkuo, N. Y. Yuan, T.W. Harris, MD.S.R. Roni, R. Jahan, G. Li, M. R. Stephen, D.A. Steeber, D. C. Stafford, J. M. Cook, L. A. Arnold. (2017, May). Automated Patch Clamp for Determining the Pharmacology and GABA_A Receptor Subtype Selectivity of Imidazobenzodiazepines. Poster Presented at Chemistry and Biochemistry Research Symposium, Milwaukee, WI

Jahan, R., Stephen, M. R., Forkuo, G. S., Kodali, R., Guthrie, M. L., **Nieman, A. N.**, . . . Arnold, L. A. (2017). Optimization of substituted imidazobenzodiazepines as novel asthma treatments. *Eur J Med Chem*, 126, 550-560. doi: 10.1016/j.ejmech.2016.11.045

Amanda N. Nieman, G. S. Forkuo, M. L. Guthrie, N. Y. Yuan, O. B. Yu, R. Kodali, R. Jahan, M. R. Stephen, M. M. Poe, B. Hartzler, C. W. Emala, J. M. Cook, D. C. Stafford, L. A. Arnold. (2016, October). Targeting the Immune System with Subtype-Selective GABA_A Receptor Modulators to Alleviate Asthma Symptoms. Poster Presented at Graduate Student Research Symposium for Math, Engineering, and the Natural Sciences, Milwaukee, WI

Amanda N. Nieman, G. S. Forkuo, M. L. Guthrie, N. Y. Yuan, O. B. Yu, R. Kodali, R. Jahan, M. R. Stephen, M. M. Poe, B. Hartzler, C. W. Emala, J. M. Cook, D. C. Stafford, L. A. Arnold. (2016, October). Alleviating Asthma Symptoms with Subtype-selective GABA_A Receptor Modulators. Poster Presented at Chemical Biology, Madison, WI

Amanda N. Nieman, G. S. Forkuo, M. L. Guthrie, N. Y. Yuan, O. B. Yu, R. Kodali, R. Jahan, M. R. Stephen, M. M. Poe, B. Hartzler, C. W. Emala, J. M. Cook, D. C. Stafford, L. A. Arnold. (2016, May). Targeting the Immune System with Subtype-Selective GABA_A Receptor Modulators to Alleviate Asthma Symptoms. Poster Presented at Chemistry and Biochemistry Research Symposium, Milwaukee, WI

Amanda N. Nieman, G. S. Forkuo, M. L. Guthrie, N. Y. Yuan, O. B. Yu, R. Kodali, R. Jahan, M. R. Stephen, M. M. Poe, B. Hartzler, C. W. Emala, J. M. Cook, D. C. Stafford, L. A. Arnold. (2016, May). Targeting the Immune System with Subtype-Selective GABA_A Receptor Modulators to Alleviate Asthma Symptoms. Poster Presented at Immunology, Seattle, WA

Forkuo, G. S., Guthrie, M. L., Yuan, N. Y., **Nieman, A. N.**, Kodali, R., Jahan, R., . . . Arnold, L. A. (2016). Development of GABA_A Receptor Subtype-Selective Imidazobenzodiazepines as Novel Asthma Treatments. *Mol Pharm*, 13(6), 2026-2038. doi: 10.1021/acs.molpharmaceut.6b00159

Amanda N. Nieman, G. S. Forkuo, O. B. Yu, M. L. Guthrie, N. Y. Yuan, R. Kodali, R. Jahan, M. R. Stephen, M. M. Poe, C. W. Emala, J. M. Cook, D. C. Stafford, L. A. Arnold. (2015, May). The Effect of γ -Aminobutyric Acid on IL-2 Production in Jurkat Cell Line. Poster Presented at Chemistry and Biochemistry Research Symposium, Milwaukee, WI

LANGUAGES

English

MEMBERSHIPS

American Association of Immunologists